

University of Warwick institutional repository: <http://go.warwick.ac.uk/wrap>

A Thesis Submitted for the Degree of PhD at the University of Warwick

<http://go.warwick.ac.uk/wrap/49815>

This thesis is made available online and is protected by original copyright.

Please scroll down to view the document itself.

Please refer to the repository record for this item for information to help you to cite it. Our policy information is available from the repository home page.

Library Declaration and Deposit Agreement

1. STUDENT DETAILS

Please complete the following:

Full name:

University ID number:

2. THESIS DEPOSIT

2.1 I understand that under my registration at the University, I am required to deposit my thesis with the University in BOTH hard copy and in digital format. The digital version should normally be saved as a single pdf file.

2.2 The hard copy will be housed in the University Library. The digital version will be deposited in the University's Institutional Repository (WRAP). Unless otherwise indicated (see 2.3 below) this will be made openly accessible on the Internet and will be supplied to the British Library to be made available online via its Electronic Theses Online Service (EThOS) service.

[At present, theses submitted for a Master's degree by Research (MA, MSc, LL.M, MS or MMedSci) are not being deposited in WRAP and not being made available via EThOS. This may change in future.]

2.3 In exceptional circumstances, the Chair of the Board of Graduate Studies may grant permission for an embargo to be placed on public access to the hard copy thesis for a limited period. It is also possible to apply separately for an embargo on the digital version. (Further information is available in the *Guide to Examinations for Higher Degrees by Research*.)

2.4 If you are depositing a thesis for a Master's degree by Research, please complete section (a) below. For all other research degrees, please complete both sections (a) and (b) below:

(a) Hard Copy

I hereby deposit a hard copy of my thesis in the University Library to be made publicly available to readers (please delete as appropriate) EITHER immediately OR after an embargo period of months/years as agreed by the Chair of the Board of Graduate Studies.

I agree that my thesis may be photocopied. YES / NO (Please delete as appropriate)

(b) Digital Copy

I hereby deposit a digital copy of my thesis to be held in WRAP and made available via EThOS.

Please choose one of the following options:

EITHER My thesis can be made publicly available online. YES / NO (Please delete as appropriate)

OR My thesis can be made publicly available only after.....[date] (Please give date)
YES / NO (Please delete as appropriate)

OR My full thesis cannot be made publicly available online but I am submitting a separately identified additional, abridged version that can be made available online.
YES / NO (Please delete as appropriate)

OR My thesis cannot be made publicly available online. YES / NO (Please delete as appropriate)

3. **GRANTING OF NON-EXCLUSIVE RIGHTS**

Whether I deposit my Work personally or through an assistant or other agent, I agree to the following:

Rights granted to the University of Warwick and the British Library and the user of the thesis through this agreement are non-exclusive. I retain all rights in the thesis in its present version or future versions. I agree that the institutional repository administrators and the British Library or their agents may, without changing content, digitise and migrate the thesis to any medium or format for the purpose of future preservation and accessibility.

4. **DECLARATIONS**

(a) I DECLARE THAT:

- I am the author and owner of the copyright in the thesis and/or I have the authority of the authors and owners of the copyright in the thesis to make this agreement. Reproduction of any part of this thesis for teaching or in academic or other forms of publication is subject to the normal limitations on the use of copyrighted materials and to the proper and full acknowledgement of its source.
- The digital version of the thesis I am supplying is the same version as the final, hard-bound copy submitted in completion of my degree, once any minor corrections have been completed.
- I have exercised reasonable care to ensure that the thesis is original, and does not to the best of my knowledge break any UK law or other Intellectual Property Right, or contain any confidential material.
- I understand that, through the medium of the Internet, files will be available to automated agents, and may be searched and copied by, for example, text mining and plagiarism detection software.

(b) IF I HAVE AGREED (in Section 2 above) TO MAKE MY THESIS PUBLICLY AVAILABLE DIGITALLY, I ALSO DECLARE THAT:

- I grant the University of Warwick and the British Library a licence to make available on the Internet the thesis in digitised format through the Institutional Repository and through the British Library via the EThOS service.
- If my thesis does include any substantial subsidiary material owned by third-party copyright holders, I have sought and obtained permission to include it in any version of my thesis available in digital format and that this permission encompasses the rights that I have granted to the University of Warwick and to the British Library.

5. **LEGAL INFRINGEMENTS**

I understand that neither the University of Warwick nor the British Library have any obligation to take legal action on behalf of myself, or other rights holders, in the event of infringement of intellectual property rights, breach of contract or of any other right, in the thesis.

Please sign this agreement and return it to the Graduate School Office when you submit your thesis.

Student's signature: Date:

Synthesis and post- Polymerisation Functionalisation of Aliphatic Poly(carbonate)s

Sarah Tempelaar, MSc.

A thesis submitted in partial fulfillment of the requirements
for the degree of

Doctor of Philosophy in Chemistry

University of Warwick
Department of Chemistry

March 2012

Table of Contents

Table of Contents	ii
List of Figures	ix
List of Schemes	xix
List of Tables	xxi
Abbreviations	xxiii
Acknowledgements	xxvi
Declaration	xxvii
Abstract	xxviii
Chapter 1. Synthesis and post-Polymerisation Modifications of Aliphatic Poly(Carbonate)s prepared by Ring-Opening Polymerisation	1
1.1. Introduction	2
1.2. Synthesis Routes to Functional Cyclic Carbonates	5
1.2.1. Functional Cyclic Carbonates derived from 2,2-bishydroxy(methyl)propionic acid (bis-MPA)	5
1.2.2. Functional cyclic carbonates derived from pentaerythriol, glycerol and trimethylolalkanes	8
1.2.3. Functional Cyclic Carbonates derived from amino acids or sugars	10
1.2.4. Synthesis of functional cyclic carbonates from other resources	12
1.3. Ring-opening polymerisation of functional cyclic carbonates	14
1.3.1. Alkyl functional monomers	14
1.3.2. Aryl functional monomers	18
1.3.3. Alkene and alkyne functional cyclic carbonates	23
1.3.4. Halogenated and azide functional cyclic carbonates	28

1.3.5. Monomers with nitrogen-containing functionalities: Amino-, amido, carbamate and urea functional cyclic carbonates	31
1.3.6. Protected sugar functional cyclic carbonates	35
1.3.7. Macromonomers, bis- and tris- carbonates	37
1.3.8. Other functional monomers	42
1.4. Post-polymerisation modification of functional poly(carbonate)s	44
1.4.1. Deprotection of aryl and alkyl functional poly(carbonate)s	44
1.4.2. Post-polymerisation modifications of alkene functional poly(carbonate)s	48
1.4.3. Post-polymerisation modifications of poly(carbonate)s <i>via</i> alkyne-azide cycloadditions	52
1.4.4. Quaternisation of halogen functional poly(carbonate)s	54
1.4.5. Deprotection of carbamate functional poly(carbonate)s	55
1.4.6. Other post-polymerisation modifications of functional poly(carbonate)s	56
1.5. Conclusion	58
1.6. Overview of cyclic carbonates	59
1.6.1. Overview of cyclic carbonate monomers	59
1.6.2. Quaternisation of halogen functional poly(carbonate)s	65
1.6. References	66
Chapter 2. Organocatalytic Synthesis and post-Polymerisation	
Functionalisation of Allyl-Functional Poly(carbonate)s	79
2.1. Introduction	80
2.2. Results and Discussion	81
2.2.1. Synthesis of 5-methyl-5-allyloxycarbonyl-1,3-dioxan-2-one, MAC.	81

2.2.2. Organocatalytic Ring-Opening Polymerisation of 5-methyl-5-allyloxycarbonyl-1,3-dioxan-2-one, MAC	82
2.2.2.1. Organocatalytic Ring-Opening Polymerisation of 5-methyl-5-allyloxycarbonyl-1,3-dioxan-2-one, MAC: Choice of catalyst	82
2.2.2.2. Organocatalytic Ring-Opening Polymerisation of 5-methyl-5-allyloxycarbonyl-1,3-dioxan-2-one, MAC: Polymerisation control	87
2.2.2.3. Organocatalytic Ring-Opening Polymerisation of 5-methyl-5-allyloxycarbonyl-1,3-dioxan-2-one, MAC: Telechelics and block copolymers	90
2.2.3. Post-polymerisation functionalisation of allyl-functional poly(carbonate), PMAC, <i>via</i> radical addition of a thiol	97
2.2.3.1. Post-polymerisation functionalisation of allyl-functional poly(carbonate), PMAC, <i>via</i> radical addition of a thiol: Optimisation of conditions	97
2.2.3.2. Post-polymerisation functionalisation of allyl-functional poly(carbonate), PMAC, <i>via</i> radical addition of a thiol: Functionalisation and characterisation	100
2.2.4. Thermal analysis of functional poly(carbonate)s derived from PMAC.	107
2.3. Conclusions	109
2.4. References	110
Chapter 3. Organocatalytic Synthesis and post-Polymerisation Functionalisation of Propargyl-Functional Poly(Carbonate)s	113
3.1. Introduction	114
3.2. Results and Discussion	116
3.2.1. Synthesis of 5-methyl-5-propargyloxycarbonyl-1,3-dioxan-2-one, MPC	116

3.2.2. Organocatalytic Ring-Opening Polymerisation of 5-methyl-5-propargyloxycarbonyl-1,3-dioxan-2-one, MPC	117
3.2.2.1. Organocatalytic Ring-Opening Polymerisation of 5-methyl-5-propargyloxycarbonyl-1,3-dioxan-2-one, MPC: Polymerisation control with the bifunctional 1-(3,5-bis(trifluoromethyl)phenyl)-3-cyclohexylthiourea/(-)-sparteine catalyst system	117
3.2.2.2. Organocatalytic Ring-Opening Polymerisation of 5-methyl-5-propargyloxycarbonyl-1,3-dioxan-2-one, MPC: Polymerisation control with the bifunctional 1-(3,5-bis(trifluoromethyl)phenyl)-3-cyclohexylthiourea/DBU catalyst system	124
3.2.2.3. Organocatalytic Ring-Opening Polymerisation of 5-methyl-5-propargyloxycarbonyl-1,3-dioxan-2-one, MPC: Telechelics and block copolymers	130
3.2.3. Post-polymerisation functionalisation of propargyl-functional poly(carbonate), PMPC, <i>via</i> copper(I) catalysed Huisgen 1,3-dipolar cycloaddition	135
3.2.3.1. Post-polymerisation functionalisation of propargyl-functional poly(carbonate), PMPC, <i>via</i> copper(I) catalysed Huisgen 1,3-dipolar cycloaddition: Optimisation of conditions.	135
3.2.3.2. Post-polymerisation functionalisation of propargyl-functional poly(carbonate), PMPC, <i>via</i> copper(I) catalysed Huisgen 1,3-dipolar cycloaddition: Functionalisation and characterisation.	139
3.2.4. Post-polymerisation functionalisation of propargyl-functional poly(carbonate), PMPC, <i>via</i> radical addition of thiols	152
3.3. Conclusions	161
3.4. References	162
Chapter 4. Synthesis and Orthogonal post-Polymerisation Functionalisation of Allyl and Propargyl Functional Poly(Carbonate)s	164

4.1. Introduction	165
4.2. Results and Discussion	167
4.2.1. Copolymerisations of 5-methyl-5-allyloxycarbonyl-1,3-dioxan-2-one (MAC) and 5-methyl-5-propargyloxycarbonyl-1,3-dioxan-2-one (MPC)	167
4.2.2. Functionalisation of the propargyl groups in an allyl- and propargyl- functional poly(carbonate)	179
4.2.3. Functionalisation of the allyl groups in an allyl- and propargyl- functional poly(carbonate)	186
4.3. Conclusions	194
4.4. References	195
Chapter 5. Synthesis, Stereo-complexation and post-Polymerisation Functionalisation of Functional Poly(Ester-Carbonate)s	197
5.1. Introduction	198
5.2. Results and Discussion	201
5.2.1. Copolymerisations of <i>L</i> - and <i>D</i> -lactide with 5-methyl-5-allyloxycarbonyl-1,3-dioxan-2-one, MAC, and 5-methyl-5-propargyloxycarbonyl-1,3-dioxan-2-one, MPC	201
5.2.2. Post-polymerisation functionalisations of allyl- and propargyl functional poly(ester-carbonate)s	208
5.2.3. Thermal analysis of poly(ester-carbonate)s	212
5.2.4. Thermal analysis of poly(ester-carbonate) blends	218
5.3. Conclusions	228
5.4. References	229
Chapter 6. Conclusions	233
6.1. Conclusions	234

Chapter 7. Experimental	238
7.1. Materials	239
7.2. General considerations	240
7.3. Experimental details for Chapter 2	243
7.3.1. Synthesis of 5-methyl-5-allyloxycarbonyl-1,3-dioxan-2-one, MAC	243
7.3.2. Organocatalytic ROP of 5-methyl-5-allyloxycarbonyl-1,3-dioxan-2-one (MAC)	244
7.3.3. Synthesis of PMAC block copolymers	245
7.3.3.1. Synthesis of PEO-PMAC block copolymer	245
7.3.3.2. Synthesis of PLA-PMAC block copolymers	245
7.3.4. Post-polymerisation functionalisation of PMAC	246
7.4. Experimental details for Chapter 3	250
7.4.1. Synthesis of 5-methyl-5-propargyloxycarbonyl-1,3-dioxan-2-one, MPC	250
7.4.2. Organocatalytic ROP of 5-methyl-5-propargyloxycarbonyl-1,3-dioxan-2-one (MPC)	251
7.4.3. Synthesis of PMPC block copolymers	252
7.4.3.1. Synthesis of PEO-PMPC block copolymers	254
7.4.3.2. Synthesis of PLLA-PMPC block copolymers	254
7.4.3.3. Synthesis of PMPC-PMAC block copolymer	253
7.4.4. Post-polymerisation functionalisation of PMPC	254
7.4.4.1. Post-polymerisation functionalisation of PMPC <i>via</i> Huisgens 1,3-dipolar Cycloaddition	254
7.4.4.2. Post-polymerisation functionalisation of PMPC <i>via</i> radical addition of a thiol	257
7.5. Experimental details for Chapter 4	259

7.5.1. Organocatalytic ROP of 5-methyl-5-allyloxycarbonyl-1,3-dioxan-2-one (MAC) and 5-methyl-5-propargyloxycarbonyl-1,3-dioxan-2-one (MPC)	259
7.5.2. Post-polymerisation functionalisations of P(MAC- <i>co</i> -MPC)	260
7.5.2.1. Functionalisation of the propargyl groups of P(MAC- <i>co</i> -MPC)	260
7.5.2.2. Functionalisation of the allyl groups of P(MAC- <i>co</i> -MPC)	261
7.6. Experimental details for Chapter 4	262
7.6.1. Copolymerisations of <i>L</i> - and <i>D</i> -Lactide with functional cyclic carbonates	262
7.6.1.1. Copolymerisations of <i>L</i> - or <i>D</i> -lactide and MAC	262
7.6.1.2. Copolymerisations of <i>L</i> -lactide and MPC	263
7.6.2. Post-polymerisation functionalisation of poly(ester-carbonate)s	264
7.6.2.1. Functionalisation of the allyl groups in P(LLA- <i>co</i> -MAC)	264
7.6.2.2. Functionalisation of the propargyl groups in P(LLA- <i>co</i> -MPC)	265
7.7. References.	266
Appendices	267

List of Figures

Figure 1.1. Alkyl functional cyclic carbonate monomers.	15
Figure 1.2. Ring opening of alkyl functional monomers with a substituent at the α -position.	17
Figure 1.3. Aryl functional cyclic carbonate monomers.	19
Figure 1.4. Methoxy- and nitro- substituted aryl functional cyclic carbonate monomers.	22
Figure 1.5. Alkene functional cyclic carbonate monomers.	24
Figure 1.6. Halogenated and azide functional cyclic carbonate monomers.	28
Figure 1.7. Cyclic carbonates with halogenated functional groups derived from <i>bis</i> -MPA.	30
Figure 1.8. Cyclic carbonate monomers with pendant carbamate functionalities.	32
Figure 1.9. Nitrogen containing functional cyclic carbonate monomers.	34
Figure 1.10. Sugar functional cyclic carbonate monomers	36
Figure 1.11. Cyclic carbonate macromonomers.	38
Figure 1.12. Polymerisation with and from cyclic carbonate M68 .	40
Figure 1.13. Bis- and tris- cyclic carbonate cross-linkers.	41
Figure 1.14. Other functional cyclic carbonate monomers.	42
Figure 1.15. Sulphide and disulphide functional cyclic carbonate monomers.	43
Figure 2.1. Organic catalysts screened for the ring-opening polymerisation of MAC.	82
Figure 2.2. Comparison of the ^1H NMR spectra of MAC (top) and of PMAC (bottom) initiated from benzyl alcohol (CDCl_3 ; 400 MHz, 298 K). Shifts in the methyl (●) and the methylene (●) resonances are observed upon polymerisation.	83
Figure 2.3. Plot of number-average molecular weight (M_n ; ■) and polydispersity (M_w/M_n ; □) against % monomer conversion in the ring-opening polymerisation of MAC. Conditions: $[\text{MAC}] = 0.5 \text{ M}$ CDCl_3 at $25 \text{ }^\circ\text{C}$, 5 mol% 2 , 10 mol% 3 , $[\text{M}]/[\text{I}] = 20$ using benzyl alcohol as initiator.	87
Figure 2.4. Plot of number-average molecular weight (M_n ; ■) and polydispersity (M_w/M_n ; □) against initial monomer-to-initiator ratio, $[\text{M}]_0/[\text{I}]_0$, in the ring-opening polymerisation of MAC. Conditions:	

- [MAC] = 0.5 M CDCl₃ at 25 °C, 5 mol% **2**, 10 mol% **3**, using benzyl alcohol as initiator. 88
- Figure 2.5.** ¹H NMR in CDCl₃ of PMAC₁₁ initiated from benzyl alcohol using 5 mol% **2** and 10 mol% **3** (400 MHz, 293 K; * = residual CDCl₃, ** = H₂O). 89
- Figure 2.6.** MALDI-TOF MS analysis of PMAC (DP = 11) initiated from benzyl alcohol using 5 mol% **2** and 10 mol% **3**. 89
- Figure 2.7.** Bifunctional initiators used in the ring-opening polymerisation of MAC. 91
- Figure 2.8.** MALDI-TOF MS analysis of telechelic PMAC (DP = 20) initiated from **6** using 5 mol% **2** and 10 mol% **3**. Two distributions (both DP = 10) are observed due to the retro-Diels Alder reaction caused by the energy from the laser. Experimental and calculated *m/z* values for both maleimide (●) and furan (●) terminated polymers are given in Table 2.3. 93
- Figure 2.9.** GPC traces of MeO-PEO₁₁₄-OH (*M_n* = 7 520 g mol⁻¹, PDI = 1.03) and MeO-PEO₁₁₄-PMAC₂₀-OH block copolymer (*M_n* = 11 900 g mol⁻¹, PDI = 1.06). 94
- Figure 2.10.** Expansion of the δ 3.00- 4.60 ppm region of the ¹H NMR spectra of BnO-PMAC-*b*-PLA-OH (top) and BnO-PLA-*b*-PMAC-OH (bottom) (400 MHz, CDCl₃, 293 K). The BnO-PLA-*b*-PMAC-OH spectrum shows the CH₂OH end group resonance from the final PMAC block, whereas this resonance is absent in the ¹H NMR spectrum of BnO-PMAC-*b*-PLA-OH. 95
- Figure 2.11.** GPC traces of BnO-PLA₂₀-OH (*M_n* = 2 020 g mol⁻¹, PDI = 1.17) and BnO-PLA₂₀-PMAC₂₀-OH block copolymer (*M_n* = 7 130 g mol⁻¹, PDI = 1.17). 95
- Figure 2.12.** ¹H NMR in CDCl₃ of PMAC₁₁ after post-polymerisation radical functionalisation with 1-dodecanethiol (400 MHz, 293 K; * = residual CDCl₃, ** = H₂O). 100
- Figure 2.13.** GPC traces of BnO-PMAC₁₀₀-OH before (*M_n* = 15 100 g mol⁻¹, PDI = 1.23) and after post-polymerisation functionalisation with 1-dodecanethiol (*M_n* = 25 000 g mol⁻¹, PDI = 1.22). 101
- Figure 2.14.** MALDI-ToF-MS of PMAC (DP = 11) after post-polymerisation functionalisation with 1-dodecanethiol. The second lower distribution represents a PMAC chain that is not fully functionalised and has one pendant allyl group left. 102

- Figure 2.15.** ^1H NMR spectra in d-DMSO of BnO-PMAC₁₀₀-OH after post-polymerisation functionalisation with (i) mercaptoacetic acid, (ii) 1-thioglycerol and (iii) mercaptoethanol (400 MHz, 293 K; * = H₂O, ** = residual d-DMSO). 103
- Figure 2.16.** GPC traces of BnO-PMAC₁₀₀-OH before ($M_n = 17\,160\text{ g mol}^{-1}$, PDI = 1.18) and after post-polymerisation functionalisation with (i) mercaptoethanol ($M_n = 26\,050\text{ g mol}^{-1}$, PDI = 1.27) and (ii) 1-thioglycerol ($M_n = 29\,340\text{ g mol}^{-1}$, PDI = 1.34). 104
- Figure 2.17.** MALDI-ToF-MS of PMAC (DP = 11) after post-polymerisation functionalisation with benzyl mercaptan. An increase in repeat unit is observed from 200 m/z to 324 m/z . 106
- Figure 3.1.** Organic catalysts used in the ring-opening polymerisation of MPC. 117
- Figure 3.2.** Comparison of the ^1H NMR spectra of MPC (top) and of PMPC (bottom) initiated from benzyl alcohol (CDCl₃; 400 MHz, 298 K). Shifts in the methyl (●) and the methylene (●) resonances are observed upon polymerisation. 118
- Figure 3.3.** Plot of number-average molecular weight (M_n ; ■) and polydispersity (M_w/M_n ; □) against % monomer conversion in the ring-opening polymerisation of MPC. Conditions: [MPC] = 0.5 M CDCl₃ at 25 °C, 5 mol% **2**, 10 mol% **1**, [M]/[I] = 20 using benzyl alcohol as initiator. 119
- Figure 3.4.** Plot of number-average molecular weight (M_n ; ■) and polydispersity (M_w/M_n ; □) against initial monomer-to-initiator ratio, [M]₀/[I]₀, in the ring-opening polymerisation of MPC. Conditions: [MPC] = 0.5 M CDCl₃ at 25 °C, 5 mol% **2** (to initiator), 10 mol% **1** (to monomer), using benzyl alcohol as initiator. 120
- Figure 3.5.** ^1H NMR in CDCl₃ of PMPC₁₀ initiated from benzyl alcohol using 5 mol% **1** and 10 mol% **2** (500 MHz, 298 K; * = residual CDCl₃, ** = H₂O). 121
- Figure 3.6.** MALDI-ToF MS analysis of PMPC (DP = 10) initiated from benzyl alcohol using 5 mol% **2** and 10 mol% **1**. 122
- Figure 3.7.** MALDI-ToF MS analysis of PMPC polymers initiated from benzyl alcohol obtained from polymerisations ran dichloromethane (top) and CDCl₃. (bottom) using **2** (5 mol%) and **1** (10 mol%) as catalysts. 123
- Figure 3.8.** Schematic representation of the isotope pattern expected for DP10 peaks of PMPC (top), PMPC with all acetylenic protons

- exchanged with deuterium (bottom) and the isotope pattern expected for a mixture of polymer chains (DP10) with 1, 2 and 3 propargylic protons substituted in a 1:1:1 ratio. 124
- Figure 3.9.** GPC trace of BnO-PMPC100-OH ($M_n = 16\,540\text{ g}\cdot\text{mol}^{-1}$, PDI = 1.11) prepared by the ROP of MPC ($[\text{MPC}] = 0.5\text{M}$) catalysed by 5 mol% **3** and 1 mol% DBU using benzyl alcohol as initiator. 125
- Figure 3.10.** Plot of number-average molecular weight (M_n ; ■) and polydispersity (M_w/M_n ; □) against % monomer conversion in the ring-opening polymerisation of MPC catalysed by **1** and DBU. Conditions: $[\text{MPC}] = 0.5\text{ M}$ CDCl_3 at $25\text{ }^\circ\text{C}$, 1 mol% **3**, 5 mol% **1**, $[\text{M}]/[\text{I}] = 45$ using benzyl alcohol as initiator. 126
- Figure 3.11.** Plot of number-average molecular weight (M_n ; ■) and polydispersity (M_w/M_n ; □) against initial monomer-to-initiator ratio, $[\text{M}]_0/[\text{I}]_0$, in the ring-opening polymerization of MPC. Conditions: $[\text{MPC}] = 0.5\text{ M}$ CDCl_3 at $25\text{ }^\circ\text{C}$, 1 mol% **3**, 5 mol% **1**, using benzyl alcohol as initiator. 127
- Figure 3.12.** Comparison of plots of number-average molecular weight (M_n) against initial monomer-to-initiator ratio, $[\text{M}]_0/[\text{I}]_0$, in the ROP of MPC ($[\text{MPC}] = 0.5\text{ M}$) using **1+2** and **1+3** as catalyst systems, respectively. 127
- Figure 3.13.** Comparison of GPC traces of resulting polymers prepared by the ROP of MPC using **1+2** ($M_n = 10\,050\text{ g}\cdot\text{mol}^{-1}$, PDI = 1.27) and **1+3** ($M_n = 8\,230\text{ g}\cdot\text{mol}^{-1}$, PDI = 1.17) as catalyst systems, respectively ($[\text{M}]/[\text{I}] = 50$; $[\text{MPC}] = 0.5\text{ M}$). 128
- Figure 3.14.** MALDI-ToF MS analysis of PMPC (DP = 12) initiated from benzyl alcohol (left) and GPC trace of BnO-PMPC₇₂-OH ($M_n = 15\,700\text{ g}\cdot\text{mol}^{-1}$, PDI = 1.13) prepared by the ROP of MPC ($[\text{MPC}] = 0.5\text{M}$) catalysed by 5 mol% **1** and 1 mol% **3**. 129
- Figure 3.15.** Bifunctional initiators used in the ring-opening polymerisation of MPC. 130
- Figure 3.16.** MALDI-ToF MS analysis of telechelic PMPC initiated from 2-hydroxyethyl disulphide, **4**, prepared by the ROP of MPC ($[\text{MPC}] = 0.5\text{M}$). 131
- Figure 3.17.** GPC traces of four block copolymers and their corresponding macro-initiator. Top left: BnO-PLLA₁₈-OH ($M_n = 4\,200\text{ g mol}^{-1}$, PDI = 1.09) and BnO-PLLA₁₈-*b*-PMPC₂₀-OH ($M_n = 8\,740\text{ g mol}^{-1}$, PDI = 1.08), top right: BnO-PMPC₂₀-OH ($M_n = 4\,540\text{ g mol}^{-1}$, PDI = 1.12) and BnO-PMPC₂₀-*b*-PLLA₂₄-OH ($M_n = 10\,350\text{ g mol}^{-1}$, PDI = 1.09), bottom left: MeO-PEO₁₁₄-OH ($M_n = 6\,790\text{ g mol}^{-1}$, PDI = 1.03) and MeO-PEO₁₁₄-*b*-

- PMPC₁₈-OH ($M_n = 11\,020\text{ g mol}^{-1}$, PDI = 1.06), bottom right: BnO-PMPC₁₇-OH ($M_n = 4\,010\text{ g mol}^{-1}$, PDI = 1.11) and BnO-PMPC₁₇-*b*-PMAC₁₉-OH ($M_n = 8\,110\text{ g mol}^{-1}$, PDI = 1.09). **134**
- Figure 3.18.** MALDI-TOF MS analysis of PMPC (M/I = 20) initiated from benzyl alcohol before (top) and after (bottom) functionalisation *via* cycloaddition with 1-azidooctane. In accordance to the addition of 1-azidooctane, the repeat unit increases from 198-199 m/z for PMPC (top) to 353 m/z after functionalisation (bottom). Theoretical and observed m/z values of the indicated peaks (●/●) are given in Table 3.5. **138**
- Figure 3.19.** ¹H NMR in CDCl₃ of PMPC₇₂ after functionalisation with 1-azidooctane (400 MHz, 298 K; * = residual CDCl₃). **140**
- Figure 3.20.** GPC traces of BnO-PMAC₇₂-OH before ($M_n = 9\,350\text{ g mol}^{-1}$, PDI = 1.11) and after post-polymerisation functionalisation with 1-azidooctane ($M_n = 12\,740\text{ g mol}^{-1}$, PDI = 1.15). **141**
- Figure 3.21.** MALDI-ToF-MS spectra of PMPC (DP = 10) after post-polymerisation functionalisation with 1-azidooctane. Samples prepared without (top) and with (bottom) sodium TFA show polymer chains ionised with residual copper from the functionalisation reaction. **142**
- Figure 3.22.** Functional azides for post-polymerisation alteration of propargyl-functional poly(carbonate)s *via* copper(I)-catalysed 1,3-dipolar cycloaddition. **143**
- Figure 3.23.** ¹H NMR in CDCl₃ of PMPC₇₂ after functionalisation with benzyl azide (top) and ¹H NMR of PMPC₇₂ after functionalisation with 3-azido-7-hydroxylcoumarin (bottom) in *d*-DMSO (400 MHz, 298 K; * = residual CDCl₃, ** = H₂O, *** = residual *d*-DMSO). **144**
- Figure 3.24.** GPC traces of (left) BnO-PMAC₇₂-OH using THF as eluent before ($M_n = 9\,350\text{ g mol}^{-1}$, PDI = 1.11) and after post-polymerisation functionalisation with benzyl azide ($M_n = 9\,700\text{ g mol}^{-1}$, PDI = 1.15) and of (right) BnO-PMAC₇₂-OH using DMF as eluent before ($M_n = 15\,700\text{ g mol}^{-1}$, PDI = 1.13) and after post-polymerisation functionalisation with coumarin azide ($M_n = 18\,620\text{ g mol}^{-1}$, PDI = 1.23). **145**
- Figure 3.25.** MALDI-ToF-MS spectrum of PMPC₁₀ after post-polymerisation functionalisation with benzyl azide. **146**
- Figure 3.26.** MALDI-ToF-MS spectrum of PMPC₁₀ after post-polymerisation functionalisation with 3-azido-7-hydroxylcoumarin (left). The presence of propargyl-containing polymer chains confirms that post-polymerisation functionalisation did not go to completion. A close up of the region between 1620 m/z and 1800 m/z (right) shows the

- presence of a two separate species. ● = PMPC fully functionalised with 3-azido-7-hydroxycoumarin azide; ● = polymer chains with 1 propargyl group left; ● = polymer chains with 2 propargyl groups left. **147**
- Figure 3.27.** Fluorescence in 3-azido-7-hydroxycoumarin-clicked PMPC is triggered by the formation of the triazole rings. (A) From left to right: Solutions in DMF of PMPC, 3-azido-7-hydroxycoumarin, PMPC + 3-azido-7-hydroxycoumarin, PMPC after functionalisation with 3-azido-7-hydroxycoumarin (**12d**); (B) Further diluted solution of **12d** in DMF; (C) From left to right: Solutions in DMF of PMPC, 3-azido-7-hydroxycoumarin, PMPC + 3-azido-7-hydroxycoumarin, **12d**, irradiated at 365 nm with a UV lamp; (D) Further diluted solution of **12d** in DMF irradiated at 365 nm with a UV lamp. **148**
- Figure 3.28.** ^1H NMR spectra of PMPC₇₂ after functionalisation with α -mannose azide in *d*-DMSO (top; 400 MHz, 298 K) and in D₂O (bottom; 400 MHz, 298 K); * = dimethyl formamide, ** = methylene chloride, *** = H₂O, **** = residual *d*-DMSO, ***** = residual D₂O. **150**
- Figure 3.29.** COSY in *d*-DMSO of PMPC₇₂ after functionalisation with α -mannose azide (400 MHz, 298 K; * = methylene chloride, ** = H₂O). In combination with the ^1H NMR spectrum in both *d*-DMSO and D₂O and the COSY in D₂O, all mannose protons in Figure 3.28 could be assigned. **150**
- Figure 3.30.** ^1H NMR in CDCl₃ of PMPC₁₂ after post-polymerisation radical functionalisation with 1-dodecanethiol (400 MHz, 298 K; * = residual CDCl₃). **153**
- Figure 3.31.** GPC traces of BnO-PMAC₇₂-OH before ($M_n = 9\,350\text{ g mol}^{-1}$, PDI = 1.11) and after post-polymerisation functionalisation with 1-dodecanethiol ($M_n = 18\,140\text{ g mol}^{-1}$, PDI = 1.17). **154**
- Figure 3.32.** MALDI-ToF-MS spectrum of PMPC₁₂ after post-polymerisation functionalisation with 1-dodecanethiol. **155**
- Figure 3.33.** ^1H NMR spectrum in CDCl₃ of PMPC₁₂ after functionalisation with benzyl mercaptan (top) and ^1H NMR spectrum of PMPC₇₂ after functionalisation with 1-thioglycerol (bottom) in *d*-DMSO (400 MHz, 298 K; * = residual CDCl₃ / *d*-DMSO, ** = H₂O). **157**
- Figure 3.34.** GPC traces of BnO-PMPC₇₂-OH before ($M_n = 9\,350\text{ g mol}^{-1}$, PDI = 1.11) and after post-polymerisation functionalisation with benzyl mercaptan ($M_n = 14\,020\text{ g mol}^{-1}$, PDI = 1.21) and before ($M_n = 15\,700\text{ g mol}^{-1}$, PDI = 1.13) and after functionalisation with mercaptoethanol ($M_n = 24\,830\text{ g mol}^{-1}$, PDI = 1.16). **157**

- Figure 3.35.** MALDI-TOF MS analysis of PMPC₁₂ after functionalisation with benzyl mercaptan. A main distribution of fully functionalised polymer (●) is observed as well as a distribution of cross-linked, benzyl functionalised PMPC₁₂ (●). 159
- Figure 4.1.** Organic catalysts used in the ring-opening polymerisation of MAC and MPC. 168
- Figure 4.2.** ¹H NMR in CDCl₃ of P(MAC-*co*-MPC) initiated from benzyl alcohol using 5 mol % **1** and 1 mol % **2** (400 MHz, 298 K; * = residual CDCl₃, ** = H₂O). The expansion shows the slight difference in chemical shift of the methyl protons between a MAC (δ1.27 ppm) and MPC (δ1.29) repeat unit making it possible to monitor the conversions of both monomers. 169
- Figure 4.3.** Graph showing MAC (●) and MPC (●) conversion against time in a copolymerisation with a feed ratio of 50:50 (A). The expansion (B) shows the first 300 minutes of the polymerisation (B). 170
- Figure 4.4.** Plots of copolymer composition *F* versus monomer feed ratio *f* for MAC (left) and MPC (right) for experimental data (●) and best fitted curve (line). 172
- Figure 4.5.** Expansion of the ¹³C NMR spectra in CDCl₃ of poly(carbonates) initiated from benzyl alcohol using 10 mol % **1** and 5 mol % **2** (126 MHz, 298 K). The spectra show the carbonate carbonyl shifts between 156 and 153 ppm of (from top to bottom) PMAC (A), PMPC (B), P(MAC₁₁-*co*-MPC₁₂) (C) and P(MAC₁₅-*co*-MPC₅) (D). The homopolymers show the chemical shift corresponding to AA dyads in PMAC (154.52 ppm) or the BB dyads in PMPC (154.42 ppm) only, while both copolymer spectra show peaks at 154.52, 154.47 and 154.43 ppm for AA, AB, BA and BB dyads. The inset displays the different possible carbonyl environments. 175
- Figure 4.6.** MALDI-ToF MS of P(MAC₁₁-*co*-MPC₁₃) obtained from the ROP of MAC and MPC, initiated from benzyl alcohol using 5 mol % **1** and 1 mol % **3**. 176
- Figure 4.7.** Comparison of the peaks with degree of polymerisation DP = 10 of P(MPC) (top), P(MAC-*co*-MPC) (centre) and P(MAC) (bottom). The peak of the copolymer corresponds to a range of DP 10 polymer chains with different ratios of each monomer resulting in a distribution with peaks between *m/z* = 2113 and *m/z* = 2133. 178
- Figure 4.8.** Calculated isotope patterns for DP10 polymer chains of (from top to bottom) PMPC, PMAC, PMPC with deuterated acetylenic

- protons and a simplified MAC-MPC copolymer with P(MAC₃-*co*-MPC₇), P(MAC₄-*co*-MPC₆), P(MAC₅-*co*-MPC₅), P(MAC₆-*co*-MPC₄) and P(MAC₇-*co*-MPC₃) chains in a 1:1:1:1:1 ratio. 179
- Figure 4.9.** ¹H NMR in CDCl₃ of P(MAC-*co*-MPC)₂₄ after post-polymerisation functionalisation with 1-azidooctane (400 MHz, 298 K; * = residual CDCl₃, ** = H₂O). 180
- Figure 4.10.** MALDI ToF MS spectrum of BnO-P(MAC-*co*-MPC)-OH after functionalisation of the pendant propargyl groups with 1-azidooctane. Distributions in different colours represent polymer chains in which the number of functionalised repeat units is kept constant, whilst the number of repeat units with an allyl functionality is varied (●) = 3 *f* MPC units, (●) = 4 *f* MPC units, (●) = 5 *f* MPC units, (●) = 6 *f* MPC units, (●) = 7 *f* MPC units, (●) = 8 *f* MPC units, (●) = 9 *f* MPC units, (●) = 10 *f* MPC units, (●) = 11 *f* MPC units, (●) = 12 *f* MPC units and (●) = 13 *f* MPC units). 182
- Figure 4.11.** Distribution in the MALDI-ToF MS spectrum of BnO-P(MAC-*co*-*f*MPC)-OH consisting of polymer chains with 8 × 1-azidooctane functionalised propargyl repeat units and 0-13 × unfunctionalised MAC units. 183
- Figure 4.12.** Schematic representation of the MALDI ToF MS spectrum of BnO-P(MAC-*co*-MPC)-OH after functionalisation of the pendant propargyl groups with 1-azidooctane. 185
- Figure 4.13.** Contour plot of P(MAC-*co*-MPC) after functionalisation of the propargyl groups with 1-azidooctane displaying the chemical composition and intensity of the polymer chains as observed by MALDI-ToF MS analysis. 186
- Figure 4.14.** ¹H NMR in CDCl₃ of P(MAC-*co*-MPC)₂₄ after orthogonal functionalisation of the allyl and propargyl groups mercaptoethanol and 1-azidooctane, respectively (400 MHz, 298 K; * = residual CDCl₃, ** = mercaptoethanol, *** = H₂O). 187
- Figure 4.15.** GPC traces of BnO-P(MAC-MPC)-OH before functionalisation, after functionalisation of the propargyl groups with 1-azidooctane and after subsequent functionalisation of the allyl groups with mercaptoethanol. 188
- Figure 4.16.** The unassigned MALDI-ToF MS spectrum of BnO-P(MAC-*co*-MPC)-OH after orthogonal functionalisation with 1-azidooctane and mercaptoethanol shows a significant low molecular weight shoulder. 188

- Figure 4.17.** Distribution in the MALDI-ToF MS spectrum of BnO-P(MAC-*co*-MPC)-OH consisting of polymer chains with 8 1-azidooctane functionalised propargyl repeat units and 0-11 functionalised MAC units. 190
- Figure 4.18.** Schematic representation of the MALDI ToF MS spectrum of BnO-P(MAC-*co*-MPC)-OH after functionalisation of the pendant allyl- and propargyl groups with mercaptoethanol and 1-azidooctane respectively. 192
- Figure 4.19.** Contour plot of P(MAC-*co*-MPC) after functionalisation of the propargyl groups with 1-azidooctane displaying the chemical composition and intensity of the polymer chains as observed by MALDI-ToF MS analysis. 193
- Figure 5.1.** Monomers used in the preparation of poly(ester)s and functional poly(ester-carbonate)s. 200
- Figure 5.2.** Organic catalysts used in the ring-opening polymerisation of MPC. 202
- Figure 5.3.** Graph showing LLA (●) and MAC (●) conversion against time. The organocatalytic ring-opening polymerisation of *L*-lactide with MAC in CDCl₃ at RT was monitored for copolymerisations catalysed by 1+3 with *f*MAC = 0.25 (A) and for copolymerisations catalysed by 2+3 with *f*MAC = 0.25 (B) and 0.4 (C). 203
- Figure 5.4.** ¹H NMR in CDCl₃ of P(DLA-*co*-MAC) initiated from benzyl alcohol using 1 mol% 1 and 0.2 mol% 2 (400 MHz, 298 K; * = residual CDCl₃, ** = H₂O). 206
- Figure 5.5.** GPC traces of (A) P(LLA-*co*-MAC) and (B) P(LLA-*co*-MPC) initiated from benzyl alcohol using 1 mol% 1 and 0.2 mol% 3. 207
- Figure 5.6.** ¹H NMR in CDCl₃ of P(LLA-*co*-MPC) initiated from benzyl alcohol using 1 mol% 1 and 0.2 mol% 3 (400 MHz, 298 K; * = residual CDCl₃, ** = H₂O). 208
- Figure 5.7.** ¹H NMR in CDCl₃ of P(LLA-*co*-MAC) after post-polymerisation radical functionalisation with 1-dodecanethiol (400 MHz, 298 K; * = residual CDCl₃). 210
- Figure 5.8.** GPC traces of (A) P(LLA-*co*-MAC) before (●) and after (●) post-polymerisation functionalisation with 1-dodecanethiol and (B) P(LLA-*co*-MPC) before (●) and after (●) postpolymerisation with 1-azidooctane. 210

- Figure 5.9.** ^1H NMR in CDCl_3 of P(LLA-*co*-MPC) after post-polymerisation functionalisation with 1-azidooctane *via* Huisgen 1,3-dipolar cycloaddition (400 MHz, 298 K; * = residual CDCl_3 ; ** = DMF). 212
- Figure 5.10.** Plot of $1/T_g$ (K^{-1}) versus weight percentage of MAC in LA/MAC copolymers. Experimentally obtained values (\blacklozenge) and calculated values (\square) are displayed. 215
- Figure 5.11.** DSC thermogram of P(LLA-*co*-MAC_{5.4%}) after functionalisation with 1-dodecanethiol (**18**) obtained by melt crystallisation showing a clear glass transition (A), crystallisation (B) and melting peak (C). 217
- Figure 5.12.** DSC thermogram of an equimolar blend of PLLA and PDLA obtained from the melt. The thermogram displays a glass transition (A), crystallisation peak for PDLA and PLLA stereocomplexation (B) and the melting point of the resulting SC-[PLLA/PDLA] (C). 219
- Figure 5.13.** DSC thermograms of blends of PDLA with **17** (top; 1) and **18** (bottom, 2) from melt crystallised samples. The DSC thermograms display peaks corresponding to the glass transition of the blend (A(1); A(2)) and crystallisation (B(1); B(2)) and melting peak (C(1); C(2)) of SC-[PDLA/**17**] and SC-[PDLA/**18**]. 221
- Figure 5.14.** DSC thermograms of **18** (blue), PDLA (red) and a blend of PDLA with **18** (black) of samples obtained from solution casting. The thermograms displays peak corresponding to the melting of **18** (A), PDLA (B) and SC-[**18**/PDLA] (SC-[AB]). 223
- Figure 5.15.** DSC thermograms of blends of PDLA with **15b** with ratios of 5:95, 25:75, 50:50, 75:25 and 95:5 (from top to bottom) from samples obtained by solution casting. The DSC thermograms display melting peaks for PDLA (\bullet), **15b** (\bullet) and SC-[PDLA/**15b**] (\bullet). 224
- Figure 5.16.** DSC thermograms of blends of PDLA with **15b** with ratios of 5:95, 25:75, 50:50, 75:25 and 95:5 (from top to bottom) from melt crystallised samples. The DSC thermograms display peaks corresponding to crystallisation (A) and melting (B) of SC-[PDLA/**15b**]. 225
- Figure 5.17.** DSC thermogram of blends of **16** with **15c** from melt crystallised samples. The DSC thermograms display peaks corresponding to glass transition (A), crystallisation (B) and melting peak (C) of SC-[**16**/**15c**]. 226

List of Schemes

- Scheme 1.1.** The synthesis of functional six-membered cyclic carbonates from 1,3-diols using phosgene derivatives, 1,1'-carbonyldiimidazole (CDI) or bis(pentafluorophenyl)carbonate (PFC) with an alcohol or amine (RXH). 5
- Scheme 1.2.** Synthesis of functional cyclic carbonates derived from *bis*-MPA. 6
- Scheme 1.3.** Synthesis of functional cyclic carbonates derived from pentaerythriol (top), glycerol and trimethylolalkanes (bottom). 8
- Scheme 1.4.** Preparation of amino-acid derived cyclic carbonate monomers. 11
- Scheme 1.5.** Synthesis of cyclic carbonates from *D*-glucose (A) and *D*-xylose (B). 11
- Scheme 1.6.** Synthesis of functional six-membered cyclic carbonates derived from oxetanes, malonic acid diethyl ester and dihydroxy acetone. 13
- Scheme 1.7.** Deprotection of furan-protected maleimide functional monomer **M33** *via retro*- Diels Alder reaction to yield the maleimide functional cyclic carbonate **M34**. 27
- Scheme 1.8.** Schematic representation of deprotection of benzyl-functional poly(carbonate)s to carboxylic acid- (A) and hydroxyl- (B) functional poly(carbonate)s. 44
- Scheme 1.9.** Schematic representation of post-polymerisation modifications of alkene-functional poly(carbonate)s: cross-linking (A), addition of a thiol (B) and epoxidation (C). 49
- Scheme 1.10.** Schematic representation of post-polymerisation modifications of alkyne-, azide- and bromide functional poly(carbonate)s through alkyne/azide cycloadditions. 53
- Scheme 1.11.** Schematic representation of the quaternisation of halide-functional poly(carbonate)s. 55
- Scheme 1.12.** Conversion of poly(**M3**) to hydroxyacetone functional poly(carbonate). 57
- Scheme 2.1.** Synthesis and ring-opening polymerisation of 5-methyl-5-allyloxycarbonyl-1,3-dioxan-2-one, MAC. Conditions: (i) allyl bromide, KOH, DMF, 100 °C (1h), then 45 °C (16h); (ii) ethyl chloroformate, NEt₃, THF, 0 °C; (iii) ROH, catalyst, CDCl₃, RT. 81

-
- Scheme 2.2.** Possible reaction pathways for initiation of cyclic carbonates in the presence of DBU: DBU could act as an alcohol activating species (A) or as an initiator (B). In addition, DBU could promote transesterification of the resulting poly(carbonate)s. 85
- Scheme 2.3.** Initiation of cyclic carbonates from ROH catalysed by the bifunctional catalyst system of sparteine and thiourea **3**. As a result of the low basicity of (-)-sparteine and a preference for **3** to coordinate cyclic monomers, no transesterification occurs. 86
- Scheme 2.4.** Possible routes for the formation of the secondary species observed in the MALDI-ToF spectra of 1,3-propanediol and 2-hydroxyethyl disulphide. 92
- Scheme 2.5.** Radical Addition of a Thiol (RSH) to the PMAC. 97
- Scheme 2.6.** The radical addition of thiophenol to allyl acetate with AIBN as radical initiator, was used as a model reaction for the optimisation of conditions for PMAC functionalisation. 98
- Scheme 3.1.** Synthesis and ring-opening polymerisation of 5-methyl-5-propargyloxycarbonyl-1,3-dioxan-2-one, MPC. Conditions: (i) allyl bromide, KOH, acetone, reflux (16h); (ii) ethyl chloroformate, NEt₃, THF, 0 °C; (iii) ROH, catalyst, CDCl₃, RT. 116
- Scheme 3.2.** Huisgen cycloaddition of an azide (N₃R) to PMPC polymers. 135
- Scheme 3.3.** The copper mediated cycloaddition of 1-azidooctane to propargyl acetate was used as a model reaction for the optimisation of conditions for PMPC functionalisation. 136
- Scheme 3.4.** Radical addition of thiols (RSH) to PMPC polymers. 153
- Scheme 4.1.** Ring-opening polymerisation of 5-methyl-5-allyloxycarbonyl-1,3-dioxan-2-one, MAC, and 5-methyl-5-propargyloxycarbonyl-1,3-dioxan-2-one, MPC. Reactions were performed in CDCl₃ at RT using catalyst system **1/2** or **1/3**. 167
- Scheme 5.1.** Ring-opening polymerisation of 5-methyl-5-allyloxycarbonyl-1,3-dioxan-2-one (MAC) and *L*-lactide (LLA). Conditions: ROH, catalyst system **1/2** or **1/3**, CDCl₃, RT. 201
- Scheme 5.2.** Post-polymerisation functionalisation of allyl-functional poly(ester-carbonate)s with 1-dodecanethiol. 209
- Scheme 5.3.** Post-polymerisation functionalisation of propargyl-functional poly(ester-carbonate)s with 1-azidooctane. 211

List of Tables

Table 2.1. Catalyst screening for the ring-opening polymerisation of MAC.	84
Table 2.2. Theoretical and observed m/z values of PMAC ₁₁ (Figure 2.6).	90
Table 2.3. Theoretical and observed m/z values of the indicated peaks (●/●) in Figure 2.8.	93
Table 2.4. Telechelics and block copolymers of MAC.	96
Table 2.5. Optimisation of the reaction conditions for the radical addition of thiophenol to allyl acetate.	99
Table 2.6. Theoretical and observed m/z values of the indicated peaks in Figure 2.14.	102
Table 2.7. Post-polymerisation radical thiol-ene functionalisation of poly(carbonates).	105
Table 2.8. Theoretical and observed m/z values of the indicated peaks in Figure 2.14.	106
Table 2.9. Thermal analysis of functionalised poly(carbonates).	108
Table 3.1. Theoretical and observed m/z values of PMPC ₁₀ (Figure 3.6).	122
Table 3.2. Estimated and observed m/z values of HO-PMPC-O(CH ₂) ₂ S-S(CH ₂) ₂ O-PMPC-OH (Figure 3.16).	131
Table 3.3. Telechelics and block copolymers of MPC.	132
Table 3.4. Optimisation of reaction conditions for the copper mediated cycloaddition of propargyl acetate and octyl azide model reaction.	137
Table 3.5. Theoretical and observed m/z values of the indicated peaks (●/●) in Figure 3.18.	138
Table 3.6. Theoretical and observed m/z values of the indicated peaks (●/●) in Figure 3.19.	142
Table 3.7. Theoretical and observed m/z values of PMPC ₁₀ after functionalisation with benzyl azide (Figure 3.25).	146
Table 3.8. Theoretical and observed m/z values of the indicated peaks (●/●) in Figure 3.26.	148
Table 3.9. Post-polymerisation functionalisation of poly(carbonates) <i>via</i> copper assisted alkyne-azide cycloaddition.	151
Table 3.10. Theoretical and observed m/z values of PMPC ₁₀ after functionalisation with 1-dodecanethiol (Figure 3.32).	155
Table 3.11. Theoretical and observed m/z values of PMPC ₁₀ after functionalisation with benzyl mercaptan (Figure 3.35).	159

Table 3.12. Post-polymerisation radical ‘thiol-yne’ functionalisation of poly(carbonates).	160
Table 4.1. Average values for molar fraction of monomer in the feed and experimental copolymer composition in the organocatalytic ROP of MAC and MPC in CDCl ₃ .	171
Table 4.2. Reactivity ratios and rate values for the organocatalytic ROP of MAC and MPC catalysed by 2+3 in CDCl ₃ .	173
Table 4.3. Theoretical and observed <i>m/z</i> values of P(MAC ₁₁ - <i>co</i> -MPC ₁₃) (Figure 4.6).	176
Table 4.4. Theoretical and observed <i>m/z</i> values of the distribution within P(MAC ₁₁ - <i>co</i> -MPC ₁₃) after functionalisation with 1-azidooctane displayed in Figure 4.11.	183
Table 4.5. Theoretical and observed <i>m/z</i> values of the distribution with 8 <i>f</i> MPC repeat units within P(MAC ₁₁ - <i>co</i> -MPC ₁₃) after functionalisation with 1-azidooctane and mercaptoethanol displayed in Figure 4.17.	190
Table 5.1. Results from lactide polymerisations and copolymerisation of lactide with MAC.	205
Table 5.2. Thermal analysis of poly(ester-carbonate)s.	213
Table 5.3. Thermal analysis of poly(ester-carbonate)s blends with PDLA.	220
Table 5.4. Thermal analysis of poly(ester-carbonate)s blends with P(DLA- <i>co</i> -MAC _{15.6%}) (7).	227

Abbreviations

δ	Chemical shift
AIBN	2,2-Azobisisobutyronitrile
BEMP	2-tert-Butylimino-2-diethylamino-1,3-dimethylperhydro-1,3,2-diazaphosphorine
<i>bis</i> -MPA	2,2-Bishydroxy(methyl)propionic acid
BL	β -Butyrolactone
Boc	<i>tert</i> -Butoxycarbonyl
CDI	1,1'-Carbonyldiimidazole
CMC	Critical micelle concentration
COSY	Correlation spectroscopy
DBU	1,8-Diazabicyclo[5.4.0]undec-7-ene
DCC	<i>N,N'</i> -Dicyclohexylcarbodiimide
DCTB	trans-2-[3-(4- <i>tert</i> -Butylphenyl)-2-methyl-2-propylidene]malonitrile
DIC	<i>N,N'</i> -Diisopropylcarbodiimide
DIPEA	Diisopropylethylamine
DLA	<i>D</i> -Lactic acid (also used for <i>D</i> -lactide)
DMF	Dimethyl formamide
DMO	<i>L</i> -3- <i>D,L</i> -Dimethyl-2,5-morpholinedione
DMSO	Dimethyl sulfoxide
DP	Degree of polymerisation
DRI	Differential refractive index
DSC	Differential scanning calorimetry
DTC	Dimethyl trimethylene carbonate
<i>E</i>	Molar mass of the end group
EDC	1-Ethyl-3-(3-dimethylaminopropyl) carbodiimide
<i>f</i>	Molar fraction of monomer in the feed

Abbreviations

F	Molar fraction of monomer in the polymer
f_{MAC}	Functionalised 5-methyl-5-allyloxycarbonyl-1,3-dioxan-2-one repeat unit
f_{MPC}	Functionalised 5-methyl-5-propargyloxycarbonyl-1,3-dioxan-2-one repeat unit
GPC	Gel permeation chromatography
HOBt	Hydroxybenzotriazole
k	Rate constant
LA	Lactic acid (also used for lactide)
LLA	<i>L</i> -Lactic acid (also used for <i>L</i> -lactide)
LS	Light scattering
M^+	Molar mass of the cation
M_n	Number-averaged molecular weight
M_w	Weight-averaged molecular weight
MW	Molecular weight
MAC	5-Methyl-5-allyloxycarbonyl-1,3-dioxan-2-one
MALDI-ToF MS	Matrix-assisted laser desorption ionisation-time of flight mass spectrometry
MBC	5-Methyl-5-benzyloxycarbonyl-1,3-dioxan-2-one
<i>m</i> -CPBA	<i>meta</i> -chloroperoxybenzoic acid
MEC	5-Methyl-5-ethyloxycarbonyl-1,3-dioxan-2-one
MPC	5-Methyl-5-propargyloxycarbonyl-1,3-dioxan-2-one
NaAsc	Sodium ascorbate
NaTFA	Sodium trifluoroacetate
NMR	Nuclear magnetic resonance
PDI	Polydispersity index
PDLA	Poly(<i>D</i> -lactic acid) or poly(<i>D</i> -lactide)
PEO	Poly(ethylene oxide)
PFC	Bis(pentafluorophenyl)carbonate

Abbreviations

PLA	Poly(lactic acid) or poly(lactide)
PLLA	Poly(<i>L</i> -lactic acid) or poly(<i>L</i> -lactide)
PMAC	Poly(5-methyl-5-allyloxycarbonyl-1,3-dioxan-2-one)
PMPC	Poly(5-methyl-5-propargyloxycarbonyl-1,3-dioxan-2-one)
PTMC	Poly(trimethylene carbonate)
<i>r</i>	Reactivity ratio
ROP	Ring-opening polymerisation
SC	Stereocomplex
$T_{5\%}$	Temperature at 5% weight degradation
$T_{50\%}$	Temperature at 50% weight degradation
T_c	Crystallisation temperature
T_g	Glass transition temperature
T_m	Melting transition temperature
TBD	1,4,7-Triazabicyclodecene
TGA	Thermogravimetric analysis
THF	Tetrahydrofuran
TMC	Trimethylene carbonate
UV	Ultraviolet
<i>w</i>	Weight fraction of monomer in polymer

Acknowledgements

First, I would like to thank Andrew Dove for giving me the opportunity to do this research and for all his advice and encouragement over the past three years and three months. I would also like to thank the EPSRC for providing me with the funding.

I would like to thank all the past and current members of the Dove group, especially Robin, Mike and Danny who have become really great friends. Thanks for the many laughs, the jokes, the tea breaks and Robin for introducing me to the concept of the 'dutch oven'. Richard, a special thanks goes to you: You have seen all my good and bad sides whilst working next to me for two years and still want to spend more time with me!

I would also like to acknowledge Laetitia Mespouille and Prof. Philippe Dubois for their help with Chapter 2, and Danny, Vinh and Remzi for providing me with the azides for Chapter 3.

Als laatste wil ik mijn familie en vrienden in Nederland bedanken voor hun steun en begrip tijdens de afgelopen negendertig maanden. Zeker gedurende het afgelopen jaar toen ik geen tijd had om naar Nederland te komen, zelfs niet voor kerst en sinterklaas.

Declaration

Experimental work contained in this thesis is original research carried out by the author, unless otherwise stated, in the Department of Chemistry at the University of Warwick, between January 2009 and March 2012. No material contained herein has been submitted for any other degree, or at any other institution.

Results from other authors are referenced in the usual manner throughout the text.

_____ Date: _____

Sarah Tempelaar

Abstract

This work describes the controlled organocatalytic ring-opening polymerisation (ROP) of cyclic carbonates with pendant groups for the preparation of functional aliphatic poly(carbonate)s and poly(ester-carbonate)s. Their subsequent post-polymerisation functionalisations were studied yielding a range of functional aliphatic poly(carbonate)s.

Chapter 1 reviews the preparation of cyclic carbonates with pendant functionalities, their ring-opening polymerisation and the post-polymerisation modifications of the resulting poly(carbonate)s. The properties and some applications of functional poly(carbonate)s are also discussed.

Chapter 2, 3 and 4 describe the controlled ring-opening polymerisation of allyl- functional cyclic carbonate MAC (5-Methyl-5-allyloxycarbonyl-1,3-dioxan-2-one) and propargyl- functional cyclic carbonate MPC (5-Methyl-5-propargyloxycarbonyl-1,3-dioxan-2-one) using organic catalysts. Successful functionalisation of allyl-functional poly(carbonate)s was achieved *via* radical addition of thiol-containing molecules to the pendant allyl esters (Chapter 2), while functionalisation of propargyl-functional poly(carbonate)s was realised *via* the Huisgen 1,3-dipolar cycloaddition of azides to the pendant propargyl groups (Chapter 3). In addition, the copolymerisation of MAC and MPC and the subsequent orthogonal functionalisation of a copolymer was investigated (Chapter 4). Chapter 5 describes the copolymerisation of MAC (and MPC) with stereopure lactide, with resulting copolymers with opposite chiralities being successfully applied in stereocomplexation.

Chapters 6 summarises the results obtained in Chapters 2, 3, 4 and 5 whilst Chapter 7 provides the experimental methodologies.

Chapter 1

Synthesis and post-Polymerisation Modifications of Aliphatic Poly(Carbonate)s prepared by Ring- Opening Polymerisation

Owing to their low toxicity, biocompatibility and biodegradability, aliphatic poly(carbonate)s have been studied by many groups. In this chapter, the synthesis and ring-opening polymerisation of functional cyclic carbonates that have been reported in the literature in the past decade are discussed, as well as the post-polymerisation modifications methods applied to the resulting homopolymers and copolymers.

1.1. Introduction

Aliphatic poly(carbonate)s are, together with aliphatic poly(ester)s, important biodegradable materials that have received considerable attention.¹⁻³ These materials are excellent candidates for pharmaceutical applications as a consequence of their low toxicity, biocompatibility, and biodegradability. Copolymers of trimethylene carbonate (TMC) with other cyclic monomers such as lactide and glycolide have already found application as sutures and in other biomedical applications such as controlled drug delivery.^{4,5} In addition, it has been proposed that materials prepared from poly(trimethylene carbonate) (PTMC) may have an advantage over poly(ester)-based materials in many applications because they degrade *in vivo* by surface erosion, whereas poly(ester)s show bulk degradation behaviour. Furthermore, poly(ester) degradation products can lead to increased levels of acidity that may be hazardous to drugs loaded in the system.⁶⁻⁹

Poly(carbonate) synthesis is commonly achieved either by the copolymerisation of epoxides with carbon dioxide or by the ring-opening polymerisation (ROP) of cyclic carbonate monomers.^{1-3,10-13} The synthesis of poly(carbonate)s *via* CO₂/epoxide copolymerisation is a potential method of utilising CO₂; however, the formation of five-membered cyclic carbonate by-product, the presence of ether linkages, and the use of air-sensitive coordination compounds make its application synthetically challenging. Consequently, despite the requirement to synthesise the monomers, the ROP

of cyclic carbonates has received significantly more attention and consequently provides an attractive and versatile methodology for the synthesis of functionalised poly(carbonate)s that has been studied by many groups.^{1,3,14} The ring-opening polymerisation of cyclic carbonates can be realised using cationic, anionic, coordination-insertion, organocatalytic, and enzymatic methods and these methods have demonstrated high levels of control over polymer molecular weight, polydispersity and end-group fidelity.¹⁵⁻²⁴

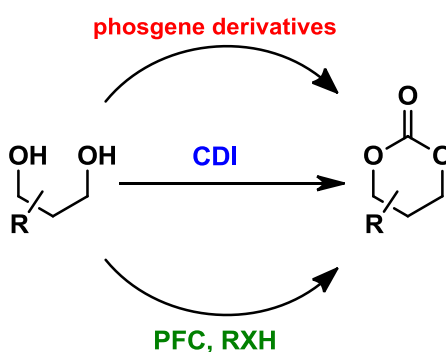
For their use in biomedical applications, such as targeted drug delivery and tissue engineering, it is advantageous to be able to tailor the poly(carbonate) structure to promote specific interactions with cells or organs. Although the properties of poly(carbonate)s derived from cyclic carbonate trimethylene carbonate (TMC) can be tuned by copolymerisation and blending with other biodegradable polymers (*i.e.* poly(lactide), poly(glycolide), poly(caprolactone)) and the introduction of functional end-groups.²⁵⁻³² Precise control over the physical properties or the addition of biologically active molecules to the poly(carbonate) structure is achieved by manipulation of pendant functionalities in the polymer backbone. Pendant functionalities may be introduced *via* the ring opening polymerisation of cyclic carbonate monomers bearing the desired functionality. However, not all functional groups are compatible with the ring-opening polymerisation process and in some cases the added functionality limits the polymerisation efficiency.³³ As a

result further modification of the polymer backbone post-polymerisation is often required. Although many further functionalisations of pendant moieties in the poly(carbonate) backbone have been reported, these modifications usually involve a number of steps and typically only partial functionalisation is achieved. In recent years, however, post-polymerisation modifications of functional poly(carbonate)s using more efficient chemistries have been reported. In addition, many copolymerisations of functional cyclic carbonates with simple cyclic esters (*i.e.* lactide, ϵ -caprolactone) have been reported due to the inherent lack of functionality in the parent poly(ester) backbone and the challenging nature of functional cyclic ester synthesis.³⁴⁻³⁶

Herein the synthesis and polymerisation of cyclic carbonates reported in the literature including post-polymerisation modifications of the resulting homo- and copolymers are discussed with a specific focus on progress made in the area in the past decade.

1.2. Synthesis Routes to Functional Cyclic Carbonates

Synthesis of cyclic carbonates can be achieved in a number of ways, although these commonly involve multistep syntheses using toxic phosgene derivatives for carbonate formation from a 1,3-diol (Scheme 1.1).^{1,3} Alternative methods that do not involve the use of phosgene include the reaction of oxetane with CO₂, a two-step procedure using a pentafluorophenyl ester intermediate and the use of 1,1'-carbonyldiimidazole (CDI).^{37,38}

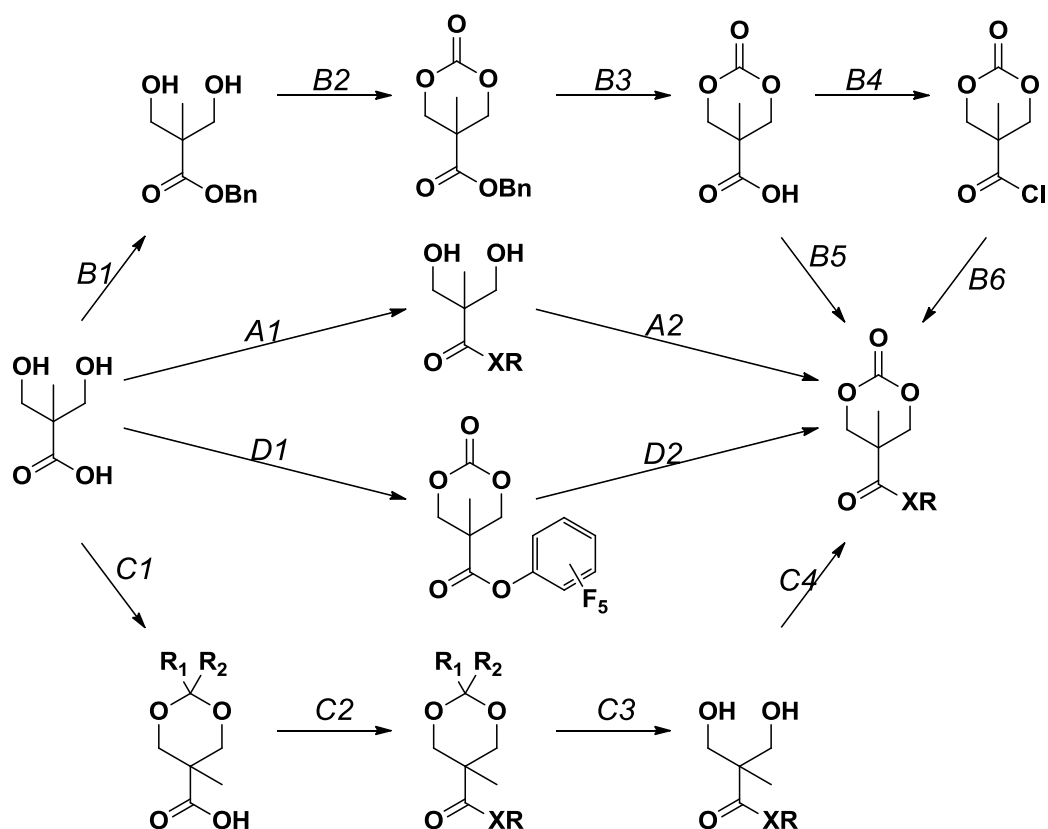


Scheme 1.1. The synthesis of functional six-membered cyclic carbonates from 1,3-diols using phosgene derivatives, 1,1'-carbonyldiimidazole (CDI) or bis(pentafluorophenyl)carbonate (PFC) with an alcohol or amine (RXH).^{1,3,37,38}

1.2.1. Functional Cyclic Carbonates derived from 2,2-bishydroxy(methyl)propionic acid (*bis*-MPA).

2,2-Bishydroxy(methyl)propionic acid (*bis*-MPA; Scheme 1.2), which has also been widely used in the preparation of biocompatible dendrimers^{39,40}, was first used for the synthesis of cyclic carbonates by Gross and co-workers in 1999.⁴¹

The reported cyclic carbonate could be prepared by direct functionalisation of the acid group in *bis*-MPA immediately using acidic or basic conditions (Scheme 1.2.; route A1), before formation of the carbonate using phosgene or a phosgene derivative such as ethyl chloroformate, di- or triphosgene (Scheme 1.2.; route A2).^{41,42} Other possible synthetic pathways from the *bis*-MPA scaffold to provide functional cyclic carbonates have since been reported. Alternative pathways B and C are more suitable for the synthesis of monomers that have more sensitive substituents. Cyclic carbonate synthesis using route B involves protection of the acid functionality by conversion to a

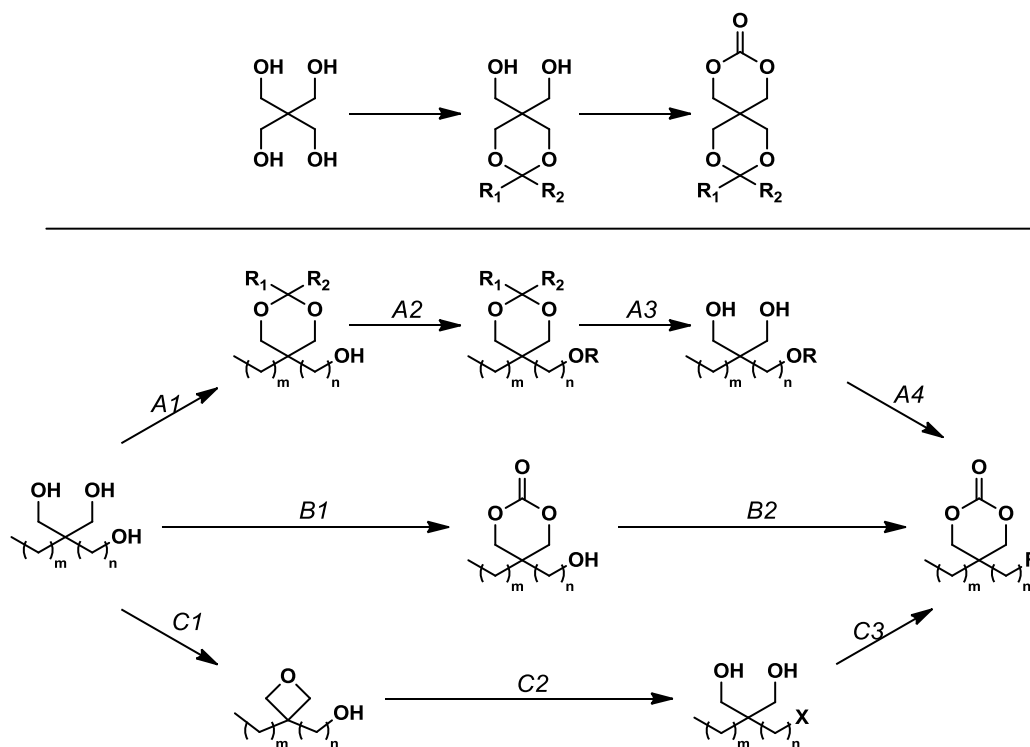


Scheme 1.2. Synthesis of functional cyclic carbonates derived from *bis*-MPA.

benzyl ester (Scheme 1.2; route B1) followed by the synthesis of benzyl functional cyclic carbonate, 5-methyl-5-benzyloxycarbonyl-1,3-dioxan-2-one (MBC; route B2), and subsequent deprotection of the acid functionality (route B3). The free carboxylic acid was then activated, typically by use of dicyclohexylcarbodiimide (DCC) (route B5) or by conversion to the acyl chloride (route B4),⁴³ before reaction with an alcohol or amine. In path C, the alcohol functionalities are acetonide protected (route C1) before functionalisation of the carboxylic acid is carried out (route C2), followed by deprotection (C3) and formation of the functional cyclic carbonate (C4). Path D, proposed in a recent publication by Hedrick and co-workers, provides an excellent alternative to the use of phosgene derivatives and multi-step procedures by the synthesis of the pentafluorophenyl functionalised carbonate, 5-methyl-5-pentafluorophenyloxycarbonyl-1,3-dioxan-2-one, from *bis*-MPA in one step using bis(pentafluorophenyl)carbonate in the presence of caesium fluoride (route D1). This was then followed by reaction of the pentafluorophenyl group with amines or alcohols (route D2).³⁷ In summary, 2,2-bishydroxy(methyl)propionic acid (*bis*-MPA) is an excellent choice as biocompatible and versatile scaffold for the preparation of cyclic carbonate monomers.

1.2.2. Functional cyclic carbonates derived from pentaerythriol, glycerol and trimethylolalkanes.

The preparation of functional cyclic carbonates has also been reported in many cases using 1,3-diol containing compounds that have not two but three or four hydroxyl groups in their molecular structure. Common precursors are pentaerythriol, glycerol and trimethylolalkenes which, including benzyl protection of the hydroxyl functionality (or functionalities), can be used in the synthesis of other functional cyclic carbonates (Scheme 1.3).⁴⁴⁻⁴⁹



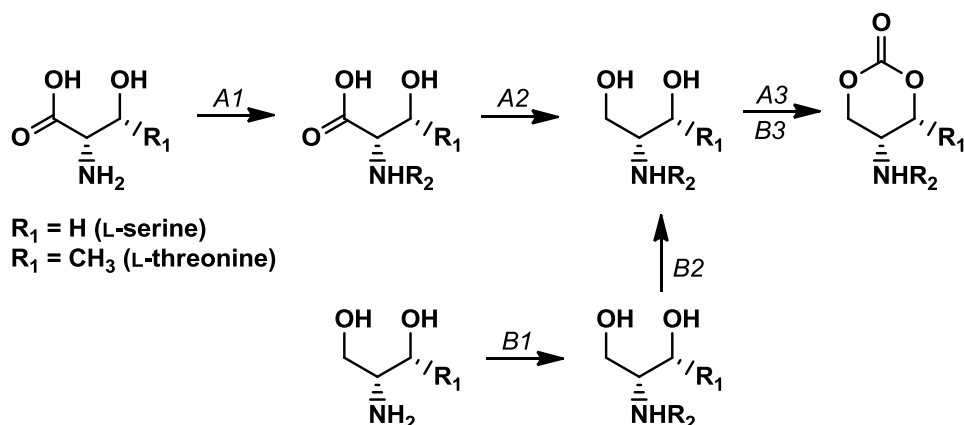
Scheme 1.3. Synthesis of functional cyclic carbonates derived from pentaerythriol (top), glycerol and trimethylolalkanes (bottom).

A number of synthetic pathways are described in the literature that use glycerol or trimethylolalkenes as a basic scaffold from which cyclic carbonates with a pendant functionality can be prepared. In Scheme 1.3, two of the available hydroxyl groups are acetonide or benzylidene protected (route A1) before further reaction of the residual alcohol with an acid chloride or *via* DCC coupling with a carboxylic acid-functional molecule (route A2). This is then followed by deprotection of the diol and conversion to the cyclic carbonate (Scheme 1.3; routes A3, A4). Alternatively, the precursor has been reacted with a dialkyl carbonate mediated by immobilised *Candida antarctica* lipase B yielding a hydroxyl functional cyclic carbonate intermediate (Scheme 1.3; route B1). The hydroxyl functionality can then be further functionalised using the abovementioned chemistries (route B2). In a report by Hatti-Kaul and co-workers the dialkyl carbonates were also used in the functionalisation of the hydroxyl group.⁵⁰ In path C, a dialkyl carbonate is used under basic conditions to form an oxetane by transesterification and subsequent decarboxylation (Scheme 1.3; routes C1, C2). The oxetane can then be ring-opened with HX to give a 1,3-diol (C3) that can be converted to the corresponding halogen-containing carbonate (C4). Synthesis of functional monomers derived from pentaerythritol is, in all reported cases, realised by partial functionalisation/protection of two of the hydroxyl functionalities leaving a 1,3-diol that can react with a phosgene derivative to form the cyclic carbonate (Scheme 1.3; top). In conclusion, glycerol and trimethylolalkenes

are good alternatives to *bis*-MPA in the synthesis of functional cyclic carbonates, whilst pentaerythritol provides an excellent opportunity to introduce two hydroxyl groups per monomer unit into the poly(carbonate) backbone.

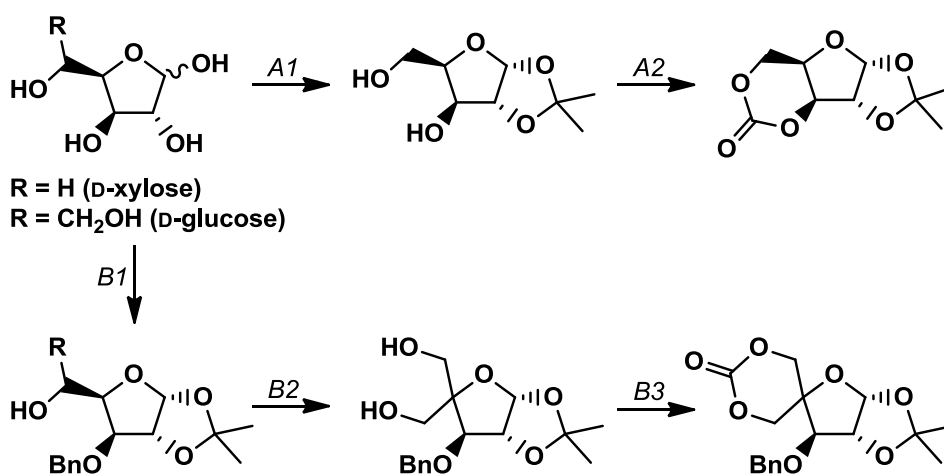
1.2.3. Functional Cyclic Carbonates derived from amino acids or sugars.

Amino acids and sugars are natural products that are indispensable for life processes, thus poly(amino acid)s and poly(saccharide)s or sugar-based polymers are highly attractive biocompatible materials. In view of the biocompatibility of the resulting polymers and their degradation products cyclic carbonates derived from amino acids and sugars have been reported by Sanda *et al.* and Gross and co-workers, respectively.⁵¹⁻⁵⁴ The synthesis of cyclic carbonate monomers derived from *L*-serine and *L*-threonine was realised by protection of these amino acids *via* conversion of the amino groups to a carbamic acid benzyl esters or carbamic acid *tert*-butyl ester (Boc) followed by reduction and carbonate formation with triphosgene (Scheme 1.4; route A1-3).⁵¹ In an alternative report, the serine-derived cyclic carbonate was prepared from the alcohol analogue of serine, serinol, instead (route B1-3).⁵⁴



Scheme 1.4. Preparation of amino-acid derived cyclic carbonate monomers.

Sugar-derived cyclic carbonate monomers have also been prepared from the furanose forms of *D*-xylose and *D*-glucose.^{52,53,55} Synthesis from *D*-xylose involves the acetonide protection of two of the hydroxyl groups to form a 1,3-diol, which is commercially available (Scheme 1.5; route A1). This 1,3-diol was then converted to the cyclic carbonate using ethyl chloroformate (route



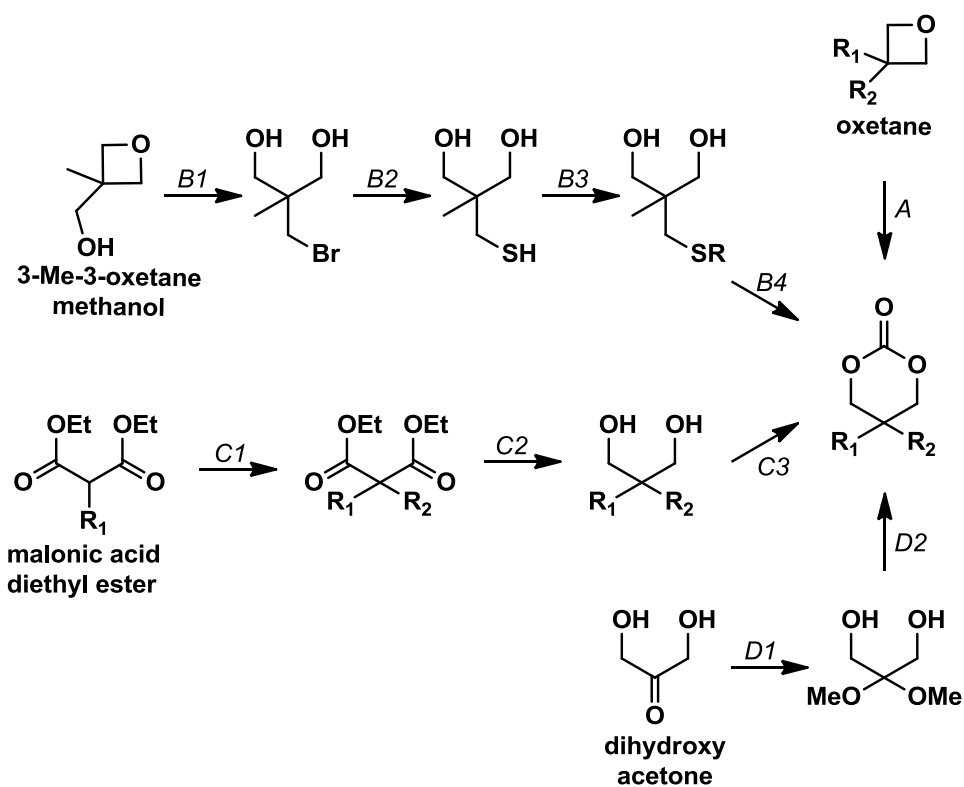
Scheme 1.5. Synthesis of cyclic carbonates from *D*-glucose (A) and *D*-xylose (B).

A2). Monomers synthesis from *D*-glucose involved protection (acetonide and benzyl ester) of three of the hydroxyl groups to give a 1,2-diol (route B1) which was converted to the 1,3-diol displayed in Scheme 1.5 (route B2) through a multi-step procedure. Carbonate formation was realised by using a phosgene-derivative to yield the *D*-glucose-based cyclic carbonate (route B3).

1.2.4. Synthesis of functional cyclic carbonates from other resources.

Examples of other reported cyclic carbonate syntheses include those derived from commercially available diols, oxetanes, a malonic acid diethyl ester derivative, dihydroxy acetone and *N*-methyl diethanolamine (Scheme 1.6).⁵⁶⁻

⁶⁴ Direct synthesis of six-membered cyclic carbonates from oxetanes using CO₂ has been reported (Scheme 1.6; route A). Alternatively the ring opening of 3-methyl-3-oxetanemethanol with HBr has also been reported resulting in a bromo-functional diol (route B1). The bromide could then be replaced with a thiol by reaction with NaSH, which was subsequently reacted with an alkene to generate the desired functional 1,3-diol (Scheme 1.6; routes B2, B3). This diol was then converted to the functional cyclic carbonate monomer using ethyl chloroformate (route B4). A monomer prepared from dihydroxy acetone, a glycolytic metabolite, has been converted to the dimethoxy acetal before ring-closure prior to reaction with ethyl chloroformate (Scheme 1.6; route C1-3). In a final example, a functional malonic acid diethyl ester was



Scheme 1.6. Synthesis of functional six-membered cyclic carbonates derived from oxetanes, malonic acid diethyl ester and dihydroxy acetone.

reacted with sodium, followed by reaction with an alkyl halide followed by reduction of the ethyl ester groups using lithium aluminium hydride before reaction of the resulting diol with a diphosgene derivative to give a functional six-membered cyclic carbonate (route D1, D2).

1.3. Ring-opening polymerisation of functional cyclic carbonates.

1.3.1. Alkyl functional monomers

The introduction of a functionality along a poly(carbonate) is desirable, but homopolymerisation of functional cyclic carbonates is not always necessary. Indeed, for some applications it is even advantageous to have a polymer backbone that contain only a percentage of monomer units with a pendant functionality.^{65,66} Furthermore, in cases in which the polymerisability of a functional monomer is not optimal, copolymerisation often provides a solution.³³ In the preparation of functional poly(carbonate)s through copolymerisation, trimethylene carbonate (TMC) is often used as co-monomer, however other simple alkyl functional monomers have also been reported.⁴³ Hedrick and co-workers have recently reported copolymerisations of functional monomers with a simple ethyl functional monomer derived from *bis*-MPA, 5-methyl-5-ethyloxycarbonyl-1,3-dioxan-2-one (MEC), while Zhuo and co-workers report the use of dimethyl trimethylene carbonate (DTC) (Figure 1.1).^{37,67-77} Only one example of MEC homopolymerisation has been reported in the literature.³⁷ The polymerisation (monomer-to-initiator ratio ($[M]/[I]$) = 108) was performed in methylene chloride at room temperature using sparteine as the catalyst in combination with a thiourea type cocatalyst. This resulted in a polymer with a molecular weight of 17 100 g mol⁻¹ and a polydispersity of 1.27. In contrast, homopolymerisation of DTC has been reported using a number of catalysts.⁷⁷⁻⁸¹ The cationic ring-opening

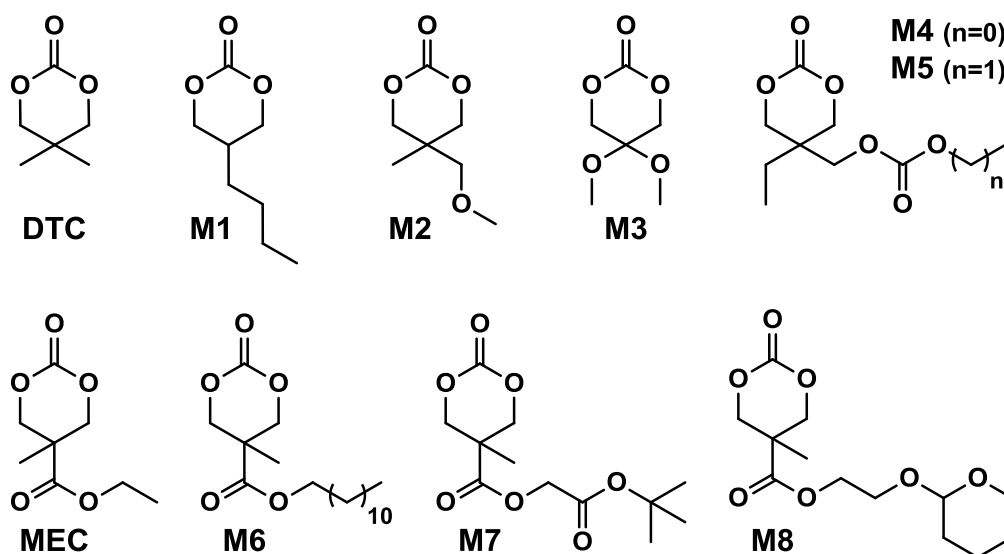


Figure 1.1. Alkyl functional cyclic carbonate monomers.

polymerisation of DTC was reported in methylene chloride at room temperature using methyl trifluoromethane sulfonate (<30% monomer conversion; $M_n = 1\ 800\text{--}2\ 100\ \text{g mol}^{-1}$; PDI = 1.30-1.38) or trifluoromethane sulfonic acid (<50% monomer conversion; $M_n = 3\ 000\text{--}3\ 500\ \text{g mol}^{-1}$; PDI = 1.10-1.11) or in nitrobenzene at 120 °C using methyl iodide (50% monomer conversion; $M_n = 1\ 100\ \text{g mol}^{-1}$; PDI = 1.52). Homopolymerisation of DTC has also been reported when catalysed by tin octanoate under bulk conditions at 120 °C and resulted in polymers with molecular weights ranging from 2 900 to 8 300 g mol^{-1} (PDI = 1.52-1.58). Other reported DTC homopolymerisations were conducted using rare earth catalysts at 0-45 °C ($M_n = 116\ 000\text{--}171\ 000\ \text{g mol}^{-1}$; PDI = 2.28-2.79). Poly(DTC) is a hydrophobic, semi-crystalline material with reported melting points of 90-93 °C and 122 °C, which results in the

slow degradation of its homopolymers and some of its reported copolymers.⁷⁷⁻

80,82

Although other alkyl functional monomers have been reported (Figure 1.1; **M1-M8**), there are few reports on the properties of their homopolymers.^{37,50,60-}

62,68,72,78,83,84 Homopolymerisation was reported for **M1** in bulk using methyl

trifluoromethanesulfonate (TfOMe) as a catalyst (60-100 °C; $M_n = 3\ 500-5\ 000$ g mol⁻¹; PDI = 1.67-2.58) or in chloro- or nitrobenzene at 120 °C initiated by

methyl iodide ($M_n = 600-800$ g mol⁻¹; PDI = 1.40-1.47),⁷⁸ whilst one example

of **M8** homopolymerisation using organic catalyst 1,8-diazabicycloundec-7-ene (DBU) in combination with a thiourea cocatalyst is reported in

dichloromethane at room temperature ($[M]/[I] = 99$; $M_n = 6\ 600$ g mol⁻¹; PDI =

1.24).³⁷ Ring opening of **M3** using a range of metal-based and organic catalysts

has recently received a lot of attention. Reported polymerisations were either

carried out in bulk at elevated temperature (130 °C), or at temperatures

between 60-110 °C in toluene.^{74,83} Ring-opening polymerisation of **M3** in bulk

resulted in a polymer with $M_n = 56\ 400$ g mol⁻¹ (PDI = 1.44), whilst good

results were obtained for both metal-based and organic catalyst 4-

dimethylaminopyridine (DMAP) in the solution polymerisation of **M3**

($[M]/[I] = 100$; $M_n = 6\ 800-17\ 000$ g mol⁻¹; PDI = 1.18-1.25) as well. Poly(**M3**)

is a rigid, brittle, amorphous material with a glass transition temperature at

39-45 °C and a slightly lower degradation temperature than PTMC.^{61,83,85,86}

Other alkyl functional monomers are 1,3-dioxaspiro[5.5]undecan-2-one,

M10⁷⁸, and α -methyl trimethylene carbonate^{48,77,82,87,88}, **M9**, which have a group at the alpha position on the carbonate ring (Figure 1.2). Endo and co-workers reported the cationic homopolymerisation of **M9** in 2001, however only very low monomer conversions were observed and the resulting polymer was not isolated.⁷⁷ Higher monomer conversions have since been reported using rare earth initiators, β -diiminate zinc complexes, aluminium triflate and organic bases.^{87,88} Good control was obtained using $\text{Al}(\text{OTf})_3$ at 110 °C and 2-tert-butylimino-2-diethylamino-1,3-dimethylperhydro-1,3,2-diazaphosphorine (BEMP) and 1,4,7-triazabicyclodecene (TBD) resulting in poly(carbonate)s with molecular weights of 10 000-5 700 g mol⁻¹ and low polydispersities. As the carbonate ring can open in two different ways, different microstructures can be expected depending on the regioselectivity of the catalysts (Figure 1.2). Guillaume and co-workers investigated the regioselectivity of the resulting polymers using a range of catalyst systems.⁸⁷

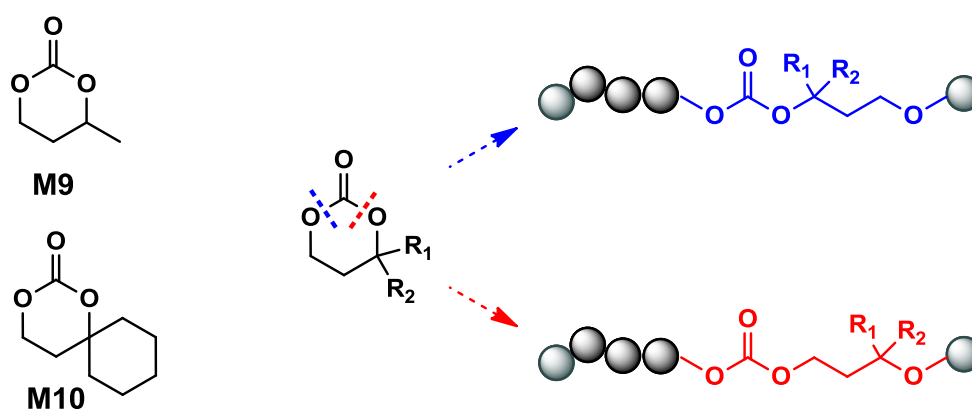


Figure 1.2. Ring opening of alkyl functional monomers with a substituent at the α -position.

Polymers with a high degree of regioregularity were obtained using β -diiminate zinc complexes, whereas organocatalysts showed poor regioselectivity. It was rationalised that this difference in regioselectivity was caused by the bulky nature of the β -diiminate surrounding ligand compared to that in the case of the aluminium triflate or organic base systems. The thermal properties of the poly(**M9**) homopolymers reveal amorphous polymers with a glass transition temperature (T_g) between -10 and -18 °C, which is very similar to that of PTMC (-15 °C).⁶⁹ In addition, **M9** was copolymerised with ϵ -caprolactone and lactide to form highly hydrophobic copolymers and was used in the synthesis of poly(butylene succinate-*co*-**M9**) by a combination of ROP and condensation polymerisation.^{48,88}

1.3.2. Aryl functional monomers

The ring-opening polymerisation of benzyl functional cyclic monomers results in polymers that are particularly hydrophobic, and many benzyl-functional monomers and poly(carbonate)s have been reported. Monomers are readily polymerised and, furthermore, the benzyl functionality can often be easily removed revealing an alcohol or carboxylic acid group. This has led to the use of benzyl functional cyclic carbonate monomers such as 5-methyl-5-benzoyloxycarbonyl-1,3-dioxan-2-one, MBC (Figure 1.3), in the preparation of hydrophilic biodegradable polymers or as intermediate in the synthesis of

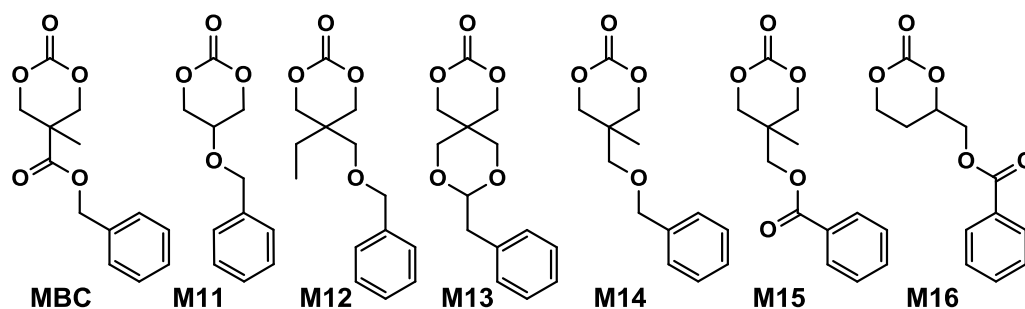


Figure 1.3. Aryl functional cyclic carbonate monomers.

carbonate monomers with more sensitive functionalities. For these reasons, benzyl functional monomers have been used extensively in the preparation of functional aliphatic poly(carbonates) and poly(ester carbonate)s in recent years. MBC and **M11**, in particular have received much attention.^{41,69,73,76,83,88-99} Homopolymerisation of MBC was first reported by Bisht and co-workers in 1999 using enzymatic methods.⁴¹ Polymerisation was studied using seven different commercially available lipases at 80 °C in bulk. Of these studied, lipase AK (from *Pseudomonas fluorescens*) gave the highest monomer conversion (97%) and molecular weight (M_n) 6 100 g mol⁻¹ with no decarboxylation was observed. Molecular weights remained low due to the initiation from water and higher molecular weights could be obtained when the lipase was dried extensively. However as the molecular weight increased, the polydispersities obtained broadened significantly ($PDI \leq 7.5$). In order to control the amount of benzyl groups in the poly(carbonate)s structure copolymerisation with TMC was conducted under the same conditions

leading to statistical copolymers.⁸⁹ Organocatalytic ring opening of MBC performed at room temperature with DBU has resulted in well-defined homopolymers with good control over molecular weights ($M_n = 4\ 500\text{-}11\ 400\ \text{g mol}^{-1}$) and with narrow molecular distributions (PDI=1.18-1.19).⁹⁶ The resulting poly(MBC) homopolymers are amorphous sticky polymers with a glass transition temperature (T_g) between 3 and 8 °C.^{89,96} Furthermore, the use of MBC in copolymerisations with lactide using tin and zinc based catalysts mostly at elevated temperatures has been reported.⁹¹⁻⁹³ As have copolymerisations with MEC or lactide (LA) using organic catalysts (DBU or thiourea-amine) at room temperature.^{69,95} In the latter case, reactivity ratios in the copolymerisation of lactide and MBC were found to be 1.1 for lactide and 0.072 for MBC. Micelles obtained from block copolymers prepared by the random copolymerisation of MBC with lactide and initiation from a PEO macroinitiator demonstrated that the introduction of carbonate moieties did not only enhance solubilisation and drug loading of the hydrophobic drug bicalutamide, but also resulted in significant reductions in the value of the critical micelle concentration (CMC) compared to micelles without MBC incorporated.

Another well reported benzyl functional monomer is 5-benzyloxy-trimethylene carbonate (**M11**). This monomer has been polymerised under bulk conditions at elevated temperatures using aluminium- and tin- based catalysts, fumaric acid, organic catalysts, porcine pancreas lipase immobilised

on silica particles or at reduced pressure without added catalyst.^{73,76,83,98,99} The poly(**M11**) homopolymers were reported to display medium to large polydispersities (PDI = 1.41-1.92) and polymer molecular weights $M_n = 8\,800$ - $22\,400\text{ g mol}^{-1}$ for polymerisations with $[M]/[I] = 1\,000$. They are rubbery materials at room temperature with a $T_g = 0$ - $6\text{ }^\circ\text{C}$ and no observed melting point.^{97,98} Reported copolymerisations include random and block copolymers with DTC, lactide and PEO.^{73,97,99} Another such example is the combined ring-opening polymerisation and polycondensation reaction of **M11** or **M12** with poly(butylene succinate) macromers.⁴⁸

Other reported aryl functional monomers, **M13-M16**, have been studied to a lesser extent.^{49,60,77,100,101} ROP of benzyl functional monomer 9-phenyl-2,4,8,10-tetraoxaspiro-[5,5]-undecan-3-one (**M13**) was investigated using diethyl zinc as initiator at $130\text{ }^\circ\text{C}$ under bulk conditions for both homopolymerisation and copolymerisations with lactide and ϵ -caprolactone.^{49,101} The resulting poly(**M13**) homopolymers displayed a $T_g = 124\text{ }^\circ\text{C}$, which is relatively high for poly(carbonate homopolymers). Cationic ROP of **M15** and **M16** to form the respective homopolymers was reported at room temperature using a range of catalysts. However, these polymerisations were heavily affected by side reaction like backbiting and decarboxylation leading to poor control and low molecular weight products.⁷⁷ Suppression of decarboxylation was achieved using MeI as initiator, but increased reaction

times and temperatures (120 °C) were needed for the polymerisation to proceed.

Apart from simple benzyl functional monomers, a number of monomers with methoxy- and nitro- substituted phenyl groups have been reported (Figure 1.4).^{77,102-104} The cationic ROP of **M17-M20** was reported by Endo and co-workers.⁷⁷ All four monomers were polymerised using methyl iodide at 120 °C yielding the respective homopolymers. The homopolymers were obtained with $M_n = 10\,000\text{ g mol}^{-1}$ (PDI = 1.22) for poly(**M17**), $M_n = 3\,400\text{ g mol}^{-1}$ (PDI = 1.88) for poly(**M18**), $M_n = 4\,400\text{ g mol}^{-1}$ (PDI = 1.58) for poly(**M19**) $M_n = 7\,100\text{ g mol}^{-1}$ (PDI = 1.39) for poly(**M20**). Polymerisation was also successfully conducted at room temperature in dichloromethane in case of **M17** and **M18** using TfOMe or TfOH as catalysts yielding polymers with $M_n = 1\,300\text{-}3\,500\text{ g mol}^{-1}$ (PDI = 1.13-1.24) and $M_n = 3\,000\text{ g mol}^{-1}$ (PDI = 1.16) respectively.

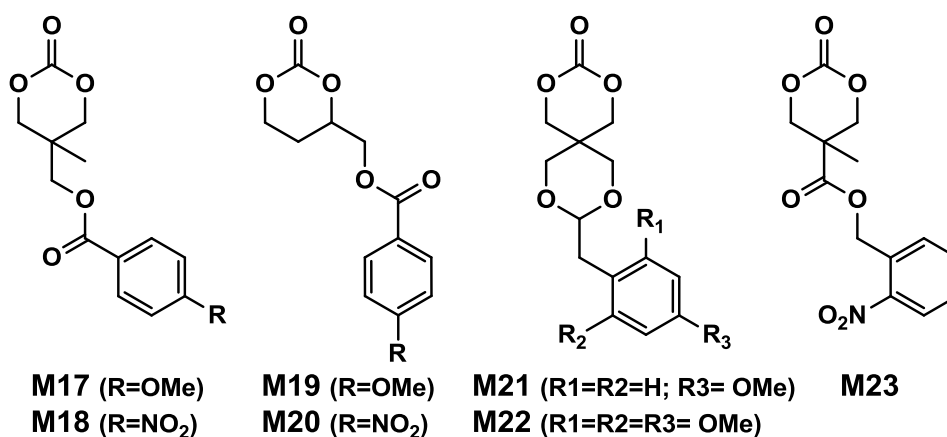


Figure 1.4. Methoxy- and nitro- substituted aryl functional cyclic carbonate monomers.

Nitrobenzyl functional monomer 5-methyl-5-(2-nitro-benzoxycarbonyl)-1,3-dioxan-2-one (**M23**) and methoxy functional monomers mono-2,4,6-trimethoxybenzylidene-pentaerythritol carbonate (**M22**) and mono-4-methoxybenzylidene-pentaerythritol carbonate (**M21**) have all been used in the synthesis of PEO block copolymers prepared by the homopolymerisation of the monomers or copolymerisation with lactide from methoxy-PEO macroinitiators.¹⁰² Polymerisations were performed using tin octanoate as catalyst under bulk conditions at 110-120 °C (**M23**) or using zinc bis[bis(trimethylsilyl)amide] in methylene chloride at 50 °C (**M21** and **M22**).¹⁰²⁻¹⁰⁴

1.3.3. Alkene and alkyne functional cyclic carbonates.

Alkene and alkyne functional groups participate in many reactions, including highly efficient and orthogonal reactions, as a consequence of their unsaturation. The introduction of such functionalities to the poly(carbonate) backbone leaves the resulting polymers open for further, efficient functionalisation.¹⁰⁵⁻¹⁰⁹ Notably, there have been several reports of the synthesis and further modification of pendant alkenes and alkyne groups in poly(ester)s.^{110,111} The introduction of pendant unsaturated groups in poly(carbonate)s prepared by the ring-opening of cyclic carbonate monomers has received increased attention in the past few years. The ring-opening

polymerisation of allyl ester functional cyclic carbonate 5-methyl-5-allyloxycarbonyl-1,3-dioxan-2-one (MAC), for example, has been described in the preparation of a range of copolymers by Mullen *et al.*, Jing and co-workers and Zhuo and co-workers (Figure 1.5).^{74,112-116} Reported homopolymerisations of MAC were either performed without added catalyst at elevated temperature (at 115 °C; $M_n = 13\,700\text{ g mol}^{-1}$; PDI = 1.8), in toluene at 95 °C using tin(II)-based poly(lactide) macroinitiator ($[M]/[I] = 40$; $M_n = 9\,200\text{ g mol}^{-1}$; PDI = 2.5), or at 110 °C catalyzed by diethyl zinc ($[M]/[I] = 200$; $M_n = 19\,000\text{ g mol}^{-1}$; PDI = 1.61)^{113,117}; however, in all cases the polymerisations showed relatively poor control and in some cases resulted in

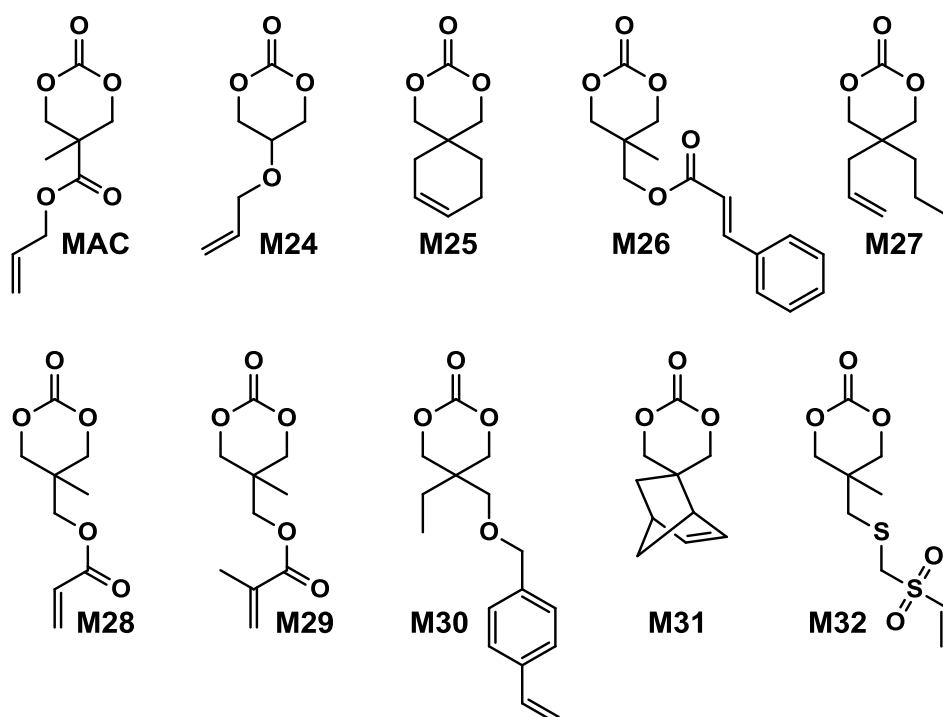


Figure 1.5. Alkene functional cyclic carbonate monomers.

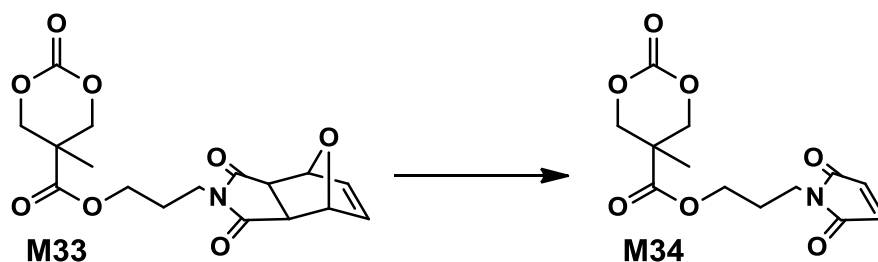
branched polymers. Studies involving MAC have mostly focused on its copolymerization with lactide and include amphiphilic block copolymers of PMAC-*co*-PLA and poly(ethylene oxide) to form micelles and polycations from poly(ethylenimine)-grafted polycarbonate.^{113,115,116} Of related allyl functional monomer 5-allyloxy-1,3-dioxan-2-one (**M24**) and 5-(2-propenyl)-5-propyl-1,3-dioxan-2-one (**M27**), polymerisation has only been reported of the former.^{44,45,64} Homopolymerisation of **M24** was reported by Parzuchowski *et al.*⁴⁴ and He *et al.*⁴⁵. Polymerisations were carried out in ethyl acetate at 65 °C using DMAP as catalyst or under bulk conditions at 120 °C using immobilised *porcine pancreas lipase* on silica or tin octanoate as catalyst. Resulting poly(**M24**) homopolymers reported showed no evidence of decarboxylation and were crystalline in nature with a melting temperature around room temperature ($T_m = 24$ °C) and a low glass transition temperature ($T_g = -40$ °C). In an effort to tune the properties of poly(carbonate)s with reactive groups, Gross and co-workers prepared the cyclohexene functional monomer 2,2-[2-pentene-1,5-diyl]-trimethylene carbonate (**M25**).^{59,118} It was hypothesised that the introduction of the cyclohexene substituent would yield poly(carbonate)s with a more rigid backbone and, as a consequence of this rigidity, a higher glass transition temperature. Indeed, polymers obtained by the metal-mediated (Al, Sn, Zn) ring-opening polymerisation of **M25** in bulk at 120 °C exhibited a T_g of 30 °C ($[M]/[I] = 200$; $M_n = 6\ 000$ -255 000 g mol⁻¹; PDI = 1.3-3.4) which is significantly higher than those reported for

allyl-functional poly(carbonate)s and TMC. In contrast, the homopolymer obtained from ROP of cinnamate functional 5-methyl-5-cinnamoyloxymethyl-1,3-dioxan-2-one (**M26**) with a molecular weight of 6 000 g mol⁻¹ (PDI = 1.87) had a T_g of 42 °C.¹¹⁹ Both its homopolymerisations and copolymerisations with *L*-lactide were performed in bulk at 120 °C using diethyl zinc as catalyst.

Acrylate functional monomer **M28** and methacrylate functional monomer **M29** were reported by Zhong and co-workers in copolymerisations with ϵ -caprolactone and lactide (incorporations <33%) and in the formation of PEO block copolymers.^{46,120,121} The monomers were polymerised in toluene using tin octanoate at 110 °C or in methylene chloride at room temperature using zinc bis[bis(trimethylsilyl)amide] as a catalyst. Styrene functional 5-ethyl-5-[(4-vinylphenyl) methoxymethyl]-1,3-dioxan-2-one (**M30**), reported by Miyagawa *et al.*, was polymerised using with polymerisations being carried out in toluene at 0 °C in the presence of potassium *tert*-butoxide (*t*-BuOK).⁴⁷ The resulting poly(**M30**) homopolymer had a $M_n = 14\ 000$ g mol⁻¹ (PDI = 1.44) and was obtained without polymerisation of the styrene moiety.

Cyclic carbonate, 5,5-(bicyclo[2.2.1]hept-2-en-5,5-ylidene)-1,3-dioxan-2-one (**M31**), with a pendant norbornene functionality was polymerised under bulk conditions with a range of amine initiators at 100-140 °C of which DBU proved to be most active.¹²² The resulting poly(**M31**)s displayed high glass transition temperatures ($T_g = 108$ °C) due to the rigidity of the norbornene

functionality. Vinyl sulfone functional carbonate **M32** was reported in the copolymerisations with TMC, caprolactone and lactide in toluene at 110 °C. The pendant vinyl sulfone remained intact during the polymerisation but copolymers obtained displayed moderate polydispersities (PDI = 1.34-1.87).⁶³ Onbulak *et al.* recently reported the synthesis and polymerisation of cyclic carbonate **M33** which has a furan protected maleimide as its pendant functionality.¹²³ The possibility to regain the maleimide functionality after polymerisation was demonstrated by the synthesis of **M34** *via* deprotection in toluene at 110 °C (Scheme 1.7). Homopolymerisation of **M33** was carried out at room temperature using DBU as catalyst and benzyl alcohol as initiator. As polymerisations became severely retarded after 60% monomer conversion, polymerisations were stopped after 50% monomer conversion to avoid transesterification resulting in poly(**M33**)s with narrow molecular weight distributions (PDI = 1.1-1.2). Copolymerisation of **M33** with lactide was carried out to overcome the poor monomer polymerisability of **M33** yielding



Scheme 1.7. Deprotection of furan-protected maleimide functional monomer **M33** *via retro-Diels Alder* reaction to yield the maleimide functional cyclic carbonate **M34**.

well defined copolymers with pendant furan-protected maleimides. Surprisingly, the only propargyl functional cyclic carbonate reported is 5-methyl-5-propargyloxycarbonyl-1,3-dioxan-2-one (MPC) and to date this monomer has only been copolymerised with lactide or trimethylene carbonate.^{43,124-128} Copolymerisations were carried out in toluene or in bulk at 100-110 °C using diethyl zinc as catalyst/initiator¹²⁴⁻¹²⁸ or in methylene chloride at room temperature using DBU and thiourea co-catalyst⁴³ and resulted in copolymers with MPC incorporations of 7-20%.

1.3.4. Halogenated and azide functional cyclic carbonates

Another large group of cyclic carbonate monomers are those with halogen containing pendant functionalities. Mindemark *et al.* recently reported the synthesis and polymerisation of another four monomers, **M35-M38** (Figure 1.6).³⁸ The resulting homopolymers of these chloro- and bromo-functional

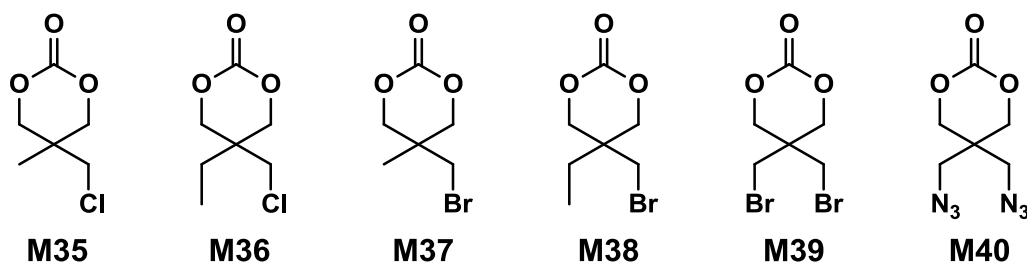


Figure 1.6. Halogenated and azide functional cyclic carbonate monomers.

monomers are all semi-crystalline in nature, with only small differences in glass transition temperature and melting temperature. However, a significant difference in solubility was observed halogenated polymers with methyl and ethyl substituents. Whilst poly(**M36**) and poly(**M38**) are insoluble in most solvents, poly(**M35**) and poly(**M37**) were found to be readily soluble in methylene chloride and tetrahydrofuran. The halogenated poly(carbonate)s were obtained by ring opening polymerisations at elevated temperature (110 °C) in bulk using stannous octanoate as a catalyst and yielded chloride-functional polymers with $M_n = 16\ 000\text{-}38\ 500\ \text{g mol}^{-1}$ and PDI = 1.46-1.81 and bromide functional polymers with $M_n = 8\ 500\text{-}31\ 900\ \text{g mol}^{-1}$ and PDI = 1.41-1.63. Glass transition temperatures and melting temperatures observed were 15 °C (T_g) and 105 °C (T_m ; $[M]/[I] = 100$) for poly(**M35**), 10-13 °C (T_g) and 131-152 °C (T_m) for poly(**M36**), 18-23 °C (T_g) and 100 °C (T_m) for poly(**M37**) and a T_g between 15-18 °C and a T_m between 121-153 °C was observed for poly(**M38**). Copolymerisation of these monomers with TMC also resulted in semicrystalline poly(carbonate)s. A similar cyclic carbonate monomer with two pendant bromide functionalities, 2,2-bis(bromomethyl)trimethylene carbonate (**M39**), has also been reported.^{56,57,129} Its homopolymerisation and its copolymerisation with ϵ -caprolactone were reported in bulk at 120 °C using tin octanoate as catalyst and resulting polymers were further modified and used for the preparation of poly(carbonate) nanoparticles. In addition, azidation of the 1,3-diol precursor to **M39**, followed by carbonate formation

using ethyl chloroformate yields diazido functional **M40**. Poly(**M40**) could be obtained at elevated temperatures under bulk conditions with tin-based catalysts ($M_n = 10\,700$ - $57\,900$ g mol⁻¹; PDI = 1.20-1.41) or using organocatalysts DBU in methylene chloride at room temperature resulting in polymers with low polydispersities (PDI <1.1). Poly(**M40**)s are also crystalline materials with a melting temperature between 50 and 100 °C and a glass transition temperature that is slightly below 0 °C.^{130,131} Furthermore, **M40** was reported in copolymerisations with DTC, lactide and in the synthesis of block copolymers, prepared by initiation from poly(ethylene oxide) macroinitiators, that were utilised for the preparation of hydrogels.^{56,57,130,131} The synthesis and polymerisation of a halogen functional cyclic carbonates derived from *bis*-MPA were reported by Hedrick and co-workers (Figure 1.7).^{37,43,67,70,132,133} This includes pentafluorophenol functional carbonate **M46** which was used as intermediate by Sanders *et al.* as outlined previously in this chapter (page 6).

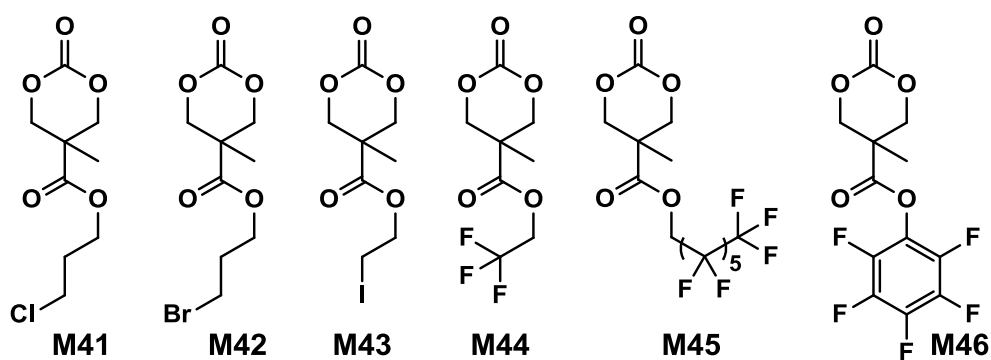


Figure 1.7. Cyclic carbonates with halogenated functional groups derived from *bis*-MPA.

The synthesis of halogen-containing poly(**M41**) ($[M]/[I] = 55$; $M_n = 12\,200$ g mol⁻¹; PDI = 1.17), poly(**M42**) ($[M]/[I] = 52$; $M_n = 11\,700$ g mol⁻¹; PDI = 1.11), poly(**M43**) ($[M]/[I] = 51$; $M_n = 10\,500$ g mol⁻¹; PDI = 1.22) and poly(**M44**) ($[M]/[I] = 54$; $M_n = 11\,500$ g mol⁻¹; PDI = 1.26) was achieved *via* organocatalytic ring-opening polymerisation at room temperature using thiourea/DBU as catalysts.^{37,70} Distribution of the pendant halogen functionalities in the poly(carbonate) backbone was achieved under these conditions in copolymerisations with MEC (**M41**, **M42**, **M43**) or TMC (**M45**) and resulted in polymers with controlled molecular weights and narrow molecular weight distributions.^{37,43,67,70,132,133}

1.3.5. Monomers with nitrogen-containing functionalities: Amino-, amido, carbamate and urea functional cyclic carbonates.

Nitrogen-containing cyclic carbonates include those with pendant amides and pendant amino, amido and urea functionalities.^{37,51,54,58,84,134,135} Cyclic carbonates with pendant amides are those with a pendant carbamic acid benzyl ester groups or a carbamic acid *tert*-butyl ester (Boc) functional groups. The Boc and benzyl ester groups are used to protect primary amines in the pendant functionality during the polymerisation. Endo and co-workers reported the anionic ring-opening polymerisation of **M48**, **M49** and **M52** (Figure 1.8) which was carried out in tetrahydrofuran at -78 to -30 °C using a

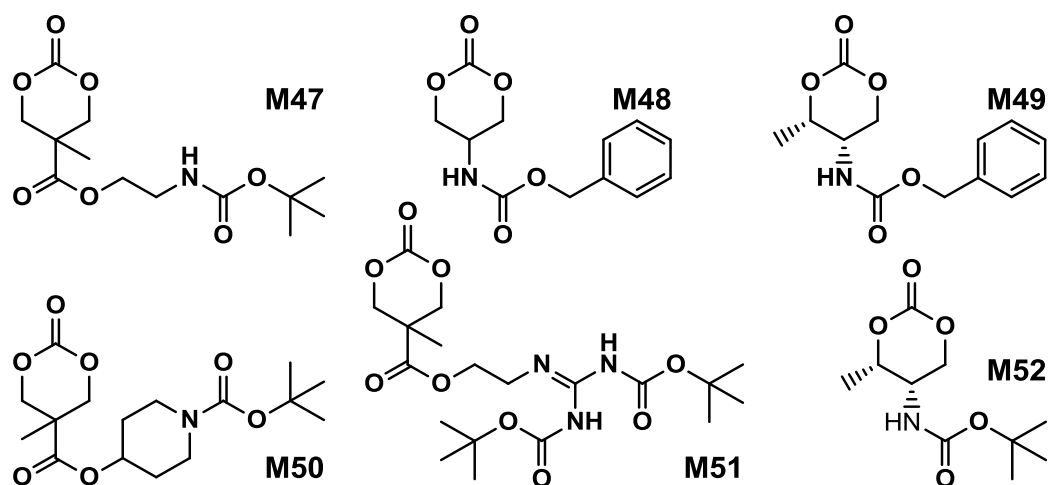


Figure 1.8. Cyclic carbonate monomers with pendant carbamate functionalities.

range of initiators.⁵¹ Molecular weights of the resulting Poly(**M48**) homopolymers ranged from 5 600 g mol⁻¹ to 20 000 g mol⁻¹ and displayed moderate polydispersities (PDI = 1.20-1.46). Interestingly, poly(**M49**) and poly(**M52**) and polymers showed inverse optical rotations compared to the respective cyclic carbonates and poly(**M49**) ($M_n = 13\ 000$ - $24\ 000$ g mol⁻¹) and poly(**M52**) homopolymers ($M_n = 5\ 700$ - $21\ 000$ g mol⁻¹) showed narrower molecular weight distributions (1.18-1.24 and 1.11-1.20, respectively) than poly(**M48**). Additionally, ring-opening of **M49** and **M52** showed a preference (9:1) for ring-opening at the non-hindered acyl bond. The bulk polymerisation of **M48** (with lactide) has also been reported at 120 °C using diethylzinc as catalyst and initiator, but did not yield poly(**M48**) with much higher molecular weight or better polydispersity ($M_n = 24\ 100$ g mol⁻¹; PDI = 1.51).⁵⁴ Although only the synthesis of Boc-protected amine **M47** has been

described, ROP of the related monomer **M50** has been reported with TMC using organic catalysts.^{37,43} The copolymerisation was performed at room temperature in methylene chloride and resulted in copolymers of **M50** and TMC with narrow molecular weight distributions (PDI = 1.07) were prepared using thiourea/DBU as catalysts at room temperature. Synthesis of poly(**M51**) homopolymers with low degrees of polymerisation (DP = 8-22) and copolymers of **M51** with other cyclic carbonate monomers was realised using thiourea/DBU in DCM at room temperature.^{84,134} Homopolymers obtained from the organocatalytic ring-opening polymerisation of **M51** exhibited low polydispersities (PDI = 1.11-1.16) and molecular weights $M_n = 3\ 800$ - $10\ 000\ \text{g mol}^{-1}$.

Although the synthesis of amido-functional cyclic carbonates **M53** and **M54** has been reported (Figure 1.9)⁴³, no report was found describing their polymerisation. No other reports of the ring-opening polymerisation of this type of amide functional cyclic carbonate monomers were found, possibly as polymerisation could be complicated by the presence of the secondary amine. In contrast, homopolymerisation of **M55**, with a tertiary amine, has been reported by Sanders *et al.* using thiourea and DBU as catalysts at room temperature reported and resulted in poly(**M55**) with $M_n = 10\ 500\ \text{g mol}^{-1}$ and PDI = 1.32 ($[M]/[I] = 63$).³⁷ The homopolymerisations of tertiary amine containing 16-membered 6,14-Dimethyl-1,3,9,11-tetraoxa-6,14-diazacyclohexadecane-2,10-dione (**M57**), which contains two carbonate groups and

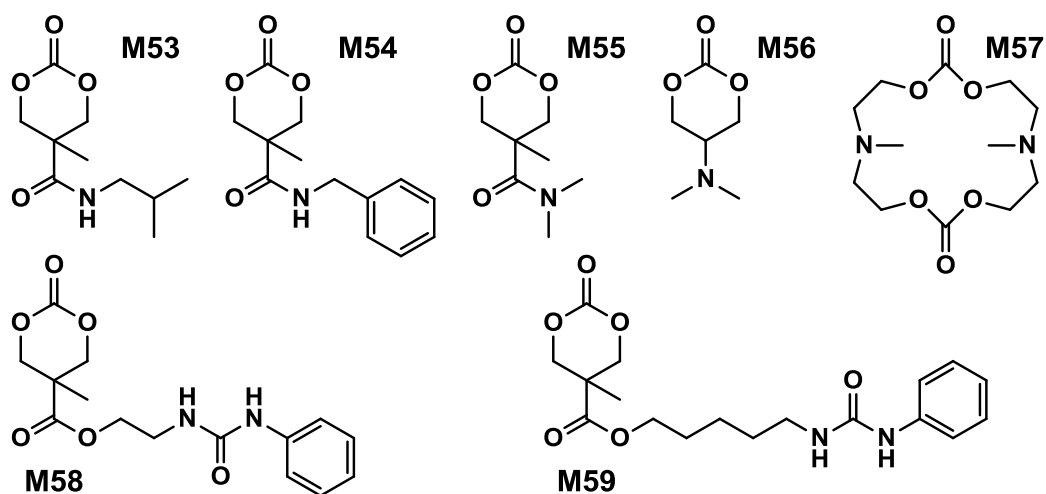


Figure 1.9. Nitrogen containing functional cyclic carbonate monomers.

two tertiary amines, was reported by Wang *et al.* in 2010.⁵⁸ Ring-opening was attempted using enzyme- and metal-based catalyst systems. Polymerisations performed in bulk at elevated temperatures (120 °C) using tin octanoate, however, resulted in decarboxylation of the monomer whilst polymerisations performed in toluene at 70-100 °C did not result in any polymerisation either. In contrast, the enzymatic ring-opening of **M57** in toluene using *Novozym-435* resulted in the formation of poly(**M57**) both at 70 °C and at room temperature and displayed living characteristics. Poly(**M57**) with a molecular weight of 8 000 g mol⁻¹ and a moderate polydispersity (PDI = 1.34) expected for enzymatic ROP was obtained. These polymers are amorphous materials that are fast-degrading and have excellent biocompatibility. Likewise, homopolymers obtained from the enzymatic ROP (60 °C; $M_n = 4900$ g mol⁻¹, PDI = 1.40) of six-membered dimethylamine-functional cyclic carbonate, 2-

dimethylaminotrimethylene carbonate (**M56**), showed low toxicity, good degradability.¹³⁵ Finally, polymerisation of urea-functional monomers **M58** and **M59** were reported using thiourea and sparteine at room temperature in DCM.¹³⁶ Poly(**M59**) was obtained with $M_n = 10\,500\text{ g mol}^{-1}$ ($[M]/[I] = 32$; PDI = 1.14) and displayed a glass transition temperatures of approximately 15 °C.¹³⁶ The synthesis of block copolymers with a poly(ethylene oxide) (PEO) block, a poly(TMC) and a poly(**M59**) or poly(**M58**) block have also been reported, as well as a block copolymer with a PEO block and a poly(MEC-*co*-**M58**) block, was reported using the same mild conditions. These block copolymers were applied in the formation of micelles that displayed low CMC's and increased stability of drug-loaded micelles due to the hydrogen-bonding interactions of the urea groups.^{69,71}

1.3.6. Protected sugar functional cyclic carbonates.

Not only are carbohydrates degradable and biocompatible, they have specific interactions with carbohydrate-binding proteins (lectins). For that reason polymers that have pendant sugar moieties can be used for targeted drug delivery.¹³⁷ Introduction of these groups on a poly(carbonate) backbone presents a non-toxic and biodegradable method to targeted drug delivery. Gross and co-workers first prepared a cyclic carbonate monomer based on the saccharide xylose, 1,2-*O*-isopropylidene-D-xylofuranose-3,5-cyclic carbonate

(**M64**, Figure 1.10).^{53,138,139} This work was extended with the synthesis and polymerisation of glucose based 1,2-*O*-isopropylidene-3-benzyloxy-pentofuranose-4,4'-cyclic carbonate (**M63**).⁵² Monomers were homopolymerised and copolymerised with *L*-lactide under bulk conditions at elevated temperatures (120-180 °C) or in dioxane (25-60 °C). Resulting poly(**M63**) and poly(**M64**) homopolymers were obtained with molecular weights of 7 900 g mol⁻¹ (PDI = 1.47; 28% yield), and 2 100-13 200 g mol⁻¹ (PDI = 1.22-92; T_g = 128 °C) respectively. As the hydroxyl groups in sugar-functional cyclic carbonates are incompatible with the ring opening process, the hydroxyl groups had to be protected before the polymerisation. Deprotection of **M64**-based polymers required the removal of the ketal group, whilst **M63**-based polymers required deprotection of the benzyl group *via* hydrogenation over palladium/carbon (90% removal) before deprotection of

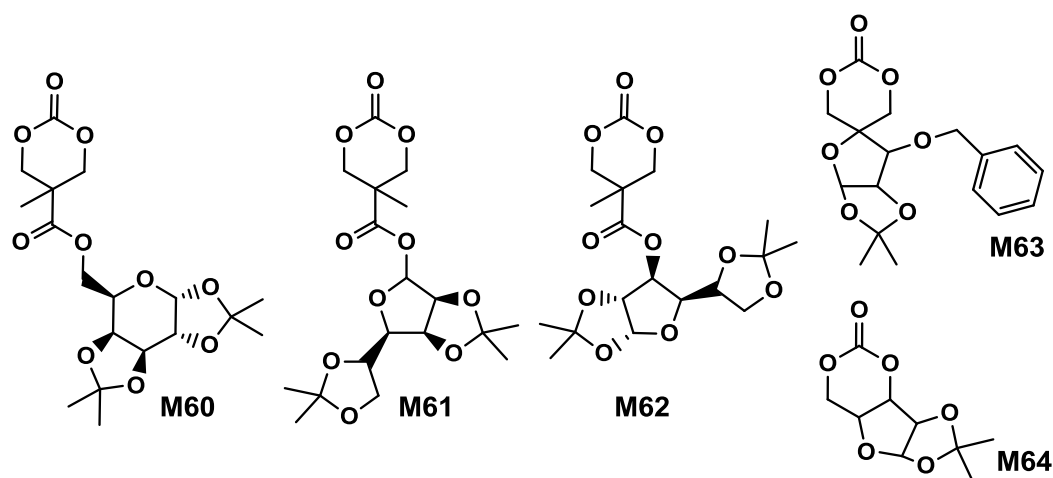


Figure 1.10. Sugar functional cyclic carbonate monomers.

the ketal groups using trifluoro acetic acid. Unfortunately deprotection results in some degradation due to the hydrolysis of the ester bonds. Thermal analysis of poly(**M63**) revealed a glass transition temperatures of 69 °C and showed a melting temperature $T_m = 76$ °C. Deprotection of the poly(**M63**) was not reported, however, deprotection of its copolymer with lactide resulted in lowering of the glass transition temperature after both deprotection steps. Homopolymerisation of cyclic carbonates **M60**, **M61** and **M62** with pendant protected saccharides was carried out at room temperature using organic catalyst system DBU/thiourea.¹⁴⁰ Homopolymers were obtained with molecular weights of 17 000-19 000 g mol⁻¹ and polydispersities 1.20-1.28. Regeneration of the hydroxyl groups was carried out by deprotection of the acetonide groups with formic acid solution without degradation. The use of block copolymers of **M60-62** with TMC was reported in the preparation of micelles in aqueous solutions, and were prepared by sequential addition of TMC to poly(**M60**), poly(**M61**) and poly(**M62**).

1.3.7. Macromonomers, bis- and tris- carbonates.

A number of cyclic carbonate containing macromonomers and cross-linkers have been reported.^{33,37,43,68,75,84,136} In particular those containing ethylene glycol moieties (**M65**, **M66**) have received increased interest in recent years (Figure 1.11). Poly(ethylene oxide) cyclic carbonate macromonomers (**M65**),

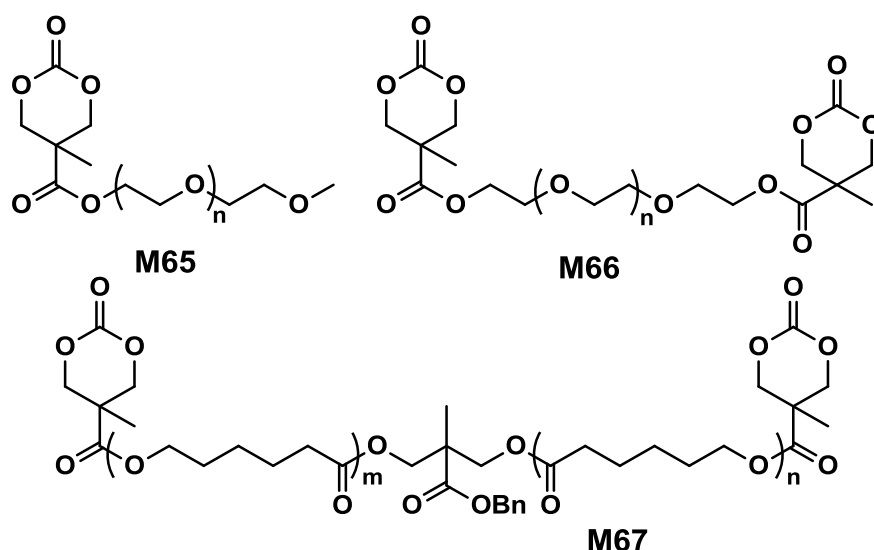


Figure 1.11. Cyclic carbonate macromonomers.

prepared from methoxy poly(ethylene oxide)s, have been reported with molecular weights ranging from 350 g mol^{-1} to $1\,900 \text{ g mol}^{-1}$ (PDI = 1.03-1.14). Although homopolymerisation of **M65** (with $M_n = 1\,900 \text{ g mol}^{-1}$ and PDI = 1.03) in methylene chloride solution at room temperature using DBU as a catalyst was possible, the reaction showed a maximum at 55% monomer conversion.³³ The limited, low concentration of the cyclic carbonate (0.2 M), due to the large poly(ethylene oxide) pendant chain, was thought to cause the ring-chain equilibrium to dominate such that a high molecular weight polymers could not be obtained. To obtain higher molecular weight polymers, the cyclic carbonate concentration was increased by copolymerisation of **M65** with TMC.^{33,43} Random copolymerisation of **M65**s were further reported with dimethyltrimethylene carbonate (DTC) from a poly(ϵ -caprolactone)

macroinitiator at 130 °C in bulk using tin octanoate as a catalyst or with dodecyl-functional monomer **M6** in methylene chloride at room temperature using organic catalysts.^{68,75} It was shown that the resulting block/graft copolymers could be self-assembled, with the latter example showing thermoresponsive behaviour caused by the combination of hydrophilic/hydrophobic groups in the second block. An organocatalytic approach to hydrogels was presented by Nederberg *et al.* by the synthesis of a bifunctional cyclic carbonate macromonomer from poly(ethylene oxide) diols.³³ Poly(ethylene oxide)- α,ω -methylcarboxytrimethylene carbonate crosslinkers, **M66s**, were prepared with $M_n = 3\,400\text{ g mol}^{-1}$, $8\,000\text{ g mol}^{-1}$ and $18\,500\text{ g mol}^{-1}$ and copolymerised with TMC in methylene chloride at room temperature in the presence of DBU to poly(carbonate)/poly(ethylene oxide) cross-linked hydrogel networks. Hydrogels prepared with increased amounts of TMC showed hydrophobic PTMC domains. The introduction of these hydrophobic domains can increase the toughness of formed hydrogels.^{33,136} This led to further investigation by synthesis of telechelic, carbonate functional poly(ϵ -caprolactone), **M67**, with a molecular weight of $8\,000\text{ g mol}^{-1}$ (PDI = 1.40; DP = 70). Copolymerisations of this hydrophobic cross-linker with **M66** ($8\,000\text{ g mol}^{-1}$) and TMC were performed to introduce hydrophobic segments which resulted in the isolation of particularly tough materials with phase-separated hydrophobic domains. Furthermore hydrogels prepared from copolymerisation from a poly(carbonate) macroinitiator bearing pendant urea

functionalities (*i.e.* poly(**M59**)) are presented as another method to strengthen the resulting network *via* hydrogen bonding with the poly(ethylene oxide) crosslinkers.^{33,84,136}

The synthesis of a triazolium-based cyclic carbonate, **M68**, that can act as an initiator for the anionic ring-opening polymerisation of β -butyrolactone (BL) at elevated temperatures was reported by Dubois and co-workers (Figure 1.12).¹⁴¹ To prove that the carbene catalyst was selective for the polymerisation of β -butyrolactone, the synthesis of a poly(β -butyrolactone) cyclic carbonate macromonomer (**M69**) with a narrow molecular weight distribution (PDI = 1.21) was realised at 90 °C under bulk conditions. Alternatively, **M68** could be copolymerised trimethylene carbonate at room

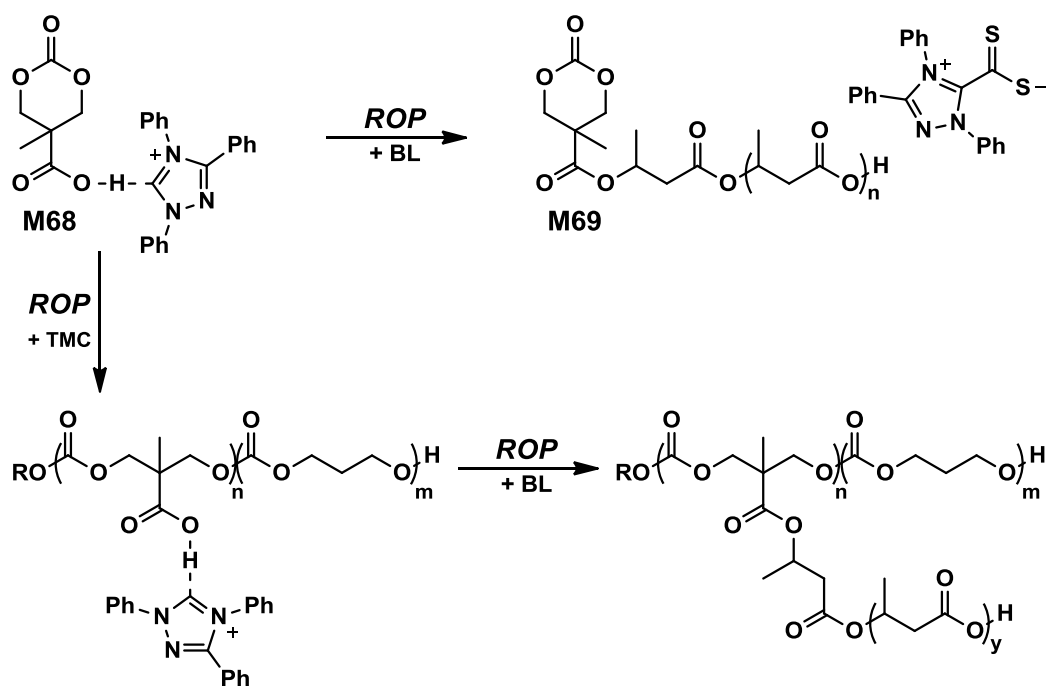


Figure 1.12. Polymerisation with and from cyclic carbonate **M68**.

temperature using sparteine and 4-chlorophenol as catalysts to give a copoly(carbonate) with pendant triazolium groups ($M_n = 4\ 100\ \text{g mol}^{-1}$; PDI = 1.19) in a controlled manner, which could then be used as initiator for the ROP of β -butyrolactone in the preparation of graft copolymers.

A range of other bis-cyclic carbonate cross-linkers and one tris-cyclic carbonate cross-linker have been reported (M70-76) for use in biodegradable cross-linked networks (Figure 1.13).^{43,142} M73 exists in both the *trans*- and *cis*-isomer which could be separated by column chromatography and isolated in a 1:1 ratio. Cross-linked networks were reported by copolymerisation of the

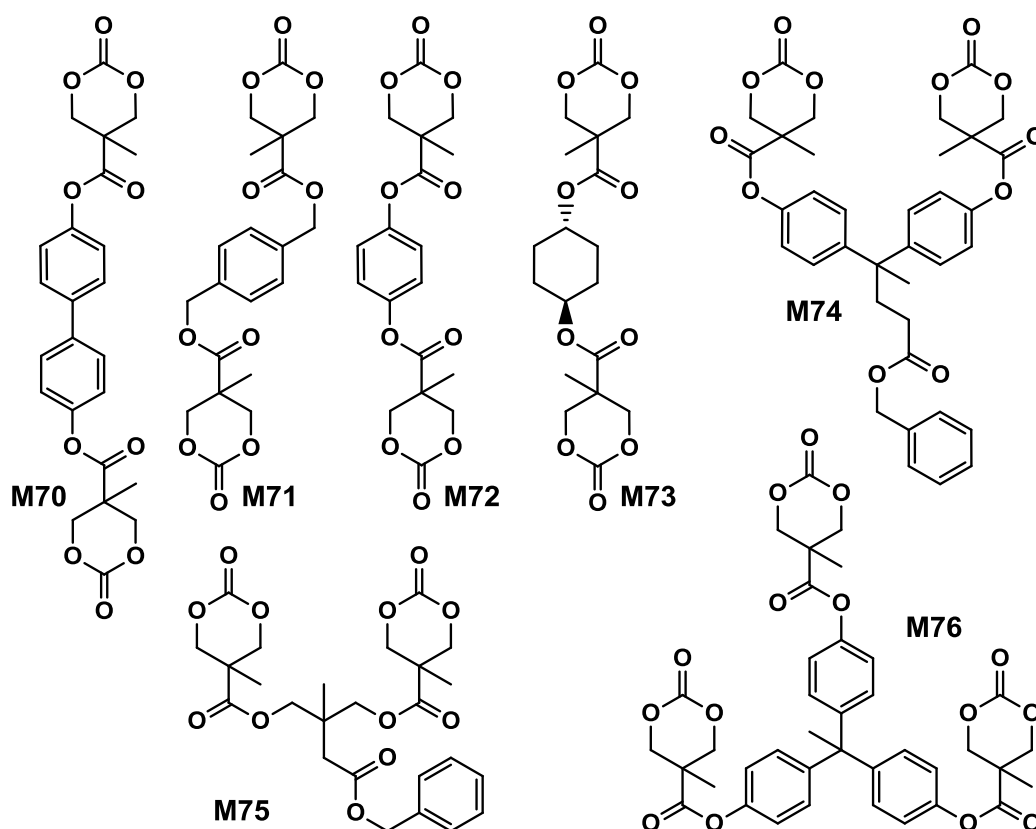


Figure 1.13. Bis- and tris- cyclic carbonate cross-linkers.

cross-linkers with TMC and ϵ -caprolactone at 140 °C in bulk in the presence of tin octanoate. As expected, cross-linked networks displayed increased glass transition temperatures with increased amount of crosslinker.

1.3.8. Other functional monomers.

Other functional monomers reported include epoxide functional, **M77**, which could be converted to bifunctional cyclic carbonate 5-(2-oxo-1,3-dioxolan-4-yl)methyl-5-propyl-1,3-dioxan-2-one (**M78**, Figure 1.14).⁶⁴ The selective polymerisation of the six-membered cyclic carbonate at 60 °C with DBU was achieved and the resulting homopolymer, with the pendant five-membered cyclic carbonate intact, was obtained in 50% yield and had a molecular weight of 14 900 g mol⁻¹ (PDI = 1.41). Hydroxyl functional monomers **M80**

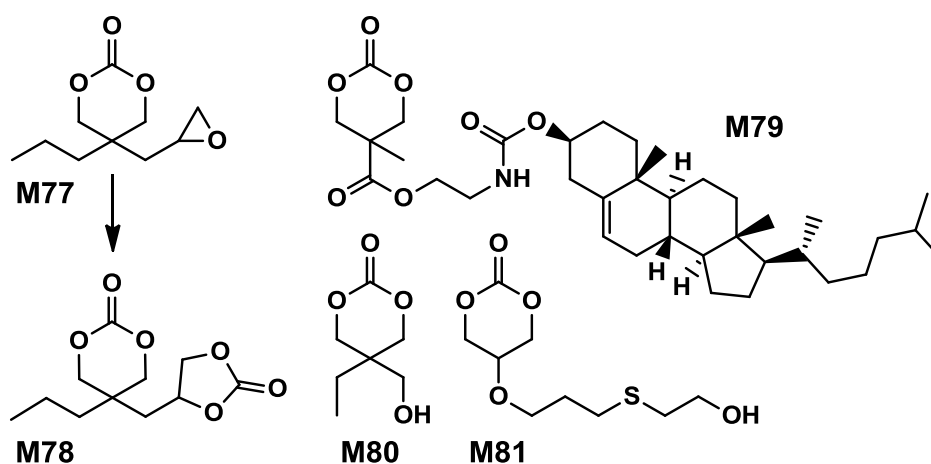


Figure 1.14 Other functional cyclic carbonate monomers.

and **M81** are incompatible in the controlled ring opening process as the hydroxyl functionality acts as an initiating species. However, advantage was taken of this fact to prepare biodegradable, hydrophilic, hyperbranched polymers.^{44,143,144}

In a recent report by Lee *et al.*, a cyclic carbonate with a pendant cholesterol functionality, cholesteryl-2-(5-methyl-2-oxo-1,3-dioxane-5-carboxyloxy) ethyl carbamate (**M79**) was homopolymerised (DP 11) and copolymerised with TMC from a PEO macroinitiator using organic catalysts DBU and a thiourea cocatalyst.¹⁴⁸ Micelles prepared from the abovementioned block copolymers showed increased loading of the anticancer drug paclitaxel. It was hypothesised that this excellent compatibility is a result of the rigid aromatic structure of cholesterol and its available stereocenters that may interact with those in paclitaxel. Sulphide and disulphide functional cyclic carbonates **M82**, **M83** and **M84** (Figure 1.15) have been reported, but their polymerisation has not been reported yet.^{37,43}

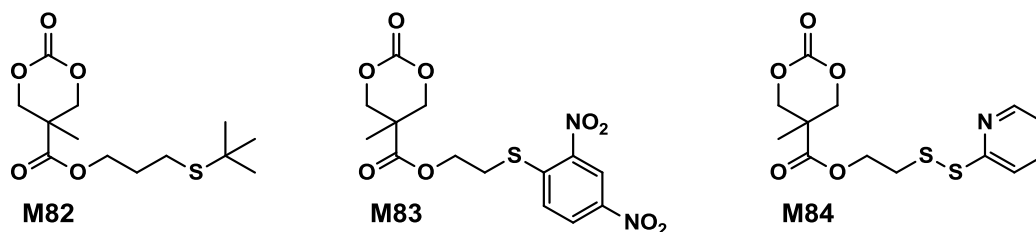
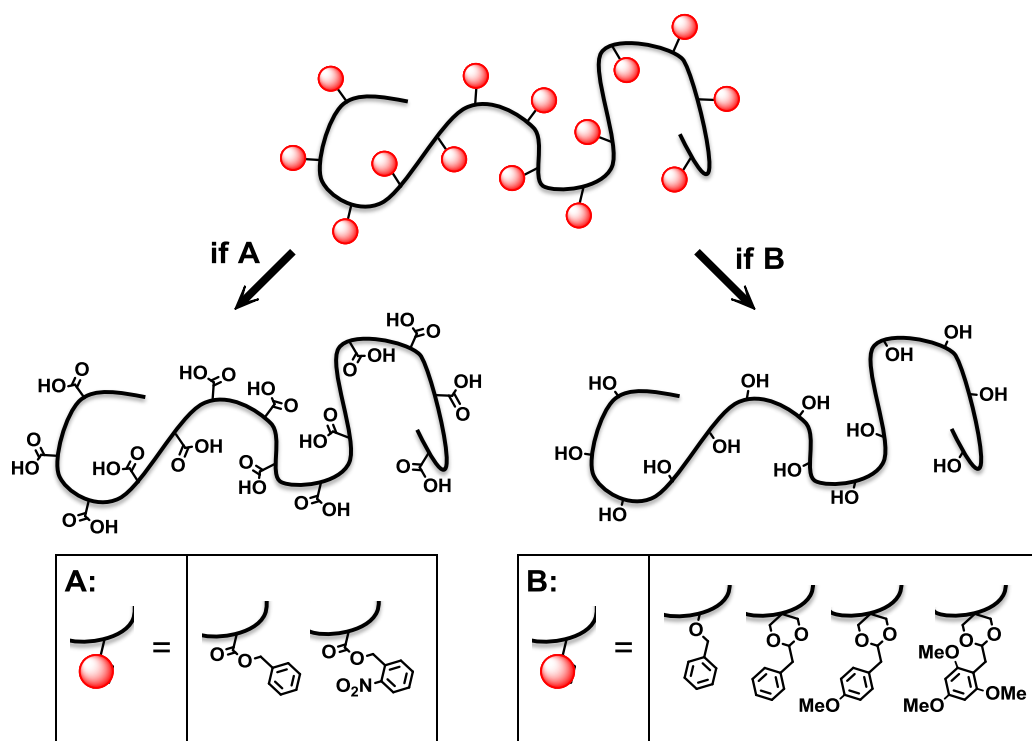


Figure 1.15. Sulphide and disulphide functional cyclic carbonate monomers.

1.4. Post-polymerisation modification of functional poly(carbonate)s.

1.4.1. Deprotection of aryl and alkyl functional poly(carbonate)s.

Alkyl and aryl functional groups are inert under most polymerisation conditions and are therefore often used to protect functional groups that may be incompatible with the ring-opening polymerisation process. Poly(carbonate)s and poly(ester)s bearing pendant hydroxyl or carboxylic acid functional groups are therefore usually obtained by deprotection of benzyl ether or benzyl ester functional polymers (Scheme 1.8). Deprotection of the benzyl functionality in poly(carbonate)s poly(MBC) and poly(M11) was



Scheme 1.8. Schematic representation of deprotection of benzyl-functional poly(carbonate)s to carboxylic acid- (A) and hydroxyl- (B) functional poly(carbonate)s.

carried out by hydrogenation over palladium on carbon or palladium hydroxide on carbon and lead to carboxyl- and hydroxyl- functional poly(carbonate)s.^{41,76,87,89,90,92-99,101,145-147} In both cases, the reduction in the molecular weight was confirmed by a shift to higher retention time observed by GPC analysis. Poly(**M11**) and poly(MBC) are highly hydrophobic materials before deprotection, but the resulting hydroxyl and carboxylic acid functional polymers are hydrophilic materials that show enhanced biocompatibility after deprotection of the benzyl functionality.^{92,99} Homopolymers and copolymers of MBC also reveal a change in glass transition temperature after deprotection. Poly(MBC), a sticky amorphous polymer before benzyl deprotection with $T_g \approx 3$ °C, was converted to semicrystalline white powders. These new carboxylic acid functional polymers had a higher T_g (47-60 °C) and display a melting temperature (T_m) around 170 °C. Poly(**M11**) homopolymers displayed an impressive 64-fold increase in water absorption after debenzilation. The auto-degradation process of lactide was increased in copolymers with **M11** after benzyl deprotection due to the presence of the hydroxyl groups. Faster degradation of the materials was observed under acidic conditions (pH = 4.4) compared to neutral conditions (pH = 7.4).⁹⁷ In a similar manner, hydroxyl functional polymers were obtained by removal of the benzylidene group in polymers prepared from **M13**.⁴⁹ In contrast to poly(**M11**), poly(**M13**) contains two hydroxyl groups per repeat unit due to the double hydroxyl protection of the benzylidene group. Although no

thermal properties are reported for poly(**M13**), lactide copolymers with 10% incorporation of the benzylidene group already show a decrease in T_g of 14 °C due to the increased flexibility of the polymer chains after removal of the rigid benzylidene groups. These lactide copolymers show surface degradation in contrast to pure poly(lactide) which display bulk degradation.

Facile deprotection of the benzylidene group could be achieved under acidic conditions in case of block copolymers of poly(ethylene oxide) and poly(**M21**) or poly(**M22**). In poly(**M21**) and poly(**M22**) the benzylidene groups are substituted with methoxy groups at the *para* position and the *ortho*- and *para*-positions respectively.¹⁰² Micelles prepared from the protected block copolymers were stable at pH = 7.4, but deprotection of the methoxy benzylidene groups at lower pH (4-5) did not cause dissociation of the micelles. However, micelles loaded with the hydrophobic anti-cancer drugs paclitaxel and doxorubicin did show increased drug release at lower pH. Although highly hydrophilic, poly(carbonate)s derived from pentaerythritol are not soluble in water.^{102,149}

Another example of a poly(carbonate) that deprotects under acidic conditions is the with an acid labile functional group was reported by Fukushima *et al.* Deprotection of tetrahydropyranyloxy protecting groups in poly(**M8**) was carried out at 50 °C using an ion-exchange resin to reveal hydroxyl functional polymers.⁷² The hydroxyl functionalities then acted as initiating sites in further ROP of stereopure lactide to form graft-copolymers with a

polycarbonate backbone and stereopure poly(lactide) grafts. By self-assembling PEO-poly(carbonate) block-copolymers with grafts of opposite chirality, micelles could be formed at extremely low concentrations due to the stereocomplexation of the lactide grafts within the core of the micelles.

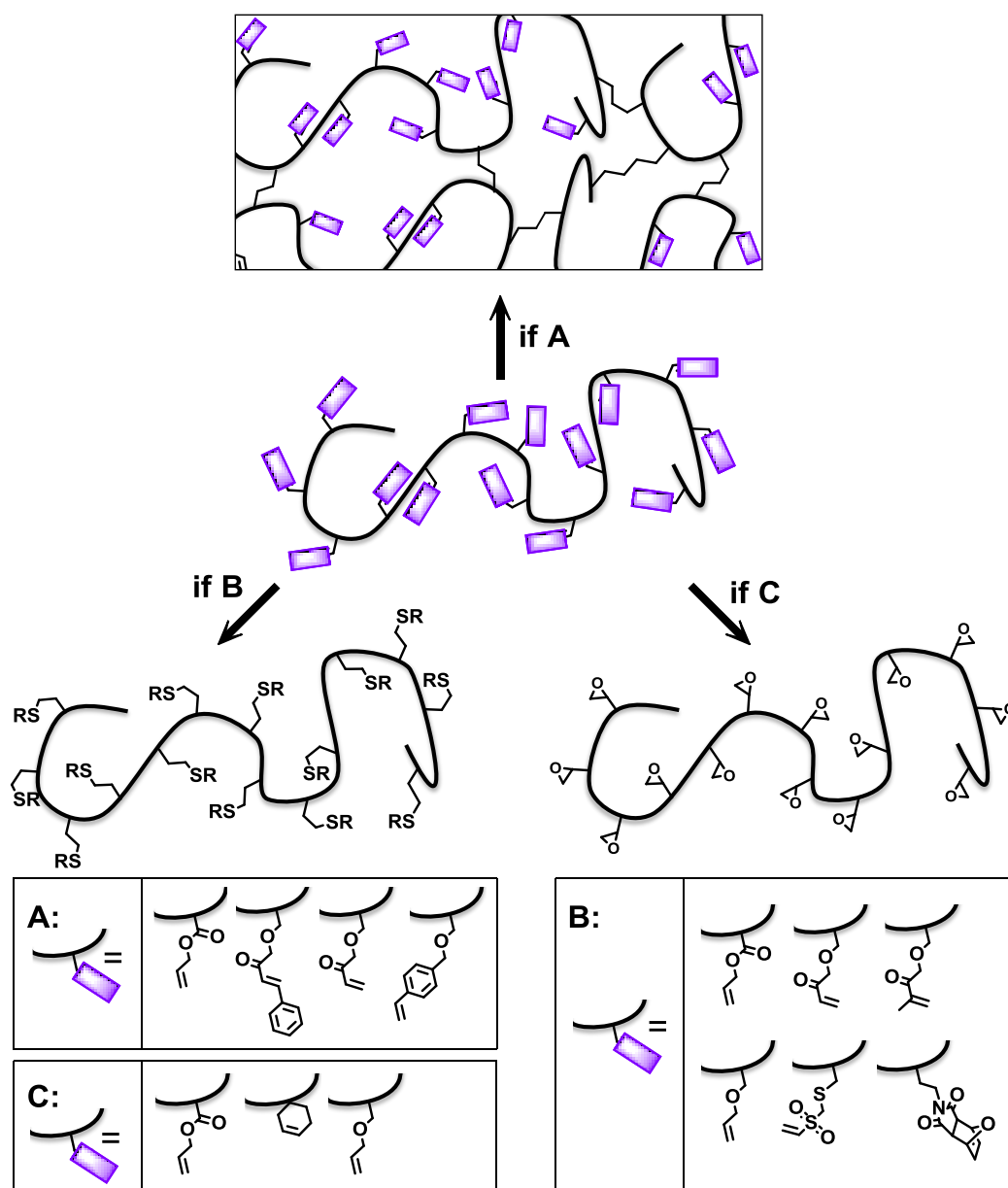
The nitrobenzyl group in the poly(carbonate)-containing blocks of poly(ethylene oxide) and poly(M23) block copolymers could be deprotected by UV irradiation at 365 nm converting the poly(carbonate) block from a hydrophobic block to a hydrophilic carboxylic acid functional block. Micelles prepared from these protected PEO/poly(carbonate) block copolymers therefore dissociate readily when irradiated due to conversion of the amphiphilic block copolymers to hydrophilic polymers.^{103,104}

The newly available carboxylic acid and hydroxyl groups after deprotection are also open to further reaction. Further modification of carboxylic acid functional polymers were reported *via* *N,N'*-diisopropylcarbodiimide (DIC), 1-ethyl-3-(3-dimethylaminopropyl) carbodiimide (EDC) or DCC couplings with free alcohol groups in biologically active molecules or with *N*-hydroxysuccinimide (NHS) or hydroxybenzotriazole (HOBT) for further reaction with amines.^{92,93,95-97} Conjugation using these methods is limited as quantitative conversion of the acid groups is rarely observed and can be as low as 20% in some reported cases. Examples of post-polymerisation modifications of acid-functional polymers obtained after deprotection included conjugation with aliphatic amines in the formation of DNA/polymer

nanoparticles, the grafting of PEO-amines to form amphiphilic copolymers with a hydrophobic backbone and hydrophilic grafts that self-assemble in aqueous environments and conjugation with peptides or drugs such as heparin, docetaxel and paclitaxel.^{90,92,93,95,96} Further modifications of hydroxyl functional monomers include reaction of the hydroxyl groups with acid chlorides (e.g. 4-isobutylmethylphenyl acetic acid).⁹⁷

1.4.2. Post-polymerisation modifications of alkene functional poly(carbonate)s.

Alkenes participate in many reactions and are for that reason have been utilised extensively. In the post-polymerisation functionalisation of biodegradable polymers, pendant carbon-carbon double bonds have been utilised in cross-linking reactions and in the addition of new pendant functional moieties.¹¹⁰ Reported post-polymerisation functionalisations of alkenyl functional poly(carbonate)s could be divided into three general categories: cross-linking, thiol additions and epoxidations (Scheme 1.9). Cross-linking of the hydrophobic core of micelles prepared from block copolymers with hydrophilic poly(ethylene oxide) blocks and hydrophobic poly(ester-carbonate) blocks with pendant allyl- or acryloyl- groups was realised by heating in the presence of azoisobutyronitrile (AIBN) at 60 °C and by UV irradiation of the micelles in the presence of a biocompatible



Scheme 1.9. Schematic representation of post-polymerisation modifications of alkene-functional poly(carbonate)s: cross-linking (A), addition of a thiol (B) and epoxidation (C).

photoinitiator respectively.^{112,113,120} Micelles with cross-linked poly(ester-carbonate)s cores, loaded with anti-cancer drug paclitaxel and with galactose groups at the micelle surface for specific targeting displayed enhanced antitumor efficacy in *in vivo* studies. In another example, the radical cross-

linking of a poly(carbonate) homopolymer with pendant styrene groups (poly(**M30**) was realised in the presence of the radical initiator benzoyl peroxide.⁴⁷ The cross-linking was carried out in the presence of styrene creating a poly(carbonate)/poly(styrene) network. Notably, the resulting cross-linked networks could be decross-linked in the presence of *t*-BuOK, resulting in poly(styrene) with pendant six-membered cyclic carbonates. Photo-crosslinking of poly(ester-carbonates) (copolymers of *L*-lactide and **M26**) with pendant cinnamate functionalities could be cross-linked by UV irradiation at 365 nm providing biodegradable networks.¹¹⁹ This type of cross-linking occurs *via* dimerisation through the [2+2] cycloaddition reaction of two cinnamate moieties upon irradiation with UV light.

The reaction of thiols and alkenes ('thiol-ene') has been utilised extensively as an efficient method in the preparation of functional polymers. Reactions proceed either *via* the free-radical addition of thiols to carbon-carbon double bonds or *via* the Michael-type addition of thiols to electron-deficient carbon-carbon double bonds.¹⁰⁸ Radical-type addition of thiols to the poly(carbonate) backbone has been reported for polymers containing pendant allyl functionalities.^{44,113,115} Copolymers prepared *via* the ROP of lactide and allyl functional monomers (MAC, **M24**) could be functionalised with a number of thiols by UV irradiation at 254 nm in the presence of 1-hydroxycyclohexylphenyl ketone as radical initiator or without radical initiator.^{44,115} Although the reaction proceeds to high conversion at equimolar

ene-thiol ratios, an excess was necessary to achieve full conversion (5:1). Functionalisation of poly(ester-carbonates) with folic acid *via* radical thiol addition resulted in polymers which displayed increased cell affinity.¹¹³ Similarly, a range of alkene functional poly(carbonate)s could be modified with thiols *via* Michael-type conjugation.⁴⁶ Lactide and ϵ -caprolactone polymers with low incorporations of acryloyl or methacryloyl functional cyclic carbonate (**M28**, **M29**), were further functionalised in dimethylformamide at room temperature with a number of thiols.⁴⁶ Quantitative conversion (using 10 equivalents of thiol) of the pendant (meth)acrylates was obtained for functionalisation with mercaptoethanol, cysteine and 2-mercaptoethylamine, but conjugation with a peptide only proceeded to 58% conversion whilst mercaptopropanoic acid only displayed a conversion of 30%. Conjugation of poly(ethylene oxide)s with small acryloyl-functional poly(carbonate) blocks (DP<20) with thiolated chitosan resulted in *in situ* hydrogel formation.¹²¹ Notably, the pendant functionalities in films of vinyl sulfone functional co-poly(carbonate)s and poly(ester-carbonate)s, obtained from the copolymerisation of **M32** with other cyclic monomers, could be quantitatively functionalised *via* Michael-type addition of thiols to the vinyl group without catalyst under aqueous conditions.⁶³ Another example of functionalisation of poly(carbonate)s and poly(ester-carbonate)s *via* Michael-type addition of thiols was presented by Onbulak *et al.*¹²³ Polymers with pendant furan-protected maleimides were deprotected *via*

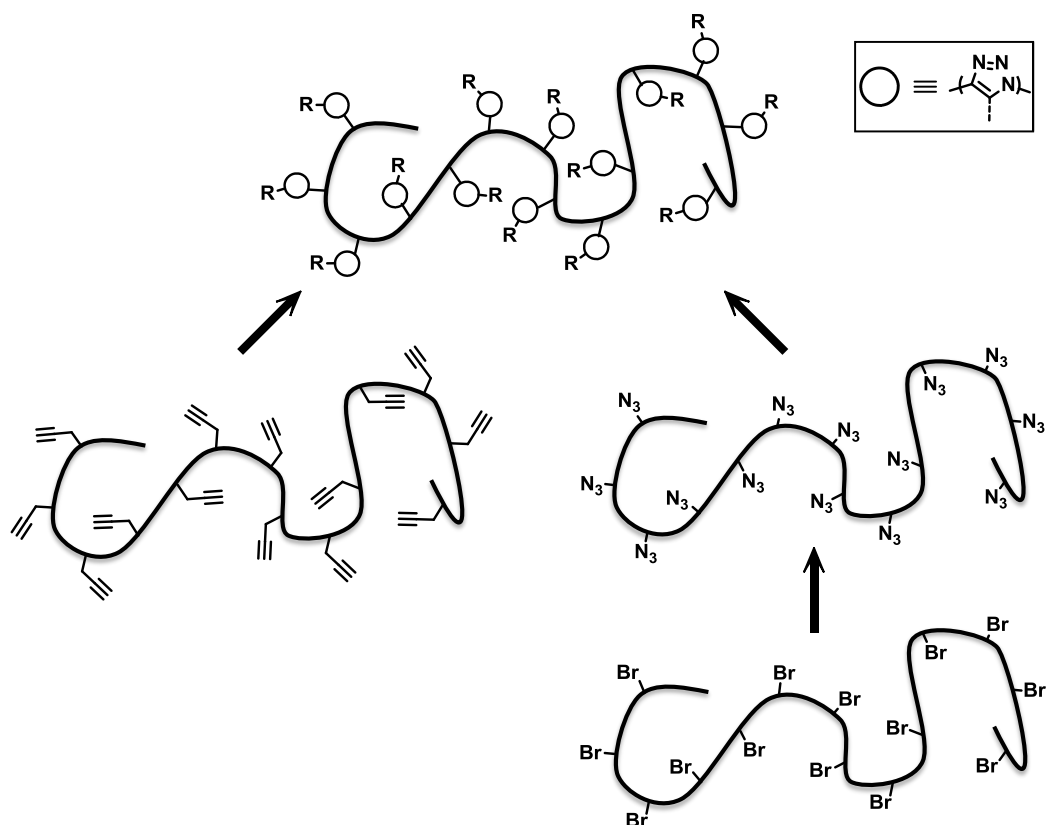
thermal *retro*-Diels Alder to give maleimide functional polymers that were further functionalised with thiol-containing molecules 6-(ferrocenyl)hexanethiol and 1-hexanethiol in the presence of triethylamine. Both deprotection and thiol addition proceed without degradation of the polymer backbone.

Finally, alkene functional poly(carbonate)s could also be epoxidised using *meta*-chloroperoxybenzoic acid (*m*-CPBA). Epoxidation of functional aliphatic poly(carbonate)s and poly(ester-carbonates) was reported for pendant allyl groups and pendant cyclohexenyl groups with efficiencies of 35-99% with hydrolysis of the epoxide groups occurring in some cases.^{45,74,116-118}

In case of epoxidation of PMAC homopolymers an increase in glass transition temperature from -12 °C to 14 °C was observed. The introduction of this new reactive functionality was applied in the grafting of poly(ethylene imine) to the poly(carbonate) backbone in the formation of biodegradable polycations and polycation/DNA polyplexes by Zhuo and co-workers.¹¹⁶

1.4.3. Post-polymerisation modifications of poly(carbonate)s *via* alkyne-azide cycloadditions.

Alkyne- and azide functional poly(carbonate)s and poly(ester-carbonate)s were successfully functionalised *via* 1,3-dipolar cycloaddition reactions (Scheme 1.10).^{56,57, 67, 71, 120-123, 150} Modifications of poly(ester-carbonates)



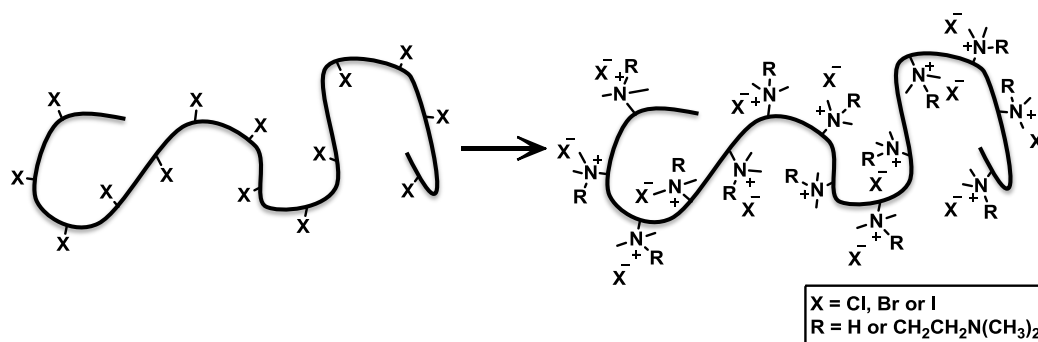
Scheme 1.10. Schematic representation of post-polymerisation modifications of alkyne-, azide- and bromide functional poly(carbonate)s through alkyne/azide cycloadditions.

obtained from copolymerisation of MPC with lactide were successfully functionalised with azide containing molecules using copper (II) sulfate pentahydrate and sodium ascorbate in water/DMSO mixtures.^{124,127,128} Modifications with glucose and galactose azides led to much higher levels of biocompatibility and enhanced hydrophilicity and cellular affinity of resulting polymers.¹²⁸ Similarly polymers were modified with CO-protected Hemoglobin and proteins Testis-specific protease 50 (TSP50), a breast cancer sensitive protease, and bovine serum albumin (BSA). The latter achieved only low grafting efficiencies of 0.7-1.6 mol%.^{124,127} Alternatively, azide functional

poly(carbonate)s could be obtained *via* polymerisation of azide functional cyclic carbonates or *via* modification of bromide functional poly(carbonate)s with sodium azide in DMF at various temperatures. The latter method, however, has limitations as azidation of bromide functional polymers did not exceed 25% for homopolymers and degradation of the poly(carbonate) backbone was observed in both bromide functional homopolymers and copolymers.^{56,57} Successful cycloaddition of alkyne-functional molecules to azido-functional poly(carbonate)s *via* copper catalysed methods (CuAAC) and *via* strain-promoted methods (SPAAC) was reported by Song and co-workers and used in the preparation of hydrogels by cross-linking of poly(carbonate)s with DABCO-terminated poly(ethylene oxide)s.^{130,131}

1.4.4. Quaternisation of halogen functional poly(carbonate)s.

A range of polymers containing quaternary amines have shown to exhibit antimicrobial activity. These polymers are, however, often not degradable which limits their use. As amines are readily quaternised by reaction with halogen containing compounds, poly(carbonate) homopolymers and copolymers bearing pendant halogen functionalities could be reacted with tertiary amines such as trimethylamine and *N,N,N',N'*-tetramethylethylenediamine (Scheme 1.11). Recently, Yang and coworkers reported the first example of quaternised poly(carbonate) nanoparticles



Scheme 1.11. Schematic representation of the quaternisation of halide-functional poly(carbonate)s.

prepared from PTMC and chloro functional poly(carbonate) P(M41) block copolymers.¹³³ Investigation of quaternisation conditions revealed a dependence on the halogen substituent on the pendant chain. Whereas chloro-functional poly(carbonate)s required heating at 90 °C, bromo- and iodo-functional poly(carbonate)s could be converted at room temperature. Another application for these cationic poly(carbonate)s was found in the synthesis of poly(carbonate)/DNA complexes.^{67,70,132,133}

1.4.5. Deprotection of carbamate functional poly(carbonate)s.

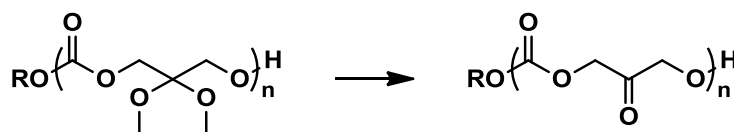
Poly(carbonate)s with pendant primary amines can be prepared *via* the ring opening polymerisation of monomers in which the primary amines are protected by conversion to benzyl- or *tert*-butyl- carbamate groups. Deprotection of the benzyl carbamate groups in homopolymers of M48, M49,

M52 and copolymers of lactide and **M48** was carried out *via* hydrogenation catalysed by palladium and *tert*-butyl- carbamate groups were removed using trifluoroacetic acid.^{51,54} Resulting primary amine functional poly(carbonate)s and poly(ester-carbonate)s could be obtained whilst retaining narrow polydispersities. After deprotection a reduction in molecular weight was observed and polymers were highly hydrophilic in contrast to the protected polymers. Primary amine functional poly(ester-carbonate)s could be further modified by reaction with peptides in the presence of carbonyldiimidazole, with films of the resulting polymers showing increased cell adhesion and spreading.⁵⁴ In another report, two Boc-protecting groups were removed to reveal pendant guanidinium groups.^{84,134} Hydrogels prepared from bis(carbonate) poly(ethylene oxide) cross-linker, Boc protected guanidinium functional cyclic carbonate and *tert*-butoxy protected carboxylic acid functional cyclic carbonate showed additional stabilisation of the hydrogel network after removal of the protecting groups with trifluoro acetic acid as a result of the hydrogen bonding between the free guanidinium and carboxylic acid groups.

1.4.6. Other post-polymerisation modifications of functional poly(carbonate)s.

Post-polymerisation modification of functional poly(carbonate)s derived from dihydroxyacetone was achieved by the conversion di(methoxy) groups in

poly(**M3**) homopolymers and copolymers (Scheme 1.12).⁶² The conversion to dihydroxyacetone functional polycarbonates was accomplished by refluxing poly(**M3**) with iodine in acetone resulting in a change in glass transition temperatures in the homopolymers 45 to 68 °C. In addition, resulting polymers showed very low solubility in common solvents and copolymers of lactide with the dihydroxyacetone functional carbonate showed very interesting degradation with degradation occurring more rapidly in copolymers with a higher carbonate content.



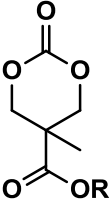
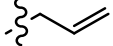
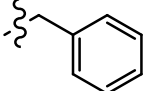
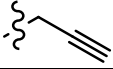
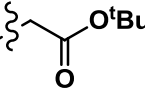
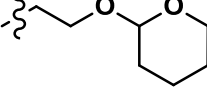
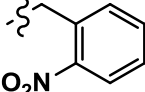
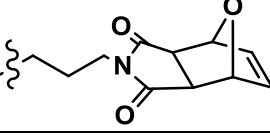
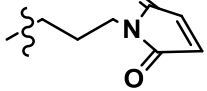
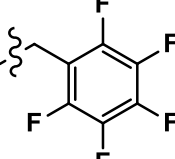
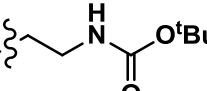
Scheme 1.12. Conversion of poly(**M3**) to hydroxyacetone functional poly(carbonate).

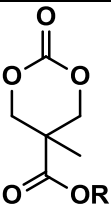
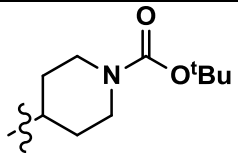
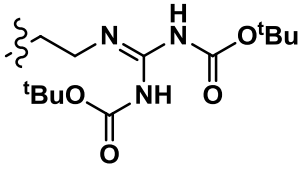
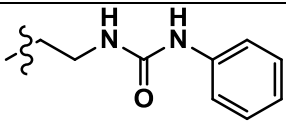
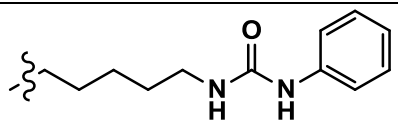
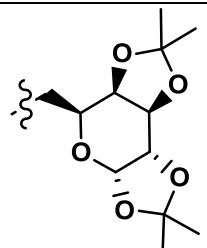
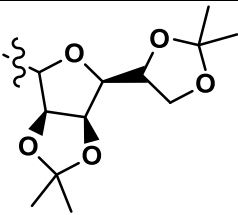
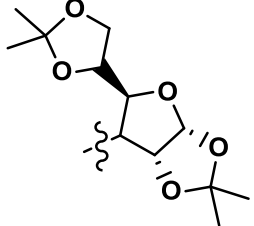
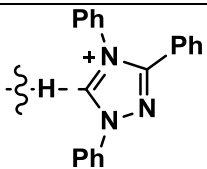
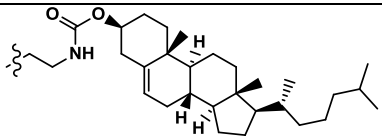
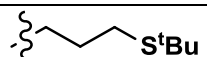
1.5. Conclusion

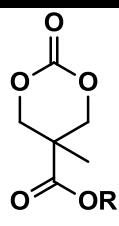
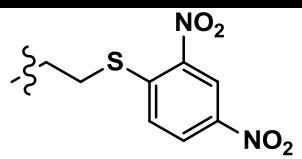
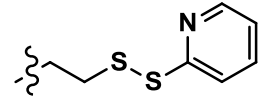
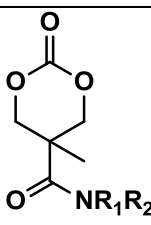
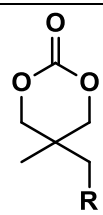
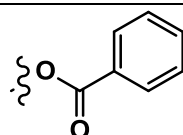
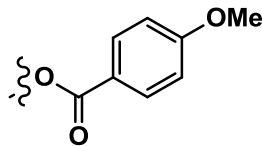
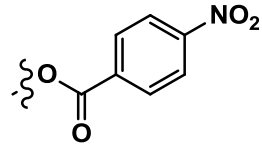
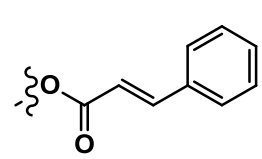
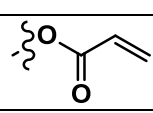
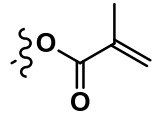
The combination of the many versatile methods reported for the synthesis of functional cyclic carbonate monomers from a range of biocompatible scaffolds with the excellent control in their ring opening polymerisation, have led to preparation of a multitude of functional poly(carbonate)s with controlled molecular weights, narrow polydispersities and high end-groups fidelity. Although post-polymerisation modifications of functional poly(carbonate)s have been investigated, only few reports exist that show both excellent control in the synthesis of functional homopolymers synthesis followed with further functionalisations that show quantitative conversions. The further development of controlled poly(carbonate) synthesis in combination with efficient chemistries could opened up new ways to exactly control the properties of these biodegradable materials and promote their biomedical application.

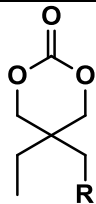
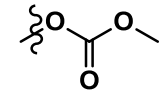
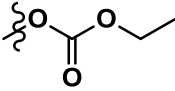
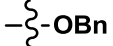
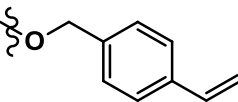
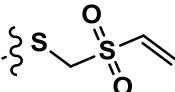
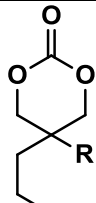
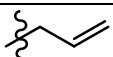
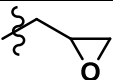
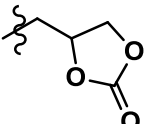
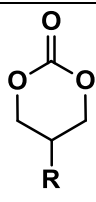
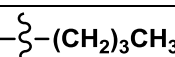
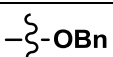
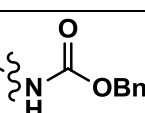
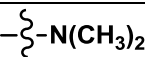
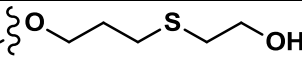
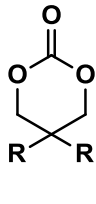
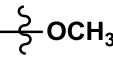
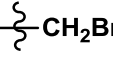
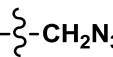
1.6. Overview of cyclic carbonates

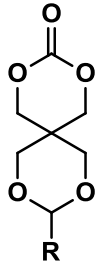
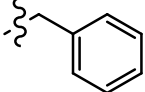
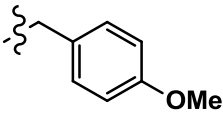
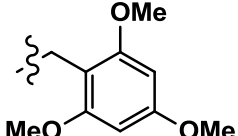
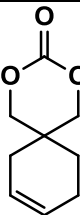
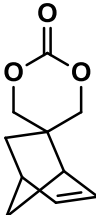
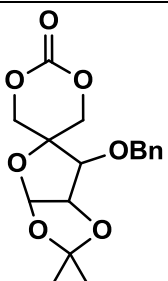
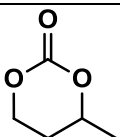
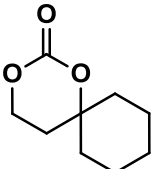
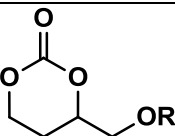
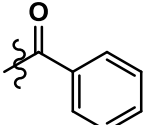
1.6.1. Overview of cyclic carbonate monomers

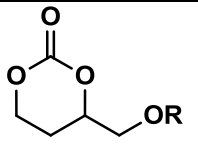
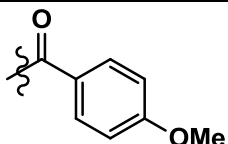
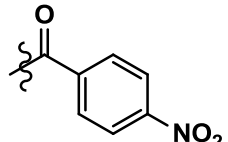
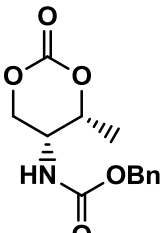
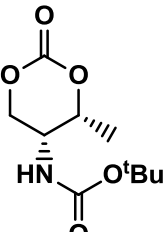
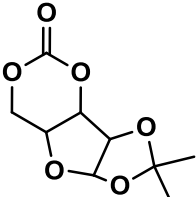
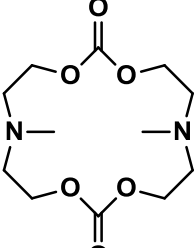
Monomer structure	Name	Pages	References	
	R=			
		MAC	24, 25, 49-52	74, 112-116
		MBC	6, 7, 18-20, 44, 45	41, 69, 89-96
	$-\zeta-\text{CH}_2\text{CH}_3$	MEC	14, 15, 20, 31, 35	37, 67-72
		MPC	28, 53	43, 124-128
	$-(\text{CH}_2)_{11}\text{CH}_3$	M6	15, 16, 39	68
		M7	15, 16	84
		M8	15, 16, 47	37, 72
		M23	22, 23, 44, 47	103, 104
		M33	27, 49, 51	123
		M34	27, 51	123
	$-\zeta-(\text{CH}_2)_3\text{Cl}$	M41	30, 31, 54, 55	37, 43, 67, 70, 133
	$-\zeta-(\text{CH}_2)_3\text{Br}$	M42	30, 31, 54, 55	37, 70, 132
	$-\zeta-(\text{CH}_2)_2\text{I}$	M43	30, 31, 54, 55	70
	$-\zeta-\text{CH}_2\text{CF}_3$	M44	30, 31	43
	$-\zeta-\text{CH}_2(\text{CF}_2)_5\text{CF}_3$	M45	30, 31	37
		M46	6, 30	37
	M47	32	37, 43	

Monomer structure	Name	Pages	References	
		M50	31, 33	43
		M51	31, 33, 56	84, 134
		M58	34, 35	69, 71, 136
		M59	34, 35	69, 71, 136
		M60	36, 37	140
		M61	36, 37	140
		M62	36, 37	140
	$-\zeta-(\text{CH}_2\text{CH}_2\text{O})_n\text{CH}_3$	M65	37, 38	33, 43, 68, 75
		M68	40	141
	$-\zeta-(\text{C}(\text{CH}_3)\text{CH}_2\text{C}(\text{O})\text{O})_n\text{H}$	M69	40	141
	M79	42, 43	148	
	M82	43	43	

Monomer structure	Name	Pages	References		
		M83	43	37	
		M84	43	37, 43	
	R1=	R2=			
	- ζ -H	- ζ -CH ₂ CH(CH ₃) ₂	M53	33, 34	43
	- ζ -H	- ζ -CH ₂ C ₆ H ₅	M54	33, 34	43
	- ζ -CH ₃	- ζ -CH ₃	M55	33, 34	37
	R=				
	- ζ -H	DTC	14, 15, 21, 30, 38	73-82	
	- ζ -OCH ₃	M2	15, 16	60	
	- ζ -OBn	M14	19, 21	60	
		M15	19, 21	77	
		M17	22	77	
		M18	22	77	
		M26	24, 26, 49, 50	119	
		M28	24, 26, 49, 51	46, 120, 121	
		M29	24, 26, 49, 51	46	
	- ζ -Cl	M35	28, 29	38	
	- ζ -Br	M37	28, 29	38	

Monomer structure	Name	Pages	References	
	R=			
		M4	15, 16	50
		M5	15, 16	50
		M12	19, 21	48
		M30	24, 26, 49, 50	47
		M32	24, 27, 49, 51	69
		M36	28, 29	38
		M38	28, 29	38
		M80	42, 43	143, 144
	R=			
		M27	24, 25	64
		M77	42	64
	M78	42	64	
	R=			
		M1	15, 16	78
		M11	19, 20, 21, 44, 45	48, 73, 76, 83, 97-99
		M24	24, 25, 49, 50	44, 45
		M48	31, 32, 55, 56	51, 54
		M56	34, 35	135
	M81	42, 43	44	
	R=			
		M3	15, 16, 57	61, 62, 83
		M39	28, 29, 54	56, 57
	M40	28, 30, 53, 54	56, 57, 130, 131	

Monomer structure	Name	Pages	References	
	R=			
		M13	19, 21, 44-46	49, 100, 101
		M21	22, 23, 44, 46	102
		M22	22, 23, 45, 47	102
	M25	24, 25, 49, 52	59, 118	
	M31	24, 26	122	
	M63	11, 12, 36, 37	52	
	M9	17, 18	48, 77, 82, 87, 88	
	M10	16, 17	78	
	R=			
		M16	19, 21	77

Monomer structure	Name	Pages	References
	 M19	22	77
	 M20	22	77
	M49	31, 32, 55, 56	51
	M52	31, 32, 55, 56	51
	M64	11, 12, 36, 37	53, 138, 139
	M57	33, 34	58

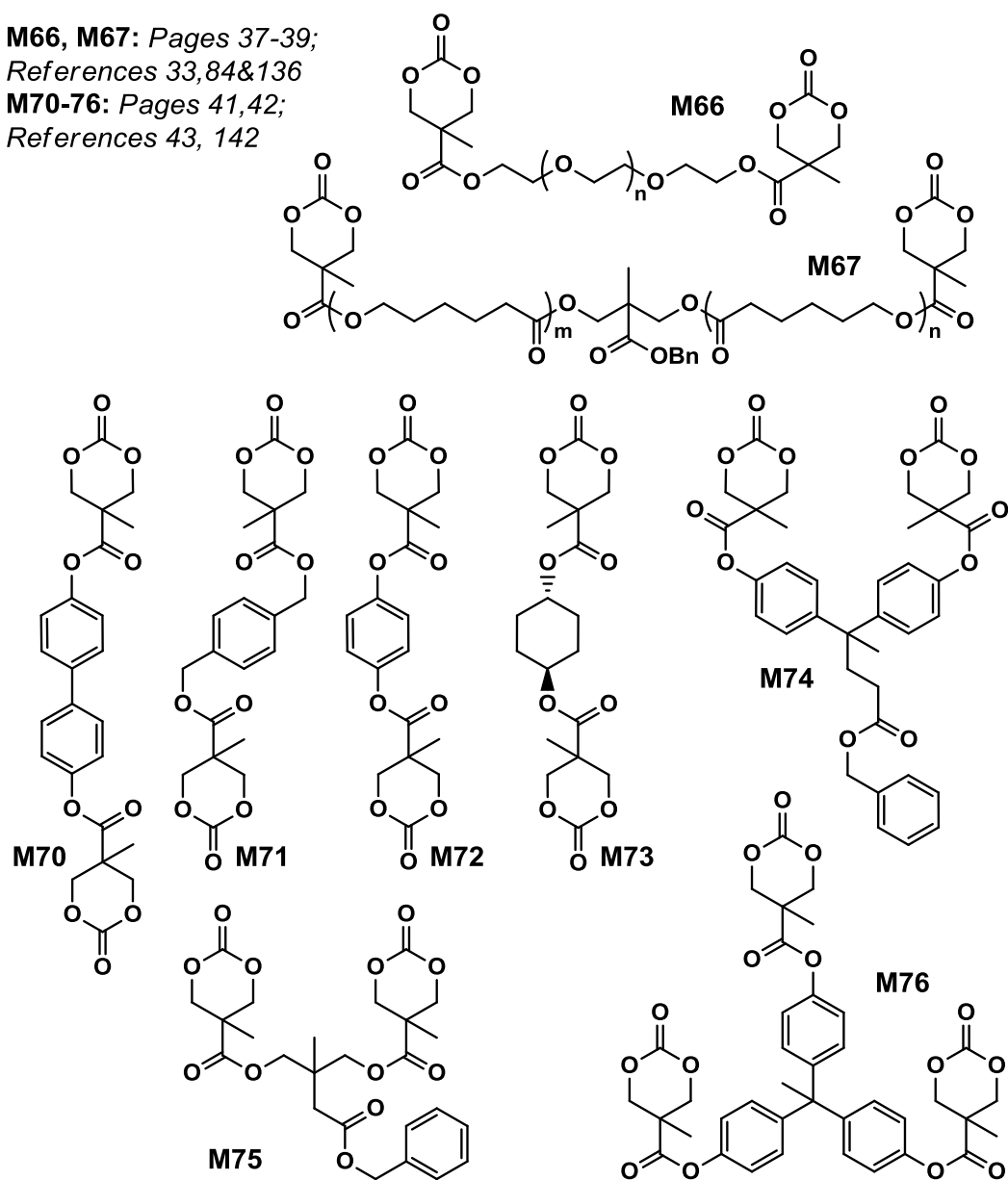
1.6.2. Overview of cyclic carbonate cross-linkers

M66, M67: Pages 37-39;

References 33,84&136

M70-76: Pages 41,42;

References 43, 142



1.7. References

1. Rokicki, G. *Prog. Polym. Sci.* **2000**, *25*, 259–342.
2. Uhrich, K. E.; Cannizzaro, S. M.; Langer, R. S.; Shakesheff, K. M. *Chem. Rev.* **1999**, *99*, 3181–3198.
3. Keul, H. *Polycarbonates*; Wiley-VCH Verlag GmbH & Co. KGaA: New York, **2009**; 307–327.
4. Zhang, Z.; Grijpma, D. W.; Feijen, J. *J. Control. Release* **2006**, *111*, 263–270.
5. Seyednejad, H.; Ghassemi, A. H.; van Nostrum, C. F.; Vermonden, T.; Hennink, W. E. *J. Control. Release* **2011**, *152*, 168–176.
6. Pitt, C. G.; Gu, Z. W. *J. Control. Release* **1987**, *4*, 283–292.
7. Fu, K.; Pack, D. W.; Klibanov, A. M.; Langer, R. *Pharm. Res.* **2000**, *17*, 100–106.
8. Pêgo, A.P.; Van Luyn, M. J. A.; Brouwer, L. A.; Van Wachem, P. B.; Poot, A. A.; Grijpma, D. W.; Feijen, J.; *J. Biomed. Mater. Res., Part A* **2003**, *67A*, 1044–1054.
9. Zhang, Z.; Kuijter, R.; Bulstra, S.K.; Grijpma, D.W.; Feijen, J. *Biomaterials* **2006**, *27*, 1741–1748.
10. Ochiai, B.; Endo, T. *Prog. Polym. Sci.* **2005**, *30*, 183–215.
11. Coates, G. W.; Moore, D. R. *Angew. Chem., Int. Ed.* **2004**, *43*, 6618–6639.
12. Darensbourg, D. J. *Chem. Rev.* **2007**, *107*, 2388–2410.

13. Darensbourg, D. J.; Mackiewicz, R. M.; Phelps, A. L.; Billodeaux, D. R. *Acc. Chem. Res.* **2004**, *37*, 836–844.
14. Feng, J.; Zhuo, R. X.; Zhang X. Z., *Prog. Polym. Sci.* **2012**, *37*, 211–236.
15. Kobayashi, S. *Macromol. Rapid Commun.* **2009**, *30*, 237–266.
16. Dove, A. P. *Chem. Commun.* **2008**, 6446–6470.
17. Matsumura, S.; Tsukada, K.; Toshima, K. *Macromolecules* **1997**, *30*, 3122–3124.
18. Storey, R. F.; Mullen, B. D.; Desai, G. S.; Sherman, J. W.; Tang, C. N. *J Polym. Sci. Part A: Polym. Chem.* **2002**, *40*, 3434–3442.
19. Kamber, N. E.; Jeong, W.; Waymouth, R. M.; Pratt, R. C.; Lohmeijer, B. G. G.; Hedrick, J. L. *Chem. Rev.* **2007**, *107*, 5813–5840.
20. Nederberg, F.; Lohmeijer, B. G. G.; Leibfarth, F.; Pratt, R. C.; Choi, J.; Dove, A. P.; Waymouth, R. M.; Hedrick, J. L. *Biomacromolecules* **2007**, *8*, 153–160.
21. Coulembier, O.; Sanders, D. P.; Nelson, A.; Hollenbeck, A. N.; Horn, H. W.; Rice, J. E.; Fujiwara, M.; Dubois, P.; Hedrick, J. L. *Angew. Chem., Int. Ed.* **2009**, *48*, 5170–5173.
22. Pastusiak, M.; Dobrzynski, P.; Kaczmarczyk, B.; Kasperczyk, J. *J. Polym. Sci., Part A: Polym. Chem.* **2011**, *49*, 2504–2512.
23. Yamamoto, Y.; Kaihara, S.; Toshima, K.; Matsumura, S. *Macromol. Biosci.* **2009**, *9*, 968–978.

24. Matsumura, S.; Tsukada, K.; Toshima, K. *Macromolecules* **1997**, *30*, 3122-3124.
25. Odelius, K.; Albertsson, A. C. *J. Polym. Sci., Part A: Polym. Chem.* **2008**, *46*, 1249-1264.
26. Dargaville, B. L.; Vaquette, C.; Peng, H.; Rasoul, F.; Chau, Y. Q.; Cooper-White, J. J.; Campbell, J. H.; Whittaker A. K. *Biomacromolecules* **2011**, *12*, 3856-3869.
27. Dai, S.; Xue, L.; Li, Z. *ACS Catal.* **2011**, *1*, 1421-1429.
28. Normand, M.; Kirillov, E.; Carpentier, J. F.; Guillaume, S. M. *Macromolecules* **2012**, *45*, 1122-1130.
29. Liu, J.; Zhang, C.; Liu, L. *J. Appl. Polym. Sci.* **2008**, *107*, 3275-3279.
30. Chapanian, R.; Tse, M. Y.; Pang, S. C.; Amsden, B. G., *J. Pharm. Sci.* **2012**, *101*, 588-597.
31. Ma, Z.; Hong, Y.; Nelson, D. M.; Pichamuthu, J. E.; Leeson, C. E.; Wagner, W. R. *Biomacromolecules* **2011**, *12*, 3265-3274.
32. Helou, M.; Moriceau, G.; Huang, Z. W.; Cammas-Marion, S.; Guillaume, S. M. *Polym. Chem.* **2011**, *2*, 840-850.
33. Nederberg, F.; Trang, V.; Pratt, R. C.; Mason, A. F.; Frank, C. W.; Waymouth, R. M.; Hedrick, J. L. *Biomacromolecules* **2007**, *8*, 3294-3297.
34. du Boullay, O. T.; Saffon, N.; Diehl, J.-P.; Martin-Vaca, B.; Bourissou, D. *Biomacromolecules* **2010**, *11*, 1921-1929.

35. Pounder, R. J.; Dove, A. P. *Biomacromolecules* **2010**, *11*, 1930–1939.
36. Pounder, R. J.; Dove, A. P. *Polym. Chem.* **2010**, *1*, 260.
37. Sanders, D. P.; Fukushima, K.; Coady, D. J.; Nelson, A.; Fujiwara, M.; Yasumoto, M.; Hedrick, J. L. *J. Am. Chem. Soc.* **2010**, *132*, 14724–14726.
38. Mindemark, J.; Bowden, T. *Polymer* **2011**, *52*, 5716–5722.
39. Wu, P.; Malkoch, M.; Hunt, J. N.; Vestberg, R.; Kaltgrad, E.; Finn, M. G.; Fokin, V. V.; Sharpless, K. B.; Hawker, C. J. *Chem. Commun.*, **2005**, 5775–5777.
40. Malkoch, M.; Malmstrom, E.; Hult, A. *Macromolecules* **2002**, *35*, 8307–8314.
41. Al-Azemi T. F.; Bisht, K. S. *Macromolecules* **1999**, *32*, 6536–6540.
42. Weilandt, K. D.; Keul, H.; Hocker, H. *Macromol. Chem. Phys.* **1996**, *197*, 3851–3868.
43. Pratt, R. C.; Nederberg, F.; Waymouth, R. M.; Hedrick, J. L. *Chem. Commun.* **2008**, 114–116.
44. Parzuchowski, P. G.; Jaroch, M.; Tryznowski, M.; Rokicki, G. *Macromolecules* **2008**, *41*, 3859–3865.
45. He, F.; Wang, Y. P.; Liu, G.; Jia, H. L.; Feng, J.; Zhuo, R. X. *Polymer* **2008**, *49*, 1185–1190.
46. Chen, W.; Yang, H.; Wang, R.; Cheng, R.; Meng, F.; Wei, W.; Zhong, Z. *Macromolecules* **2010**, *43*, 201–207.

47. Miyagawa, T.; Shimizu, M.; Sanda, F.; Endo, T. *Macromolecules* **2005**, *38*, 7944-7949.
48. Yang, J.; Hao, Q.; Liu, X.; Ba, C.; Cao, A. *Biomacromolecules* **2004**, *5*, 209-218.
49. Xie, Z.; Lu, C.; Chen, X.; Chen, L.; Wang, Y.; Hu, X.; Shi, Q.; Jing, X. *J. Polym. Sci., Part A: Polym. Chem.* **2007**, *45*, 1737-1745.
50. Pyo, S. H.; Persson, P.; Lundmark, S.; Hatti-Kaul, R. *Green Chem.* **2011**, *13*, 976-982.
51. Sanda, F.; Kamatani, J.; Endo, T. *Macromolecules* **2001**, *34*, 1564-1569.
52. Kumar, R.; Gao, W.; Gross, R. A. *Macromolecules* **2002**, *35*, 6835-6844.
53. Chen, X.; Gross, R. A. *Macromolecules* **1999**, *32*, 308-314.
54. Hu, X.; Chen, X.; Xie, Z.; Cheng, H.; Jing, X. *J. Polym. Sci., Part A: Polym. Chem.* **2008**, *46*, 7022-7032.
55. Youssefyeh, R. D.; Verheyden, J. P. H.; Moffatt, J. G. *J. Org. Chem.* **1979**, *44*, 1301-1309.
56. Zhang, X.; Zhong, Z.; Zhuo, R. *Macromolecules* **2011**, *44*, 1755-1759.
57. Zhu, W. P.; Wang, Y.; Zhang, Q.; Shen, Z. *J. Polym. Sci., Part A: Polym. Chem.* **2011**, *49*, 4886-4893.
58. Wang, H. F.; Su, W.; Zhang, C.; Luo, X.; Feng, J. *Biomacromolecules* **2010**, *11*, 2550-2557.
59. Chen, X.; McCarthy, S. P.; Gross, R. A. *Macromolecules* **1997**, *30*, 3470-3476.

60. Darensbourg, D. J.; Moncada, A. I.; Wei, S. H. *Macromolecules* **2011**, *44*, 2568–2576.
61. Helou, M.; Brusson, J. M.; Carpentier J. F.; Guillaume, S. M.; *Polym. Chem.* **2011**, *2*, 2789-2795.
62. Weiser, J. R.; Zawaneh, P. N.; Putnam, D. *Biomacromolecules* **2011**, *12*, 977–986.
63. Wang, R.; Chen, W.; Meng, F.; Cheng, R.; Deng, C.; Feijen, J.; Zhong, Z. *Macromolecules*, **2011**, *44*, 6009–6016.
64. Endo, T.; Kakimoto, K.; Ochiai, B.; Nagai, D. *Macromolecules* **2005**, *38*, 8177-8182.
65. van der Ende, A. E.; Kravitz, E. J.; Harth, E. *J. Am. Chem. Soc.* **2008**, *130*, 8706-8713.
66. van der Ende, A. E.; Harrell, J.; Sathiyakumar, V.; Meschievitz, M.; Katz, J.; Adcock, K.; Harth, E. *Macromolecules* **2010**, *43*, 5665–5671.
67. Qiao, Y.; Yang, C.; Coady, D. J.; Ong, Z. Y.; Hedrick, J. L.; Yang, Y. Y. *Biomaterials* **2012**, *33*, 1146-1153.
68. Kim, S. H.; Tan, J. P. K.; Fukushima, K.; Nederberg, F.; Yang, Y. Y.; Waymouth, R. M.; Hedrick, J. L.; *Biomaterials* **2011**, *32*, 5505-5514.
69. Nederberg, F.; Fukushima, K.; Colson, J.; Yang, C.; Nelson, A.; Yang, Y. Y.; Hedrick, J. L. *Biomaterials* **2010**, *31*, 8063-8071.
70. Ong, Z. Y.; Fukushima, K.; Coady, D. J.; Yang, Y. Y.; Ee, P. L. R.; Hedrick, J. L. *J. Control. Release* **2011**, *152*, 120–126.

71. Tan, J. P.K.; Kim, S. H.; Nederberg, F.; Fukushima, K.; Coady, D. J.; Nelson, A.; Yang, Y. Y.; Hedrick, J. L. *Macromol. Rapid Commun.* **2010**, *31*, 1187–1192.
72. Fukushima, K.; Pratt, R. C.; Nederberg, F.; Tan, J. P.K.; Yang, Y. Y.; Waymouth, R. M.; Hedrick, J. L. *Biomacromolecules* **2008**, *9*, 3051–3056.
73. He, F.; Wang, Y.; Feng, J.; Zhuo, R.; Wang, X. *Polymer* **2003**, *44*, 3215–3219.
74. He, F.; Wang, C. F.; Jiang, T.; Han, B.; Zhuo, R. X., *Biomacromolecules* **2010**, *11*, 3028–3035.
75. Zhang, X.; Chen, F.; Zhong, Z.; Zhuo, R. *Macromol. Rapid Commun.* **2010**, *31*, 2155–2159.
76. Zhang, X.; Mei, H.; Hu, C.; Zhong, Z.; Zhuo, R. *Macromolecules* **2009**, *42*, 1010-1016.
77. Nemoto, N.; Sanda, F.; Endo, T.; *J. Polym. Sci., Part A: Polym. Chem.* **2001**, *39*, 1305–1317.
78. Ariga, T.; Takata, T.; Endo, T. *Macromolecules* **1997**, *30*, 737-744.
79. Ling, J.; Shen, Z.; Huang, Q. *Macromolecules* **2001**, *34*, 7613-7616.
80. Peng, H.; Ling, J.; Liu, J.; Zhu, N.; Ni, X.; Shen, Z. *Polym. Degrad. Stab.* **2010**, *95*, 643-650.
81. Liu, B.; Cui, D. *J. Appl. Polym. Sci.* **2009**, *112*, 3110–3118.
82. Cai, J.; Zhu, K. J.; Yang, S. L. *Polymer* **1998**, *39*, 4409-4415.

83. Helou, M.; Miserque, O.; Brusson, J. M.; Carpentier, J. F.; Guillaume, S. M. *Chem. Eur. J.* **2010**, *16*, 13805–13813.
84. Bartolini, C.; Mespouille, L.; Verbruggen, I.; Willem, R.; Dubois, P.; *Soft Matter* **2011**, *7*, 9628–9637.
85. Zelikin, A. N.; Zawaneh, P. N.; Putnam, D. *Biomacromolecules* **2006**, *7*, 3239–3244.
86. Zawaneh, P. N.; Doody, A. M.; Zelikin, A. N.; Putnam, D. *Biomacromolecules* **2006**, *7*, 3245–3251.
87. Brignou, P.; Carpentier, J. F.; Guillaume, S. M. *Macromolecules* **2011**, *44*, 5127–5135.
88. Ling, J.; Dai, Y.; Zhu, Y.; Sun, W.; Shen, Z. *J. Polym. Sci., Part A: Polym. Chem.* **2010**, *48*, 3807–3815.
89. Al-Azemi, T. F.; Harmon, J. P.; Bisht, K. S. *Biomacromolecules* **2000**, *1*, 493–500.
90. Gong, F.; Cheng, X.; Wang, S.; Zhao, Y.; Gao, Y.; Cai, H. *Acta Biomater.* **2010**, *6*, 534–546.
91. Yuan, Y.; Jing, X.; Xiao, H.; Chen, X.; Huang, Y.; *J. Appl. Polym. Sci.* **2011**, *121*, 2378–2385.
92. Xie, Z.; Hu, X.; Chen, X.; Lu, T.; Liu, S.; Jing, X. *J. Appl. Polym. Sci.* **2008**, *110*, 2961–2970.
93. Danquah, M.; Fujiwara, T.; Mahato, R. I. *Biomaterials* **2010**, *31*, 2358–2370.

94. Lu, W.; Li, F.; Mahato, R. I. *J. Pharm. Sci.* **2011**, *100*, 2418–2429.
95. Lu, J.; Shoichet, M. S. *Macromolecules* **2010**, *43*, 4943–4953.
96. Seow, W. Y.; Yang, Y. Y.; *J. Control. Release* **2009**, *139*, 40–47.
97. Ray III, W. C.; Grinstaff, M. W.; *Macromolecules* **2003**, *36*, 3557–3562.
98. Wang, X. L.; Zhuo, R. X.; Liu, L. J.; He, F.; Liu, G. *J. Polym. Sci., Part A: Polym. Chem.* **2002**, *40*, 70–75.
99. Feng, J.; Wang, X. L.; He, F.; Zhuo, R. X. *Macromol. Rapid Commun.* **2007**, *28*, 754–758.
100. Mei, L. L.; Yan, G. P.; Yu, X. H.; Cheng, S. X.; Wu, J. Y. *J. Appl. Polym. Sci.* **2008**, *108*, 93–98.
101. Chen, H.; Yan, G. P.; Li, L.; Ai, C. W.; Yu, X. H. *J. Appl. Polym. Sci.* **2009**, *114*, 3087–3096.
102. Chen, W.; Meng, F.; Li, F.; Ji, S. J.; Zhong, Z. *Biomacromolecules* **2009**, *10*, 1727–1735.
103. Xie, Z.; Hu, X.; Chen, X.; Mo, G.; Sun, J.; Jing, X. *Adv. Eng. Mater.* **2009**, *11*, B7–B11.
104. Xie, Z.; Hu, X.; Chen, X.; Sun, J.; Shi, Q.; Jing, X. *Biomacromolecules* **2008**, *9*, 376–380.
105. Tasdelen, M. A. *Polym. Chem.* **2011**, *2*, 2133–2145.
106. Iha, R. K.; Wooley, K. L.; Nyström, A. M.; Burke, D. J.; Kade, M. J.; Hawker, C. J.; *Chem. Rev.* **2009**, *109*, 5620–5686.
107. Meldal, M.; Tornøe, C. W. *Chem. Rev.* **2008**, *108*, 2952–3015.

108. Hoyle, C. E. Bowman, C. N. *Angew. Chem. Int. Ed.* **2010**, *49*, 1540 – 1573.
109. Konkolewicz, D.; Gray-Weale, A.; Perrier, S. *J. Am. Chem. Soc.* **2009**, *131*, 18075–18077.
110. Ates, Z.; Thornton, P. D. Heise, A. *Polym. Chem.* **2011**, *2*, 309–312.
111. Riva, R.; Schmeits, S.; Stoffelbach, F.; Jérôme, C.; Jérôme, R.; Lecomte, P. *Chem. Commun.* **2005**, 5334–5336.
112. Hu, X.; Chen, X.; Xie, Z.; Liu, S.; Jing, X. *J. Polym. Sci., Part A: Polym. Chem.* **2007** *45*, 5518–5528.
113. Hu, X.; Chen, X.; Liu, S.; Shi, Q.; Jing, X. *J. Polym. Sci., Part A: Polym. Chem.* **2008** *46*, 1852–1861.
114. Hu, X.; Chen, X.; Wei, J.; Liu, S.; Jing, X. *Macromol. Biosci.* **2009**, *9*, 456–463.
115. Yue, J.; Li, X.; Mo, G.; Wang, R.; Huang, Y.; Jing, X. *Macromolecules* **2010**, *43*, 9645–9654.
116. Wang, C. F.; Lin, Y. X.; Jiang, T.; He, F.; Zhuo, R. *Biomaterials* **2009**, *30*, 4824–4832.
117. Mullen, B. D.; Tang, C. N.; Storey, R. F. *J. Polym. Sci., Part A: Polym. Chem.* **2003**, *41*, 1978–1991.
118. Chen, X.; McCarthy, S. P.; Gross, R. A. *Macromolecules* **1998**, *31*, 662–668.

119. Hu, X.; Chen, X.; Cheng, H.; Jing, X. *J. Polym. Sci., Part A: Polym. Chem.* **2009**, *47*, 161–169.
120. Yang, R.; Meng, F.; Ma, S.; Huang, F.; Liu, H.; Zhong, Z. *Biomacromolecules* **2011**, *12*, 3047–3055.
121. Yu, Y.; Deng, C.; Meng, F.; Shi, Q.; Feijen, J.; Zhong, Z. *J. Biomed. Mater. Res., Part A* **2011**, *99A*, 316–326.
122. Murayama, M.; Sanda F.; Endo, T. *Macromolecules* **1998**, *31*, 919–923.
123. Onbulak, S.; Tempelaar, S.; Pounder, R. J.; Gok, O.; Sanyal, R.; Dove, A. P.; Sanyal, A. *Macromolecules* **2012**, *45*, 1715–1722.
124. Lia, T.; Jing, X.; Huang, Y. *Polym. Adv. Technol.* **2011**, *22* 1266–1271.
125. Y.; Han, Quan Shi, Junli Hu, Qing Du, Xuesi Chen, Xiabin Jing, *Macromol. Biosci.* **2008**, *8*, 638–644.
126. Shia, Q.; Chena, X.; Lua T.; Jing, X. *Biomaterials* **2008**, *29*, 1118–1126.
127. Shi, Q.; Huang, Y.; Chen, X.; Wu, M.; Sun, J.; Jing, X. *Biomaterials* **2009**, *30*, 5077–5085.
128. Lu, C.; Shi, Q.; Chen, X.; Lu, T.; Xie, Z.; Hu, X.; Ma, J.; Jing, X. *J. Polym. Sci., Part A: Polym. Chem.* **2007**, *45*, 3204–3217.
129. Gou, P. F.; Zhu, W. P.; Shen, Z. Q. *Polym. Chem.*, **2010**, *1*, 1205–1214.
130. Xu, J.; Filion, T. M.; Prifti, F.; Song, J. *Chem. Asian J.* **2011**, *6*, 2730–2737.
131. Xu, J.; Prifti, F.; Song, J. *Macromolecules* **2011**, *44*, 2660–2667.

132. Yang, C.; Ong, Z. Y.; Yang, Y. Y.; Ee, P. L. R.; Hedrick, J. L. *Macromol. Rapid Commun.* **2011**, *32*, 1826–1833.
133. Nederberg, F.; Zhang, Tan, Y.; J. P. K.; Xu, K.; Wang, H.; Yang, C.; Gao, S.; Guo, X. D.; Fukushima, K.; Li, L.; Hedrick, J. L.; Yang, Y. Y. *Nat. Chem.* **2011**, *3*, 409–414.
134. Cooley, C. B.; Trantow, B. M.; Nederberg, F.; Kiesewetter, M. K.; Hedrick, J. L.; Waymouth, R. M.; Wender, P. A. *J. Am. Chem. Soc.* **2009**, *131*, 16401–16403.
135. Zhang, X.; Cai, M.; Zhong, Z.; Zhuo, R. *Macromol. Rapid Commun.* **2012**, DOI: 10.1002/marc.201100765.
136. Nederberg, F.; Trang, V.; Pratt, R. C.; Kim, S. H.; Colson, J.; Nelson, A.; Frank, C. W.; Hedrick, J. L.; Dubois P.; Mespouille, L. *Soft Matter*, **2010**, *6*, 2006–2012.
137. Slavin, S.; Burns, J.; Haddleton, D. M.; Becer, C. R. *Eur. Polym. J.* **2011**, *47*, 435–446.
138. Shen, Y.; Chen, X.; Gross, R. A.; *Macromolecules* **1999**, *32*, 3891–3897.
139. Shen, Y.; Chen, X.; Gross, R. A.; *Macromolecules* **1999**, *32*, 2799–2802.
140. Suriano, F.; Pratt, R.; Tan, J. P. K.; Wiradharma, N.; Nelson, A.; Yang, Y. Y.; Dubois, P.; Hedrick, J. L. *Biomaterials* **2010**, *31*, 2637–2645.
141. Coulembier, O.; Moins, S.; Dubois, P. *Macromolecules* **2011**, *44*, 7493–7497.
142. Al-Azemi, T.F.; Bisht, K. S.; *Polymer* **2002**, *43*, 2161–2167.

143. Luo, X.; Huang, F.; Qin, S.; Wang, H.; Feng, J.; Zhang, X.; Zhuo, R. *Biomaterials* **2011**, *32*, 9925-9939.
144. Su, W.; Luo, X.; Wang, H.; Li, L.; Feng, J.; Zhang, X. Z.; Zhuo, R. *Macromol. Rapid Commun.* **2011**, *32*, 390-396.
145. Li, F.; Danquah, M.; Mahato, R. I. *Biomacromolecules* **2010**, *11*, 2610-2620.
146. Lu, J.; Shi, M.; Shoichet, M. S. *Bioconjugate Chem.* **2009**, *20*, 87-94.
147. Hu, X.; Liu, S.; Chen, X.; Mo, G.; Xie, Z.; Jing, X. *Biomacromolecules* **2008**, *9*, 553-560.
148. Lee, A. L. Z.; Venkataraman, S.; Sirat, S. B. M.; Gao, S.; Hedrick, J. L.; Yang, Y. Y.; *Biomaterials* **2012**, *33*, 1921-1928.
149. Vandenberg, E. J.; Tian, D. *Macromolecules* **1999**, *32*, 3613-3619.

Chapter 2

Organocatalytic Synthesis and post-Polymerisation Functionalisation of Allyl-Functional Poly(carbonate)s

Well-defined allyl-functional poly(carbonate)s were synthesised *via* the organocatalytic ring-opening polymerisation of 5-methyl-5-allyloxycarbonyl-1,3-dioxan-2-one using the dual 1-(3,5-bis(trifluoromethyl)phenyl)-3-cyclohexylthiourea and (-)-sparteine catalyst system. The resulting allyl-functional poly(carbonate)s obtained showed low polydispersities and high end-group fidelity, with the versatility of the system being demonstrated by the synthesis of block copolymers and telechelic polymers. Further functionalisation of homopolymers with degrees of polymerisation of 11 and 100 were realised *via* the radical addition of thiols to the pendant allyl functional groups, resulting in a range of functional aliphatic poly(carbonate)s.

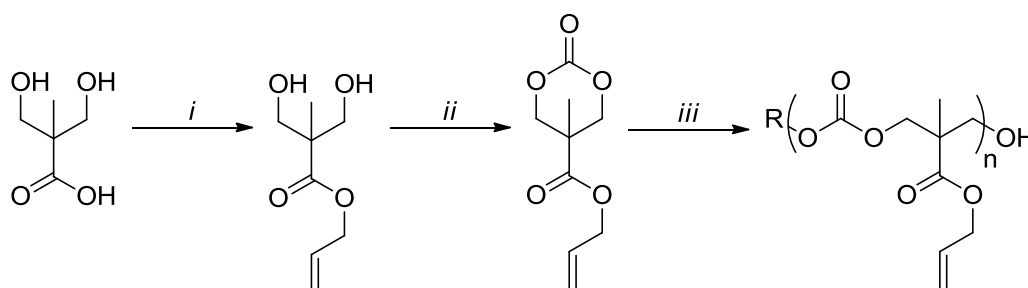
2.1. Introduction

As a consequence of their unsaturation, pendant allyl groups provide a versatile option for ready functionalisation of the polymer backbone *via* radical addition of thiols, epoxidation, halogenation, and hydroboration, among others.¹⁻⁷ The introduction of a pendant carbon-carbon double bond in a poly(carbonate) backbone has previously been reported *via* the ring-opening polymerisation (ROP) of an allyl ester functional cyclic carbonate, 5-methyl-5-allyloxycarbonyl-1,3-dioxan-2-one (MAC).⁸⁻¹¹ However, previous studies have mostly focused on its copolymerisation with lactide.⁸⁻¹⁶ The reported homopolymerisations were either performed without added catalyst at 115 °C¹⁰, or at elevated temperatures using metal-based catalysts^{8,10} and resulted in relatively poor control, large polydispersities and, in some cases, branched polymers. Recent advances in the ring-opening polymerisation of cyclic esters and cyclic carbonates have led to marked improvements in selectivity and polymerisation control, in particular the application of organocatalysts.¹⁷⁻²⁵ Herein, the utilisation of these highly specific organocatalysts for the controlled ROP of the allyl ester-functional cyclic carbonate, MAC, is reported along with its post-polymerisation functionalisation *via* radical addition of thiols to the pendant allyl groups, giving rise to a range of functional poly(carbonate)s through mild, versatile, and selective routes.

2.2. Results and Discussion

2.2.1. Synthesis of 5-methyl-5-allyloxycarbonyl-1,3-dioxan-2-one, MAC.

Owing to the electrophilic nature of allyl bromide, 5-methyl-5-allyloxycarbonyl-1,3-dioxan-2-one (MAC) was able to be synthesised in a simple two-step literature procedure (Scheme 2.1).⁸ In the first step, the allyl functionalised diol was synthesised by heating 2,2-bis(hydroxymethyl)propionic acid and potassium hydroxide in dimethyl formamide (DMF) at 100 °C for one hour to form the 2,2-bis(hydroxymethyl)propionic acid potassium salt. The allyl bromide was added and the mixture was kept at 45 °C for 16 hours. After purification by distillation, the cyclic carbonate could then be formed by ring closure using ethyl chloroformate in the presence of triethylamine to trap the hydrochloric acid by formation of the NEt₃.HCl salt. The product had to be recrystallised several times to remove all impurities and dried extensively before its use in ROP.



Scheme 2.1. Synthesis and ring-opening polymerisation of 5-methyl-5-allyloxycarbonyl-1,3-dioxan-2-one, MAC. Conditions: (i) allyl bromide, KOH, DMF, 100 °C (1h), then 45 °C (16h); (ii) ethyl chloroformate, NEt₃, THF, 0 °C; (iii) ROH, catalyst, CDCl₃, RT.

2.2.2. Organocatalytic Ring-Opening Polymerisation of 5-methyl-5-allyloxycarbonyl-1,3-dioxan-2-one, MAC.

Initial studies into the ring-opening polymerisation of MAC were performed using organic catalysts. Polymerisations were carried out in CDCl_3 or methylene chloride (0.5 M MAC) at 25 °C with monomer-to-initiator ratio, $[\text{M}]/[\text{I}] = 20$ using benzyl alcohol or neopentyl alcohol as alcohol initiator (Scheme 2.1).

2.2.2.1. Organocatalytic Ring-Opening Polymerisation of 5-methyl-5-allyloxycarbonyl-1,3-dioxan-2-one, MAC: Choice of catalyst.

The organocatalytic ROP of MAC was investigated using a range of organic catalysts that had previously been studied for the ring-opening polymerisation of lactide and trimethylene carbonate (Figure 2.1).^{20,23,24,26,27} The polymerisations could be monitored by the disappearance of the

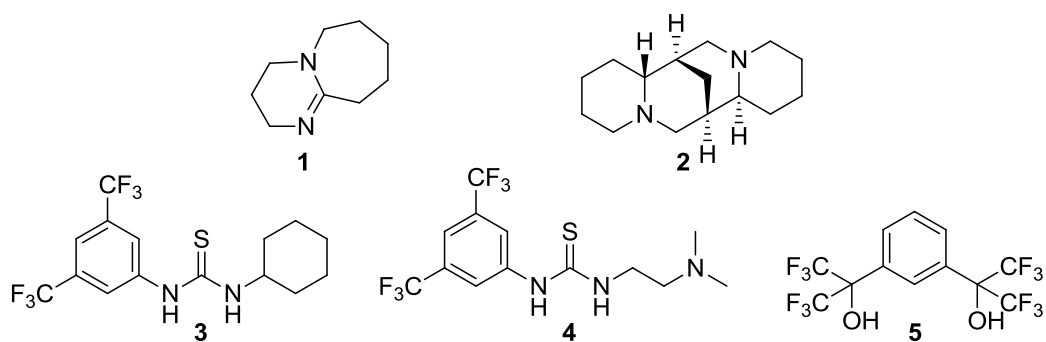


Figure 2.1. Organic catalysts screened for the ring-opening polymerisation of MAC.

methylene resonances in the carbonate ring at $\delta = 4.21$ ppm and $\delta = 4.71$ ppm and the appearance of a multiplet at $\delta = 4.23$ - 4.37 ppm corresponding to the methylene resonances in the polymer backbone and by the shift of the methyl resonance from $\delta = 1.35$ ppm in the monomer to $\delta = 1.27$ ppm in the poly(carbonate) (Figure 2.2). After precipitation from CDCl_3 or CH_2Cl_2 into cold hexanes, residual catalyst could be removed by column chromatography to yield pure polymers.

Although application of the highly active 1,8-diazabicyclo[5.4.0]undec-7-ene (1, DBU) as catalyst in the ROP of trimethylene carbonate resulted in excellent control,²³ this was not the case when used as a catalyst in the ROP

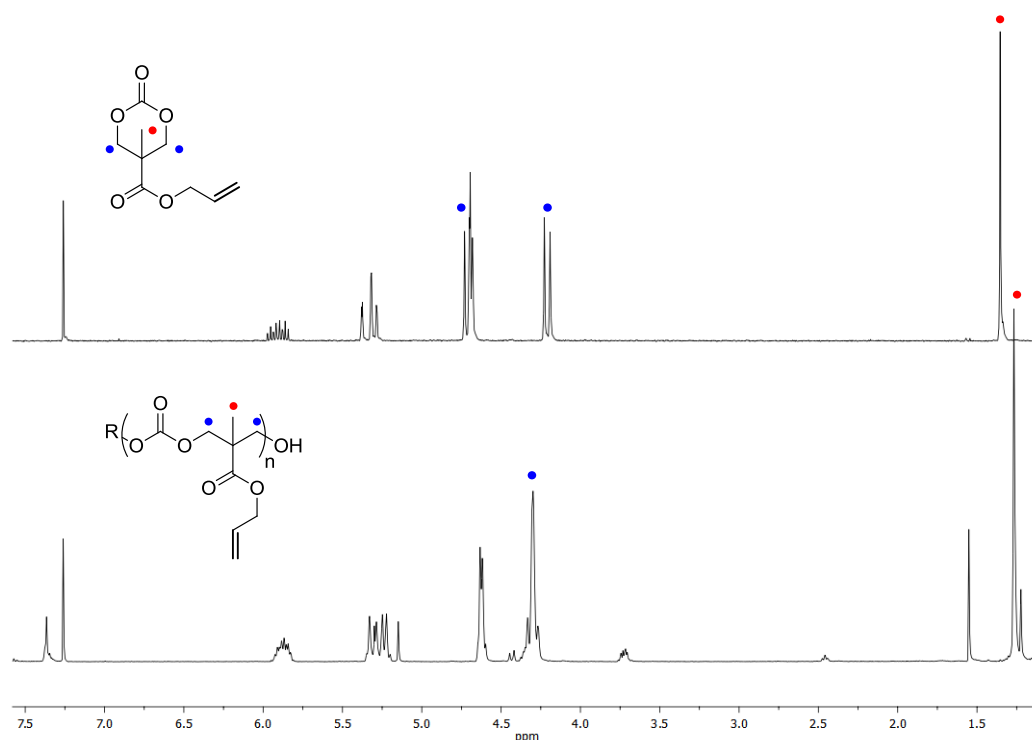


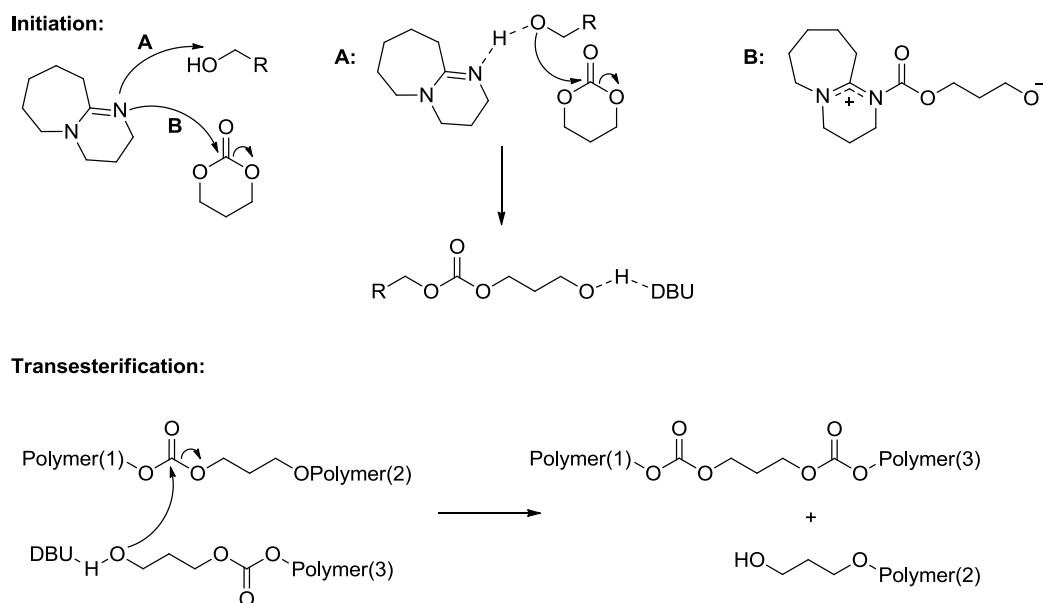
Figure 2.2. Comparison of the ^1H NMR spectra of MAC (top) and of PMAC (bottom) initiated from benzyl alcohol (CDCl_3 ; 400 MHz, 298 K). Shifts in the methyl (●) and the methylene (●) resonances are observed upon polymerisation.

of MAC. ^1H NMR spectroscopic analysis of the polymerisation revealed a linear increase of monomer conversion against time when using 5 mol% DBU until *ca.* 70% monomer conversion, at which point the polymerisations became severely retarded with isolated polymers displaying broadening molecular weight distributions (from PDI = 1.15 to >1.80) ultimately leading to bimodal gel permeation chromatography (GPC) traces (Table 2.1; entry 1). Indeed a highly active catalyst such as DBU is a strong enough base ($\text{p}K_{\text{a}} = 24.3$) to catalyse ROP of cyclic monomers without addition of a cocatalyst to activate the monomer (Scheme 2.2).¹⁹ In addition, DBU has also been reported to be able to act as an initiator in the ROP of cyclic carbonate and is known to promote transesterification.^{19,28} For these reasons, it was hypothesised that in MAC polymerisations catalysed by DBU, transesterification of the main

Table 2.1. Catalyst screening for the ring-opening polymerisation of MAC^a

catalyst(s)	time (h)	monomer conversion (%) ^b	M_n^c (g mol ⁻¹)	PDI ^c
1 ^d	4	90	10 700	1.80
2 ^e +3 ^f	51.5	92	4600	1.12
2 ^e +4 ^f	768	94	4200	1.13
2 ^e +5 ^f	70	88	3530	1.12
1 ^d +3 ^f	4	92	10 470	1.49

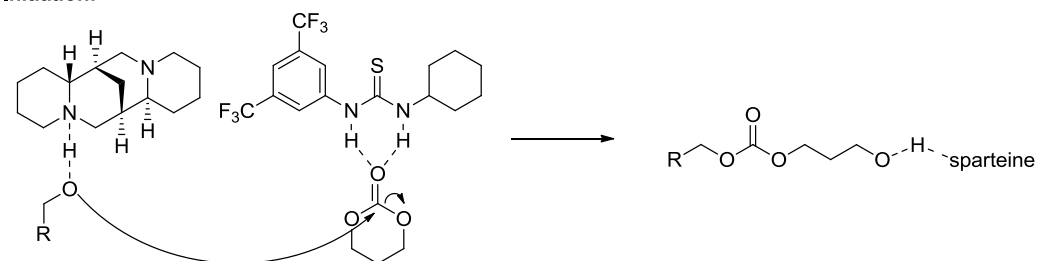
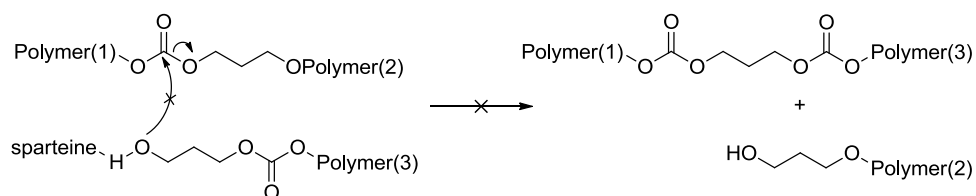
^a Reactions were performed in CDCl_3 at 25 °C, $[\text{MAC}] = 0.5 \text{ M}$, $[\text{M}]/[\text{I}] = 20$, using benzyl alcohol as initiator. ^b Measured by ^1H NMR spectroscopy. ^c Determined by GPC analysis in tetrahydrofuran (THF). ^d 5 mol% DBU (1), neopentanol was used as initiator. ^e 5 mol% (-)-sparteine (2). ^f 10 mol% co-catalyst (3-5).



Scheme 2.2. Possible reaction pathways for initiation of cyclic carbonates in the presence of DBU: DBU could act as an alcohol activating species (A) or as an initiator (B). In addition, DBU could promote transesterification of the resulting poly(carbonate)s.

chains and side chains was the main event taking place after *ca.* 70% monomer conversion leading to molecular scrambling and broadening of the molecular weight distribution. As such, the focus was turned to the bifunctional catalyst systems. These systems use sparteine, a catalyst that is less basic ($pK_a = 17.5$) and does not catalyse the ROP of cyclic monomers without an added cocatalyst for monomer activation. Furthermore, NMR studies involving thiourea cocatalyst **3** have shown that pronounced hydrogen bonding occurs with cyclic carbonates or esters, while significantly less hydrogen bonding is observed between **3** and ring-opened esters and carbonates (Scheme 2.3).^{19,20,23,24} For the ring-opening polymerisation of MAC using (-)-sparteine, **2** (5 mol%), in combination with either thiourea, **3** or **4**,

or $\alpha,\alpha,\alpha',\alpha'$ -tetrakis-(trifluoromethyl)-1,3-benzenedimethanol (**5**) (10 mol%), good control of the polymerisation was observed (Table 2.1; entries 2-4). Of these systems, the **2/3** system resulted in the best combination of activity and polymerisation control and was therefore chosen as catalyst system for the ring-opening polymerisation of MAC.

Initiation:**Transesterification:**

Scheme 2.3. Initiation of cyclic carbonates from ROH catalysed by the bifunctional catalyst system of sparteine and thiourea **3**. As a result of the low basicity of (-)-sparteine and a preference for **3** to coordinate cyclic monomers, no transesterification occurs.

2.2.2.2. Organocatalytic Ring-Opening Polymerisation of 5-methyl-5-allyloxycarbonyl-1,3-dioxan-2-one, MAC: Polymerisation control.

Investigation of the living characteristics of the polymerisation catalysed by **3** and (-)-sparteine (**2**) led to the observation of a linear correlation between number average molecular weight (M_n) against monomer conversion (Figure 2.3) and initial monomer-to-initiator ratio ($[M]_0/[I]_0$) while retaining low PDI values throughout the polymerisation (Figure 2.4).

Analysis of DP10 and DP100 polymer using ^1H NMR spectroscopy confirmed degrees of polymerisation (DP) of 11 and 100, respectively, by comparison of the integration of the resonances at $\delta = 7.37$ (ArH) and 5.15 (CH₂) ppm

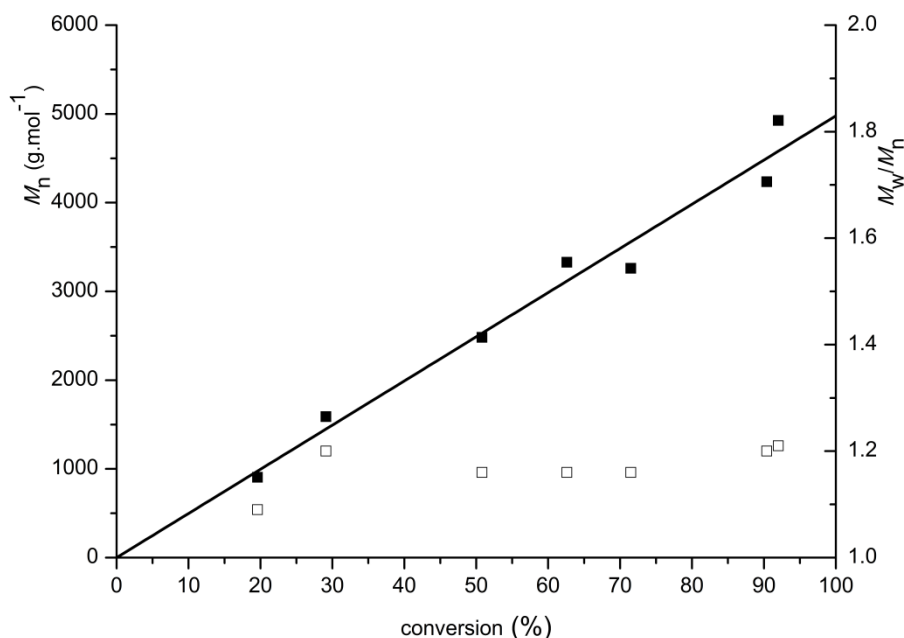


Figure 2.3. Plot of number-average molecular weight (M_n ; ■) and polydispersity (M_w/M_n ; □) against % monomer conversion in the ring-opening polymerisation of MAC. Conditions: [MAC] = 0.5 M CDCl_3 at 25 °C, 5 mol% **2**, 10 mol% **3**, $[M]/[I] = 20$ using benzyl alcohol as initiator.

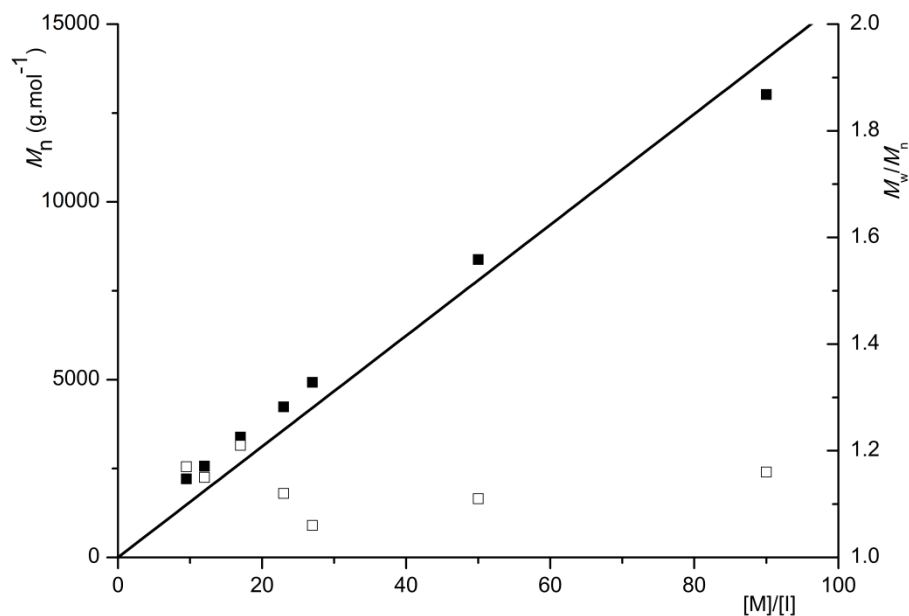


Figure 2.4. Plot of number-average molecular weight (M_n ; ■) and polydispersity (M_w/M_n ; □) against initial monomer-to-initiator ratio, $[M]_0/[I]_0$, in the ring-opening polymerisation of MAC. Conditions: $[MAC] = 0.5$ M $CDCl_3$ at 25 °C, 5 mol% **2**, 10 mol% **3**, using benzyl alcohol as initiator.

originating from the benzyl alcohol initiator group against the methylene and methyl resonances on the polymer backbone (Figure 2.5). The 1H NMR spectrum of the DP11 polymer, reveals resonances corresponding to the monomer unit at the hydroxyl chain end at $\delta = 3.72$ ppm (CH_2OH), 1.22 ppm (CH_3) and 2.46 ppm (OH). Further analysis of the DP10 polymer by MALDI-ToF MS revealed a single distribution with a spacing of 200 m/z , which is equal to that of a repeat unit (Figure 2.6; Table 2.2). The main peak at $m/z = 2533$ corresponds to a sodium charged polymer chain of DP12 with a benzyl alcohol end group. All observations suggest that the **2+3** catalysed ring-opening polymerisation of MAC proceeds in a controlled and living manner.

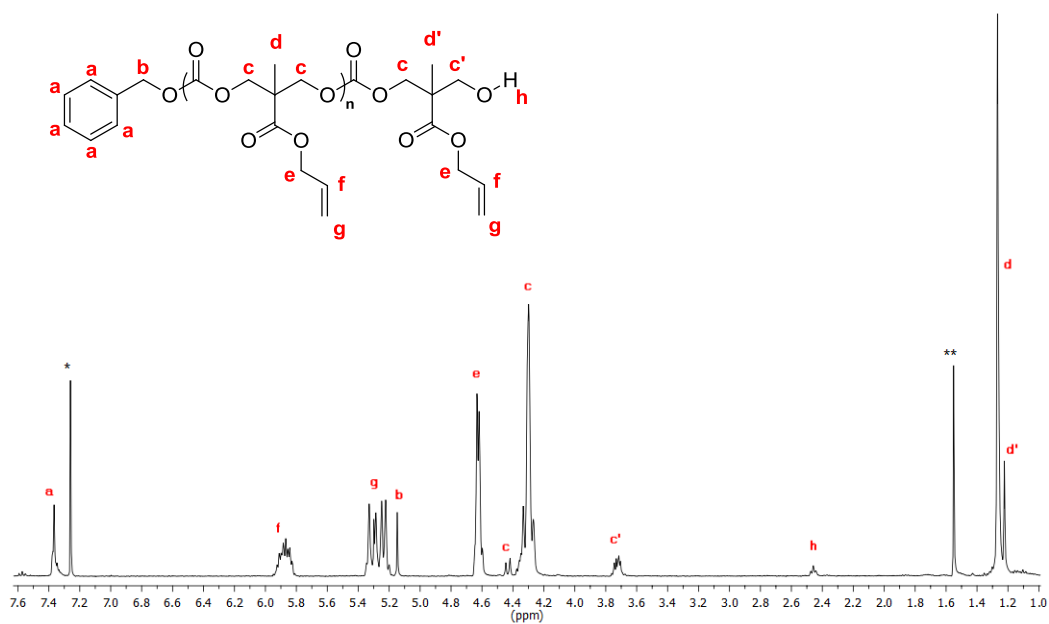


Figure 2.5. ^1H NMR in CDCl_3 of PMAC_{11} initiated from benzyl alcohol using 5 mol% **2** and 10 mol% **3** (400 MHz, 293 K; * = residual CDCl_3 , ** = H_2O).

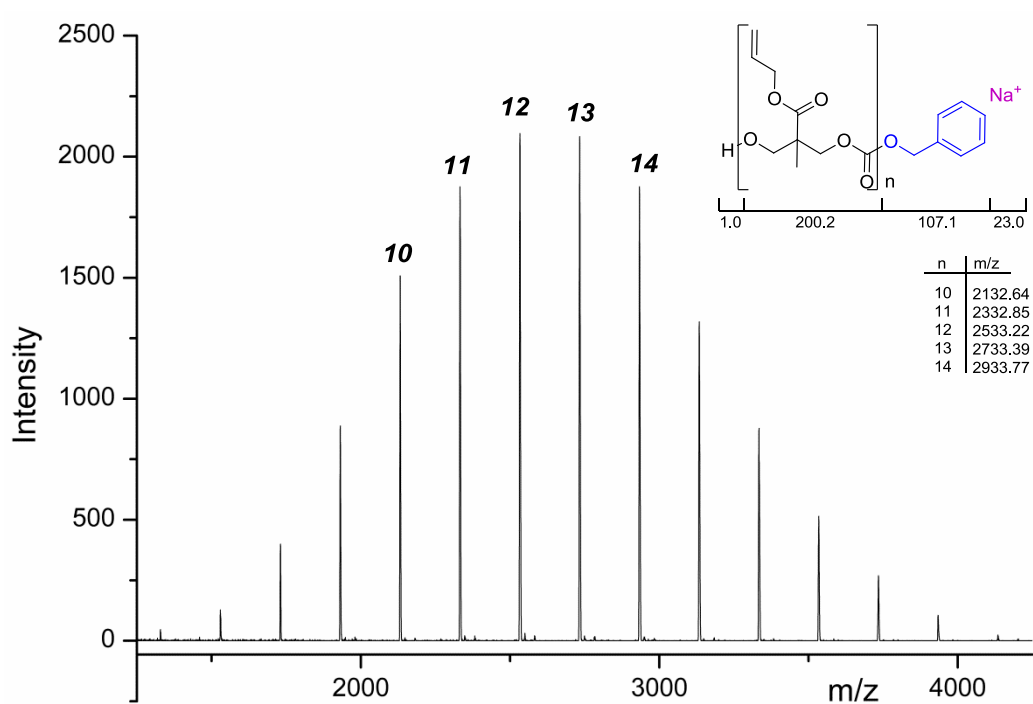


Figure 2.6. MALDI-TOF MS analysis of PMAC ($\text{DP} = 11$) initiated from benzyl alcohol using 5 mol% **2** and 10 mol% **3**.

Table 2.2. Theoretical and observed m/z values of PMAC₁₁ (Figure 2.6).

DP	Experimental m/z	Calculated m/z
10	2132.6	2132.7
11	2332.9	2332.8
12	2533.2	2532.9
13	2733.4	2732.9
14	2933.8	2933.0

2.2.2.3. Organocatalytic Ring-Opening Polymerisation of 5-methyl-5-allyloxycarbonyl-1,3-dioxan-2-one, MAC: Telechelics and block copolymers.

Initiator versatility was investigated by the synthesis of telechelic PMAC ($[M]/[I] = 10$ per hydroxyl group) initiated from 1,3-propanediol (**6**), 2-hydroxyethyl disulphide (**7**), **8** and **9** (Figure 2.7). ¹H NMR spectroscopic analysis of these polymers revealed resonances expected for the initiating alcohols with integration against the main chain polymer resonances being consistent with polymers with a total degree of polymerisation of 18, 24, 16 and 20, respectively. MALDI-ToF MS analysis of all polymers showed distributions with a spacing of 200 m/z . The main peaks in the spectra of 1,3-propanediol and 2-hydroxyethyl disulphide at $m/z = 3502$ (DP17) and $m/z = 4380$ (DP21), respectively, both correspond to the values expected for telechelic PMAC initiated from **6** and **7**. In both the cases, however, a second smaller

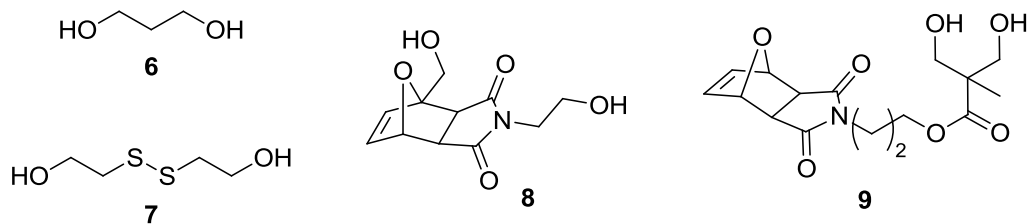
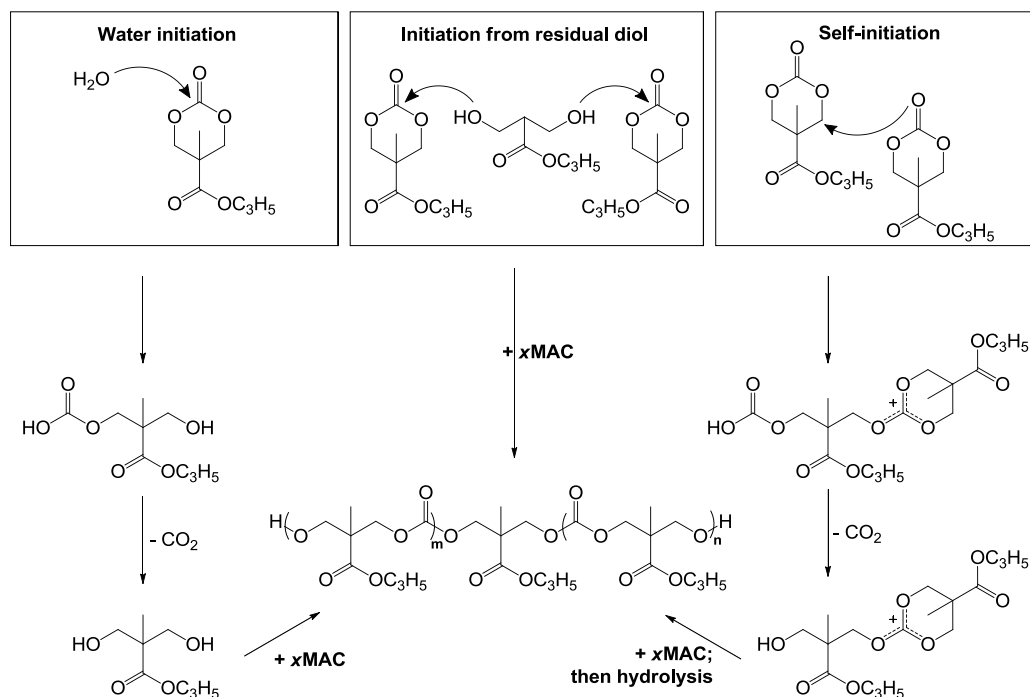


Figure 2.7. Bifunctional initiators used in the ring-opening polymerisation of MAC.

distribution could be observed by MALDI-ToF MS. This distribution could originate either by initiation from allyl diol impurities, by monomer initiated ROP according to an active chain-end mechanism as recently proposed by Delcroix *et al.*²⁹, but are most likely due to residual water within the system (Scheme 2.4). In the case of protected maleimide type initiators (**8** and **9**) distributions could be observed corresponding to the products obtained after retro-Diels Alder reaction. The reaction was most likely induced by the energy released by the laser during analysis as the NMR spectra of both polymers correspond to polymers initiated from **8** and **9**. No resonances corresponding to species obtained by retro-Diels Alder reaction were observed in the NMR spectra. In the case of **9** a distribution was observed with a main peak at $m/z = 4898$ (DP23), whereas in the case of **8** two distributions were observed with main peaks at $m/z = 2166$ (DP10) and $m/z = 2123$ (DP10) corresponding to PMAC with a furan chain end and PMAC with a maleimide chain end (Figure 2.8; Table 2.3).



Scheme 2.4. Possible routes for the formation of the secondary species observed in the MALDI-ToF spectra of 1,3-propanediol and 2-hydroxyethyl disulphide.

Initiator versatility was further demonstrated by the synthesis of a MeO-PEO₁₁₄-*b*-PMAC₂₀-OH block copolymer by initiation of MAC polymerisation from commercially available poly(ethylene oxide) monomethyl ether-5K that when characterized by GPC analysis in THF against poly(styrene) standards (comparable to the PMAC polymers) revealed a $M_n = 7\,520\text{ g mol}^{-1}$ (PDI = 1.03). Chain growth was confirmed by GPC analysis with the block copolymer showing a shift to higher molecular weight ($M_n = 11\,900\text{ g mol}^{-1}$; PDI = 1.06; Figure 2.9). To further demonstrate the living nature of the system, block copolymers of PMAC with poly(lactide), PLA, were synthesized both by chain growth of PMAC from a PLA synthesised using the same

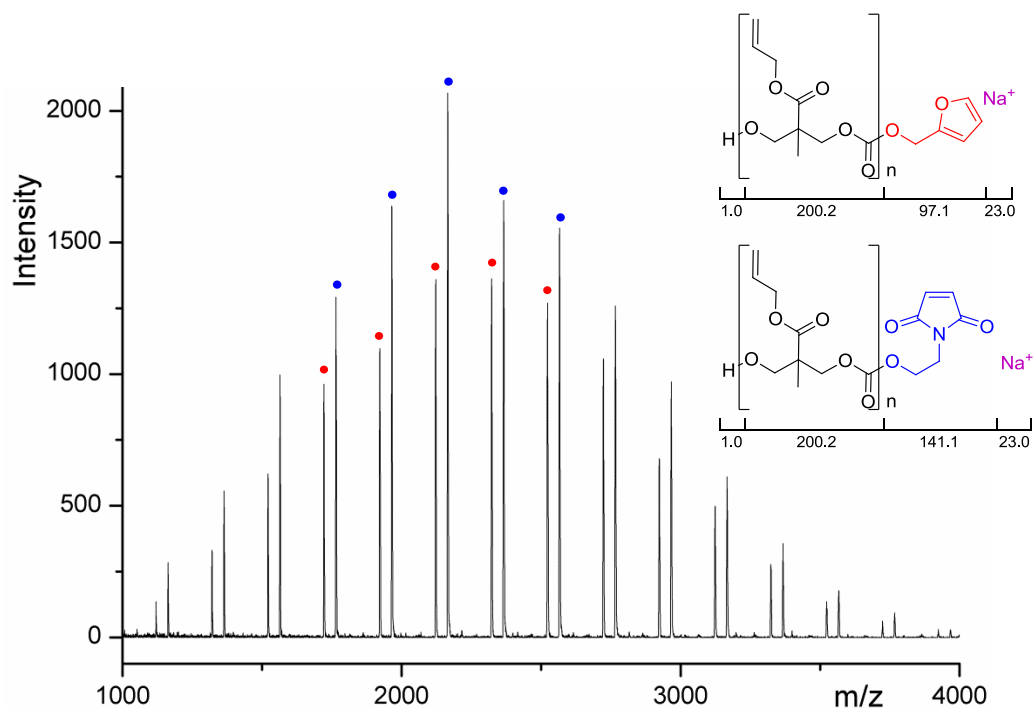


Figure 2.8. MALDI-TOF MS analysis of telechelic PMAC (DP = 20) initiated from **8** using 5 mol% **2** and 10 mol% **3**. Two distributions (both DP = 10) are observed due to the retro-Diels Alder reaction caused by the energy from the laser. Experimental and calculated m/z values for both maleimide (●) and furan (●) terminated polymers are given in Table 2.3.

Table 2.3. Theoretical and observed m/z values of the indicated peaks (●/●) in Figure 2.8.

(●) furan functional PMAC			(●) maleimide functional PMAC		
DP	Exp. m/z^a	Calc. m/z^b	DP	Exp. m/z^a	Calc. m/z^b
8	1721.0	1721.6	8	1764.5	1764.6
9	1921.8	1921.7	9	1964.8	1964.6
10	2122.1	2122.7	10	2165.3	2165.7
11	2322.4	2322.8	11	2365.8	2365.8
12	2522.6	2522.9	12	2566.1	2565.9

^a Experimentally observed m/z values ; ^b Calculated m/z values;

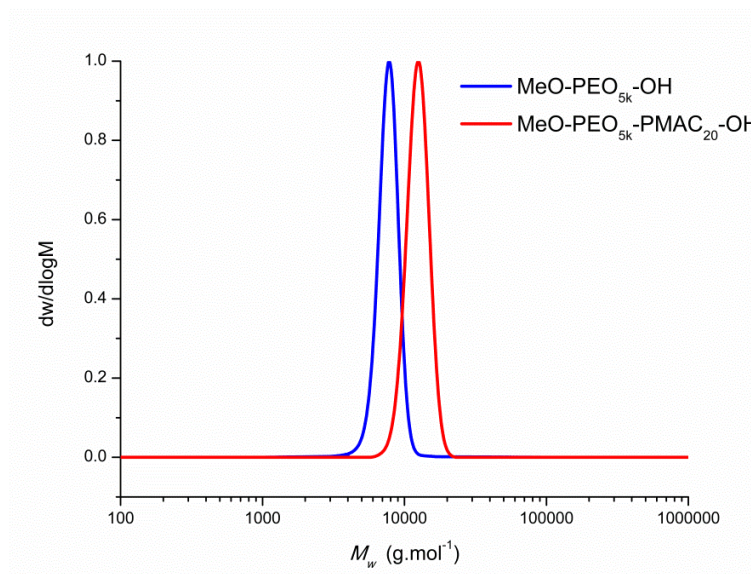


Figure 2.9. GPC traces of MeO-PEO₁₁₄-OH ($M_n = 7\,520\text{ g mol}^{-1}$, PDI = 1.03) and MeO-PEO₁₁₄-PMAC₂₀-OH block copolymer ($M_n = 11\,900\text{ g mol}^{-1}$, PDI = 1.06).

catalyst system, initiated from benzyl alcohol in a one-pot process, and by lactide ROP from a PMAC macroinitiator. BnO-PLA₂₀-*b*-PMAC₂₀-OH and BnO-PMAC₁₆-*b*-PLA₂₃-OH block copolymer synthesis was confirmed by ¹H NMR spectroscopy showing resonances corresponding to both PLA and PMAC, only differing in the resonances of the final monomer unit (hydroxyl chain end, $\delta = 3.68$ and 1.19 ppm for MAC monomer unit; $\delta = 4.27$ ppm for PLA monomer unit, Figure 2.10). Furthermore, in both cases an increase in molecular weight was observed by GPC, while maintaining a low polydispersity (Figure 2.11; Table 2.4).

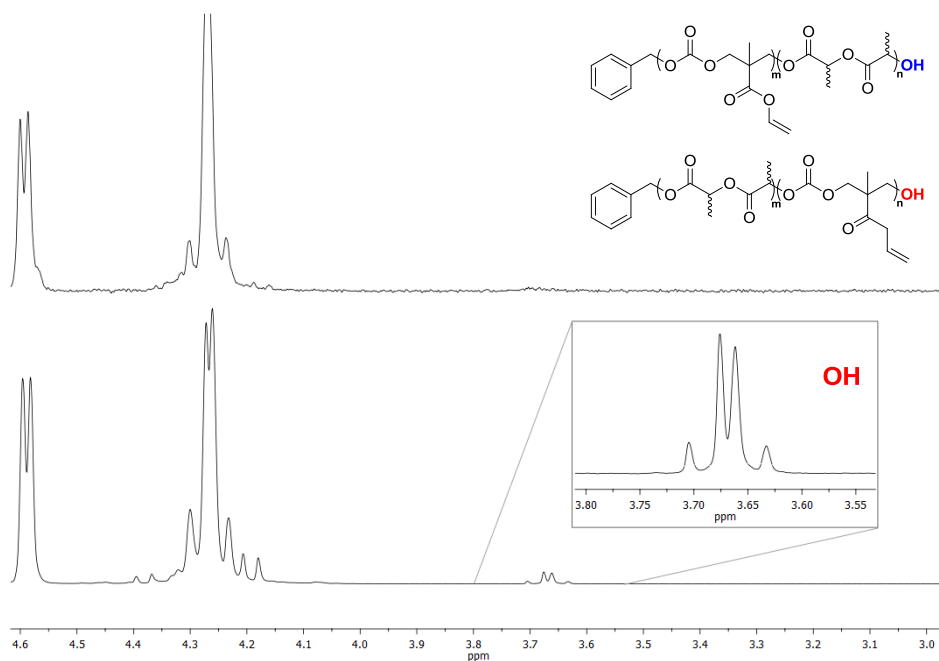


Figure 2.10. Expansion of the δ 3.00- 4.60 ppm region of the ^1H NMR spectra of BnO-PMAC-*b*-PLA-OH (top) and BnO-PLA-*b*-PMAC-OH (bottom) (400 MHz, CDCl_3 , 293 K). The BnO-PLA-*b*-PMAC-OH spectrum shows the CH_2OH end group resonance from the final PMAC block, whereas this resonance is absent in the ^1H NMR spectrum of BnO-PMAC-*b*-PLA-OH.

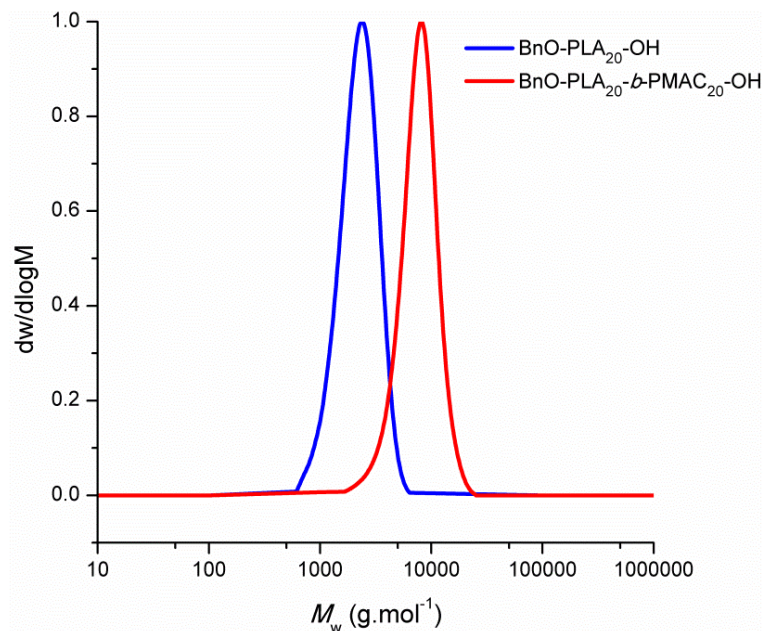


Figure 2.11. GPC traces of BnO-PLA₂₀-OH ($M_n = 2\,020\text{ g mol}^{-1}$, PDI = 1.17) and BnO-PLA₂₀-PMAC₂₀-OH block copolymer ($M_n = 7\,130\text{ g mol}^{-1}$, PDI = 1.17).

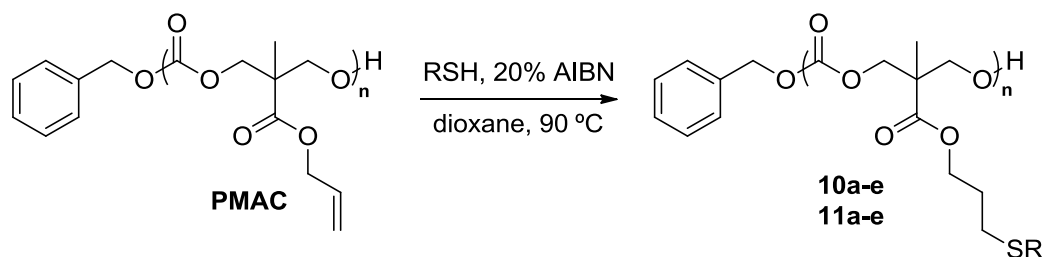
Table 2.4. Telechelics and block copolymers of MAC^a

polymer	DP ^b	M_n (NMR) ^c (g mol ⁻¹) ^b	M_n (GPC) ^d (g mol ⁻¹)	PDI ^d
HO-PMAC-O(CH ₂) ₃ O-PMAC-OH	9 ^f	3 670	5 450	1.16
HO-PMAC-O(CH ₂) ₂ S-S(CH ₂) ₂ O-PMAC-OH	12 ^f	4 960	4 050	1.23
HO-PMAC-O-(C ₁₁ H ₁₀ NO ₃)-O-PMAC-OH	8 ^f	3 440	4 290	1.29
HO-PMAC-O-(C ₁₆ H ₁₉ NO ₅)-O-PMAC-OH	10 ^f	4 110	4 240	1.17
MeO-PEO ₁₁₄ - <i>b</i> -PMAC-OH ^e	20 ^f	12 680	11 900	1.06
BnO-PLA-OH	20 ^g	1 550	2 020	1.17
BnO-PLA- <i>b</i> -PMAC-OH	20 ^f	5 550	7 130	1.17
BnO-PMAC-OH	16 ^f	3 310	4 260	1.34
BnO-PMAC- <i>b</i> -PLA-OH	23 ^g	4 970	6 620	1.28

^a Targeted degree of polymerisation (DP) = 20 (block copolymers) or 10 (telechelics). Reactions were performed in CDCl₃ at 25 °C, [MAC] = 0.5 M, [M]/[I] = 20 using 5 mol% **2** and 10 mol% **3**; ^b Experimental degree of polymerisation measured by ¹H NMR spectroscopy per OH group; ^c Determined by ¹H NMR spectroscopy; ^d Determined by GPC analysis in THF; ^e Poly(ethylene oxide) macroinitiator (DP = 114, determined as M_n = 7 520 g mol⁻¹, PDI = 1.03 by GPC analysis in THF against poly(styrene) standards). ^f DP of PMAC block. ^g DP of PLA block.

2.2.3. Post-polymerisation functionalisation of allyl-functional poly(carbonate), PMAC, *via* radical addition of a thiol.

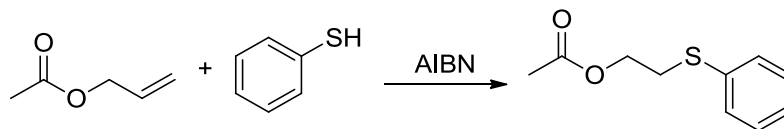
Allyl-functional poly(carbonate)s could be further functionalised *via* radical addition of a thiol (Scheme 2.5). Prior to the functionalisation of the allyl-functional poly(carbonate)s, optimisation of the required conditions for the radical addition of thiols to the allyl esters was undertaken using a model system.



Scheme 2.5. Radical Addition of a Thiol (RSH) to the PMAC.

2.2.3.1. Post-polymerisation functionalisation of allyl-functional poly(carbonate), PMAC, *via* radical addition of a thiol: Optimisation of conditions.

The model system used for the optimisation of the conditions required for quantitative conversion of the allyl esters consisted of allyl acetate and thiophenol with azobis(isobutyronitrile), AIBN, as the radical initiator (Scheme 2.6), with optimisation being performed at 90 °C. A range of solvents were investigated leading to no conversion being observed for



Scheme 2.6. The radical addition of thiophenol to allyl acetate with AIBN as radical initiator, was used as a model reaction for the optimisation of conditions for PMAC functionalisation.

dimethylformamide (DMF) and dimethyl sulfoxide (DMSO), whilst 1,4-dioxane resulted in almost a doubling in conversion over 24 h compared to reactions in which other solvents such as chloroform and ethyl acetate were applied (Table 2.5). As an excellent solvent for the poly(carbonate)s, 1,4-dioxane was hence used in further thiol-ene reactions. As expected, the amount of radical initiator did not greatly influence the reaction whereas increased concentration of the reagents led to decreased reaction times. Initial functionalisations of allyl-functional poly(carbonate)s, carried out using benzyl mercaptan, did not reach full conversion as determined by ^1H NMR spectroscopic analysis, but GPC analysis did reveal a shift to higher molecular weight compared to that of the unfunctionalised polymer. As such the concentration was further increased giving 0.15 M PMAC in dioxane at 90 °C for 24 h as optimal conditions for full functionalisation of PMAC homopolymers when an equimolar amount of thiol (to alkene) was used. However, under optimal conditions using 1 equivalent of benzyl mercaptan, initial reactions led to the observation of a high molecular weight tail by GPC analysis. This high molecular weight shoulder was attributed to cross-linking

Table 2.5. Optimisation of the reaction conditions for the radical addition of thiophenol to allyl acetate.^a

solvent	concentration	equivalents	conversion
	allyl acetate	AIBN	
chloroform	0.46	0.2	37%
THF	0.46	0.2	31%
1,2-dichloroethane	0.46	0.2	29%
ethyl acetate	0.46	0.2	33%
DMF	0.46	0.2	2%
DMSO	0.46	0.2	-
dioxane	0.46	0.2	59%
dioxane	0.46	0.5	61%
dioxane	0.46	1.0	51%
dioxane	3.68	0.2	84%
dioxane	7.36	0.2	89%
dioxane ^b	7.36	0.2	96%
dioxane ^c	3.68	0.2	quant.

^a Reactions were performed at 90 °C or refluxed for 24h under nitrogen atmosphere using 1 equivalent of thiophenol and degassed solvents and reactants. ^b Using 3 equivalents of thiophenol; ^c Using 1 equivalent of benzyl mercaptan instead of thiophenol.

of some of the pendant allyl groups. Variation of the equivalents of benzyl mercaptan between 0.5 and 3 equivalents observed cross-linked chloroform-insoluble product with 0.5 equivalent, whereas increasing the equivalents of thiol to 2 or more resulted in the observation of monomodal GPC traces with the narrow molecular weight distributions of the initial PMAC retained.

2.2.3.2. Post-polymerisation functionalisation of allyl-functional poly(carbonate), PMAC, *via* radical addition of a thiol: Functionalisation and characterisation.

Functionalisation of PMAC homopolymers (DP11 and DP100) with 1-dodecanethiol resulted in poly(carbonate)s **10a** and **11a** in which >99% conversion of the allyl groups was confirmed by the disappearance of the resonance of the vinyl resonances at $\delta = 5.87$ and 5.37-5.20 ppm and the appearance of new resonances at $\delta = 4.16$, 2.50-2.40 and 1.84 ppm and $\delta = 2.50-2.40$, 1.50, 1.30, 1.19 and 0.81 ppm consistent with the added 1-dodecyl group (Figure 2.12). Furthermore, analysis of the modified polymers by gel

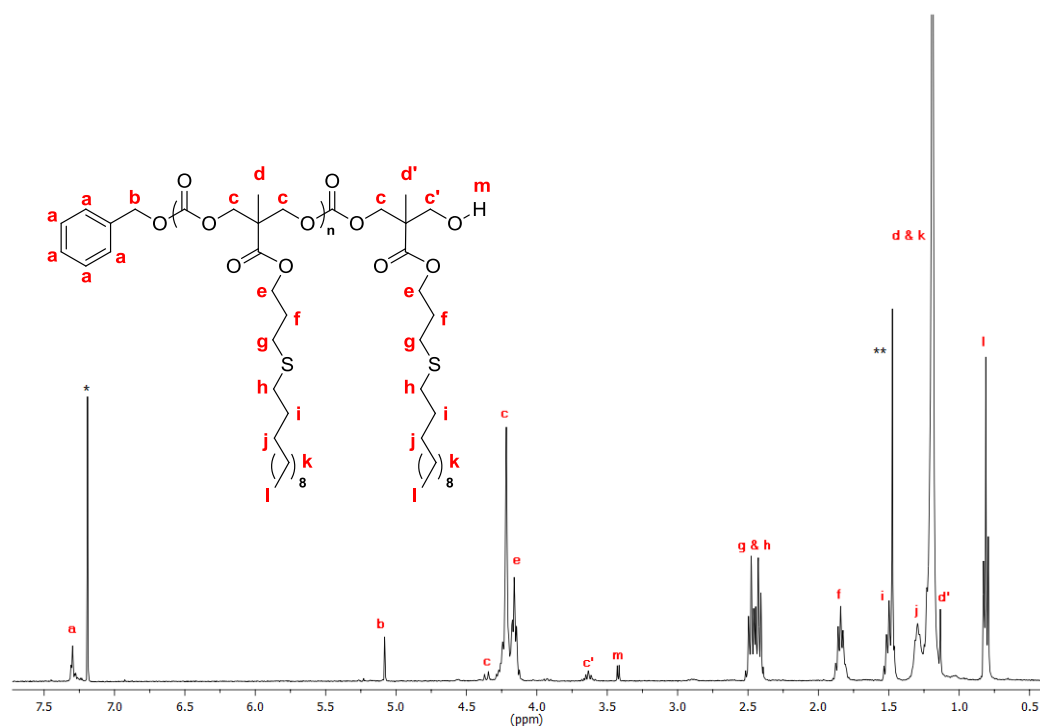


Figure 2.12. ¹H NMR in CDCl₃ of PMAC₁₁ after post-polymerisation radical functionalisation with 1-dodecanethiol (400 MHz, 293 K; * = residual CDCl₃, ** = H₂O).

permeation chromatography (Figure 2.13) revealed a shift from $M_n = 3\,440\text{ g mol}^{-1}$ (DP10) and $M_n = 15\,100\text{ g mol}^{-1}$ (DP100) to $M_n = 5\,320\text{ g mol}^{-1}$ (DP10) and $M_n = 25\,000\text{ g mol}^{-1}$ (DP100) whilst maintaining narrow, unimodal polydispersity indices (PDI= 1.16 and 1.22). MALDI-ToF MS analysis of the **10a** polymer also revealed a new distribution with repeat units that were consistent with the new polymer structure (Figure 2.14; Table 2.6). The addition of 1-dodecanethiol across the double bonds resulted in an increase in the repeating unit from 200 m/z to 402 m/z . A second distribution corresponding to a polymer chain with a single residual unfunctionalised allyl group was also observed, although in notably lower intensity, even though full conversion of the pendant alkene groups was observed by ^1H NMR spectroscopy.

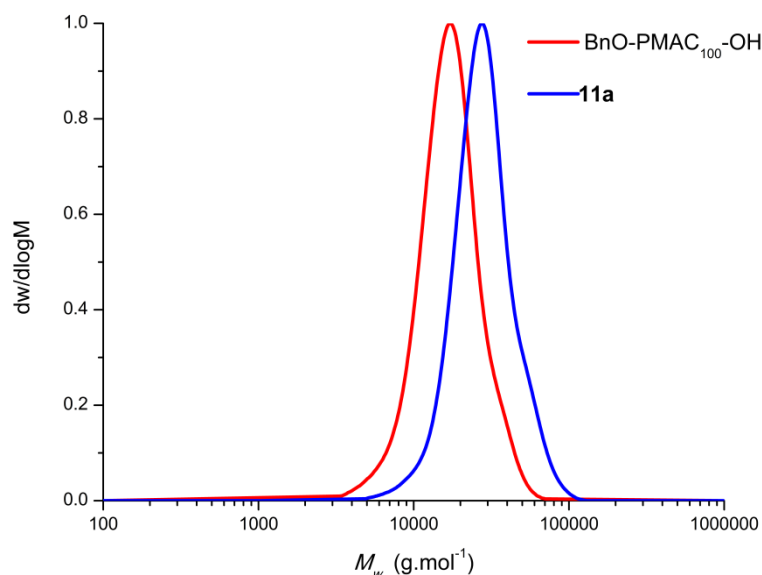


Figure 2.13. GPC traces of BnO-PMAC₁₀₀-OH before ($M_n = 15\,100\text{ g mol}^{-1}$, PDI = 1.23) and after post-polymerisation functionalisation with 1-dodecanethiol ($M_n = 25\,000\text{ g mol}^{-1}$, PDI = 1.22).

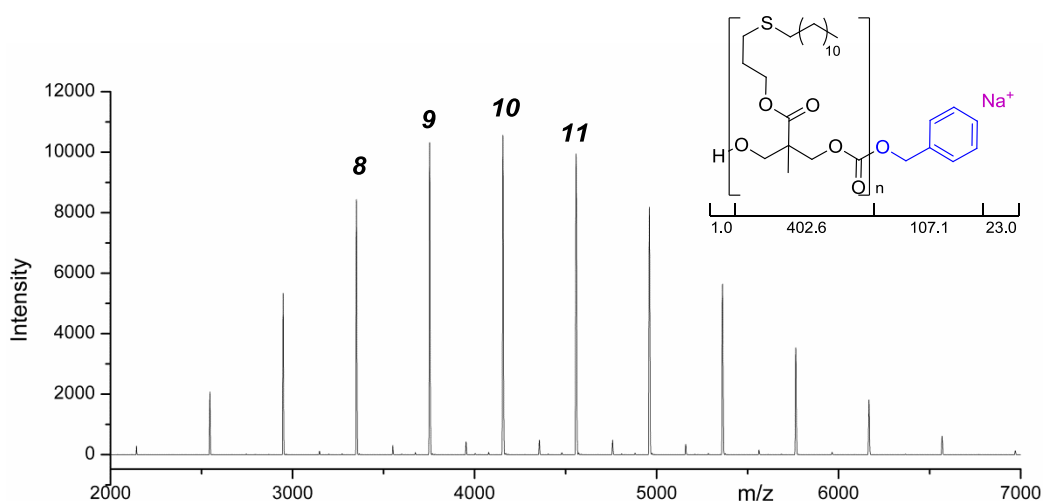


Figure 2.14. MALDI-ToF-MS of PMAC (DP = 11) after post-polymerisation functionalisation with 1-dodecanethiol. The second lower distribution represents a PMAC chain that is not fully functionalised and has one pendant allyl group left.

Table 2.6. Theoretical and observed m/z values of the indicated peaks in Figure 2.14.

DP	Experimental m/z	Calculated m/z
8	3351.4	3351.0
9	3753.9	3753.2
10	4156.2	4156.5
11	4558.5	4558.7

In order to further demonstrate the versatility of this system, PMAC homopolymers of DP11 and DP100 were functionalised with a range of thiol-containing molecules including some with functional groups that are not compatible with the ring-opening polymerisation process such as alcohol and

carboxylic acid groups (Table 2.7). In all cases ^1H NMR spectroscopic analysis of the modified polymers demonstrated that addition of the thiol to the allyl groups was occurring to >99%, evidenced by the disappearance of the vinyl resonances at $\delta = 5.87$ and 5.37-5.20 ppm and with data consistent with those expected for the modified side-chain groups (Figure 2.15). In addition, in all cases, analysis by GPC revealed shifts to lower retention times while maintaining narrow, unimodal distributions with polydispersity indices similar to that of the unmodified PMAC. GPC data were also consistent with the absence of adverse side reactions. However, addition of mercaptoacetic

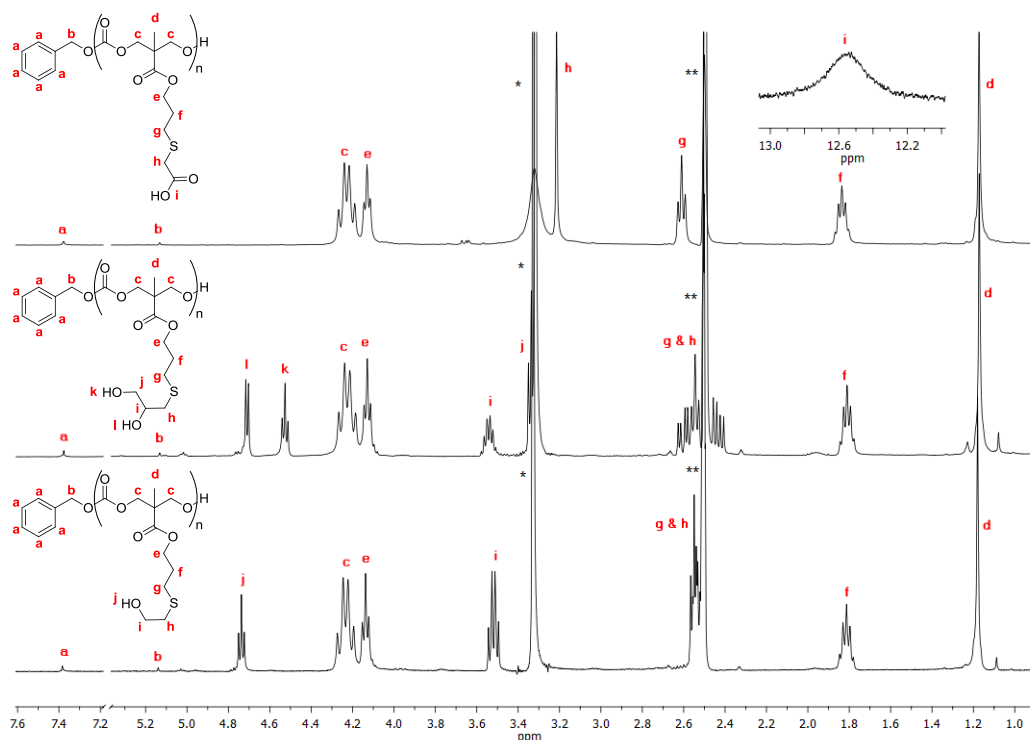


Figure 2.15. ^1H NMR spectra in *d*-DMSO of BnO-PMAC₁₀₀-OH after post-polymerisation functionalisation with (i) mercaptoacetic acid, (ii) 1-thioglycerol and (iii) mercaptoethanol (400 MHz, 293 K; * = H₂O, ** = residual *d*-DMSO).

acid resulted in the isolation of a polymer that was not soluble in solvents in which GPC analysis could be performed. Poly(carbonate)s functionalised with mercaptoethanol displayed number average molecular weights of $6\,170\text{ g mol}^{-1}$ (DP10; PDI = 1.17) and $26\,050\text{ g mol}^{-1}$ (DP100; PDI = 1.27), whilst 1-thioglycerol functionalised polymers displayed number average molecular weights of $6\,750\text{ g mol}^{-1}$ (DP10; PDI = 1.16) and $29\,340\text{ g mol}^{-1}$ (DP100; PDI = 1.34) (Figure 2.16). MALDI-ToF MS analysis of PMAC₁₁ functionalised with benzyl mercaptan further confirmed successful functionalisation revealing a single distribution consistent with the new polymer structure. This new distribution observed displayed an increase in the repeating unit from 200 m/z to 324 m/z and a main peak at $m/z = 3375$ which corresponds to a sodium charged, fully functionalised polymer chain of with DP = 10 (Figure 2.17; Table 2.8).

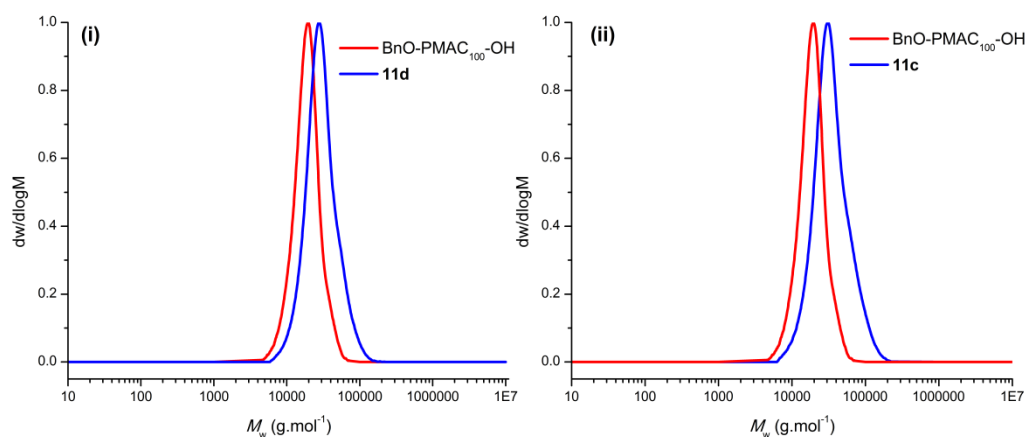


Figure 2.16. GPC traces of BnO-PMAC₁₀₀-OH before ($M_n = 17\,160\text{ g mol}^{-1}$, PDI = 1.18) and after post-polymerisation functionalisation with (i) mercaptoethanol ($M_n = 26\,050\text{ g mol}^{-1}$, PDI = 1.27) and (ii) 1-thioglycerol ($M_n = 29\,340\text{ g mol}^{-1}$, PDI = 1.34).

Table 2.7. Post-polymerisation radical thiol-ene functionalisation of poly(carbonates)^a

polymer	thiol	M_n (g mol ⁻¹)	PDI ^c
BnO-PMAC ₁₁ -OH (10)	-	3 440 ^b /3 680 ^c	1.15 ^b /1.10 ^c
BnO-PMAC ₁₀₀ -OH (11)	-	15 100 ^b /17 160 ^c	1.23 ^b /1.18 ^c
10a	1-dodecanethiol	5 320 ^b	1.16 ^b
11a	1-dodecanethiol	25 000 ^b	1.22 ^b
10b	benzyl mercaptan	3 530 ^b	1.18 ^b
11b	benzyl mercaptan	20 710 ^b	1.19 ^b
10c	1-thioglycerol	6 750 ^c	1.16 ^c
11c	1-thioglycerol	29 340 ^c	1.34 ^c
10d	mercaptoethanol	6 170 ^c	1.17 ^c
11d	mercaptoethanol	26 050 ^c	1.27 ^c

^a [PMAC] = ca. 0.15 M in 1,4-dioxane, 2 equivalent of thiol, 20 mol% AIBN, 90 C, 24 h;

^b Measured by GPC analysis using THF as eluent; ^c Measured by GPC analysis using DMF as eluent.

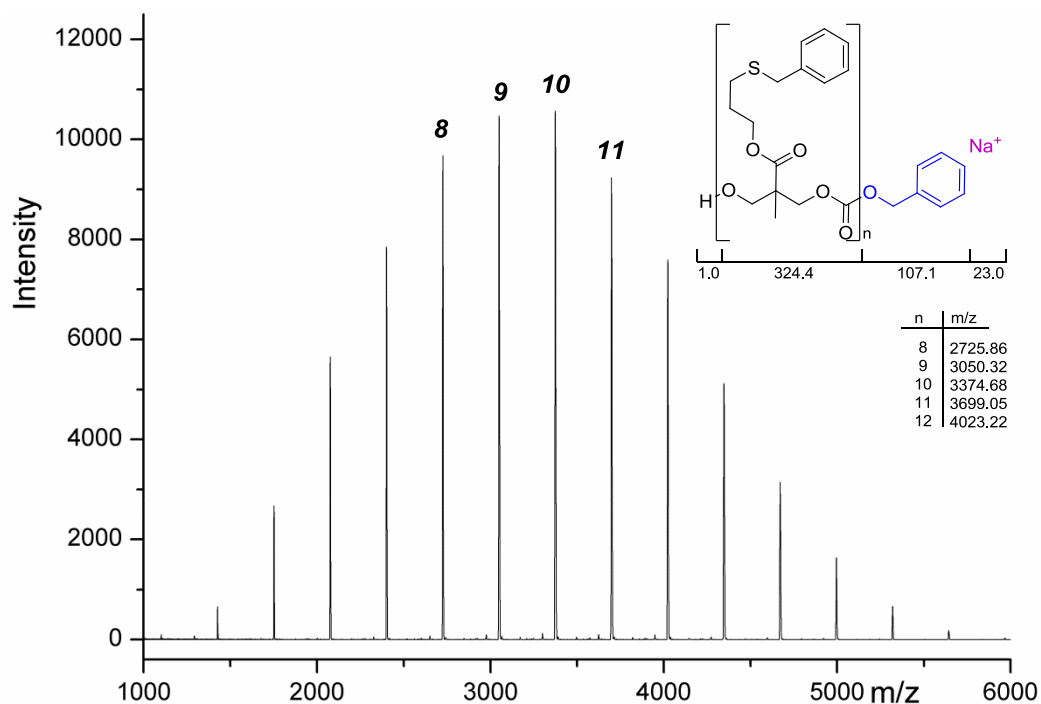


Figure 2.17. MALDI-ToF-MS of PMAC (DP = 11) after post-polymerisation functionalisation with benzyl mercaptan. An increase in repeat unit is observed from 200 m/z to 324 m/z .

Table 2.8. Theoretical and observed m/z values of the indicated peaks in Figure 2.17.

DP	Experimental m/z	Calculated m/z
8	2725.9	2725.9
9	3050.3	3050.0
10	3374.7	3374.1
11	3699.1	3699.2

2.2.4. Thermal analysis of functional poly(carbonate)s derived from PMAC.

Analysis of the DP100 functional polymers by differential scanning calorimetry (DSC) and thermogravimetric analysis (TGA) was undertaken to investigate the effect of chemical structure on the thermal properties and degradation of the functional polymers. Notably, DSC analysis of the DP100 PMAC prefunctionalisation revealed a lower glass transition temperature (T_g) of $-26.4\text{ }^\circ\text{C}$ than those previously reported ($-12.0\text{ }^\circ\text{C}$; $M_n = 19\ 000\text{ g mol}^{-1}$, PDI = 1.6 and $M_n = 9\ 200\text{ g mol}^{-1}$, PDI = 1.8).^{8,10} This further suggests that the organocatalytic ring-opening polymerisation of MAC resulted in poly(carbonate)s without any side reactions, whereas PMAC homopolymers previously reported underwent branching involving the ester side group. Post-polymerisation functionalisation of the PMAC homopolymers revealed subtle changes in the T_g values of the polymers with respect to DP100 PMAC displaying a glass transition temperature (T_g) of $-26.4\text{ }^\circ\text{C}$ (Table 2.9). While the addition of linear alkyl groups (1-dodecanethiol and mercaptoethanol) led to a slight increase in T_g , the addition of benzyl mercaptan led to the highest increase to $-5.0\text{ }^\circ\text{C}$, attributed to the steric hindrance and aromatic interactions. Notably, the 1-dodecanethiol-functionalised polymer also displayed a melting transition at $T_m = -2.9\text{ }^\circ\text{C}$, likely a consequence of crystallisation of the linear alkyl side chains.

Table 2.9. Thermal analysis of functionalised poly(carbonates).

polymer	thiol	T_g^a (°C)	T_m^b (°C)	H_m (J g ⁻¹)	$T_{5\%}^d$ (°C)	$T_{50\%}^d$ (°C)
BnO-PMAC ₁₀₀	-	-26.4	-	-	307	355
OH						
11a	1-dodecanethiol	-15.7 ^c	-2.9	27.0	282	313
11b	benzyl mercaptan	-5.1	-	-	280	347
11c	1-thioglycerol	-28.5	-	-	229	275
11d	mercaptoethanol	-16.3	-	-	284	329
11e	mercaptoacetic acid	-33.2	-	-	261	343

^a Glass transition temperature, measured by DSC analysis at the second scan; ^b Melting point, measured by DSC analysis; ^c Loss of accuracy due to proximity to the melting endotherm; ^d Temperatures at 5 and 50% weight degradation.

The thermal degradation of PMAC₁₀₀ and functionalised PMAC₁₀₀ samples (**11a-11e**) was also studied using TGA (Table 2.9). Again, the initial degradation values were shown to be largely invariant with polymer structure ranging from 311 to 360 °C, attesting for a good thermal stability whatever the nature of the pendant functional groups. The most notable outlier was the 1-thioglycerol functionalised polymer which degraded at significantly lower temperature (initial degradation temperature = 247.5 °C) most likely attributed to the dehydration of this polyol derivative. Notably, all investigated (functionalised) poly(carbonate)s display higher thermal stability than poly(trimethylene carbonate) (PTMC), which has a reported degradation temperature of ca. 230 °C.³⁰

2.3. Conclusions

In conclusion, the controlled ring-opening polymerisation of 5-methyl-5-allyloxycarbonyl-1,3-dioxan-2-one was achieved successfully by using a range of organic catalysts under mild conditions. Using the preferred system of thiourea and (-)-sparteine, the living nature of the polymerisations was demonstrated by the observation of a linear evolution of molecular weight with both monomer conversion and monomer-to-initiator ratio, low PDIs, and the synthesis of telechelic polymers and block copolymers of PMAC with PEO and PLA. Post-polymerisation functionalisation of the pendant allyl groups in the polymer backbone by facile free radical “thiol-ene” addition led to the isolation of aliphatic poly(carbonate)s with a range of pendant functionalities, without notable polymer degradation leading to precise control over the thermal properties of the polymers. Such a facile and versatile methodology provides an attractive route to the synthesis of functional aliphatic poly(carbonates).

2.4. References

1. Hoyle, C. E.; Lowe, A. B.; Bowman, C. N. *Chem. Soc. Rev.* **2010**, *39*, 1355–1387.
2. Iha, R. K.; Wooley, K. L.; Nystrom, A. M.; Burke, D. J.; Kade, M. J.; Hawker, C. J. *Chem. Rev.* **2009**, *109*, 5620–5686.
3. Parrish, B.; Quansah, J. K.; Emrick, T. *J. Polym. Sci., Part A: Polym. Chem.* **2002**, *40*, 1983–1990.
4. Hoyle, C. E.; Bowman, C. N. *Angew. Chem., Int. Ed.* **2010**, *49*, 1540–1573.
5. Stanford, M. J.; Dove, A. P. *Macromolecules* **2009**, *42*, 141–147.
6. van der Ende, A. E.; Harrell, J.; Sathiyakumar, V.; Meschievitz, M.; Katz, J.; Adcock, K.; Harth, E. *Macromolecules* **2010**, *43*, 5665–5671.
7. van der Ende, A. E.; Kravitz, E. J.; Harth, E. *J. Am. Chem. Soc.* **2008**, *130*, 8706–8713.
8. Hu, X.; Chen, X.; Liu, S.; Shi, Q.; Jing, X. *J. Polym. Sci., Part A: Polym. Chem.* **2008**, *46*, 1852–1861.
9. Hu, X.; Chen, X.; Wei, J.; Liu, S.; Jing, X. *Macromol. Biosci.* **2009**, *9*, 456–463.
10. Mullen, B. D.; Tang, C. N.; Storey, R. F. *J. Polym. Sci., Part A: Polym. Chem.* **2003**, *41*, 1978–1991.
11. Hu, X.; Chen, X.; Xie, Z.; Liu, S.; Jing, X. *J. Polym. Sci., Part A: Polym. Chem.* **2007**, *45*, 5518–5528.

12. Chen, X.; McCarthy, S. P.; Gross, R. A. *Macromolecules* **1998**, *31*, 662–668.
13. Endo, T.; Kakimoto, K.; Ochiai, B.; Nagai, D. *Macromolecules* **2005**, *38*, 8177–8182.
14. He, F.; Wang, Y.-P.; Liu, G.; Jia, H.-L.; Feng, J.; Zhuo, R.-X. *Polymer* **2008**, *49*, 1185–1190.
15. Miyagawa, T.; Shimizu, M.; Sanda, F.; Endo, T. *Macromolecules* **2005**, *38*, 7944–7949.
16. Wang, C.-F.; Lin, Y.-X.; Jiang, T.; He, F.; Zhuo, R.-X. *Biomaterials* **2009**, *30*, 4824–4832.
17. Dove, A. P. *Chem. Commun.* **2008**, 6446–6470.
18. Jerome, C.; Lecomte, P. *Adv. Drug Delivery Rev.* **2008**, *60*, 1056–1076.
19. Kamber, N. E.; Jeong, W.; Waymouth, R. M.; Pratt, R. C.; Lohmeijer, B. G. G.; Hedrick, J. L. *Chem. Rev.* **2007**, *107*, 5813–5840.
20. Dove, A. P.; Pratt, R. C.; Lohmeijer, B. G. G.; Waymouth, R. M.; Hedrick, J. L. *J. Am. Chem. Soc.* **2005**, *127*, 13798–13799.
21. du Boullay, O. T.; Saffon, N.; Diehl, J.-P.; Martin-Vaca, B.; Bourissou, D. *Biomacromolecules* **2010**, *11*, 1921–1929.
22. Pounder, R. J.; Dove, A. P. *Biomacromolecules* **2010**, *11*, 1930–1939.
23. Nederberg, F.; Lohmeijer, B. G. G.; Leibfarth, F.; Pratt, R. C.; Choi, J.; Dove, A. P.; Waymouth, R. M.; Hedrick, J. L. *Biomacromolecules* **2007**, *8*, 153–160.

24. Pratt, R. C.; Lohmeijer, B. G. G.; Long, D. A.; Lundberg, P. N. P.; Dove, A. P.; Li, H. B.; Wade, C. G.; Waymouth, R. M.; Hedrick, J. L. *Macromolecules* **2006**, *39*, 7863–7871.
25. Becker, J. M.; Tempelaar, S.; Stanford, M. J.; Pounder, R. J.; Covington, J. A.; Dove, A. P. *Chem.—Eur. J.* **2010**, *16*, 6099–6105.
26. Coulembier, O.; Sanders, D. P.; Nelson, A.; Hollenbeck, A. N.; Horn, H. W.; Rice, J. E.; Fujiwara, M.; Dubois, P.; Hedrick, J. L. *Angew. Chem., Int. Ed.* **2009**, *48*, 5170–5173.
27. Lohmeijer, B. G. G.; Pratt, R. C.; Leibfarth, F.; Logan, J. W.; Long, D. A.; Dove, A. P.; Nederberg, F.; Choi, J.; Wade, C.; Waymouth, R. M.; Hedrick, J. L. *Macromolecules* **2006**, *39*, 8574–8583.
28. Rokicki, G. *Prog. Polym. Sci.* **2000**, *25*, 259–342.
29. Delcroix, D.; Martin-Vaca, B.; Bourissou, D.; Navarro, C. *Macromolecules* **2010**, *43*, 8828–8835.
30. Nederberg, F.; Trang, V.; Pratt, R. C.; Mason, A. F.; Frank, C. W.; Waymouth, R. M.; Hedrick, J. L. *Biomacromolecules* **2007**, *8*, 3294–3297.

Chapter 3

Organocatalytic Synthesis and post-Polymerisation Functionalisation of Propargyl-Functional Poly(Carbonate)s

Well-defined propargyl-functional poly(carbonate)s were synthesised *via* the organocatalytic ring-opening polymerisation of 5-methyl-5-propargyloxycarbonyl-1,3-dioxan-2-one using the dual catalyst systems of 1-(3,5-bis(trifluoromethyl)phenyl)-3-cyclohexylthiourea and (-)-sparteine or DBU. The resulting poly(carbonate)s obtained showed low polydispersities and high end-group fidelity. Further functionalisation of homopolymers with degrees of polymerisation of 10, 12 and 72 were realised *via* the Huisgen cycloaddition of azides or *via* the radical addition of thiols to the pendant propargyl functional groups, resulting in a range of functional aliphatic poly(carbonate)s.

3.1. Introduction

The alkyne functional group is utilised in many organic reactions and the reactivity of this functionality is utilised in several reactions. Examples of reactions that involve alkynes are coupling reactions such as the Sonogashira, Glaser and Eglinton couplings, but also in cycloaddition reactions such as Diels-Alder with 1,3-dienes and the highly efficient Huisgen 1,3-dipolar cycloaddition of alkynes and azides.¹⁻⁵ The copper-catalysed Huisgen cycloaddition is used extensively in materials chemistry as a fast and quantitative method of functionalisation.^{6,7} Furthermore, in other reactions such as hydrogenation, hydroboration, halogenation and the ‘thiol-yne’ reaction, two equivalents of the corresponding reagent can be added to one alkyne group as a result of its double unsaturation.⁸ As such, the availability of a carbon-carbon triple bond in the polymer backbone offers great versatility in its post-polymerisation modification.

The introduction of a pendant propargyl functionality in a poly(carbonate) backbone has previously been reported *via* the ring-opening polymerisation of a propargyl ester functional cyclic carbonate, 5-methyl-5-propargyloxycarbonyl-1,3-dioxan-2-one (MPC).⁹⁻¹² Whilst MPC has been utilised in the copolymerisation with lactide ($M_n = 8\,700-9\,600\text{ g mol}^{-1}$; PDI = 1.21-1.32) and in the synthesis of block copolymers (PDI = 1.20-1.67), there are no previous reports of MPC homopolymerisations. These polymerisations were performed in toluene at 120 °C¹² or at 100 °C in bulk⁹ using diethyl zinc

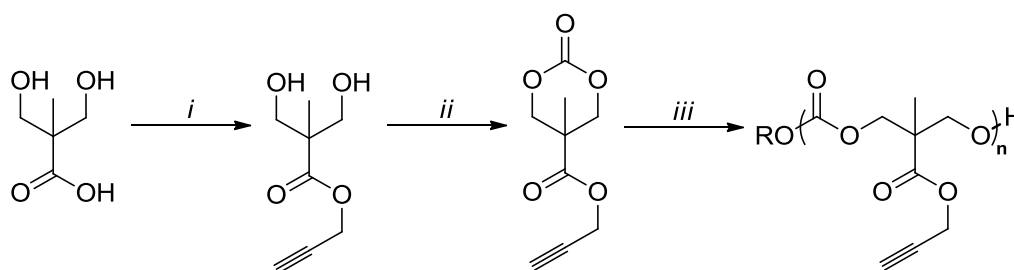
as a catalyst. Studies involving MPC include PMPC-*co*-PLA polymers to form sugar-containing, biodegradable polymers, in the immobilisation of proteins to biodegradable polymer fibres and in the preparation of protein-grafted polymer microspheres.⁹⁻¹¹

Herein, the concept of synthesising a single functional polycarbonate scaffold in a controlled manner has been further extended to those with a pendant propargyl functionality. Polymer scaffolds were prepared by the ring-opening polymerisation of MPC, followed by their post-polymerisation functionalisation *via* Huisgen cycloaddition of azide or *via* radical addition of thiols to the pendant propargyl groups, giving rise to a range of functional poly(carbonate)s.

3.2. Results and Discussion

3.2.1. Synthesis of 5-methyl-5-propargyloxycarbonyl-1,3-dioxan-2-one, MPC.

Owing to the electrophilic nature of propargyl bromide, 5-methyl-5-propargyloxycarbonyl-1,3-dioxan-2-one (MPC) could be synthesised in a simple two-step procedure as previously reported (Scheme 3.1).^{9,10} In the first step, the propargyl functionalised diol was synthesised by refluxing 2,2-bis(hydroxymethyl)propionic acid and potassium hydroxide in acetone for one hour to form the 2,2-bis(hydroxymethyl)propionic acid potassium salt before adding a solution of propargyl bromide (80 wt%) and refluxing for a further 15 hours. After purification by distillation, the cyclic carbonate could be formed by ring closure using ethyl chloroformate in the presence of triethylamine to trap the hydrochloric acid by formation of the NEt₃.HCl salt. The product had to be recrystallised several times to remove all impurities and dried extensively before its use in ROP.



Scheme 3.1. Synthesis and ring-opening polymerisation of 5-methyl-5-propargyloxycarbonyl-1,3-dioxan-2-one, MPC. Conditions: (i) allyl bromide, KOH, acetone, reflux (16h); (ii) ethyl chloroformate, NEt₃, THF, 0 °C; (iii) ROH, catalyst, CDCl₃, RT.

3.2.2. Organocatalytic Ring-Opening Polymerisation of 5-methyl-5-propargyloxycarbonyl-1,3-dioxan-2-one, MPC.

Initial studies into the ring-opening polymerisation (ROP) of MPC (Scheme 3.1.) were carried out with the dual catalyst system of 1-(3,5-bis(trifluoromethyl)phenyl)-3-cyclohexylthiourea, **3**, in combination with (-)-sparteine, **2**, as catalysts (Figure 3.1). Reactions were performed in CDCl₃ or CH₂Cl₂ (0.5 M MPC) at 25 °C using 10 mol% **1** and 5 mol% (-)-sparteine, benzyl alcohol as initiator with $[M]/[I] = 20$, as these conditions had previously shown to give excellent control in the ROP of MAC (Chapter 2).

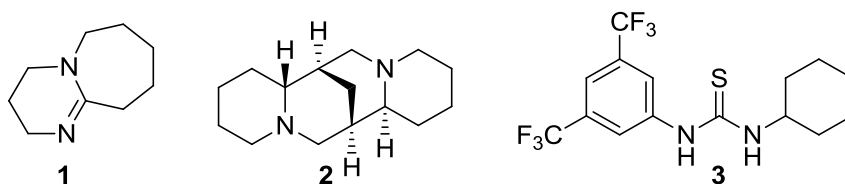


Figure 3.1. Organic catalysts used in the ring-opening polymerisation of MPC.

3.2.2.1. Organocatalytic Ring-Opening Polymerisation of 5-methyl-5-propargyloxycarbonyl-1,3-dioxan-2-one, MPC: Polymerisation control with the bifunctional 1-(3,5-bis(trifluoromethyl)phenyl)-3-cyclohexylthiourea/(-)-sparteine catalyst system.

The polymerisation of MPC could be monitored by the disappearance of the methylene resonances in the carbonate ring at $\delta = 4.22$ and 4.72 ppm and the

appearance of a multiplet at $\delta = 4.27$ - 4.40 ppm and by the shift of the methyl resonance from $\delta = 1.37$ ppm in the monomer to $\delta = 1.29$ ppm in the polymer backbone (Figure 3.2). Upon completion, pure polymers were obtained by precipitation from CDCl_3 or CH_2Cl_2 into cold hexanes and removal of residual catalyst by column chromatography. Resultant polymers showed narrow molecular weight distributions by GPC analysis ($M_n = 6\,750\text{ g mol}^{-1}$, PDI = 1.18) indicating that the polymerisation was well-controlled.

Further investigation of the living characteristics of the polymerisation catalysed by 10 mol% **3** and 5 mol% (-)-sparteine revealed a first order kinetic

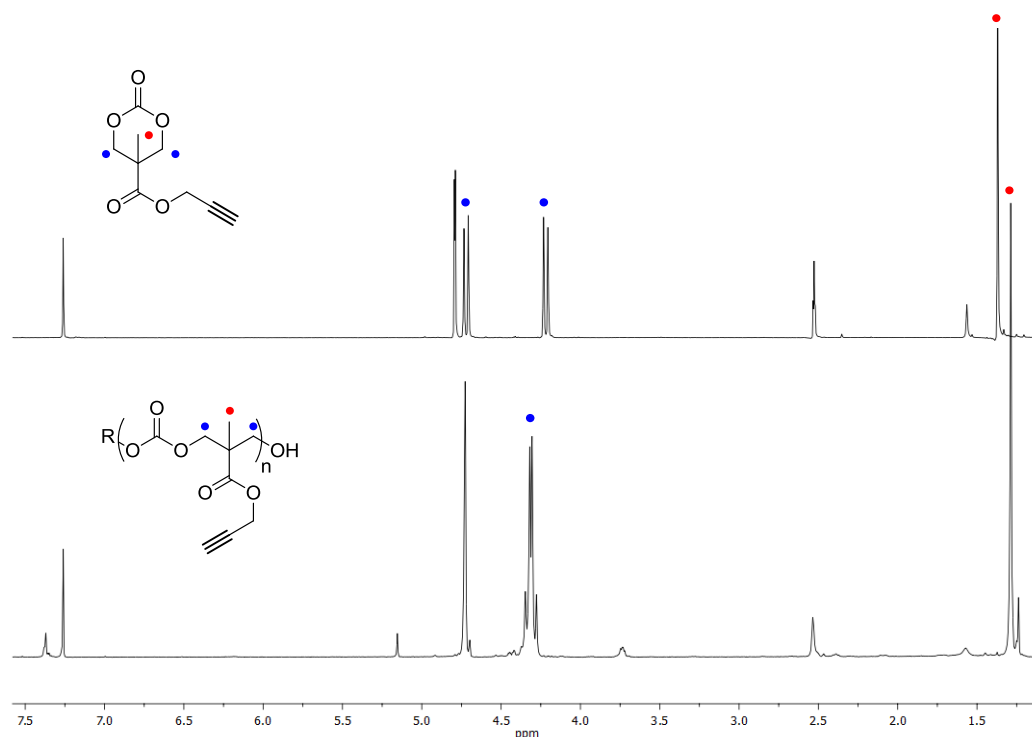


Figure 3.2. Comparison of the ^1H NMR spectra of MPC (top) and of PMPC (bottom) initiated from benzyl alcohol (CDCl_3 ; 400 MHz, 298 K). Shifts in the methyl (●) and the methylene (●) resonances are observed upon polymerisation.

plot as well as a linear correlation between number-average molecular weight (M_n) against monomer conversion while retaining low PDI values throughout the polymerisation (Figure 3.3). However, in the investigation of the correlation between number-average molecular weight (M_n) against initial monomer-to-initiator ratio ($[M]_0/[I]_0$) using the preferred conditions of 10 mol% **3** and 5 mol% (-)-sparteine (to monomer), a high molecular weight shoulder was observed in the GPC traces of polymerisations with higher $[M]/[I]$. A reduction of the high molecular weight shoulder was achieved when the (-)-sparteine to initiator ratio was kept at 1:1 and resulted in the observation of a linear correlation between M_n and $[M]_0/[I]_0$ (Figure 3.4).

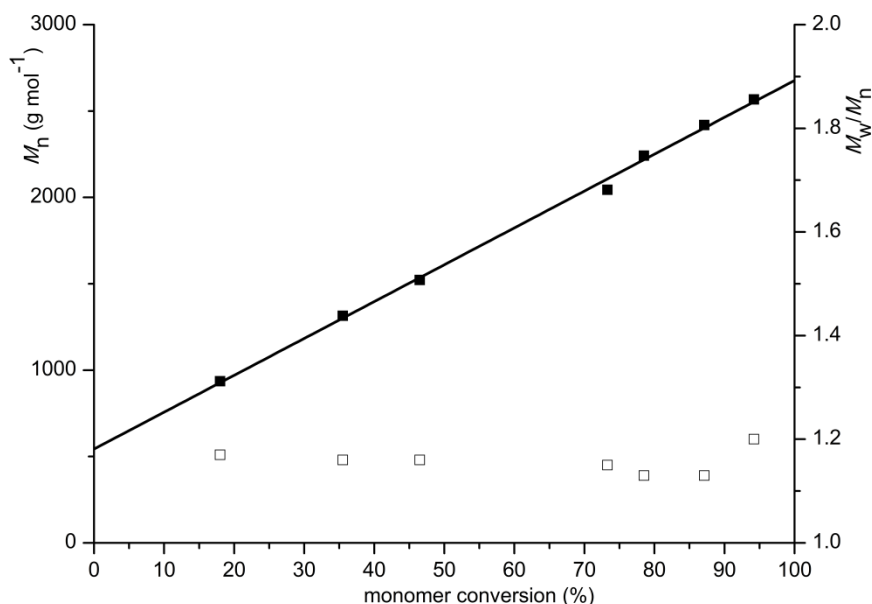


Figure 3.3. Plot of number-average molecular weight (M_n ; ■) and polydispersity (M_w/M_n ; □) against % monomer conversion in the ring-opening polymerisation of MPC. Conditions: $[MPC] = 0.5 \text{ M}$ CDCl_3 at $25 \text{ }^\circ\text{C}$, 5 mol% **2**, 10 mol% **3**, $[M]/[I] = 20$ using benzyl alcohol as initiator.

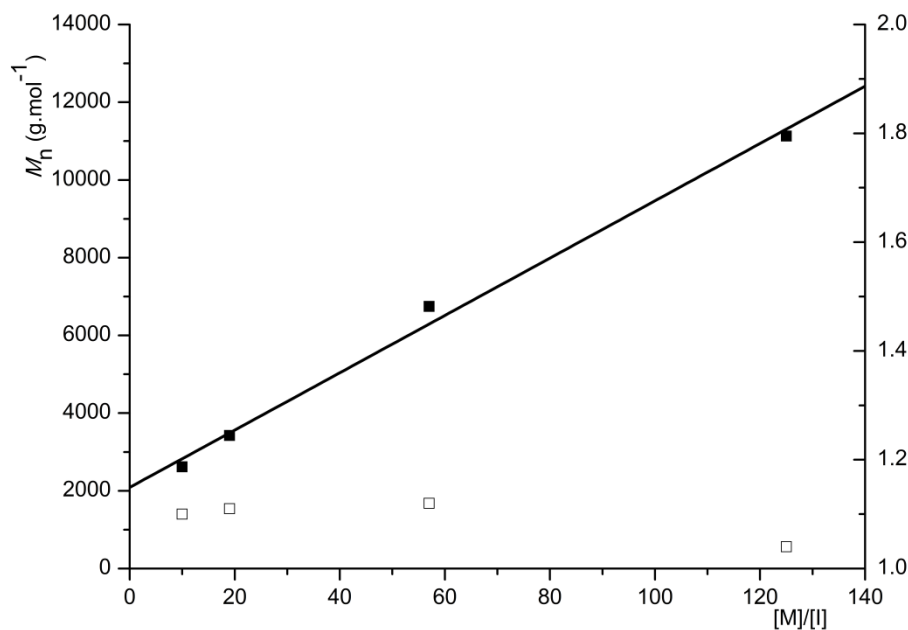


Figure 3.4. Plot of number-average molecular weight (M_n ; ■) and polydispersity (M_w/M_n ; □) against initial monomer-to-initiator ratio, $[M]_0/[I]_0$, in the ring-opening polymerisation of MPC. Conditions: $[MPC] = 0.5$ M $CDCl_3$ at 25 °C, 5 mol% **2** (to initiator), 10 mol% **3** (to monomer), using benzyl alcohol as initiator.

Interestingly, both graphs display a non-zero intercept. This observation could indicate that the initiator efficiency is poor or that initiation from another species was also occurring leading to the observation of a lower molecular weight by GPC than expected. Analysis of the resulting polymers, however, revealed polymers with degrees of polymerisation comparable to those expected for the respective monomer-to-initiator ratio used. Nevertheless, analysis of a polymerisation with $[M]/[I] = 10$ after standard work-up using 1H NMR spectroscopy confirmed degree of polymerisation (DP) of 10 by comparison of the integration of the resonances at $\delta = 7.37$

(ArH) and 5.15 (CH₂) ppm originating from the benzyl alcohol initiator group against the methylene and methyl resonances on the polymer backbone (Figure 3.5). The ¹H NMR spectrum of the DP10 polymer, also reveals resonances corresponding to the monomer unit at the hydroxyl chain end at δ = 3.73 (CH₂OH), 1.24 (CH₃) and 2.40 ppm (OH). Further analysis of the DP10 polymer by MALDI-ToF MS revealed a single distribution with a spacing of 198 *m/z*, which is equal to that of a monomer unit (Figure 3.6; Table 3.1). The main peak at *m/z* = 1914 corresponds to a sodium charged polymer chain of DP9 with a benzyl alcohol end group. These observations suggest that, at least for lower molecular weights, ROP occurs in a living manner without the occurrence of side reactions.

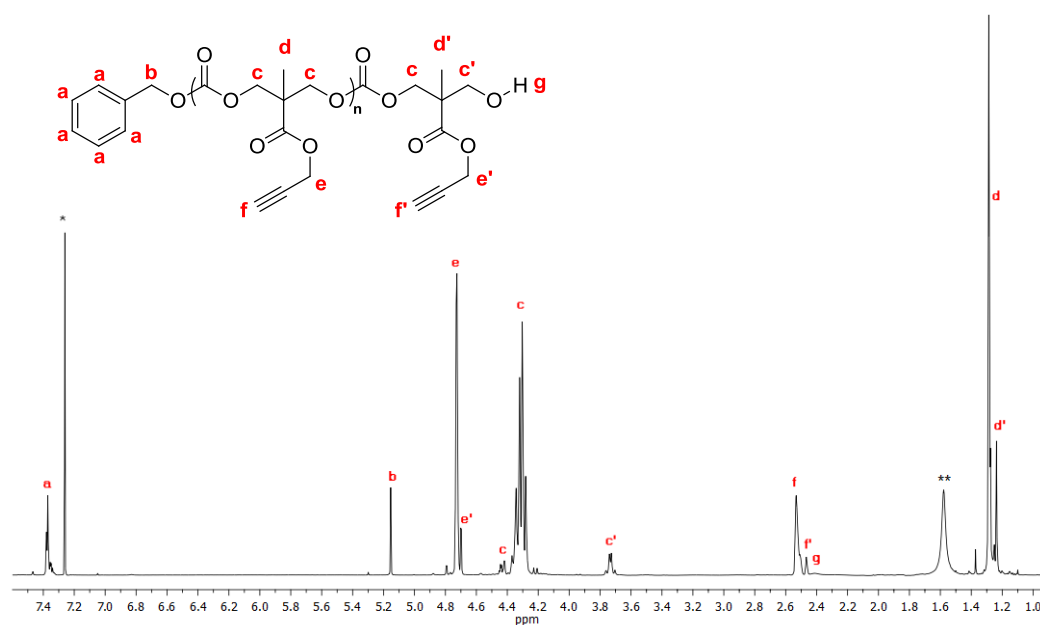


Figure 3.5. ¹H NMR in CDCl₃ of PMPC₁₀ initiated from benzyl alcohol using 5 mol% **3** and 10 mol% **2** (500 MHz, 298 K; * = residual CDCl₃, ** = H₂O).

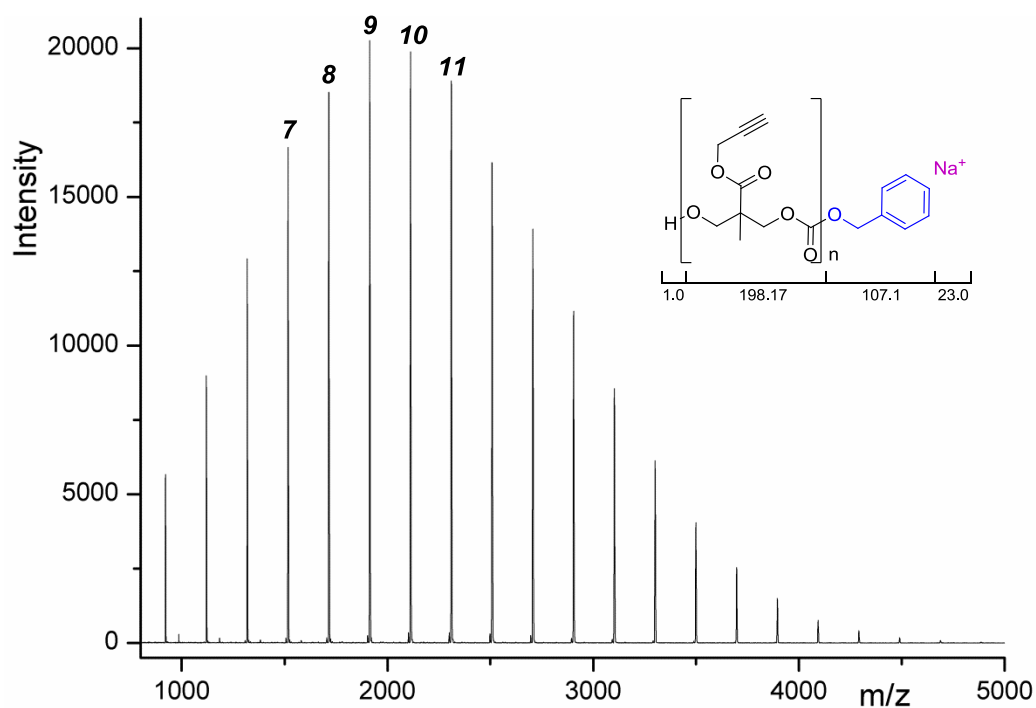


Figure 3.6. MALDI-ToF MS analysis of PMPC (DP = 10) initiated from benzyl alcohol using 5 mol% **2** and 10 mol% **3**.

Table 3.1. Theoretical and observed m/z values of PMPC₁₀ (Figure 3.6).

DP	Experimental m/z	Calculated m/z
7	1517.1	1517.4
8	1715.3	1715.5
9	1913.7	1913.5
10	2111.9	2112.6
11	2310.2	2310.6

Interestingly, polymerisations that were run in CDCl_3 showed a decrease in intensity of the propargyl proton resonance and MALDI-ToF MS analysis of the corresponding polymers revealed distributions with a repeat unit closer to 199 m/z than the expected 198 m/z (Figure 3.7). These results correspond to polymer chains in which the acetylenic proton has undergone proton-deuterium exchange with the solvent during polymerisation (Figure 3.8).

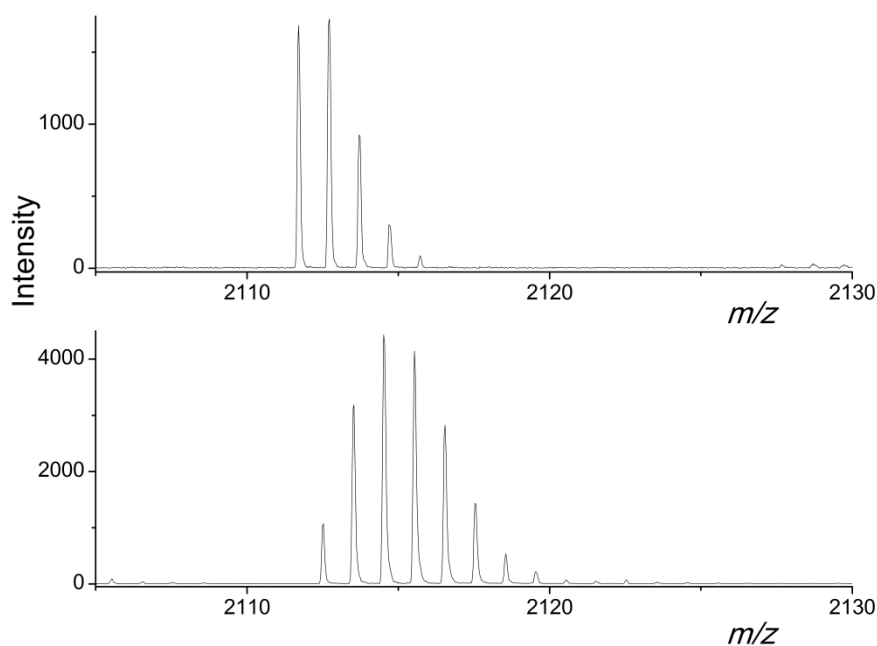


Figure 3.7. MALDI-ToF MS analysis of PMPC polymers initiated from benzyl alcohol obtained from polymerisations run dichloromethane (top) and CDCl_3 . (bottom) using **2** (5 mol%) and **3** (10 mol%) as catalysts.

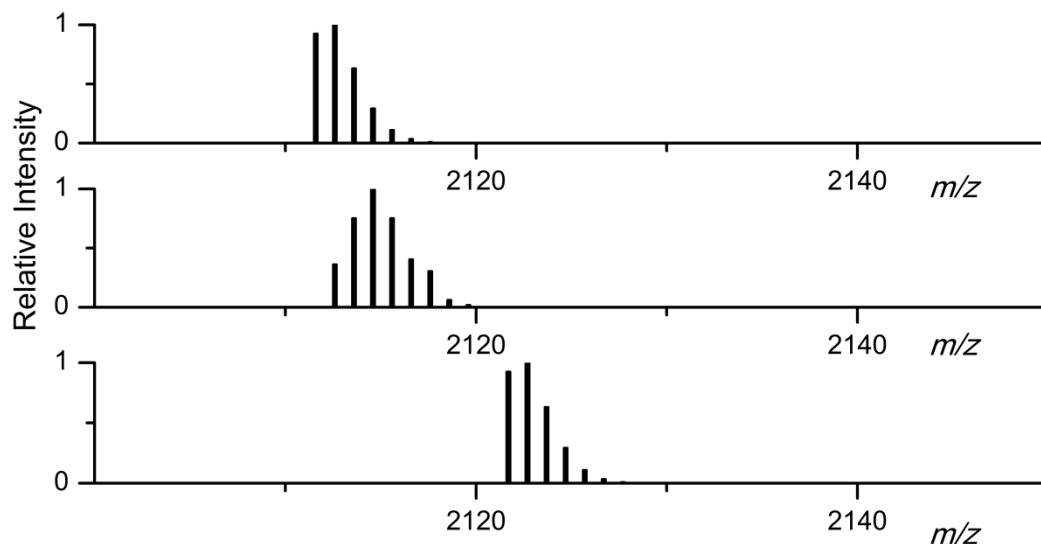


Figure 3.8. Schematic representation of the isotope pattern expected for DP10 peaks of PMPC (top), PMPC with all acetylenic protons exchanged with deuterium (bottom) and the isotope pattern expected for a mixture of polymer chains (DP10) with 1, 2 and 3 propargylic protons substituted in a 1:1:1 ratio.

3.2.2.2. Organocatalytic Ring-Opening Polymerisation of 5-methyl-5-propargyloxycarbonyl-1,3-dioxan-2-one, MPC: Polymerisation control with the bifunctional 1-(3,5-bis(trifluoromethyl)phenyl)-3-cyclohexylthiourea/DBU catalyst system.

As an alternative to the **3**/(-)-sparteine catalyst system, the ring opening polymerisation of MPC was investigated using **3** in combination with 1,8-diazabicyclo[5.4.0]undec-7-ene (**1**, DBU). The application of an alternative catalyst system was investigated as a consequence of both the limited availability of (-)-sparteine and the long reaction times when (-)-sparteine is used. Previously, the use of DBU as a catalyst in the polymerisation of MAC was investigated (Chapter 2), but resulted in the observation of bimodal GPC

traces and large polydispersities. However, its successful use in the ring-opening polymerisation of functional cyclic carbonates by Nederberg *et al.* prompted further investigation using this dual system.¹³ A possible reasons for successful application of the dual DBU/**3** system could be the excess of activated monomer species present. Initial studies into the ring-opening polymerisation of MPC were carried out using 5 mol% **3** and 1 mol% DBU. Polymerisations achieved 90+% monomer conversion within 6 hours at a monomer-to-initiator ratio of 100 ($[M]/[I] = 100$) and GPC analysis of the resultant polymer indicated that the polymerisation was well-controlled with $M_n = 16\,540\text{ g mol}^{-1}$ and PDI = 1.11 (Figure 3.9).

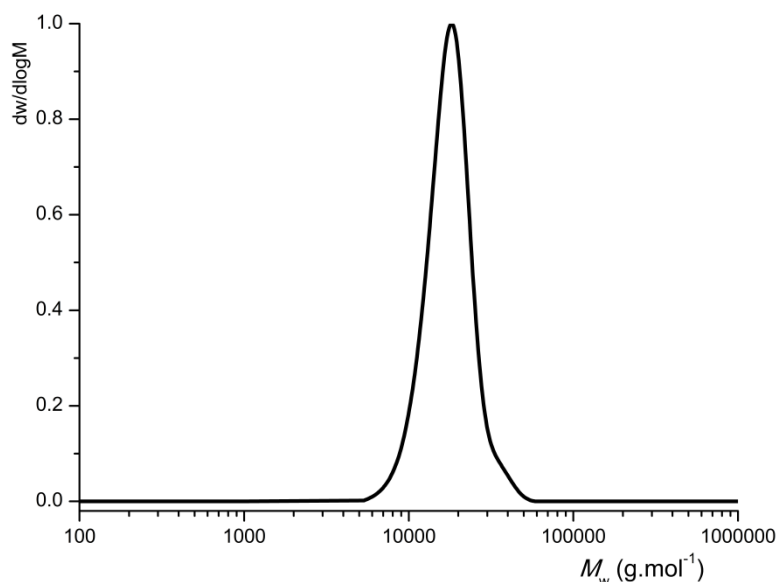


Figure 3.9. GPC trace of BnO-PMPC₁₀₀-OH ($M_n = 16\,540\text{ g.mol}^{-1}$, PDI = 1.11) prepared by the ROP of MPC ($[MPC] = 0.5M$) catalysed by 5 mol% **3** and 1 mol% DBU using benzyl alcohol as initiator.

Further investigation of the living characteristics of the polymerisation catalysed by **3** and DBU (**1**) revealed a linear correlation between number-average molecular weight (M_n) against monomer conversion (Figure 3.10) while retaining low PDI values throughout the polymerisation. A linear correlation was observed as well between number-average molecular weight (M_n) against initial monomer-to-initiator ratio ($[M]_0/[I]_0$) (Figure 3.11). The observation of a zero intercept in both graphs is in contrast with the observation of the non-zero intercept in the ROP of MPC when catalysed by (-)-sparteine and **3** (Figure 3.12).

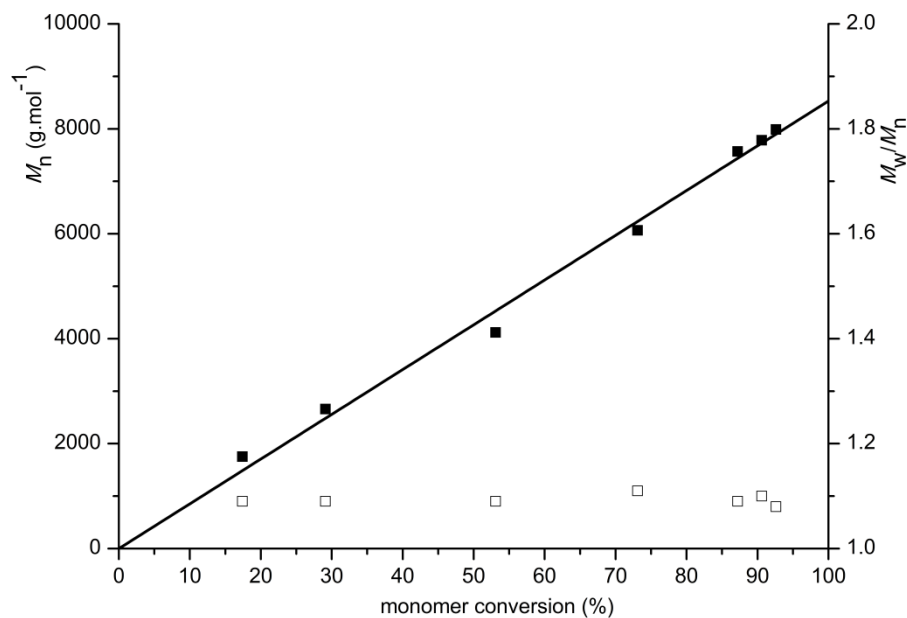


Figure 3.10. Plot of number-average molecular weight (M_n ; ■) and polydispersity (M_w/M_n ; □) against % monomer conversion in the ring-opening polymerisation of MPC catalysed by **3** and DBU. Conditions: $[MPC] = 0.5$ M $CDCl_3$ at 25 °C, 1 mol% **1**, 5 mol% **3**, $[M]/[I] = 45$ using benzyl alcohol as initiator.

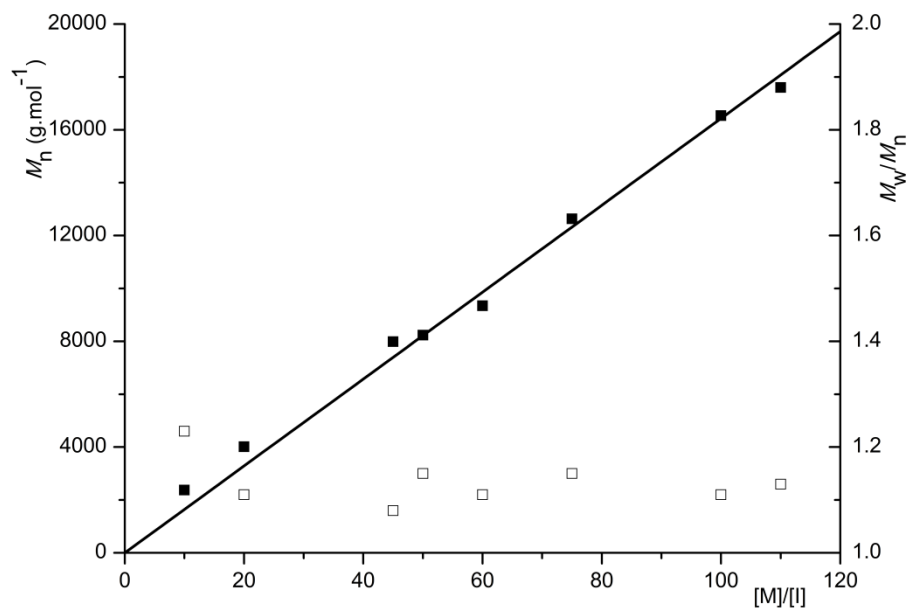


Figure 3.11. Plot of number-average molecular weight (M_n ; ■) and polydispersity (M_w/M_n ; □) against initial monomer-to-initiator ratio, $[M]_0/[I]_0$, in the ring-opening polymerization of MPC. Conditions: $[MPC] = 0.5 \text{ M}$ CDCl_3 at $25 \text{ }^\circ\text{C}$, 1 mol% **1**, 5 mol% **3**, using benzyl alcohol as initiator.

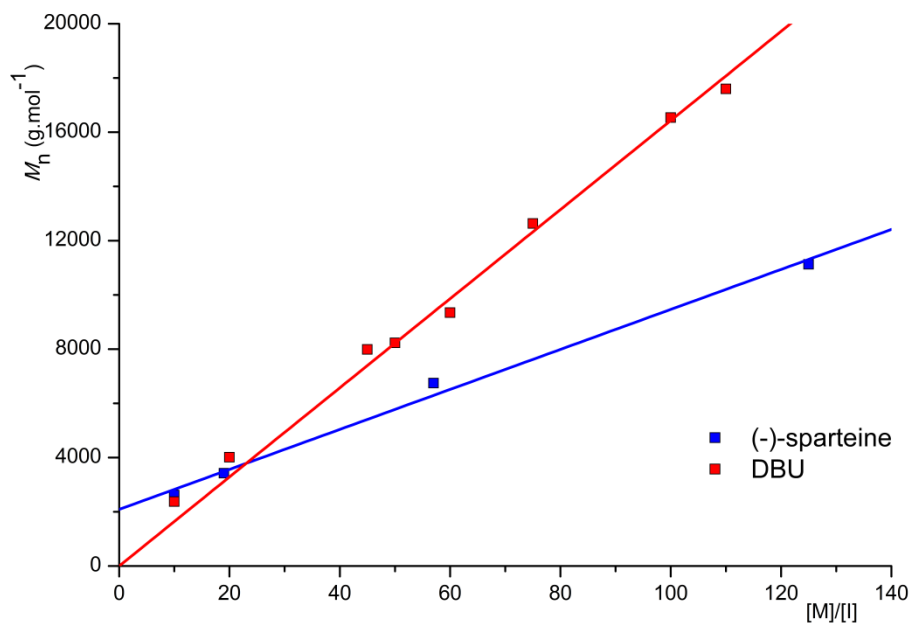


Figure 3.12. Comparison of plots of number-average molecular weight (M_n) against initial monomer-to-initiator ratio, $[M]_0/[I]_0$, in the ROP of MPC ($[MPC] = 0.5 \text{ M}$) using **2+3** and **1+3** as catalyst systems, respectively.

For a better comparison, polymerisations with $[M]/[I] = 50$ were repeated with both catalyst systems using the same batch of monomer. Interestingly, after analysis of the resulting poly(carbonate)s by gel permeation chromatography, a monomodal trace was observed when DBU was used as a catalyst in combination with **3**, whereas a bimodal trace was observed when (-)-sparteine was used in combination with **1** (Figure 3.13).

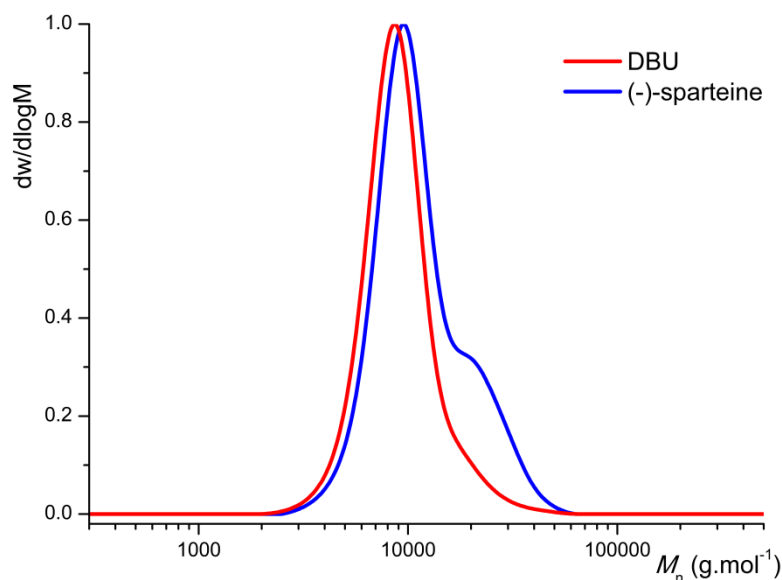


Figure 3.13. Comparison of GPC traces of resulting polymers prepared by the ROP of MPC using **2+3** ($M_n = 10\,050\ \text{g}\cdot\text{mol}^{-1}$, PDI = 1.27) and **1+3** ($M_n = 8\,230\ \text{g}\cdot\text{mol}^{-1}$, PDI = 1.17) as catalyst systems, respectively ($[M]/[I] = 50$; $[MPC] = 0.5\ \text{M}$).

This observation supports the hypothesis that secondary initiation might be taking place in the case of ROP of MPC catalysed by the **2/3** system for $M/I \geq 50$ although the cause remains unclear. Overall, the DBU/**3** catalyst system

showed superior control as well as a higher activity and was therefore chosen in preference over the **2/3** system for further polymerisations in the work described in this chapter.

Analysis of poly(carbonate)s obtained *via* the ROP of MPC catalysed by the **1/3** system by ^1H NMR spectroscopy confirmed degrees of polymerisation of 12 and 72 and in both cases GPC analysis showed narrow molecular weight distributions. Further analysis of the DP12 polymer by MALDI-ToF MS revealed a single distribution with a spacing of 198 m/z (equal to that of a monomer unit) and a main peak at $m/z = 2715$ corresponding to a sodium charged polymer chain of DP13 with a benzyl alcohol end group further confirming that ROP using the **1/3** system as catalysts is well controlled (Figure 3.14).

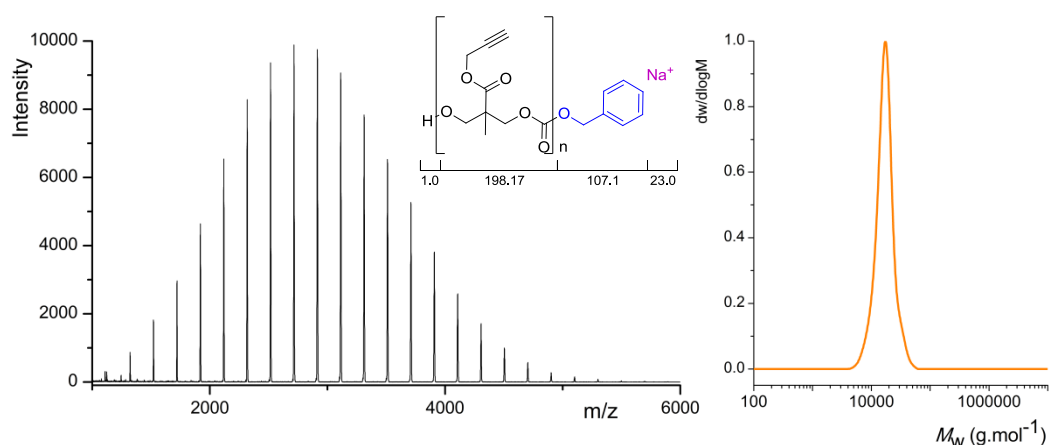


Figure 3.14. MALDI-ToF MS analysis of PMPC (DP = 12) initiated from benzyl alcohol (left) and GPC trace of BnO-PMPC₇₂-OH ($M_n = 15\,700\ \text{g}\cdot\text{mol}^{-1}$, PDI = 1.13) prepared by the ROP of MPC ($[\text{MPC}] = 0.5\text{M}$) catalysed by 5 mol% **3** and 1 mol% **1**.

3.2.2.3. Organocatalytic Ring-Opening Polymerisation of 5-methyl-5-propargyloxycarbonyl-1,3-dioxan-2-one, MPC: Telechelics and block copolymers.

Initiator versatility was investigated by the synthesis of telechelic PMPC ($[M]/[I] = 20$ per alcohol group) initiated from 2-hydroxyethyl disulphide, **7**, and furan-protected maleimide functional diol, **8** (Figure 3.15). ^1H NMR spectroscopic analysis of these polymers revealed resonances expected for the initiating alcohols with integration against the main chain polymer resonances being consistent with DP20 and DP24 polymers, respectively. MALDI-ToF MS analysis of the former showed a distribution with a spacing of 198-199 m/z and a main peak at $m/z = 5928$ (DP29) corresponding to the value expected for telechelic PMPC initiated from 2-hydroxyethyl disulphide (Figure 3.16; Table 3.2). MALDI-ToF MS analysis of PMPC initiated of **8** showed two distributions, both with a spacing of 198-199 m/z . These distributions with main peaks at $m/z = 2542$ (DP12) and $m/z = 2687$ (DP13) correspond to the polymer chains obtained after retro-Diels Alder reaction of the initiator induced by the energy supplied by the laser during analysis.

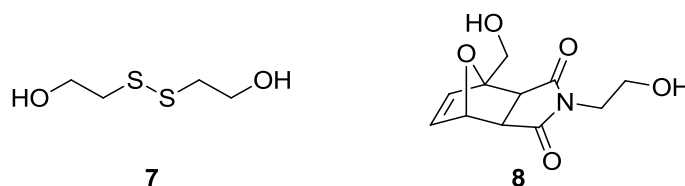


Figure 3.15. Bifunctional initiators used in the ring-opening polymerisation of MPC.

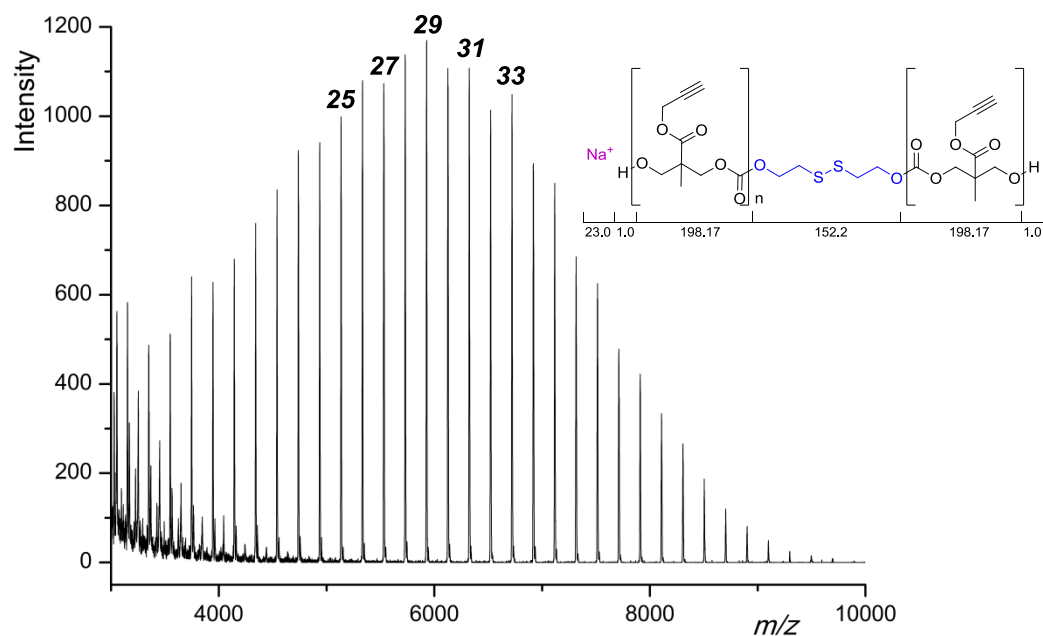


Figure 3.16. MALDI-ToF MS analysis of telechelic PMPC initiated from 2-hydroxyethyl disulphide, **7**, prepared by the ROP of MPC ([MPC] = 0.5M).

Table 3.2. Estimated and observed m/z values of HO-PMPC-O(CH₂)₂S-(CH₂)₂O-PMPC-OH (Figure 3.16).

DP	Experimental m/z	Calculated m/z^a
25	5133.8	5134.8
27	5531.4	5531.4
29	5927.7	5928.0
31	6324.3	6324.6
33	6720.2	6721.2

^a calculated m/z value for a polymer with a 13% deuteration of the acetylenic proton of the propargyl group.

Further initiator versatility was demonstrated by the synthesis of a range of block copolymers (Table 3.3). MeO-PEO₁₁₄-*b*-PMPC₁₈-OH and MeO-PEO₂₁₆-*b*-PMPC₁₂-OH block copolymers were synthesised by initiation of from commercially available poly(ethylene oxide) monomethyl ether-5K and -10K. Chain growth was confirmed by GPC analysis in THF against poly-

Table 3.3. Telechelics and block copolymers of MPC^a

polymer	DP ^b	M_n (NMR) ^c (g mol ⁻¹)	M_n (GPC) ^d (g mol ⁻¹)	PDI ^d
HO-PMPC-O-(C ₁₁ H ₁₀ NO ₃)-O-PMPC-OH	20 ^f	8170	8100	1.08
HO-PMPC-O(CH ₂) ₂ S-S(CH ₂) ₂ O-PMPC-OH	24 ^f	8480	8410	1.10
MeO-PEO ₁₁₄ - <i>b</i> -PMPC ₁₈ -OH ^e	18 ^f	8610	11 020	1.06
MeO-PEO ₂₁₆ - <i>b</i> -PMPC ₁₂ -OH ^g	12 ^f	11 930	17 870	1.06
BnO-PLLA ₁₈ -OH	18 ^h	2700	4200	1.09
BnO-PLLA ₁₈ - <i>b</i> -PMPC ₂₀ -OH	20 ^f	6670	8740	1.08
BnO-PMPC ₂₀ -OH	20 ^f	4070	4540	1.12
BnO-PMPC ₂₀ - <i>b</i> -PLLA ₂₄ -OH	24 ^h	7530	10 350	1.09
BnO-PMPC-OH	17 ^f	3480	4010	1.11
BnO-PMPC- <i>b</i> -PMAC-OH	19 ⁱ	5280	8110	1.09

^a Targeted degree of polymerisation (DP) = 20. Reactions were performed in CDCl₃ at 25 °C, [MPC] = 0.5 M, [M]/[I] = 20) using 5 mol% **3** and 1 mol% **1**. ^b Experimental degree of polymerisation measured by ¹H NMR spectroscopy per OH group. ^c Determined by ¹H NMR spectroscopy. ^d Determined by GPC analysis in THF. ^e Poly(ethylene oxide) macroinitiator (DP = 114, determined M_n = 6 790 g mol⁻¹, PDI = 1.03 by GPC analysis in THF against poly(styrene) standards), using 10 mol% **3** and 5 mol% **2** as catalysts. ^f DP of PMPC block. ^g Poly(ethylene oxide) macroinitiator (DP = 216, determined M_n = 14 820 g mol⁻¹, PDI = 1.06 by GPC analysis in THF against poly(styrene) standards), using 10 mol% **3** and 5 mol% **2** as catalysts. ^h DP of PLLA block. ⁱ DP of PMAC block.

(styrene) standards with the block copolymers exhibiting shifts to higher molecular weight in both cases. GPC analysis of MeO-PEO₁₁₄-*b*-PMPC₁₈-OH revealed a shift from $M_n = 6\,790\text{ g mol}^{-1}$ (PDI = 1.03) for the poly(ethylene oxide) macro-initiator (as characterised by GPC analysis in THF) to $M_n = 11\,020\text{ g mol}^{-1}$; PDI = 1.06 and GPC analysis of MeO-PEO₂₁₆-*b*-PMPC₁₂-OH revealed a shift from $M_n = 14\,820\text{ g mol}^{-1}$ (PDI = 1.06) to $M_n = 17\,870\text{ g mol}^{-1}$; PDI = 1.06 (Figure 3.17). The living nature of the system was further demonstrated by the synthesis of block copolymers of PMPC with poly(*L*-lactide), PLLA. PMPC-PLLA block copolymers were synthesised both by chain growth of PMPC of a PLLA synthesised using the same catalyst system (1/2), initiated from benzyl alcohol in a one-pot process, and by ROP of *L*-lactide from a PMPC macroinitiator. BnO-PLLA₁₈-*b*-PMPC₂₀-OH and BnO-PMPC₂₀-*b*-PLLA₂₄-OH block copolymer synthesis was confirmed by ¹H NMR spectroscopic analysis showing resonances corresponding to both PLA and PMPC. Furthermore, in both cases an increase in molecular weight was observed by GPC, while maintaining a low polydispersity (Figure 3.17). Finally, a block copolymer of PMPC with PMAC was synthesised in a similar fashion, using the same catalyst system and in a one-pot process yielding a poly(carbonate) with two functional blocks. The synthesis of the BnO-PMPC₁₇-*b*-PMAC₁₉-OH block copolymer was confirmed by ¹H NMR spectroscopic analysis and GPC analysis showing an increase in molecular

weight from BnO-PMPC₁₇-OH and a low polydispersity (Table 3.3; Figure 3.17).

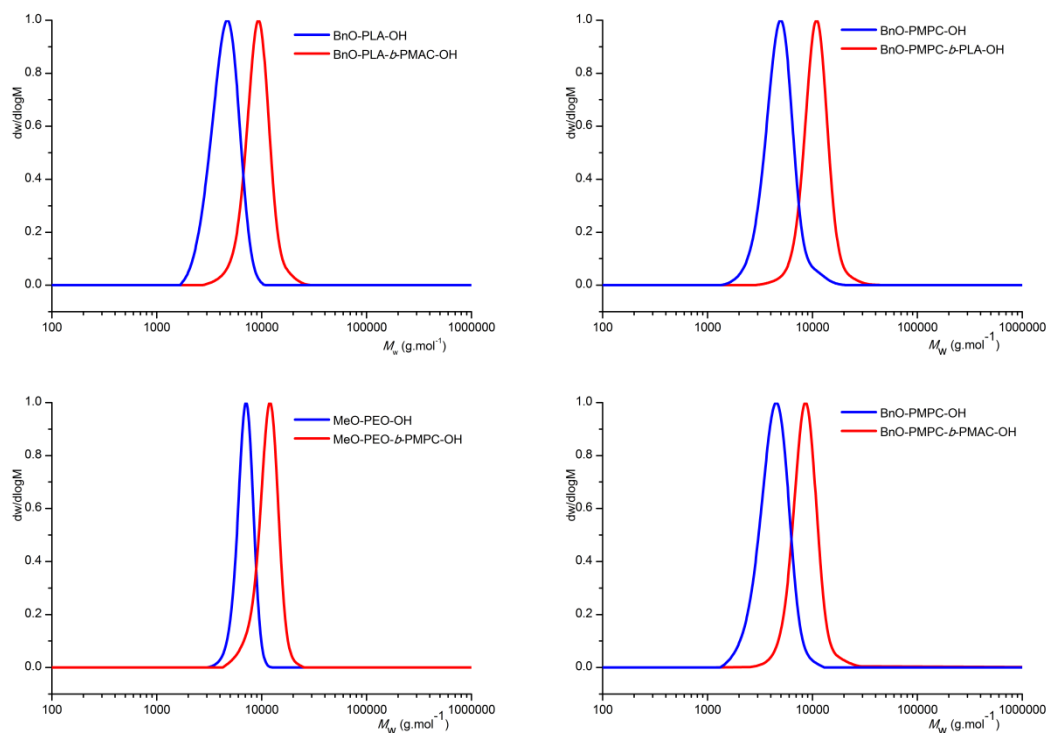
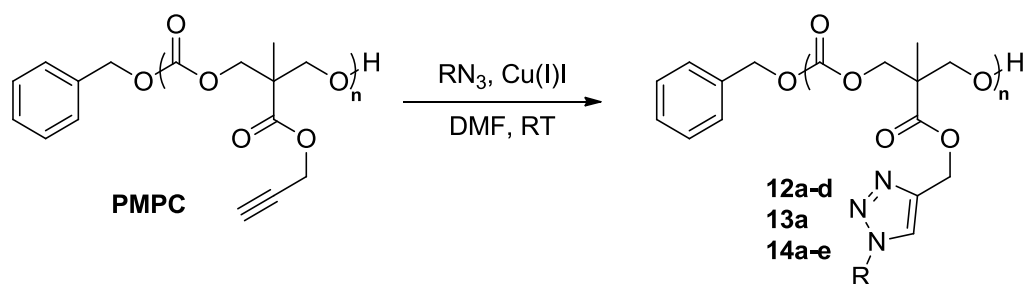


Figure 3.17. GPC traces of four block copolymers and their corresponding macro-initiator. Top left: BnO-PLLA₁₈-OH ($M_n = 4\,200\text{ g mol}^{-1}$, PDI = 1.09) and BnO-PLLA₁₈-*b*-PMPC₂₀-OH ($M_n = 8\,740\text{ g mol}^{-1}$, PDI = 1.08), top right: BnO-PMPC₂₀-OH ($M_n = 4\,540\text{ g mol}^{-1}$, PDI = 1.12) and BnO-PMPC₂₀-*b*-PLLA₂₄-OH ($M_n = 10\,350\text{ g mol}^{-1}$, PDI = 1.09), bottom left: MeO-PEO₁₁₄-OH ($M_n = 6\,790\text{ g mol}^{-1}$, PDI = 1.03) and MeO-PEO₁₁₄-*b*-PMPC₁₈-OH ($M_n = 11\,020\text{ g mol}^{-1}$, PDI = 1.06), bottom right: BnO-PMPC₁₇-OH ($M_n = 4\,010\text{ g mol}^{-1}$, PDI = 1.11) and BnO-PMPC₁₇-*b*-PMAC₁₉-OH ($M_n = 8\,110\text{ g mol}^{-1}$, PDI = 1.09).

3.2.3. Post-polymerisation functionalisation of propargyl-functional poly(carbonate), PMPC, via copper(I) catalysed Huisgen 1,3-dipolar cycloaddition.

Propargyl functional poly(carbonate)s could be further functionalised *via* the Cu(I)-catalysed Huisgen 1,3-dipolar cycloaddition (Scheme 3.2). Prior to functionalisation of polymers, optimisation of the required conditions to assure quantitative conversion of the propargyl groups in the polymer was carried out using a model system.

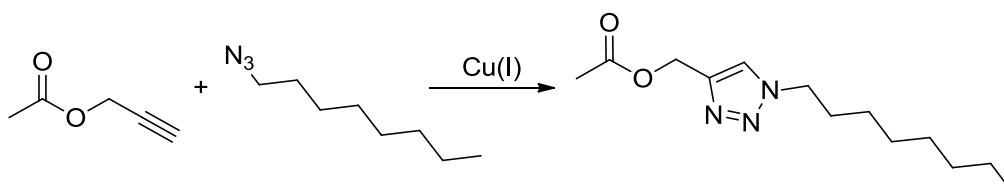


Scheme 3.2. Huisgen cycloaddition of an azide (N_3R) to PMPC polymers.

3.2.3.1. Post-polymerisation functionalisation of propargyl-functional poly(carbonate), PMPC, via copper(I) catalysed Huisgen 1,3-dipolar cycloaddition: Optimisation of conditions.

The model system used for the optimisation of the conditions required for quantitative conversion of the propargyl esters to the triazole-containing

products were carried out with propargyl acetate, 1-azidooctane and source of copper(I) (Scheme 3.3). Based on literature procedures,¹⁴⁻¹⁸ it was decided to both investigate copper(II) sulfate/sodium ascorbate in 1:1 water/organic solvent mixtures and copper(I) iodide/diisopropylethylamine (DIPEA) in organic solvents. Initial reactions were performed for 24 hours at room temperature using 1.5 equivalents of 1-azidooctane (0.33 M) and 0.4 or 0.8 equivalents of copper.



Scheme 3.3. The copper mediated cycloaddition of 1-azidooctane to propargyl acetate was used as a model reaction for the optimisation of conditions for PMPC functionalisation.

In all cases, quantitative or near quantitative conversion of the alkyne- to the triazole-containing product was observed, irrespective to which solvent or source of copper was used. Reducing the amount of 1-azidooctane from 1.5 to 1.1 equivalents for reaction in water/acetone catalysed by copper sulphate and sodium ascorbate showed 97% conversion, whereas the reaction in tetrahydrofuran catalysed by copper iodide and DIPEA showed 99% conversion. Further reduction of the amount of catalyst in the latter system to

0.1 and 0.2 equivalent of copper iodide, using 1.1 equivalent of octyl azide, showed conversions of the alkyne of 94% and 90% respectively (Table 3.4).

The optimisations was further continued using propargyl-functional poly(carbonate) with a degree of polymerisation (DP) of 20. A test reaction was performed utilising the preferred conditions of tetrahydrofuran with 0.4 equivalent of copper iodide and 0.8 equivalent of DIPEA with 1.05 equivalent

Table 3.4. Optimisation of reaction conditions for the copper mediated cycloaddition of propargyl acetate and octyl azide model reaction.^a

catalyst(s)	solvent(s)	equivalents	equivalents	conversion
		azide	catalyst(s)	(%)
Cu(II)SO ₄ / NaAsc ^b	H ₂ O/ DMSO ^d	1.5	0.8/1.6 ^c	quant.
Cu(II)SO ₄ / NaAsc ^b	H ₂ O/ dioxane ^d	1.5	0.8/1.6	quant.
Cu(II)SO ₄ / NaAsc ^b	H ₂ O/ acetone ^d	1.5	0.8/1.6	quant.
Cu(II)SO ₄ / NaAsc ^b	H ₂ O/ acetone ^d	1.1	0.8/1.6	97%
Cu(I)I/DIPEA ^c	DMF	1.5	0.4/0.8	quant.
Cu(I)I/DIPEA ^c	dioxane	1.5	0.4/0.8	quant.
Cu(I)I/DIPEA ^c	acetone	1.5	0.4/0.8	99%
Cu(I)I/DIPEA ^c	THF	1.5	0.4/0.8	quant.
Cu(I)I/DIPEA ^c	THF	1.1	0.4/0.8	99%
Cu(I)I/DIPEA ^c	THF	1.1	0.2/0.4	94%
Cu(I)I/DIPEA ^c	THF	1.1	0.1/0.2	90%

^a Reactions were performed at RT for 24h under nitrogen atmosphere using degassed solvents and reactants. ^b Using sodium ascorbate (NaAsc); ^c Using diisopropylamine (DIPEA); ^d With H₂O/ organic solvent ratio of 1:1.

1-azidooctane was performed. Reaction in an organic solvent was preferred to avoid degradation of the poly(carbonate). The reaction showed full conversion of the propargyl groups in the polymer to the octyl triazole-functional poly(carbonate) by ^1H NMR spectroscopy as well as the observation of a single distribution by MALDI-ToF MS analysis. The distribution revealed a repeat unit of 353 m/z , expected for a repeat unit after the addition of azidooctane, and a main peak at $m/z = 4725$ corresponding to a sodium charged, fully functionalised poly(carbonate) chain with a DP of 13 (Figure 3.18; Table 3.5).

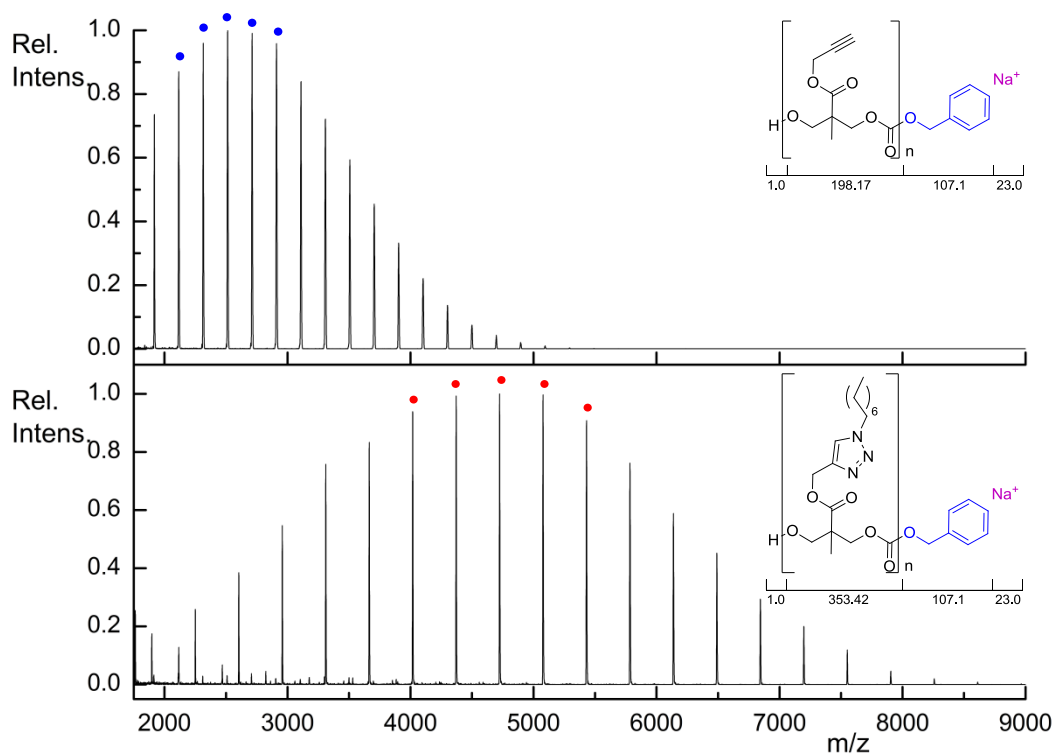


Figure 3.18. MALDI-TOF MS analysis of PMPC ($M/I = 20$) initiated from benzyl alcohol before (top) and after (bottom) functionalisation *via* cycloaddition with 1-azidooctane. In accordance to the addition of 1-azidooctane, the repeat unit increases from 198-199 m/z for PMPC (top) to 353 m/z after functionalisation (bottom). Theoretical and observed m/z values of the indicated peaks (●/●) are given in Table 3.5.

Table 3.5. Theoretical and observed m/z values of the indicated peaks (●/●) in Figure 3.18.

(●) PMPC ^a			(●) 1-azidooctane-functional PMPC		
DP	Exp. m/z^b	Calc. $m/z^c, d$	DP	Exp. m/z^b	Calc. m/z^c
10	2116.1	2117.6	11	4018.3	4018.2
11	2314.4	2315.7	12	4371.6	4371.4
12	2514.10	2514.7	13	4724.9	4724.6
13	2712.2	2712.8	14	5078.0	5078.8
14	2911.1	2911.8	15	5431.5	5432.0

^a Polymerisation performed in CDCl₃, yielding a partially deuterated polymer. ^b Experimentally observed m/z values; ^c Calculated m/z values; ^d Estimation, using the assumption that a 1:1 copolymer with repeat units of 198 and 199 m/z is formed.

3.2.3.2. Post-polymerisation functionalisation of propargyl-functional poly(carbonate), PMPC, *via* copper(I) catalysed Huisgen 1,3-dipolar cycloaddition: Functionalisation and characterisation.

Functionalisation with 1-azidooctane was successfully repeated for PMPC homopolymers with DP10 and DP72 resulting in polymers **12a** and **14a** in which >99% conversion of the propargyl groups had occurred as evidenced the disappearance of the resonance of the acetylenic proton at $\delta = 2.53$ ppm and the appearance of new resonances consistent with the triazole proton at $\delta = 7.73$ ppm and the octyl resonances at $\delta = 4.38, 1.92, 1.36-1.18$ and 0.86 ppm (Figure 3.19). Furthermore, analysis by GPC revealed a shift to higher molecular weight while maintaining narrow distributions with polydispersity indices similar to that of the unmodified PMPC. In case of the DP10 polymer

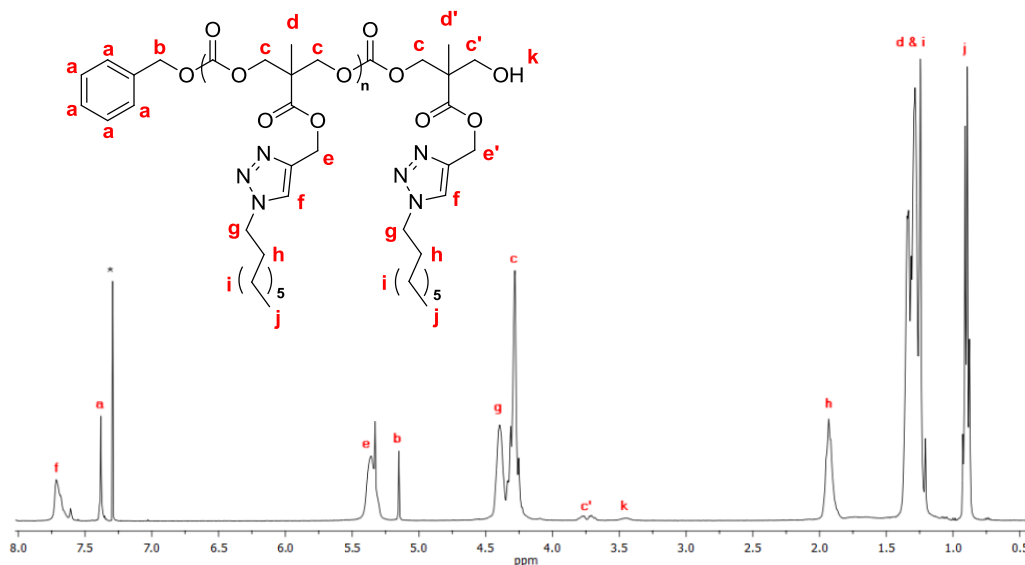


Figure 3.19. ^1H NMR in CDCl_3 of PMPC_{72} after functionalisation with 1-azido-octane (400 MHz, 298 K; * = residual CDCl_3).

a shift from $M_n = 2\,370\text{ g mol}^{-1}$ (PDI = 1.29) to $M_n = 5\,560\text{ g mol}^{-1}$ (PDI = 1.16) was observed and a shift from $M_n = 9\,350\text{ g mol}^{-1}$ (PDI = 1.11) to $M_n = 12\,690\text{ g mol}^{-1}$ (PDI = 1.15) for the DP72 polymer (Figure 3.20). Although most of the copper catalyst could be removed from the polymers by passing the polymer solution through a neutral alumina plug, removal of all copper proved difficult as evidenced by MALDI-ToF MS. Copper salts are known to act as good cationisation agents in the MALDI-ToF MS analysis of polymers such as polystyrene, polybutadiene and polyisoprene¹⁹⁻²¹ and this appeared to be true for functionalised poly(carbonate)s as a second distribution with a copper counter ion instead of the sodium counter ion expected from ionisation with sodium trifluoroacetate (NaTFA) was obtained. Preparation the MALDI-ToF

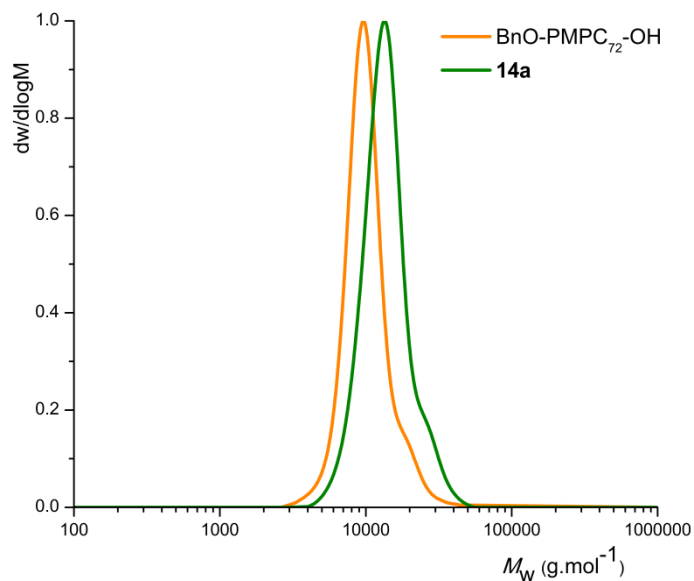


Figure 3.20. GPC traces of BnO-PMAC₇₂-OH before ($M_n = 9\,350$ g mol⁻¹, PDI = 1.11) and after post-polymerisation functionalisation with 1-azidoctane ($M_n = 12\,740$ g mol⁻¹, PDI = 1.15).

MS sample without sodium trifluoroacetate as cationisation agent resulted in the observation of a single distribution with a repeat unit of 353 m/z and a main peak at $m/z = 4765$ corresponding to a copper charged, fully functionalised polymer chain of DP13 (Figure 3.21, Table 3.6).

In order to demonstrate the versatility of this system, the PMPC homopolymers with degrees of polymerisation of 10, 12 and 72 were likewise functionalised *via* the Cu(I) assisted Huisgen 1,3-dipolar cycloaddition of the propargyl groups with a choice of azide-containing molecules including some with functional groups that are not compatible with ring-opening polymerisation process (Figure 3.22).

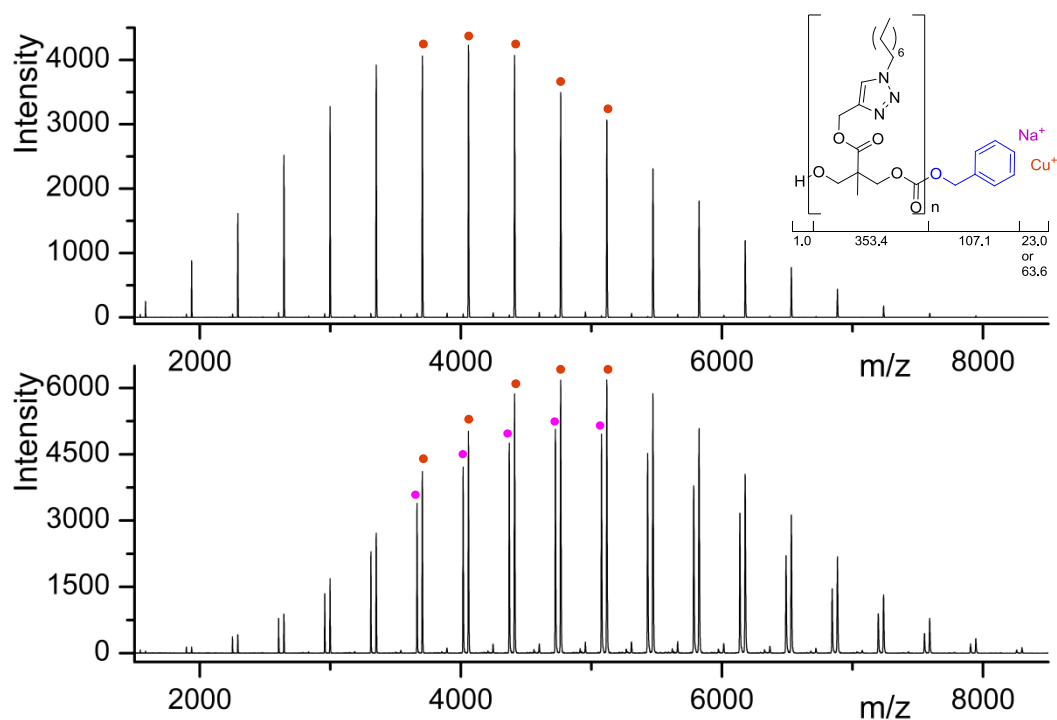


Figure 3.21. MALDI-ToF-MS spectra of PMPC (DP = 10) after post-polymerisation functionalisation with 1-azidooctane. Samples prepared without (top) and with (bottom) NaTFA show polymer chains ionised with residual copper from the functionalisation reaction.

Table 3.6. Theoretical and observed m/z values of the indicated peaks (●/●) in Figure 3.21.

DP	(●) 6a Cu ⁺		(●) 6a Na ⁺	
	Exp. m/z^b	Calc. m/z^c	Exp. m/z^b	Calc. m/z^c
10	3705.2	3704.9	3664.4	3665.0
11	4058.6	4059.1	4017.8	4018.2
12	4411.9	4412.3	4371.1	4371.4
13	4765.3	4765.5	4723.9	4724.6
14	5118.6	5118.7	5077.9	5078.8

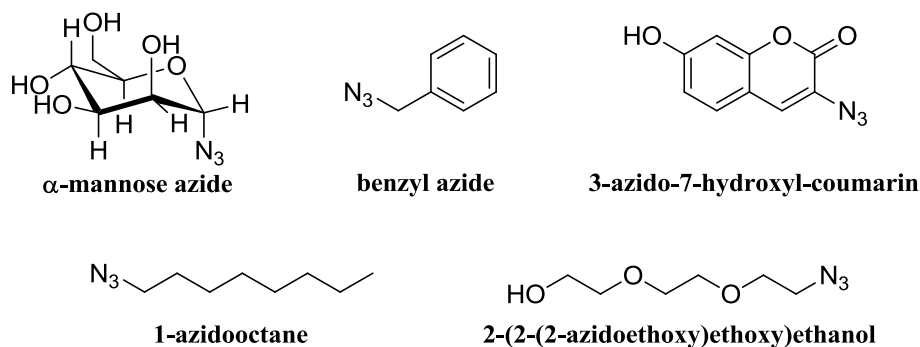


Figure 3.22. Functional azides for post-polymerisation alteration of propargyl-functional poly(carbonate)s *via* copper(I)-catalysed 1,3-dipolar cycloaddition.

Functionalisations with some azides (*i.e.* benzyl azide) could be carried out in tetrahydrofuran due to the solubility of the resulting polymers in this solvent. However, other functionalisations were expected to result in polymers insoluble in tetrahydrofuran and, as such, functionalisations were carried out in dimethylformamide. ^1H NMR spectroscopic analysis of polymers modified with 2-(2-(2-azidoethoxy)ethoxy)ethanol and benzylazide demonstrated that addition of the azide to the propargyl groups had occurred to >99% conversion, with new resonances being observed corresponding to the added functionalities. Furthermore, in these cases resonances corresponding to the triazole proton were found at $\delta = 7.6\text{--}7.8$ ppm. ^1H NMR spectroscopic analysis of DP10 and DP72 polymers modified with 3-azido-7-hydroxylcoumarin showed that, in both cases, addition of the azide to the propargyl groups had only occurred to 83-85% conversion (Figure 3.23). It was hypothesised that this lower conversion might be due to the bulky nature of the functional group

added, thereby sterically blocking the propargyl groups for further addition of 7-hydroxycoumarin. GPC data of polymers functionalised with benzyl azide only show a slight shift to lower retention time after functionalisation had occurred ($M_n = 2\,670\text{ g mol}^{-1}$, PDI = 1.33; and $M_n = 9\,700\text{ g mol}^{-1}$, PDI = 1.12; Figure 3.24), whilst retaining the narrow molecular weight distribution of the starting polymer. Such a relatively small shift was previously observed in the addition of a benzyl functionality to allyl-functional poly(carbonate)s. A similar observation was made for 2-(2-(2-azidoethoxy)ethoxy)ethanol functional poly(carbonate)s, where only a small shift to a lower retention

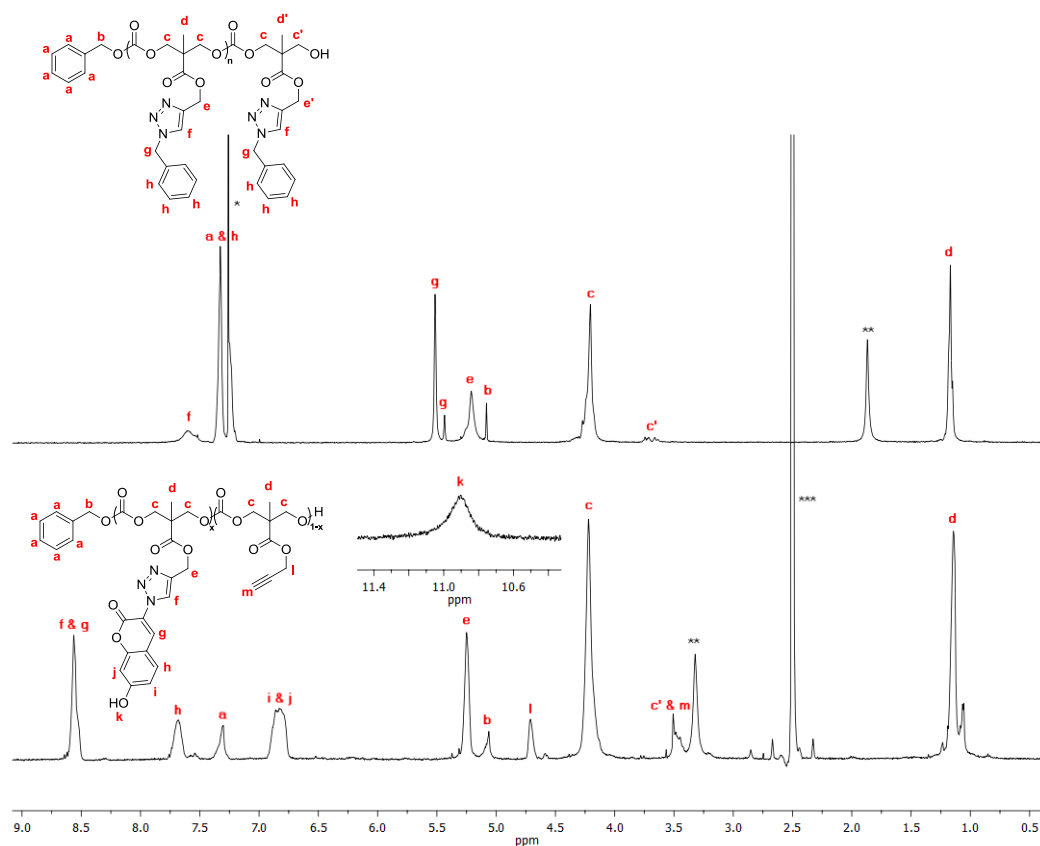


Figure 3.23. ¹H NMR in CDCl₃ of PMPC₇₂ after functionalisation with benzyl azide (top) and ¹H NMR of PMPC₇₂ after functionalisation with 3-azido-7-hydroxycoumarin (bottom) in d₂-DMSO (400 MHz, 298 K; * = residual CDCl₃, ** = H₂O, *** = residual d₂-DMSO).

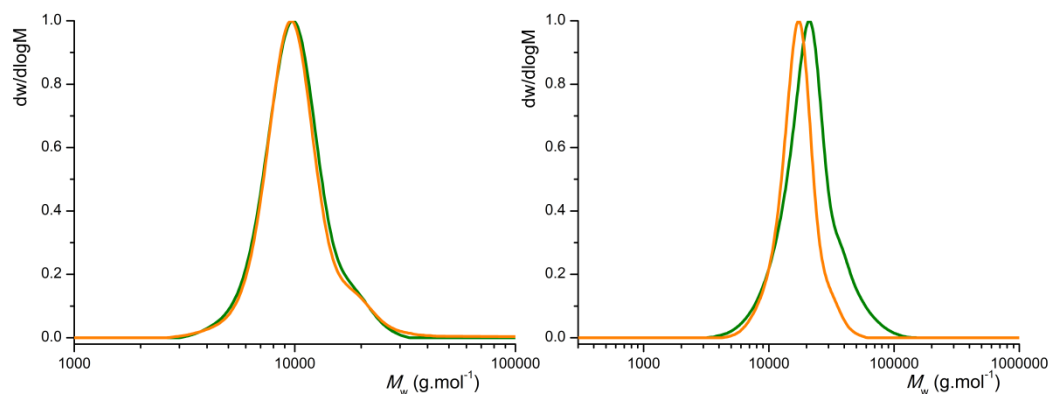


Figure 3.24. GPC traces of (left) BnO-PMAC₇₂-OH using THF as eluent before ($M_n = 9\,350\text{ g mol}^{-1}$, PDI = 1.11) and after post-polymerisation functionalisation with benzyl azide ($M_n = 9\,700\text{ g mol}^{-1}$, PDI = 1.15) and of (right) BnO-PMAC₇₂-OH using DMF as eluent before ($M_n = 15\,700\text{ g mol}^{-1}$, PDI = 1.13) and after post-polymerisation functionalisation with coumarin azide ($M_n = 18\,620\text{ g mol}^{-1}$, PDI = 1.23).

time was observed for the DP10 polymer. The DP72 polymer functionalised with 2-(2-(2-azidoethoxy)ethoxy)ethanol displayed a slightly higher retention time to that of the starting polymer. These observations were attributed to a change in interaction of the polymer backbone with the eluent after functionalisation. As such, their hydrodynamic volumes might remain similar to those observed before functionalisation even though the polymers have significantly increased in molecular weight. This hypothesis is supported by the observation of a distribution for benzyl azide functionalised PMPC₁₀ by MALDI-ToF MS analysis consistent with the new polymer structure without any residual pendant propargyl groups. The single distribution observed shows an increase in the repeating unit from 198 m/z to 331 m/z and a main

peak at $m/z = 2781$ corresponding to a sodium charged, fully functionalised polymer chain with DP = 8 (Figure 3.25; Table 3.7).

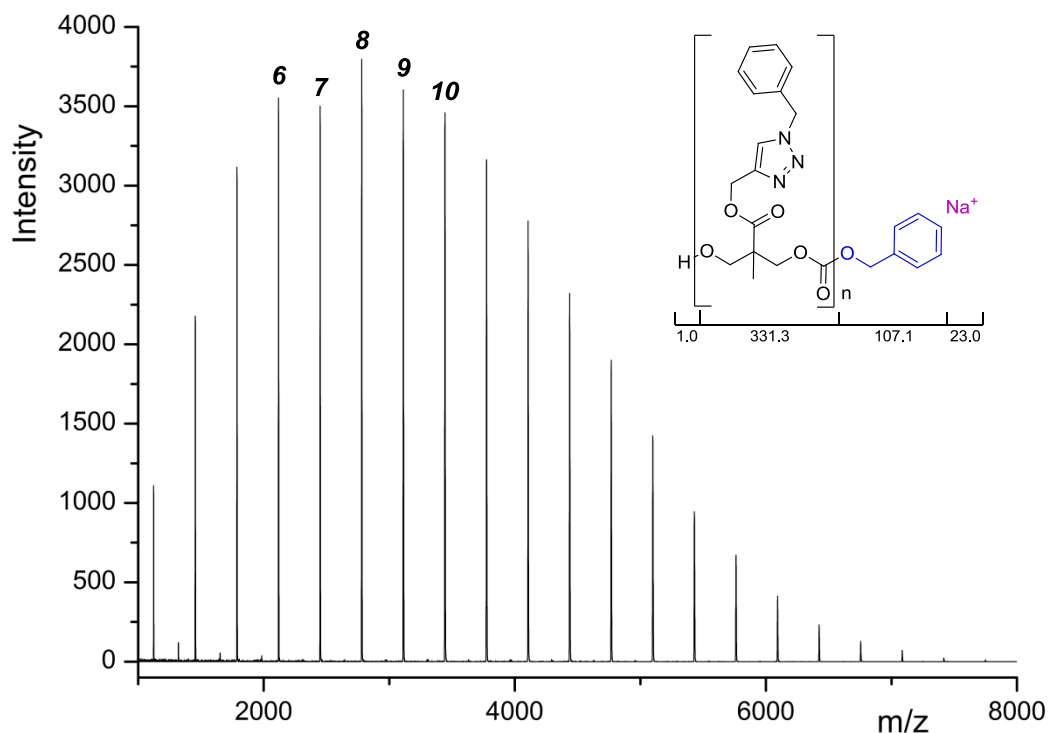


Figure 3.25. MALDI-ToF-MS spectrum of PMPC₁₀ after post-polymerisation functionalisation with benzyl azide.

Table 3.7. Theoretical and observed m/z values of PMPC₁₀ after functionalisation with benzyl azide (Figure 3.25).

DP	Experimental m/z^b	Calculated $m/z^c, d$
6	2118.3	2118.9
7	2449.7	2450.4
8	2781.1	2781.5
9	3112.6	3112.8
10	3443.7	3444.1

MALDI-ToF MS analysis of PMPC₁₀ functionalised with 3-azido-7-hydroxycoumarin, however, revealed new distributions consistent with partially functionalised polymer chains. The main three main distributions identified were with fully functionalised polymer chains and polymer chains with one and two unreacted propargyl groups (Figure 3.26, Table 3.8). Irradiation of hydroxycoumarin-modified poly(carbonate)s at 365 nm with a UV lamp provided further evidence the pendant alkynes had reacted s strong fluorescence was observed for both DP10 and DP72(Figure 3.27). 3-azido-7-hydroxycoumarin is a profluorophore and is fluorescence inactive until formation of the triazole ring. Indeed, no fluorescence was observed for the PMPC or 3-azido-7-hydroxycoumarin starting materials, or a mixture of the two.

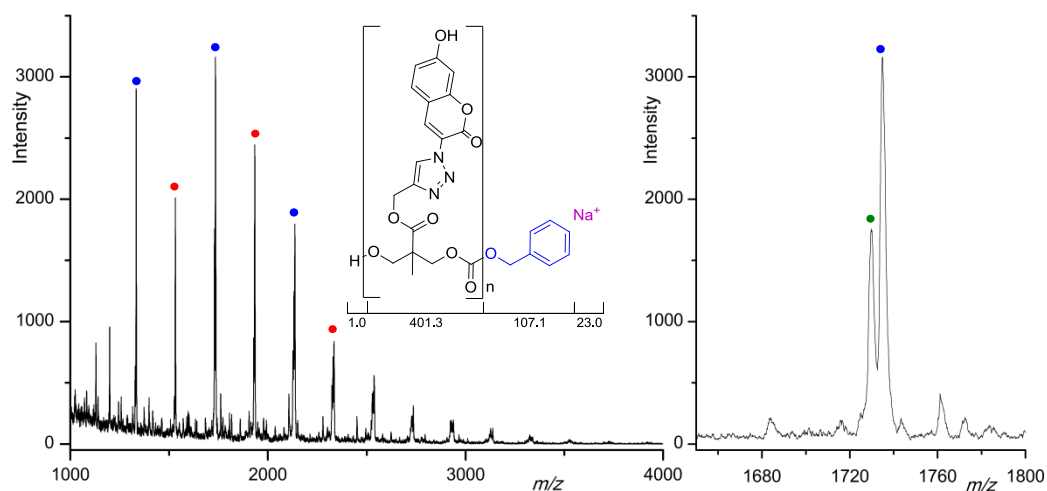


Figure 3.26. MALDI-ToF-MS spectrum of PMPC₁₀ after post-polymerisation functionalisation with 3-azido-7-hydroxycoumarin (left). The presence of propargyl-containing polymer chains confirms that post-polymerisation functionalisation did not go to completion. A close up of the region between 1620 m/z and 1800 m/z (right) shows the presence of a two separate species. ● = PMPC fully functionalised with 3-azido-7-hydroxycoumarin azide; ● = polymer chains with 1 propargyl group left; ● = polymer chains with 2 propargyl groups left.

Table 3.8. Theoretical and observed m/z values of the indicated peaks (●/●) in Figure 3.26.

(●) 6d ^a			(●) 6d ^b		
DP	Exp. m/z	Calc. m/z	DP	Exp. m/z	Calc. m/z
3	1333.4	1334.3	4	1532.1	1532.4
4	1735.4	1735.4	5	1933.7	1934.4
5	2136.4	2137.5	6	2335.1	2335.5

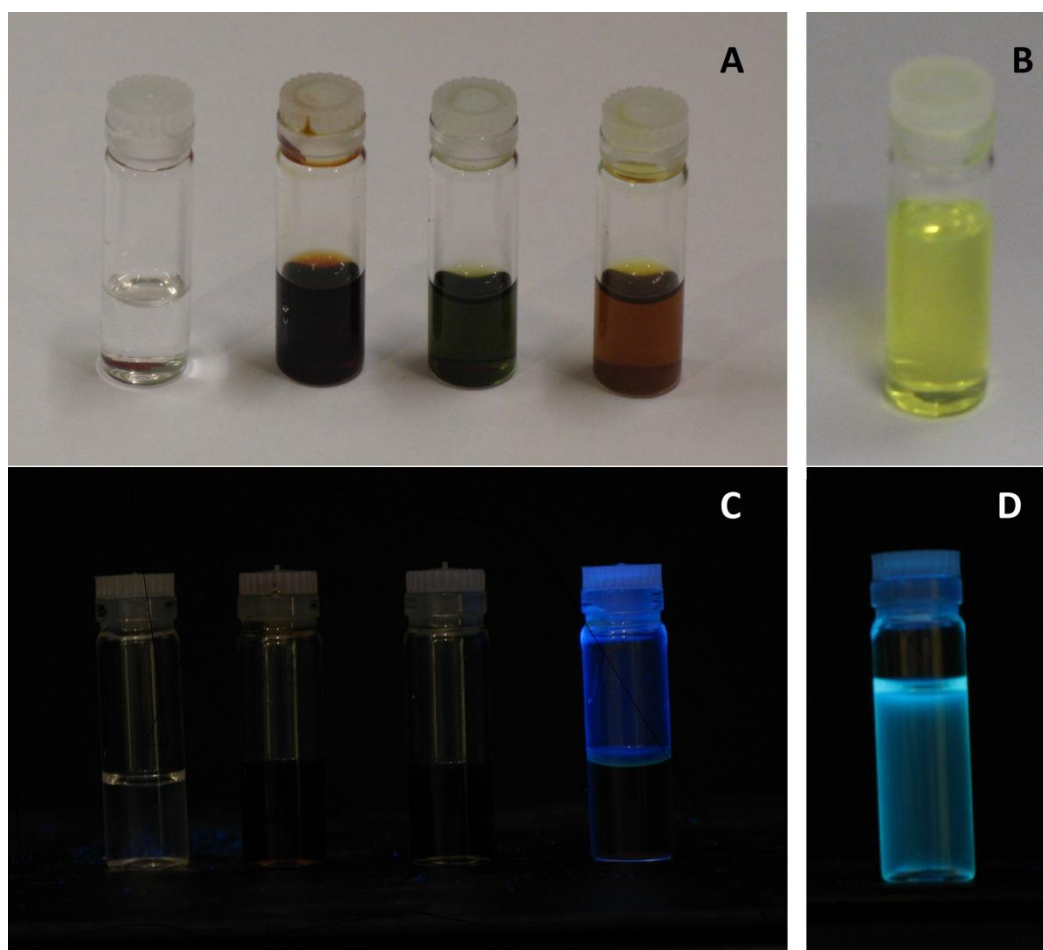


Figure 3.27. Fluorescence in 3-azido-7-hydroxycoumarin-clicked PMPC is triggered by the formation of the triazole rings.(A) From left to right: Solutions in DMF of PMPC, 3-azido-7-hydroxycoumarin, PMPC + 3-azido-7-hydroxycoumarin, PMPC after functionalisation with 3-azido-7-hydroxycoumarin (**12d**); (B) Further diluted solution of **12d** in DMF; (C) From left to right: Solutions in DMF of PMPC, 3-azido-7-hydroxycoumarin, PMPC + 3-azido-7-hydroxycoumarin, **12d**, irradiated at 365 nm with a UV lamp; (D) Further diluted solution of **12d** in DMF irradiated at 365 nm with a UV lamp.

Finally, a click reaction with mannose azide was performed. Click reactions were performed in DMF, yielding polymers that were insoluble in chloroform. ^1H NMR spectroscopic analysis of the mannose functionalised polymers of DP12 and DP72 was therefore performed in deuterated DMSO which revealed that >99 % conversion of the alkyne groups to the triazole product had occurred. ^1H NMR spectroscopic analysis in *d*-DMSO proved difficult to elucidate, therefore additional NMR analyses were performed in both D_2O and *d*-DMSO. Comparison of the ^1H NMR spectra in H_2O and *d*-DMSO revealed which resonances corresponded to the hydroxyl groups (Figure 3.28), whilst further analysis by correlation spectroscopy (COSY) made it possible to assign all resonances in the NMR spectra (Figure 3.29).

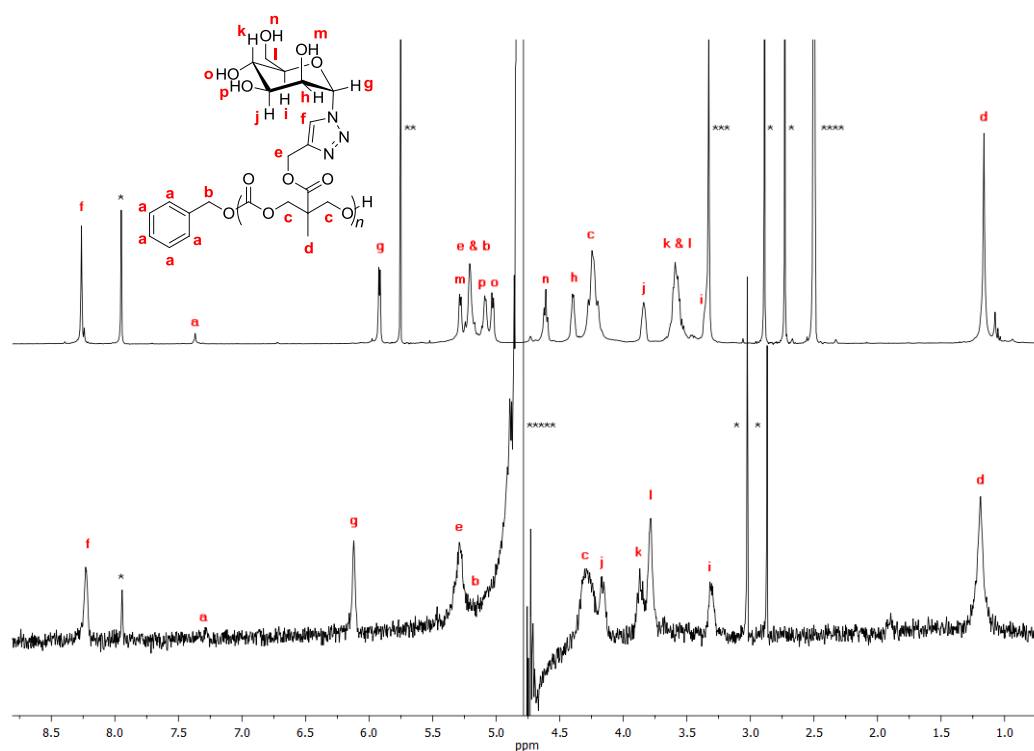


Figure 3.28. ^1H NMR spectra of PMPC₇₂ after functionalisation with α -mannose azide in *d*-DMSO (top; 400 MHz, 298 K) and in D₂O (bottom; 400 MHz, 298 K); * = dimethyl formamide, ** = methylene chloride, *** = H₂O, **** = residual *d*-DMSO, ***** = residual D₂O.

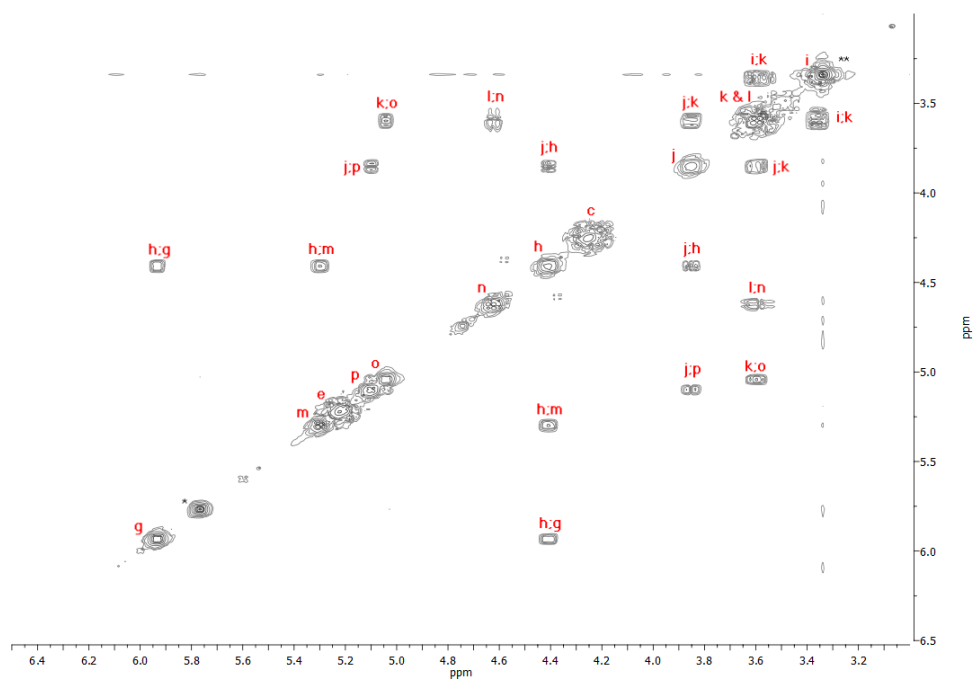


Figure 3.29. COSY in *d*-DMSO of PMPC₇₂ after functionalisation with α -mannose azide (400 MHz, 298 K; * = methylene chloride, ** = H₂O). In combination with the ^1H NMR spectrum in both *d*-DMSO and D₂O and the COSY in D₂O, all mannose protons in Figure 3.28 could be assigned.

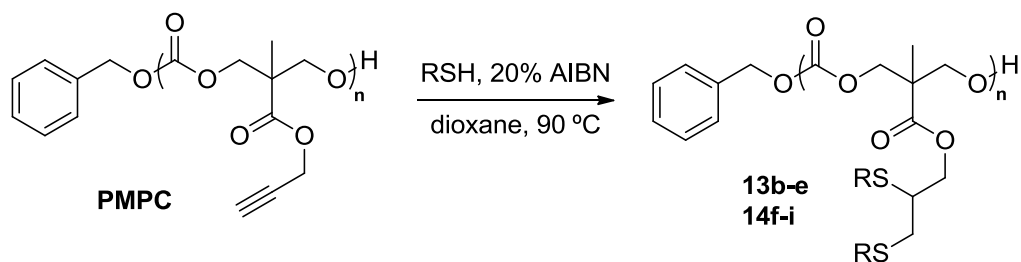
Table 3.9. Post-polymerisation functionalisation of poly(carbonates) *via* copper assisted alkyne-azide cycloaddition.^a

polymer	azide	M_n (g mol ⁻¹)	PDI ^c
BnO-PMPC ₁₀ -OH (12)	-	2240 ^b /4600 ^c	1.33 ^b /1.18 ^c
BnO-PMPC ₁₂ -OH (13)	-	2370 ^b /5810 ^c	1.29 ^b /1.17 ^c
BnO-PMPC ₇₂ -OH (14)	-	9350 ^b /15 700 ^c	1.11 ^b /1.13 ^c
12a	1-azidooctane ^d	5560 ^b	1.16 ^b
14a	1-azidooctane	12 740 ^b	1.15 ^b
12b	benzyl azide ^d	2670 ^b	1.33 ^b
14b	benzyl azide	9700 ^b	1.12 ^b
12c	TEG-azide ^d	2477 ^b	1.28 ^b
14c	TEG-azide	7000 ^b	1.21 ^b
12d	Coumarin-azide	5657 ^c	1.12 ^c
14d	Coumarin-azide	18 620 ^c	1.23 ^c
13a	Mannose-azide	8610 ^c	1.23 ^c
14e	Mannose azide	13200 ^c	1.30 ^c

^a [PMPC] = 0.34 M in THF or DMF, 1.1 equivalent of azide, 0.4 eq. CuI, 0.8 eq. DIPEA, RT, 24 h; ^b Measured by GPC analysis using THF as eluent; ^c Measured by GPC analysis using DMF as eluent; ^d reaction performed using 1.05 eq. azide; ^e Reaction performed in H₂O/acetone (1:1) using 0.8 eq. CuSO₄, 1.6 eq. RT, 24h

3.2.4. Post-polymerisation functionalisation of propargyl-functional poly(carbonate), PMPC, *via* radical addition of thiols.

Similar to the optimisation for the required conditions for the radical addition of thiols to allyl esters, the optimisations were undertaken of the radical addition of thiols to propargyl esters using a model system consisting of propargyl acetate and benzyl mercaptan with AIBN as the radical initiator. Having found the optimal conditions for the functionalisation of allyl functional poly(carbonate)s, the optimisation was started using the best conditions identified in these prior experiments (*i.e.* 0.15 M polymer in dioxane at 90 °C for 24 h with 2 equivalents of benzyl mercaptan). However, double the equivalent of thiol containing species was used as two equivalents of thiol should be added to the carbon-carbon triple bond. Using these conditions it was found that the first equivalent of thiol was added to the propargyl group, no full conversion to the doubly substituted product was achieved as evidenced by the ¹H NMR spectrum showing a mixture of products. Increasing the amount of benzyl mercaptan to 10 equivalents did show near full conversion to the doubly substituted product. Using these conditions for the functionalisation of propargyl-functional polymers of DP12 and DP72 with a range of thiols (Scheme 3.4), revealed that >99% conversion of the propargyl groups had occurred in all cases, evidenced by the disappearance of the resonance of the acetylenic proton at $\delta = 2.53$ ppm and



Scheme 3.4. Radical addition of thiols (RSH) to PMPC polymers.

the appearance of new resonances consistent with the corresponding thiol added. For example, in case of functionalisation with 1-dodecanethiol, new resonances were observed at $\delta = 2.76, 3.00$ and 4.39 ppm corresponding to the modified polymer as well as the dodecyl resonances at $\delta = 1.19-1.44, 1.58$ and 2.56 ppm (Figure 3.30). Although analysis by GPC revealed a shift to higher molecular weight, a high molecular weight shoulder was observed (Figure

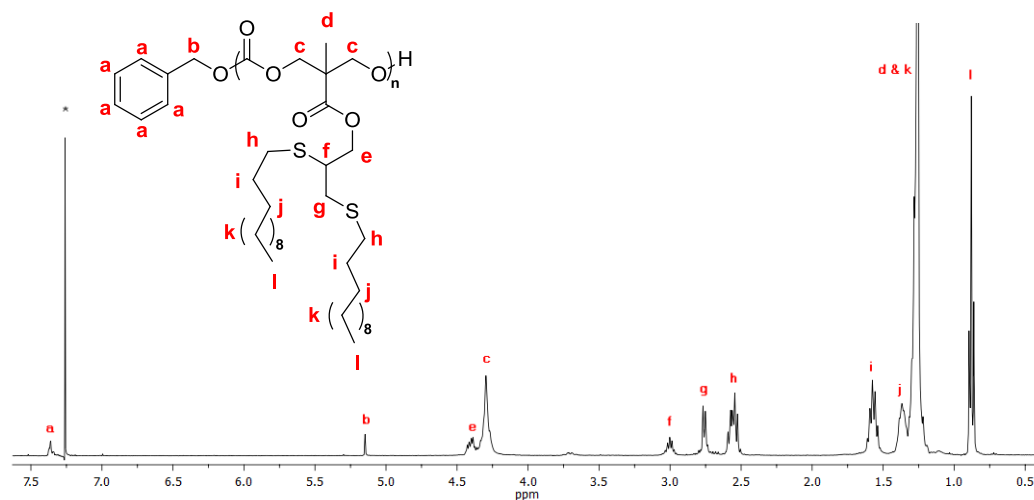


Figure 3.30. ^1H NMR in CDCl_3 of PMPC_{12} after post-polymerisation radical functionalisation with 1-dodecanethiol (400 MHz, 298 K; * = residual CDCl_3).

3.31). This shoulder and broadening of the molecular weight distribution is most likely caused by cross-linking of the propargyl groups or allyl intermediates. A shift from $M_n = 2\,370\text{ g mol}^{-1}$ (PDI = 1.29) to $M_n = 5\,700\text{ g mol}^{-1}$ (PDI = 1.80) was observed for the DP10 polymer and from $M_n = 9\,350\text{ g mol}^{-1}$ (PDI = 1.13) to $M_n = 18\,140\text{ g mol}^{-1}$ (PDI = 1.17) for the DP72 polymer.

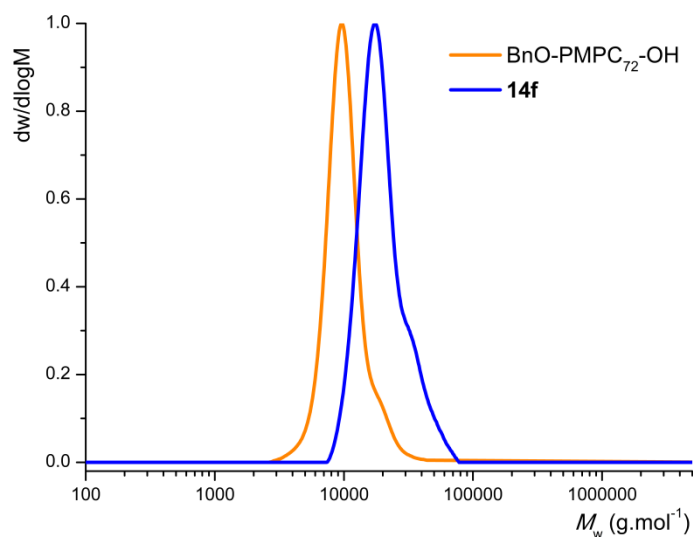


Figure 3.31. GPC traces of BnO-PMAC₇₂-OH before ($M_n = 9\,350\text{ g mol}^{-1}$, PDI = 1.11) and after post-polymerisation functionalisation with 1-dodecanethiol ($M_n = 18\,140\text{ g mol}^{-1}$, PDI = 1.17).

MALDI-ToF MS analysis of the polymer revealed a new distribution with a repeat unit that was consistent with the addition of two 1-dodecanethiol molecules ($2 \times 202\text{ g mol}^{-1}$), resulting in an increase in the repeating unit from 198 m/z to 603 m/z (Figure 3.32; Table 3.10). The main peak at $m/z = 2542$ corresponds with a sodium charged, fully functionalised polymer chain with

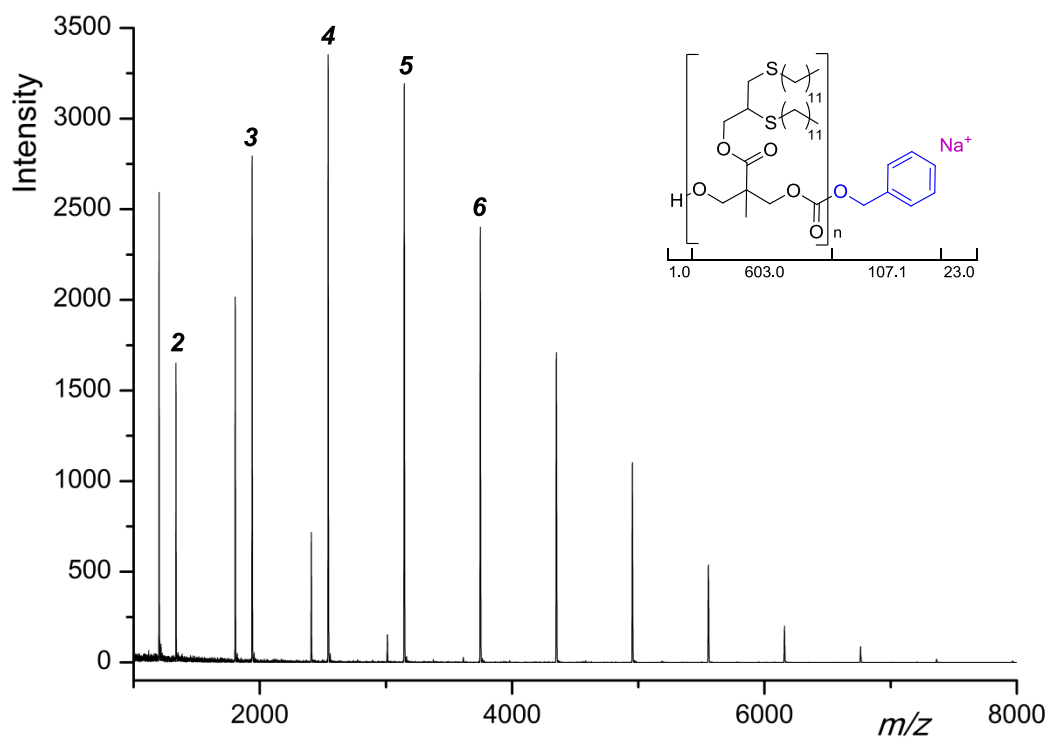


Figure 3.32. MALDI-ToF-MS spectrum of PMPC₁₂ after post-polymerisation functionalisation with 1-dodecanethiol.

Table 3.10. Theoretical and observed m/z values of PMPC₁₀ after functionalisation with 1-dodecanethiol (Figure 3.32).

DP	Experimental m/z^b	Calculated $m/z^c, d$
2	1335.1	1335.9
3	1939.4	1939.3
4	2542.3	2542.7
5	3145.2	3145.1
6	3748.1	3748.5

DP = 4. A second distribution was observed showing a loss of ~135 Da, This second distribution is only present at low m/z and is in combination with the observation of a main peak at a lower DP than expected. This could be due to mid-chain cleavages including a loss of CO leading to one distribution at a lower m/z than expected and a distribution which corresponds to the loss of the benzyl alcohol end group and CO and has most likely occurred during analysis. No peaks were observed for polymer chains with residual alkyne groups. The radical “thiol-yne” process was repeated for a range of thiol-containing molecules including those with alcohol groups which are incompatible with ring-opening polymerisation. ^1H NMR spectroscopic analysis of the modified polymers (Figure 3.33) all demonstrated that full conversion to the doubly substituted product had occurred with data consistent with those expected for the modified side-chain groups. Although GPC data revealed a shift to higher molecular weight in all cases, each also revealed a high molecular weight shoulder due to cross-linking of the propargyl groups (Figure 3.34).

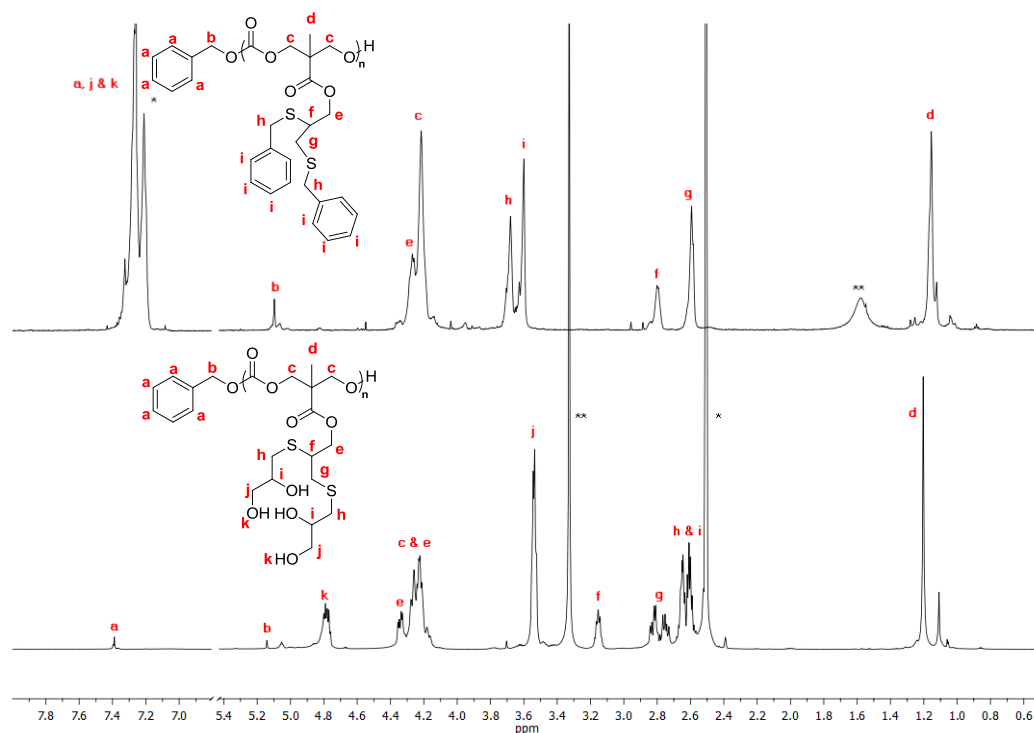


Figure 3.33. ^1H NMR spectrum in CDCl_3 of PMPC_{12} after functionalisation with benzyl mercaptan (top) and ^1H NMR spectrum of PMPC_{72} after functionalisation with 1-thioglycerol (bottom) in $d\text{-DMSO}$ (400 MHz, 298 K; * = residual CDCl_3 / $d\text{-DMSO}$, ** = H_2O).

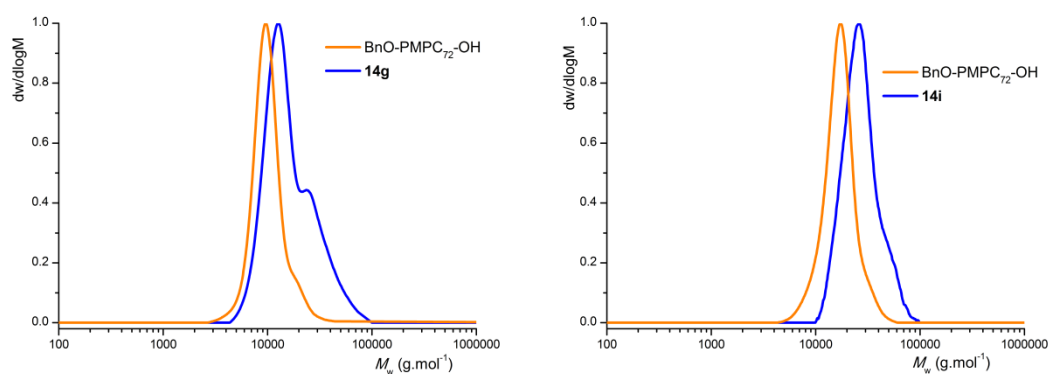


Figure 3.34. GPC traces of $\text{BnO-PMPC}_{72}\text{-OH}$ before ($M_n = 9\,350\text{ g mol}^{-1}$, PDI = 1.11) and after post-polymerisation functionalisation with benzyl mercaptan ($M_n = 14\,020\text{ g mol}^{-1}$, PDI = 1.21) and before ($M_n = 15\,700\text{ g mol}^{-1}$, PDI = 1.13) and after functionalisation with mercaptoethanol ($M_n = 24\,830\text{ g mol}^{-1}$, PDI = 1.16).

MALDI-ToF MS analysis of benzyl mercaptan functionalised PMPC₁₂ revealed a new distribution with a repeat unit of 447 m/z consistent with the addition of two benzyl mercaptan molecules. The main peak at $m/z = 2363$ corresponds to a sodium charged, fully functionalised polymer chain with a DP of 5. However, a second distribution was also observed which could correspond to a polymer chain in which two propargyl units remain. The assumption of a polymer chain with 2 remaining propargyl groups seems unlikely because of the lack of the three distributions corresponding to polymer chains in which one, two, or three benzyl mercaptan molecules have not added (Figure 3.35; Table 3.11). The second distribution most likely due to cross-linking as the apparent degree of polymerisation of the second distribution is double to that of the main distribution, although the precise structure of this second species could not be elucidated.

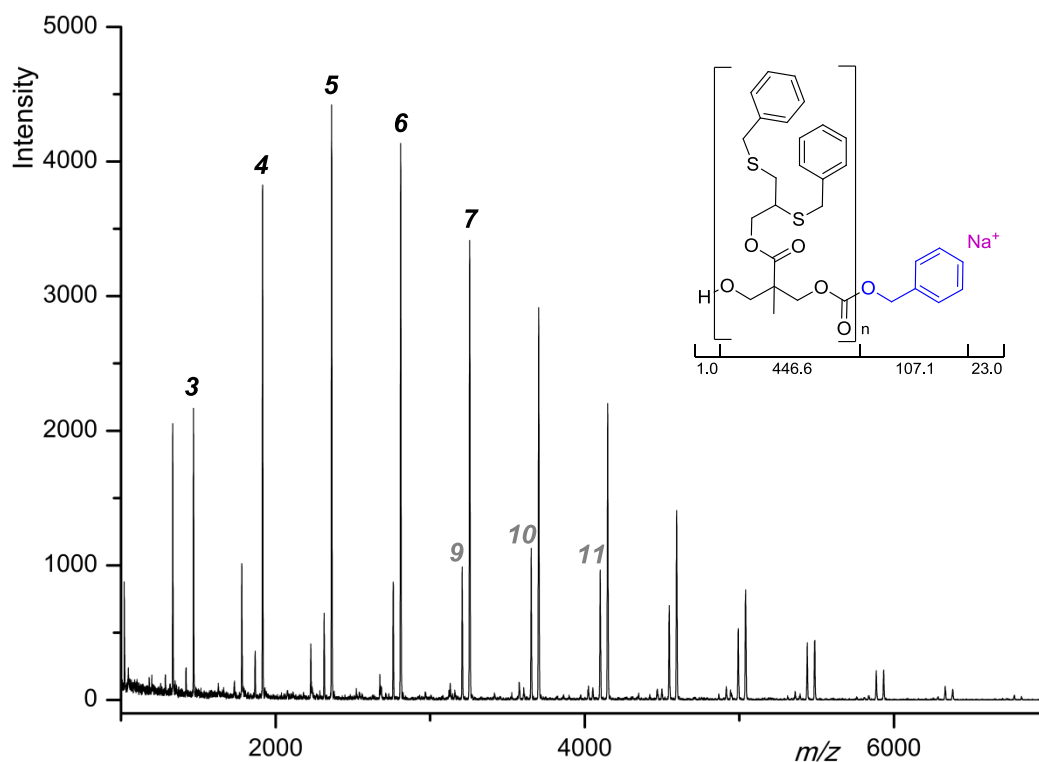


Figure 3.35. MALDI-TOF MS analysis of PMPC₁₂ after functionalisation with benzyl mercaptan. A main distribution of fully functionalised polymer (●) is observed as well as a distribution of cross-linked, benzyl functionalised PMPC₁₂ (●).

Table 3.11. Theoretical and observed m/z values of PMPC₁₀ after functionalisation with benzyl mercaptan (Figure 3.35).

(●) 7c ^a			(●) cross-linked 7c		
DP	Exp. m/z^b	Calc. $m/z^c, d$	DP	Exp. m/z^b	Calc. m/z^c
3	1468.6	1470.5	8	2761.6	2760.0
4	1916.2	1917.0	9	3207.1	3206.5
5	2362.9	2363.5	10	3653.3	3653.0
6	2809.1	2810.0	11	4100.1	4099.5
7	3255.9	3256.5	12	4545.7	4546.0

Table 3.12. Post-polymerisation radical ‘thiol-yne’ functionalisation of poly(carbonates).^a

polymer	thiol	M_n (g mol ⁻¹)	PDI ^c
BnO-PMPC ₁₂ -OH (13)	-	2370 ^b /5810 ^c	1.29 ^b /1.17 ^c
BnO-PMPC ₇₂ -OH (14)	-	9350 ^b /15700 ^c	1.11 ^b /1.13 ^c
13b	1-dodecanethiol	5700 ^b	1.80 ^b
14f	1-dodecanethiol	18 140 ^b	1.17 ^b
13c	benzyl mercaptan	3570 ^b	1.36 ^b
14g	benzyl mercaptan	14 020 ^b	1.21 ^b
13d	1-thioglycerol	7830 ^c	1.22 ^c
14h	1-thioglycerol	11 550 ^c	1.57 ^c
13e	mercaptoethanol	7830 ^c	1.36 ^c
14i	mercaptoethanol	24 830 ^c	1.16 ^c

^a Reactions performed in dioxane, 10 equivalent of thiol, 20 mol% AIBN, 90 °C, 24 h; ^b Measured by GPC analysis using THF as eluent; ^c Measured by GPC analysis using DMF as eluent.

3.3. Conclusions

In conclusion, the controlled ring-opening polymerisation of 5-methyl-5-propargyloxycarbonyl-1,3-dioxan-2-one, MPC, was achieved successfully by using thiourea and DBU. Low molecular polydispersities, the observation of a linear evolution of molecular weight with both monomer conversion and monomer-to-initiator ratio, low PDIs, and the synthesis of telechelic polymers and block copolymers of PMPC with PEO, PLA and PMAC demonstrated the living nature of the polymerisations. Post-polymerisation functionalisation of the pendant propargyl groups in the polymer backbone *via* the copper-catalysed Huisgen 1,3-dipolar cycloaddition led to the isolation of aliphatic poly(carbonate)s with a range of pendant functionalities, without notable polymer degradation. Post-polymerisation functionalisation of the polymers *via* radical 'thiol-yne', however, resulted in cross-linked polymers even when using 10 equivalents of thiol. These methodologies provide attractive routes to the synthesis of biodegradable and biocompatible functional polymers.

3.4. References

1. Sessions, L. B.; Cohen, B. R.; Grubbs, R. B. *Macromolecules*, **2007**, *40*, 1926–1933.
2. Baier, M. C.; Huber J.; Mecking, S. *J. Am. Chem. Soc.*, **2009**, *131*, 14267–14273.
3. Abe, H.; Kurokawa, H.; Chida, Y.; Inouye, M. *J. Org. Chem.*, **2011**, *76*, 309–311.
4. Stumpe, K.; Komber, H.; Voit, B. I. *Macromol. Chem. Phys.*, **2006**, *207*, 1825–1833.
5. Meldal, M.; Tornøe, C. W. *Chem. Rev.*, **2008**, *108*, 2952–3015.
6. Lutz, J. F. *Angew. Chem. Int. Ed.*, **2007**, *46*, 1018–1025.
7. Binder, W. H.; Sachsenhofer, R. *Macromol. Rapid Commun.*, **2007**, *28*, 15–54.
8. Konkolewicz, D.; Gray-Weale, A.; Perrier, S. *J. Am. Chem. Soc.*, **2009**, *131*, 18075–18077.
9. C. Lu, Q. Shi, X. Chen, T. Lu, Z. Xie, X. Hu, J. Ma, X. Jing, *J. Polym. Sci. Part A: Polym. Chem.*, **2007**, *45*, 3204–3217.
10. Shia, Q.; Chen, X.; Lu, T.; Jing, X. *Biomaterials*, **2008**, *29*, 1118–1126.
11. Han, Y.; Shi, Q.; Hu, J.; Du, Q.; Chen, X.; Jing, X. *Macromol. Biosci.*, **2008**, *8*, 638–644.
12. Shi, Q.; Huang, Y.; Chen, X.; Wu, M.; Sun, J.; Jing, X. *Biomaterials*, **2009**, *30*, 5077–5085.

13. F. Nederberg, Y. Zhang, J. P. K. Tan, K. Xu, H. Wang, C. Yang, S. Gao, X. D. Guo, K. Fukushima, L. Li, J. L. Hedrick & Y. Y. Yang, *Nat. Chem.* **2011**, *3*, 409–414.
14. Fijten, M. W. M.; Haensch, C.; van Lankvelt, B. M.; Hoogenboom, R.; Schubert, U. S. *Macromol. Chem. Phys.* **2008**, *209*, 1887–1895.
15. Ngai, M. H.; Yang, P. Y.; Liu, K.; Shen, Y.; Wenk, M. R.; Yao, S. Q.; Lear, M. J. *Chem. Commun.*, **2010**, *46*, 8335–8337.
16. Xie, M.; Shi, J.; Ding, L.; Li, J.; Han, H.; Zhang, Y. *J. Polym. Sci., Part A: Polym. Chem.* **2009**, *47*, 3022–3033.
17. Parrish, B.; Breitenkamp, R. B.; Emrick, T. *J. Am. Chem. Soc.* **2005**, *127*, 7404–7410.
18. Riva, R.; Schmeits, S.; Stoffelbach, F.; Jérôme, C.; Jérôme, R.; Lecomte, P. *Chem. Commun.* **2005**, 5334–5336.
19. Kéki, S.; Deák G.; Zsuga, M. *Rapid Commun. Mass Spectrom.* **2001**, *15*, 675–678.
20. Nielen, M. W.F. *Mass Spectrom. Rev.* **1999**, *18*, 309–344.
21. Knochenmuss, R.; Lehmann, E.; Zenobi, R. *Eur. Mass Spectrom.* **1998**, *4*, 421–427.

Chapter 4

Synthesis and Orthogonal post-Polymerisation Functionalisation of Allyl and Propargyl Functional Poly(Carbonate)s

Allyl- and propargyl-functional cyclic carbonates were copolymerised using organic catalysts resulting in well-defined poly(carbonate)s with the two pendant functionalities. The resulting poly(carbonate)s obtained showed low polydispersities and high end-group fidelity. Orthogonal functionalisation of a copolymer with a degree of polymerization of 24 was realised via the Huisgen cycloaddition of azides to the propargyl functionalities followed by the radical addition of thiols to the pendant allyl functional groups, resulting in a new, functional, amphiphilic aliphatic poly(carbonate).

4.1. Introduction

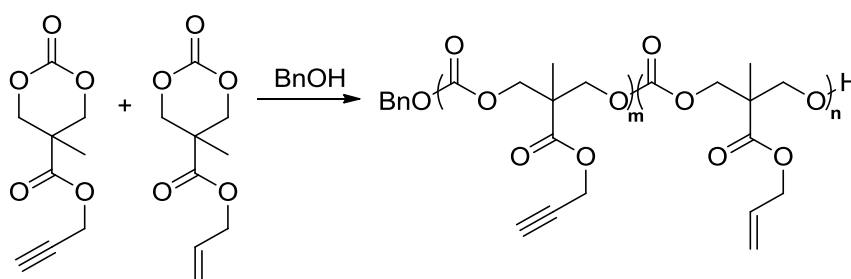
Highly functionalised biodegradable macromolecules are materials which offer good potential for use in drug delivery applications. The ability to control their properties and structure by applying facile post-polymerisation techniques is key to their development. In the ring-opening process, functionalities that are susceptible to further facile reactions can be easily introduced to the α -chain end by employing an appropriate alcohol initiator.^{1,2} Functionalisation of the ω -chain end poses more of a challenge but successful examples of such processes have been reported.³ The application of monomers with pendant functionalities further offers a route to complex materials such as multi-functionalised homo- and copolymers. Facile post-polymerisation functionalisation of biodegradable homopolymers and copolymers with a pendant functionality have been previously reported and were discussed in Chapters 1, 2 and 3. Although these materials lead to a control of the polymer structure, more precise control and more complex structures could be prepared by orthogonal functionalisation of two or more functionalities in the polymer backbone. Orthogonal approaches to polymer functionalisation have been successfully applied for the facile preparation non-degradable polymers,⁴⁻⁸ partially degradable polymers,⁹ in the synthesis of biodegradable dendrons¹⁰ and helical block copoly(α -peptide)s.¹¹ Orthogonal functionalisation in the backbone of biodegradable polymers have also been reported using robust and efficient techniques such as the 1,3-

dipolar cycloaddition of alkynes and azides,^{12,13} Michael-type or radical addition of thiols to alkenes and Diels Alder reactions^{5,8}. Herein the preparation of allyl- and propargyl- functional aliphatic copoly(carbonate)s *via* organocatalytic ring-opening polymerisation (ROP) and the orthogonal post-polymerisation functionalisation of the pendant alkyne and alkene functionalities in one copolymer is reported.

4.2. Results and Discussion

4.2.1. Copolymerisations of 5-methyl-5-allyloxycarbonyl-1,3-dioxan-2-one (MAC) and 5-methyl-5-propargyloxycarbonyl-1,3-dioxan-2-one (MPC).

The synthesis of allyl- and propargyl functional aliphatic poly(carbonate)s was achieved *via* the ROP of 5-methyl-5-allyloxycarbonyl-1,3-dioxan-2-one (MAC) and 5-methyl-5-propargyloxycarbonyl-1,3-dioxan-2-one (MPC) with organic catalysts (Scheme 4.1). Reactions were performed in CDCl_3 ($[\text{M}] = 0.5 \text{ M}$) at $25 \text{ }^\circ\text{C}$, using benzyl alcohol as initiator with $[\text{M}]/[\text{I}] = 20$ and polymerisations were catalysed by the dual catalyst system of 10 mol% 1-(3,5-bis(trifluoromethyl)phenyl)-3-cyclohexylthiourea, **3**, in combination with 5 mol% (-)-sparteine (**2**) or the dual catalyst system of 5 mol % 1-(3,5-bis(trifluoromethyl)phenyl)-3-cyclohexylthiourea, **3**, in combination with 1 mol % 1,8-diazabicyclo[5.4.0]undec-7-ene (**1**, DBU) (Figure 4.1), which showed excellent control in the homopolymerisation of MAC and MPC as



Scheme 4.1. Ring-opening polymerisation of 5-methyl-5-allyloxycarbonyl-1,3-dioxan-2-one, MAC, and 5-methyl-5-propargyloxycarbonyl-1,3-dioxan-2-one, MPC. Reactions were performed in CDCl_3 at RT using catalyst system **2/3** or **1/3**.

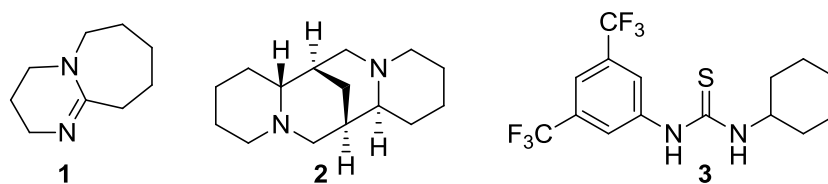


Figure 4.1. Organic catalysts used in the ring-opening polymerisation of MAC and MPC.

previously discussed in Chapters 2 and 3. The polymerisation could be followed by ¹H NMR spectroscopic analysis by monitoring the disappearance of the methylene resonances of the carbonate rings at $\delta = 4.22$ and 4.72 ppm and the appearance of a multiplet at $\delta = 4.23$ – 4.39 ppm. The conversion of each monomer could be individually established by integration of the resonance attributed to the methyl group since a slight difference in the chemical shift is observed both monomers and both polymer repeat units. The methyl resonance in the MAC monomer shifts from $\delta = 1.35$ ppm to $\delta = 1.27$ ppm in the polymer backbone, whereas the methyl resonance in the MPC monomer shifts from $\delta = 1.37$ ppm to $\delta = 1.29$ ppm upon polymerisation (Figure 4.2). Conversion of both monomers was followed against time for copolymerisations catalysed by **2+3** with molar fractions of MAC and MPC in the feed $f_{\text{MAC}} = f_{\text{MPC}} = 0.5$ and with $f_{\text{MAC}}/f_{\text{MPC}} = 0.75/0.25$. Upon $\geq 90\%$ monomer conversion, pure polymers were obtained by repeated precipitation into cold hexanes. Resultant polymers showed narrow distributions by gel permeation chromatography (GPC) analysis (DP23, $M_n = 6\,170$ g mol⁻¹, PDI = 1.18; DP20,

$M_n = 4\,670\text{ g mol}^{-1}$, PDI = 1.17) and incorporations of MAC and MPC
 $F_{MAC}/F_{MPC} = 0.48/0.52$ and $0.75/0.25$, respectively, for polymerisations with
 $f_{MAC}/f_{MPC} = 0.5/0.5$ and $0.75/0.25$.

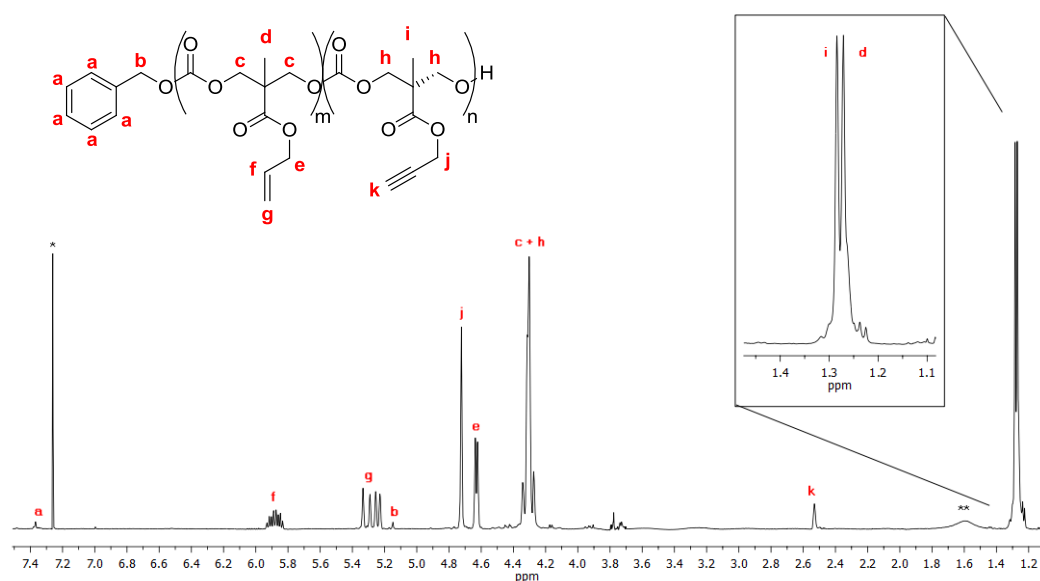


Figure 4.2. ^1H NMR in CDCl_3 of $\text{P}(\text{MAC-co-MPC})$ initiated from benzyl alcohol using 5 mol % **3** and 1 mol % **2** (400 MHz, 298 K; * = residual CDCl_3 , ** = H_2O). The expansion shows the slight difference in chemical shift of the methyl protons between a MAC (δ 1.27 ppm) and MPC (δ 1.29) repeat unit making it possible to monitor the conversions of both monomers.

In situ ^1H NMR spectroscopic analysis during the polymerisation allowed for the conversions of the individual monomers to be followed by integration of the methyl resonances of each monomer and their corresponding repeat units in the polymer (Figure 4.3), making determination of the reactivity ratios of the monomers possible. In order to determine the reactivity ratios, polymerisations with molar fractions of monomer in the feed ranging from

0.1-0.9 were carried out. The average molar fraction compositions of the copolymers (F_{MAC} and F_{MPC}) and the exact molar fraction composition of the monomers in the feed (f_{MAC} and f_{MPC}) were obtained from the ^1H NMR spectra of the MAC-MPC copolymerisations at low conversions (typically $\leq 10\%$). The reactivity ratios for MAC-MPC copolymerisations in CDCl_3 were determined from the average values obtained for each monomer feed ratio (Table 4.1) using software designed by van Herk and *co*-workers.

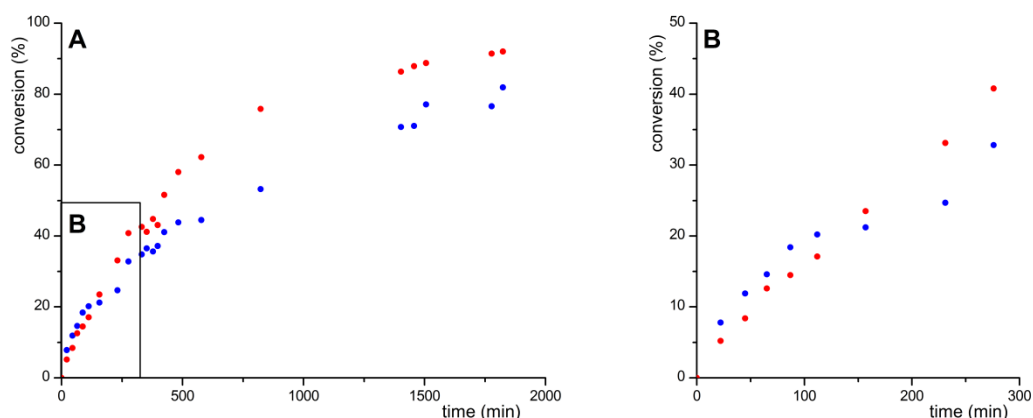


Figure 4.3. Graph showing MAC (●) and MPC (●) conversion against time in a copolymerisation with a feed ratio of 50:50 (A). The expansion (B) shows the first 300 minutes of the polymerisation (B).

This software calculates the best fitting curve, and thus reactivity ratios for the obtained experimental values by finding the minimal value for the sum of squares of the differences between experimental values and calculated copolymer composition.^{14,15}

Table 4.1. Average values for molar fraction of monomer in the feed and experimental copolymer composition in the organocatalytic ROP of MAC and MPC in CDCl₃.^a

$f_{MAC}^{b,c}$	$F_{MAC}^{c,d}$	$f_{MPC}^{b,c}$	$F_{MPC}^{c,d}$	<i>Error</i>
0.12	0.20	0.89	0.80	0.034
0.21	0.29	0.79	0.71	0.009
0.32	0.47	0.68	0.53	0.037
0.40	0.60	0.60	0.40	0.024
0.47	0.66	0.53	0.34	0.030
0.52	0.74	0.48	0.26	0.035
0.62	0.84	0.38	0.16	0.017
0.72	0.88	0.28	0.12	0.028
0.80	0.93	0.20	0.074	-
0.90	1.00	0.10	0	0.003

^a Polymerisations were carried out with [monomer] = 0.5 M in CDCl₃ at RT. ^b Average molar fraction of monomer in the feed (f). ^c Determined by ¹H NMR spectroscopic analysis. ^d Average copolymer composition (F).

Using this non-linear least-squares method,¹⁶ reactivity ratios for MAC, r_{MAC} = 3.74 ± 0.006, and for MPC, r_{MPC} = 0.92, ± 0.004, were calculated. Using these reactivity ratios, the corresponding best fitting curves were calculated using the Mayo-Lewis equation:

$$F_{MAC} = 1 - F_{MPC} = \frac{r_{MAC}f_{MAC}^2 + f_{MAC}f_{MPC}}{r_{MAC}f_{MAC}^2 + 2f_{MAC}f_{MPC} + r_{MPC}f_{MPC}^2}$$

Plotting the calculated curves with the experimentally obtained data in a polymer composition (F) versus monomer feed (f) plots for both monomers shows satisfactory agreement between experimental and calculated data (Figure 4.4). The aforementioned calculations and fittings are based on the assumption that the rate to add a new monomer unit to the growing polymer chain is dependent only on the incorporated unit at the chain end. If this is true for the copolymerisation of MAC and MPC, the rate constants $k_{\text{MAC-MAC}}$ and $k_{\text{MPC-MPC}}$ of the homopropagation steps should in theory be equal to those found in the respective homopolymerisations ($k_{\text{MAC}} = 0.053 \text{ s}^{-1}$ and $k_{\text{MPC}} = 0.002 \text{ s}^{-1}$). The rate constants $k_{\text{MAC-MPC}}$ and $k_{\text{MPC-MAC}}$ of the cross-propagation steps are related to $k_{\text{MAC-MAC}}$ and $k_{\text{MPC-MPC}}$ through the reactivity ratios, $r_{\text{MAC}} = k_{\text{MAC-MAC}}/k_{\text{MAC-MPC}}$ and $r_{\text{MPC}} = k_{\text{MPC-MPC}}/k_{\text{MPC-MAC}}$ (Table 4.2). The results for the reactivity ratios and rate constants above show that $r_{\text{MAC}} > 1$ and $r_{\text{MPC}} < 1$, which

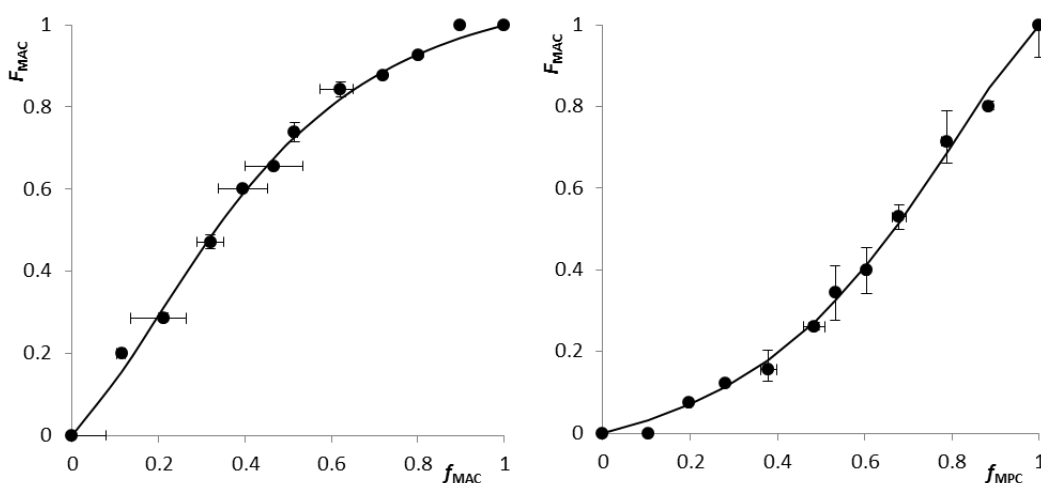


Figure 4.4. Plots of copolymer composition F versus monomer feed ratio f for MAC (left) and MPC (right) for experimental data (\bullet) and best fitted curve (line).

Table 4.2. Reactivity ratios and rate values for the organocatalytic ROP of MAC and MPC catalysed by **2+3** in CDCl₃.^a

r_{MAC}	3.74	± 0.006
$k_{\text{MAC-MAC}}$	5.3×10^{-2}	± 0.004
$k_{\text{MAC-MPC}}$	1.4×10^{-2}	± 0.001
r_{MPC}	0.92	± 0.004
$k_{\text{MPC-MPC}}$	2.0×10^{-3}	± 0.001
$k_{\text{MPC-MAC}}$	2.2×10^{-3}	± 0.001

^a Polymerisations were carried out with [monomer] = 0.5 M in CDCl₃ at RT.

indicates that MAC is more reactive than MPC and will be incorporated faster at the start of the polymerisation. Because $k_{\text{MAC-MAC}} > k_{\text{MAC-MPC}} > k_{\text{MPC-MAC}} \approx k_{\text{MPC-MPC}}$ there will be a preference for homopropagation of MAC, but due to r_{MPC} being close to one there will be only a slight preference for cross-propagation after an MPC unit is incorporated. As neither reactivity ratios are large or approaching zero, the repeat unit distribution in P(MAC-*co*-MPC) is still expected to be approximately random, which is confirmed by the *in situ* NMR data throughout the polymerisation.

¹³C NMR spectroscopic analysis of P(MAC₁₁-*co*-MPC₁₂) and P(MAC₁₅-*co*-PMPC₅) obtained from ROP using **2+3** as catalysts and of P(MAC₁₁-*co*-MPC₁₃) using **1+3** as catalysts, provided additional information on the distribution of the individual monomers in the copolymer structure. After verifying the

structure by ^{13}C NMR spectroscopic analysis, the region in the spectrum showing the chemical shift of the carbonyl carbon from the carbonate in the polymer backbone was investigated. The carbonyl carbon is sensitive to its environment and it is therefore possible to determine the statistical, alternating or blocky nature of the copolymers by analysis of the interaction of every repeat unit with its neighbouring repeat unit(s). For copolymers of MAC (A) and MPC (B) there are 4 different dyads possible: AA, AB, BA and BB. ^{13}C NMR spectroscopic analysis of allyl- and propargyl-functional poly(carbonate) homopolymers showed resonances at $\delta = 154.52$ ppm (AA dyad) and $\delta = 154.42$ ppm (BB dyad) respectively, for the carbon of their carbonate bond. In the copolymers a new signal at $\delta = 154.47$ ppm is observed (Figure 4.5). This new signal was assigned to carbonate bonds between an allyl and a propargyl functionality *i.e.* for AB and BA dyads. The resonance at $\delta = 154.516$ ppm was assigned to carbonyl carbons between two allyl functionalities *i.e.* an AA dyad, whereas the resonance at $\delta = 154.424$ ppm was assigned to carbonyl carbons between two propargyl functionalities *i.e.* a BB dyad. The intensities of the peaks indicate that a random copolymer is formed, as block copolymers would, apart from the block junction, only show the resonances at $\delta = 154.516$ and 154.424 ppm and an alternating copolymer would only show a resonance at $\delta = 154.472$ ppm. Irrespective of catalyst used a statistical random copolymer structure was found for these copolymers.

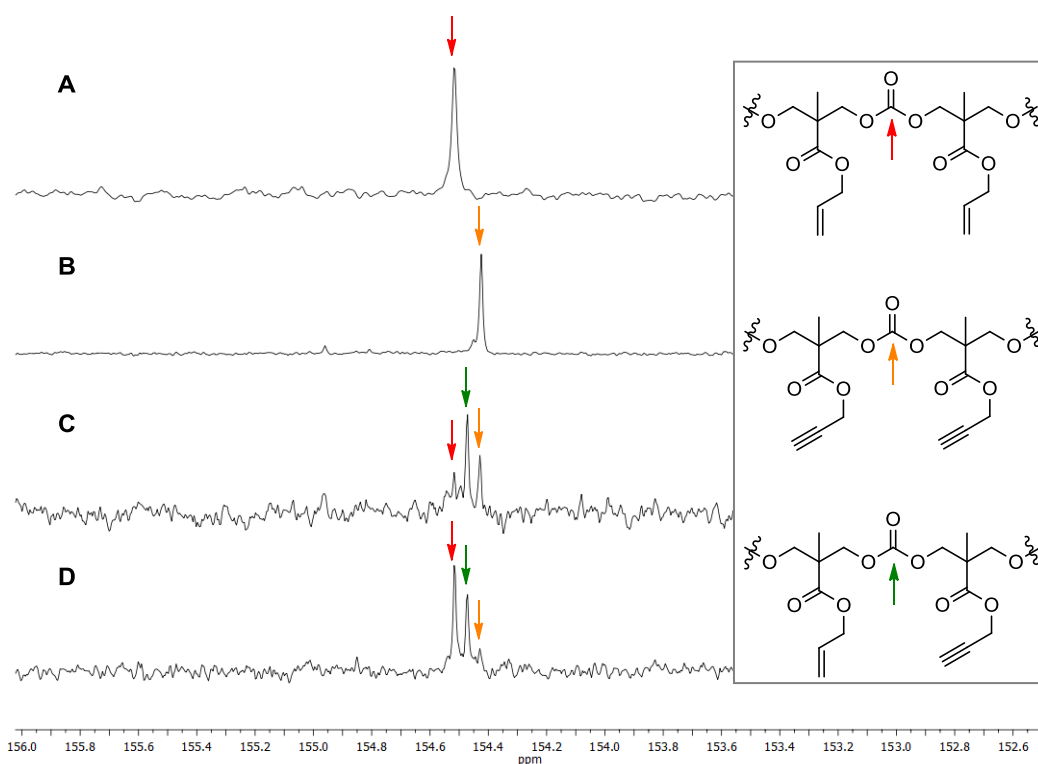


Figure 4.5. Expansion of the ^{13}C NMR spectra in CDCl_3 of poly(carbonates) initiated from benzyl alcohol using 10 mol % **3** and 5 mol % **2** (126 MHz, 298 K). The spectra show the carbonate carbonyl shifts between 156 and 153 ppm of (from top to bottom) PMAC (A), PMPC (B), P(MAC₁₁-*co*-MPC₁₂) (C) and P(MAC₁₅-*co*-MPC₅) (D). The homopolymers show the chemical shift corresponding to AA dyads in PMAC ($\delta = 154.52$ ppm) or the BB dyads in PMPC ($\delta = 154.42$ ppm) only, while both copolymer spectra show peaks at $\delta = 154.52$, 154.47 and 154.43 ppm for AA, AB, BA and BB dyads. The inset displays the different possible carbonyl environments.

Further analysis of the P(MAC-*co*-MPC) structure was carried out by MALDI-ToF MS spectroscopy. The MALDI-ToF MS reveals what appears to be a single distribution in linear detection mode with a repeat unit of *ca.* 199 *m/z* (Figure 4.6; Table 4.3). MALDI-ToF MS analysis of the polymer was repeated in reflectron detection mode, in which the presence of a distribution within each peak was revealed. Sodium charged allyl functional poly(carbonate)

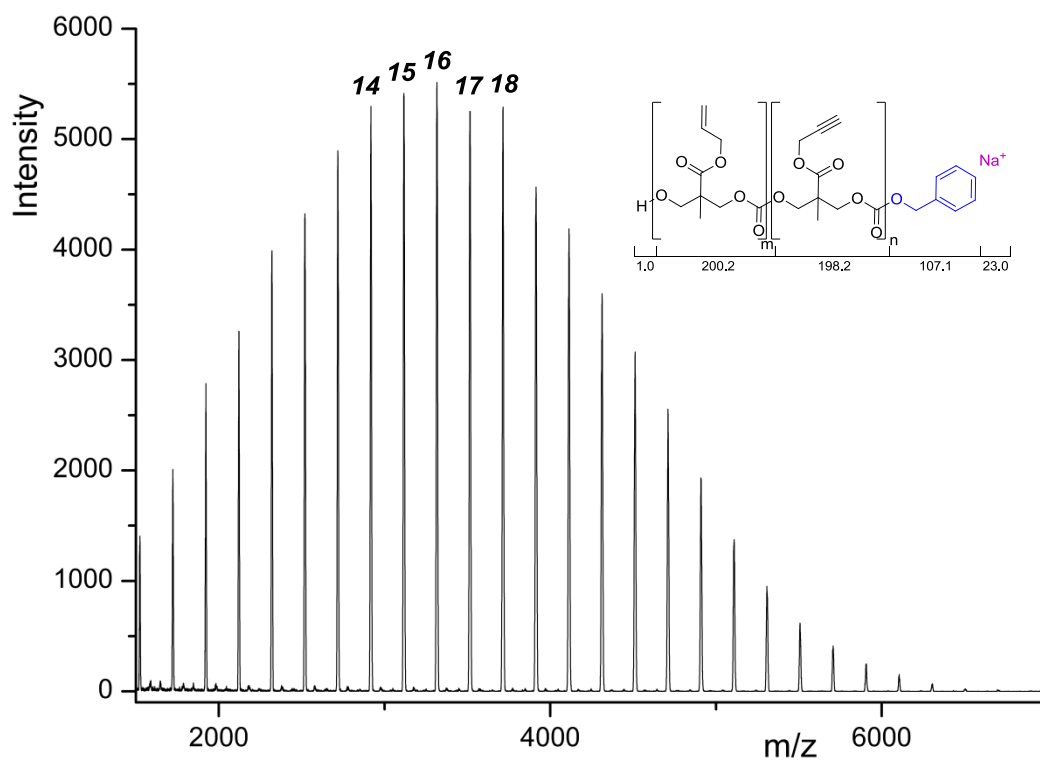


Figure 4.6. MALDI-ToF MS of P(MAC₁₁-*co*-MPC₁₃) obtained from the ROP of MAC and MPC, initiated from benzyl alcohol using 5 mol % **3** and 1 mol % **1**.

Table 4.3. Theoretical and observed m/z values of P(MAC₁₁-*co*-MPC₁₃) (Figure 4.6).

DP	Experimental m/z	Calculated m/z^a
14	2918.6	2918.9
15	3116.4	3118.0
16	3315.9	3317.0
17	3515.9	3516.1
18	3713.5	3716.1

^a calculated m/z value for copolymer chains with a 1:1 MAC/MPC copolymer composition.

homopolymers initiated from benzyl alcohol reveal a peak with highest intensity at $m/z = 2133$ within the isotope pattern of a DP10 polymer and an isotope pattern corresponding to the calculated isotope pattern for a PMAC homopolymer of DP10. Sodium charged propargyl-functional poly(carbonate)s with a DP = 10 initiated from benzyl alcohol also which reveals an isotope pattern corresponding to that expected for the DP10 homopolymer and a peak at $m/z = 2113$. Expansion of the copolymer peak with a degree of polymerisation of 10, however, shows a distribution ranging from 2113 m/z to 2133 m/z within its peak, exactly between the values found for PMAC and PMPC homopolymer, and a peak with the highest intensity at $m/z = 2123$. This distribution within the DP10 peak in the copolymer arises from DP10 polymer chains with varying amounts of MAC and MPC incorporations, each with their own isotope patterns and intensities (Figure 4.7). In this case, the distribution is further complicated due to the incorporation of MPC units that have a deuterated terminal alkyne functionality, which is caused by proton-deuterium exchange of the acetylenic proton in MPC with deuterium in the polymerisation solvent (Figure 4.8).

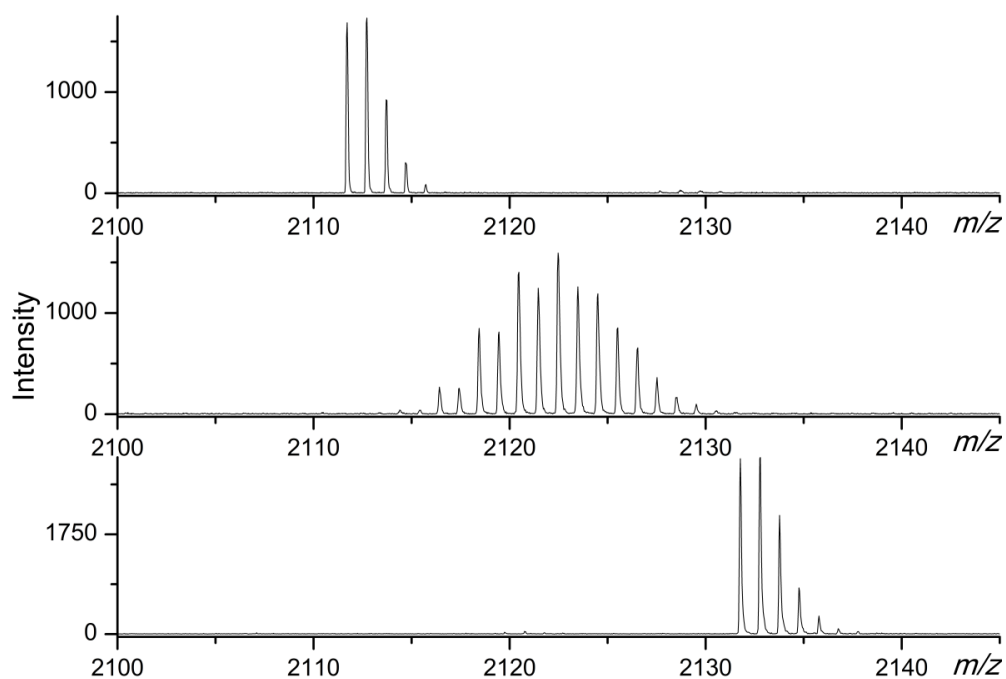


Figure 4.7. Comparison of the peaks with degree of polymerisation DP = 10 of P(MPC) (top), P(MAC-*co*-MPC) (centre) and P(MAC) (bottom). The peak of the copolymer corresponds to a range of DP 10 polymer chains with different ratios of each monomer resulting in a distribution with peaks between $m/z = 2113$ and $m/z = 2133$.

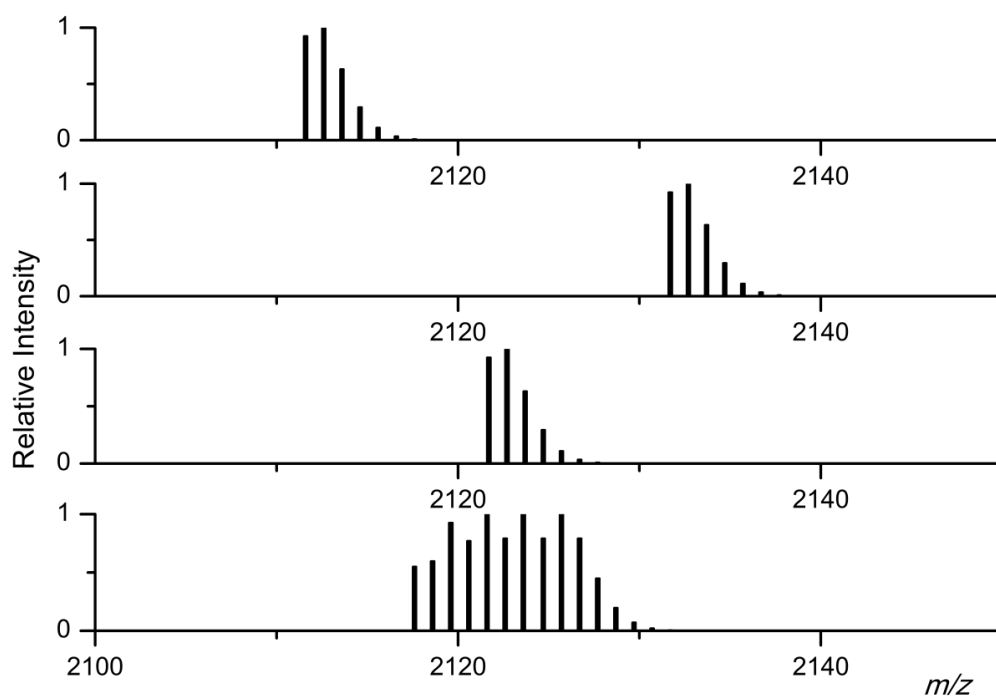


Figure 4.8. Calculated isotope patterns for DP10 polymer chains of (from top to bottom) PMPC, PMAC, PMPC with deuterated acetylenic protons and a simplified MAC-MPC copolymer with P(MAC₃-*co*-MPC₇), P(MAC₄-*co*-MPC₆), P(MAC₅-*co*-MPC₅), P(MAC₆-*co*-MPC₄) and P(MAC₇-*co*-MPC₃) chains in a 1:1:1:1:1 ratio.

4.2.2. Functionalisation of the propargyl groups in an allyl- and propargyl-functional poly(carbonate).

Functionalisation of the propargyl groups in P(MAC-*co*-MPC) copolymers was carried out in a similar manner to that reported in Chapter 3 for PMPC homopolymers, using 1.5 equivalent azide, 0.4 equivalent CuI and 0.8 equivalent diisopropylethylamine, in degassed tetrahydrofuran for 24 hours at room temperature. Upon completion, the reaction was quenched by addition of tetrahydrofuran and AmberlystTM (acidic) ion exchange resin, followed by the removal of copper by passing the mixture over an alumina plug and precipitation into hexanes to afford a partially functionalised BnO-P(MAC-*co*-MPC) copolymer. ¹H NMR spectroscopic analysis revealed >99% conversion of the propargyl groups had occurred, evidenced by the disappearance of the resonance of the propargyl protons at $\delta = 2.50$ ppm and the appearance of a new signal for the triazole protons at $\delta = 7.63$ ppm and new signals consistent with the 1-octyl groups (Figure 4.9). ¹³C NMR spectra of P(MAC₁₁-*co*-MPC₁₃) after propargyl functionalisation confirms the formation of the new copolymer structure with the triazole resonances observed at $\delta = 142.2$ and 123.8 ppm as well as the addition of resonances corresponding to the carbons from the octyl group. A shift was also observed in the carbonyl resonance of the pendant ester from $\delta = 171.5$ ppm for the propargyl ester to $\delta = 172.1$ ppm for the triazole ester. The resonance arising from the carbonyl bond in the carbonate, however, did not change much. The

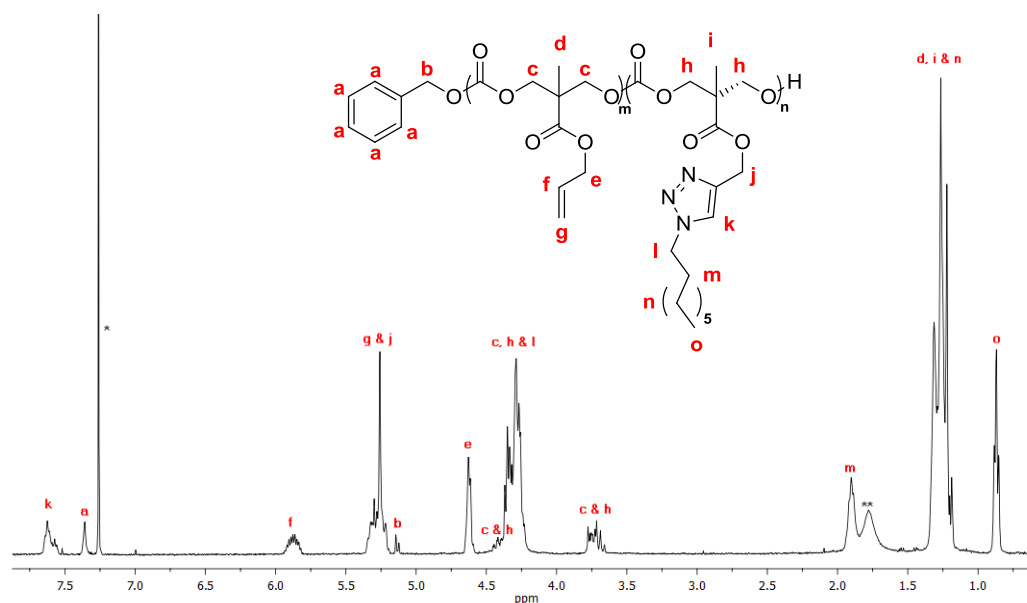


Figure 4.9. ^1H NMR in CDCl_3 of $\text{P}(\text{MAC-co-MPC})_{24}$ after post-polymerisation functionalisation with 1-azidooctane (400 MHz, 298 K; * = residual CDCl_3 , ** = H_2O).

resonance corresponding to a carbonyl carbon with two neighbouring MAC repeat units (AA dyad) remained at $\delta = 154.51$ ppm, whilst the resonance corresponding to a carbonyl carbon with two neighbouring MPC units (BB dyad) had shifted slightly from $\delta = 154.43$ ppm before functionalisation to $\delta = 154.42$ ppm after functionalisation (CC dyad). The chemical shift at $\delta = 154.47$ ppm was assigned to AC and CA dyads. Analysis of the copolymer by gel permeation chromatography further revealed that successful functionalisation of the propargyl groups had occurred by the observation of a shift to lower retention time from $M_n = 4\,670$ g mol^{-1} before functionalisation to $M_n = 5\,210$ g mol^{-1} after functionalisation with 1-azidooctane, while maintaining a low polydispersity (PDI = 1.11).

MALDI-ToF MS analysis of the copolymer after functionalisation of the carbon-carbon triple bond (Figure 4.10) reveals a new complex spectrum with repeat units of $m/z = 200$ and $m/z = 353$ compared to that of the unfunctionalised copolymer which showed an average repeat unit of $m/z \approx 199$. The spectrum was assigned to ascertain that only the expected “clicked” copolymer was present. The MALDI-TOF MS spectrum of the copolymer could be deconvoluted by employing the following equation:

$$m_{calc} = n_1MW_1 + n_2MW_2 + E_\alpha + E_\omega + M^+$$

Where n_1MW_1 and n_2MW_2 represent the molar mass and number of the two repeating units, E_α and E_ω represent the molar mass of the end groups at the α and ω ends of the polymer chain, and M^+ the molar mass of the cation. To simplify the MALDI-TOF MS spectrum, the spectrum was separated into distributions in which $n_2MW_2 + E_\alpha + E_\omega + M^+$ was kept constant with n_2MW_2 being the number and molar mass of 1-azidooctane functional MPC repeat units (f -MPC). For example, a distribution could be extrapolated from the copolymer spectrum consisting of polymer chains with n MAC repeat units with $m/z = 200$, $8 \times$ 1-azidooctane functionalised MPC repeat units ($n_2MW_2 = 8 \times 353$), with end groups corresponding to initiation from benzyl alcohol ($E_\alpha + E_\omega = 108.1 \text{ g mol}^{-1}$) and a Na^+ cation (Figure 4.11; Table 4.4). This extrapolated spectrum has a repeat unit of 200 m/z corresponding to the MAC

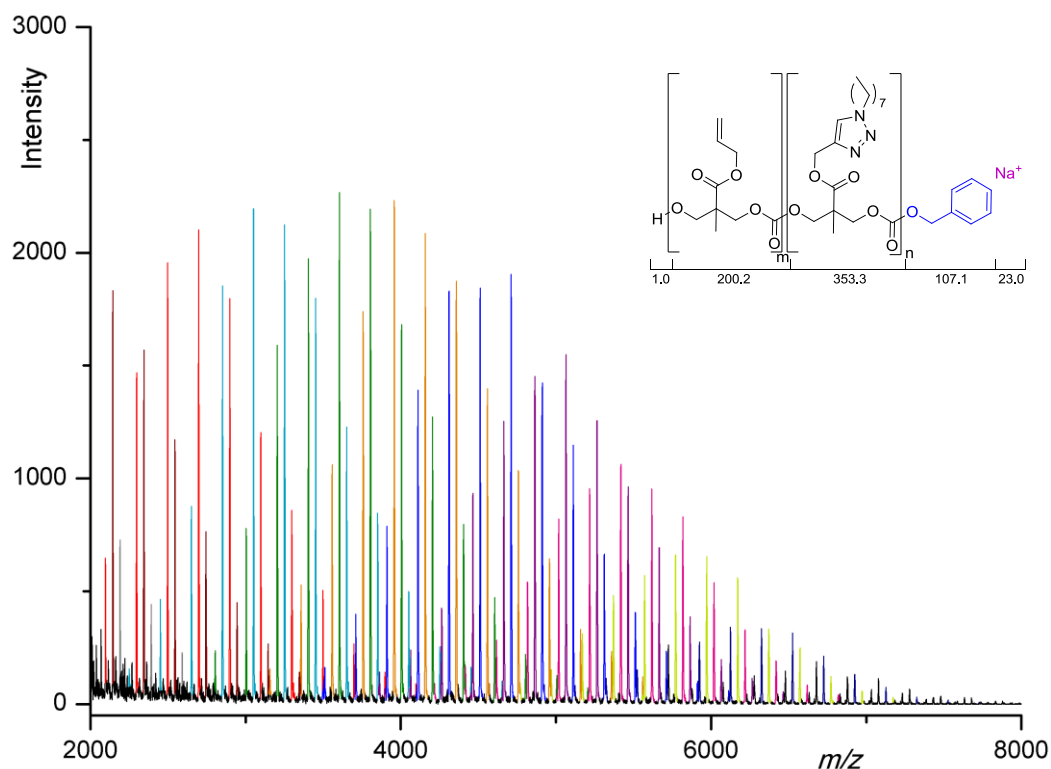


Figure 4.10. MALDI ToF MS spectrum of BnO-P(MAC-*co*-MPC)-OH after functionalisation of the pendant propargyl groups with 1-azido-octane. Distributions in different colours represent polymer chains in which the number of functionalised repeat units is kept constant, whilst the number of repeat units with an allyl functionality is varied (●) = 3 *f*MPC units, (●) = 4 *f*MPC units, (●) = 5 *f*MPC units, (●) = 6 *f*MPC units, (●) = 7 *f*MPC units, (●) = 8 *f*MPC units, (●) = 9 *f*MPC units, (●) = 10 *f*MPC units, (●) = 11 *f*MPC units, (●) = 12 *f*MPC units and (●) = 13 *f*MPC units).

repeating unit and a main peak at $m/z = 3958$ corresponding to a sodium charged, benzyl alcohol initiated, fully functionalised copolymer chain with a degree of polymerisation of 13 and with a chemical composition of $5 \times$ MAC repeat units and $8 \times$ 1-azido-octane functionalised MPC repeat units. Using this method, a schematic representation of the distributions within the spectrum was prepared by establishing the number of MAC and *f*MPC units of each peak in the MALDI-ToF MS spectrum of the copolymer and assigning each peak to a distribution corresponding to the amount of functionalised

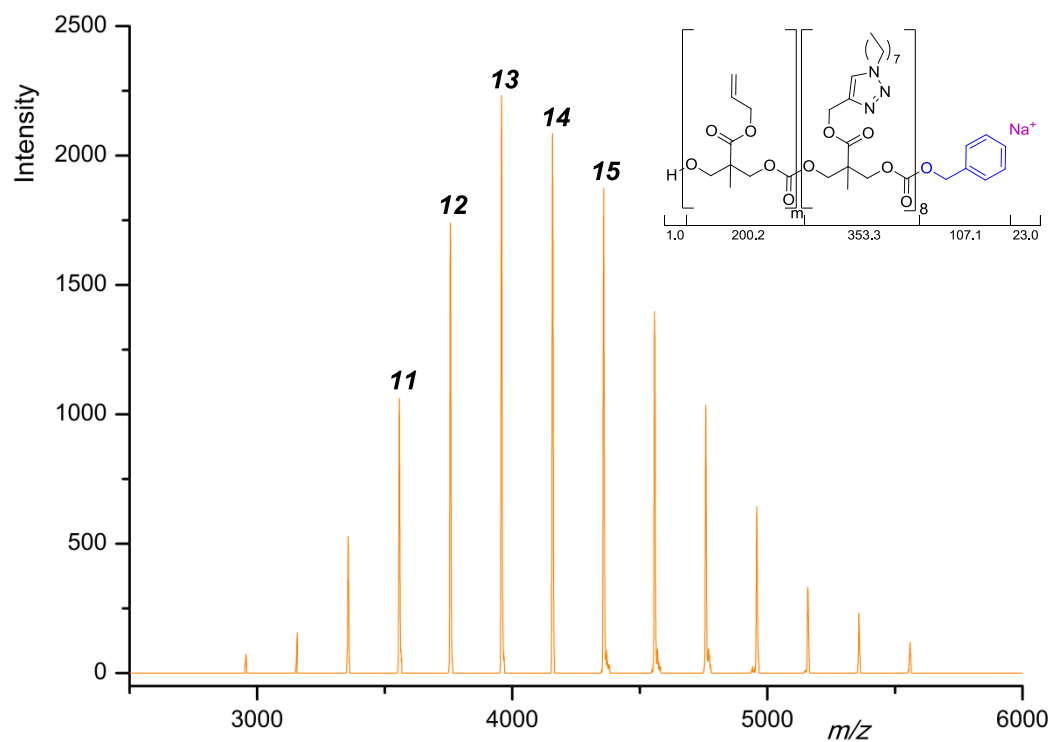


Figure 4.11. Distribution in the MALDI-ToF MS spectrum of BnO-P(MAC-*co*-MPC)-OH consisting of polymer chains with $8 \times$ 1-azido-octane functionalised propargyl repeat units and 0 - $13 \times$ unfunctionalised MAC units.

Table 4.4. Theoretical and observed m/z values of the distribution within P(MAC₁₁-*co*-MPC₁₃) after functionalisation with 1-azido-octane displayed in Figure 4.11.

DP	Experimental m/z	Calculated m/z^a
11	3557.4	3558.8
12	3757.6	3758.9
13	3957.7	3959.0
14	4158.0	4159.0
15	4358.1	4359.1

MPC units in the polymer chain. All distributions correspond to sodium charged, fully functionalised polymer chains with n_1 MAC and n_2 functionalised MPC repeat units and an end group corresponding to initiation from benzyl alcohol (Figure 4.12). The copolymer chemical composition could also be visualised in the form of a contour plot (Figure 4.13) by creating a matrix composed of the composition and intensity of the copolymer chains. The contour plot shows that in the MALDI-ToF MS spectrum obtained from the copolymer, the highest intensities are obtained for copolymer chains with 4-6 MAC units and 5-8 functionalised propargyl units. A slightly lower incorporation of the MAC monomer compared to the MPC is also observed by ^1H NMR spectroscopic analysis *i.e.* $11\times$ MAC and $13\times$ MPC. The lower observed average degree of polymerisation (~ 11) does not correspond to that expected from ^1H NMR spectroscopic analysis of the copolymer after functionalisation and MALDI-ToF analysis of the copolymer before functionalisation which show a degree of polymerisation of 24 and 16, respectively. Calculations of the average number molecular weight obtained by MALDI-ToF analysis of the copolymer after propargyl functionalisation, $M_n = 2\,630\text{ g mol}^{-1}$ (PDI = 1.10), also does not correspond to that observed by GPC ($M_n = 5\,210\text{ g mol}^{-1}$; PDI = 1.11). This apparent lower molecular weight is most likely due to a preference for chains with lower molecular weights to fly during MALDI-ToF analysis.

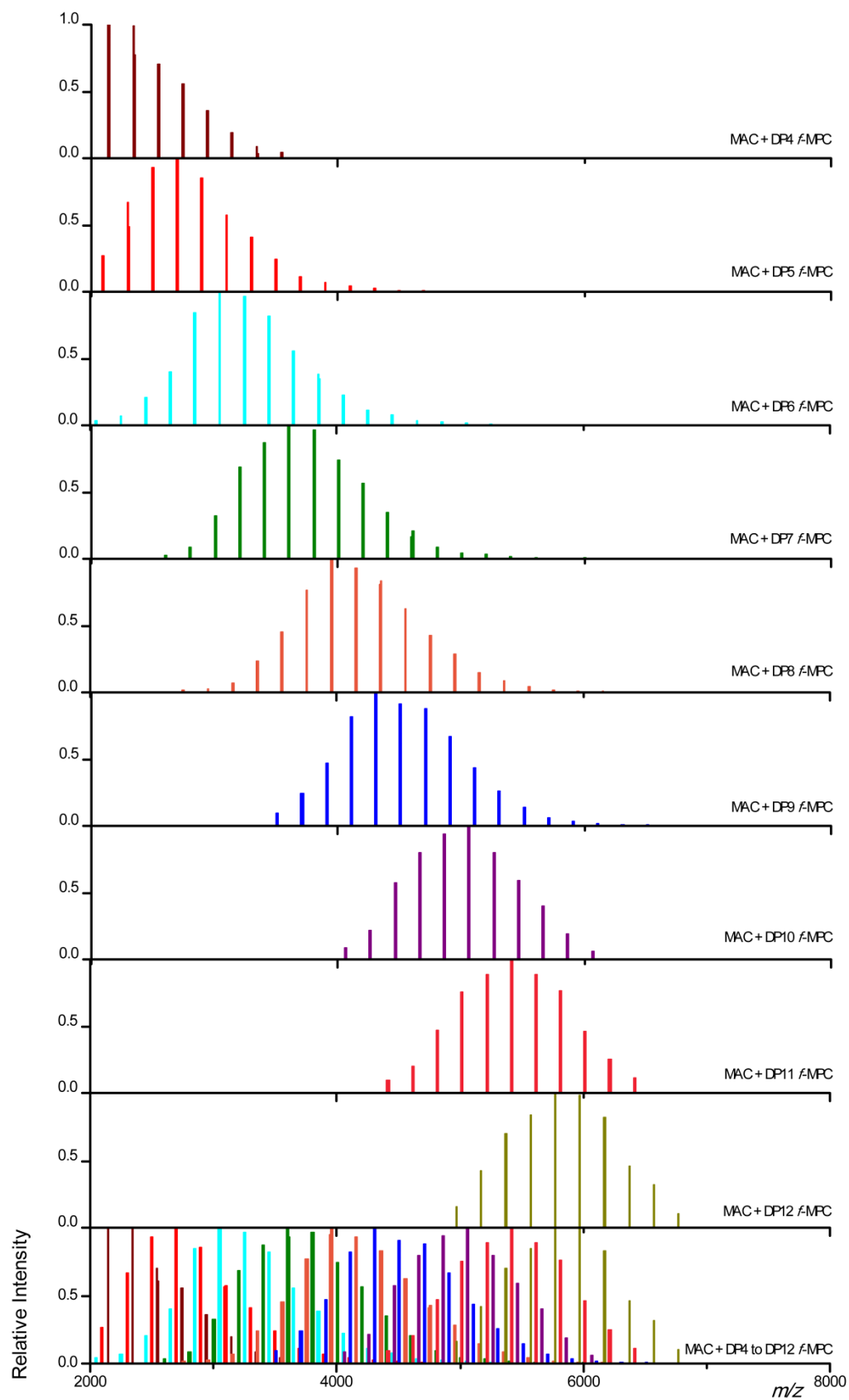


Figure 4.12. Schematic representation of the MALDI ToF MS spectrum of BnO-P(MAC-co-MPC)-OH after functionalisation of the pendant propargyl groups with 1-azidoctane.

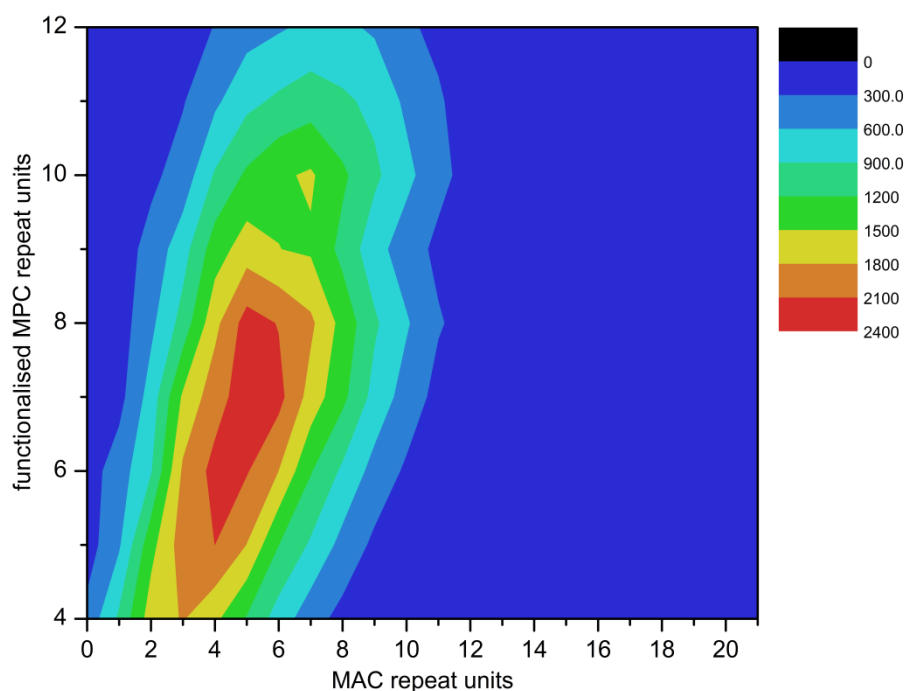


Figure 4.13. Contour plot of P(MAC-*co*-MPC) after functionalisation of the propargyl groups with 1-azidooctane displaying the chemical composition and intensity of the polymer chains as observed by MALDI-ToF MS analysis.

4.2.3. Functionalisation of the allyl groups in an allyl- and propargyl-functional poly(carbonate).

After successful functionalisation of pendant propargyl groups with 1-azidooctane, the pendant allyl functionalities in P(MAC-*co*-MPC) were reacted with mercaptoethanol *via* radical addition of the thiol to the carbon-carbon double bond. Functionalisation was carried out using an excess of thiol to avoid cross-linking as previously discussed for PMAC homopolymers. The excess thiol, however, proved difficult to remove by precipitation. ^1H NMR spectroscopic analysis revealed that >99% conversion of the allyl groups had

occurred, evidenced by the disappearance of the resonances of the allyl functionality at $\delta = 5.88$ and 5.36 - 5.19 ppm and the appearance of new signals consistent with the addition of mercaptoethanol (Figure 4.14).

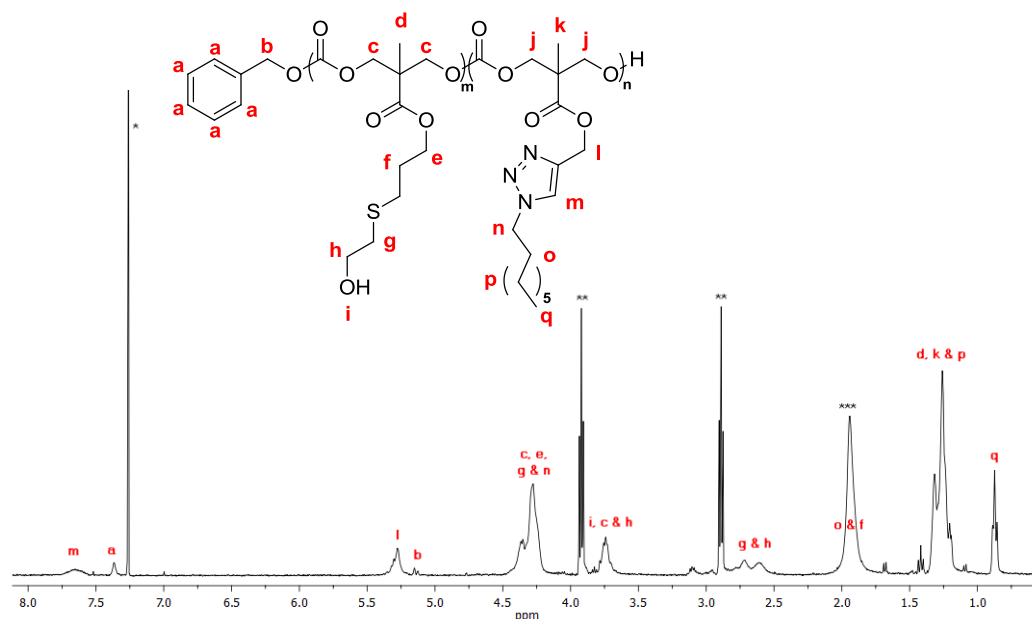


Figure 4.14. ^1H NMR in CDCl_3 of $\text{P}(\text{MAC-co-MPC})_{24}$ after orthogonal functionalisation of the allyl and propargyl groups mercaptoethanol and 1-azidooctane, respectively (400 MHz, 298 K; * = residual CDCl_3 , ** = mercaptoethanol, *** = H_2O).

Full functionalisation seemed to have occurred and analysis of the copolymer by gel permeation chromatography reveals a main distribution that has shifted to a lower retention time compared to both the polymer before orthogonal functionalisation and the 1-azidooctane functionalised copolymer (Figure 4.15). However, a shoulder is observed at higher retention time which is most likely due to degradation before the addition of mercaptoethanol or degradation of the amphiphilic copolymer during work-up.

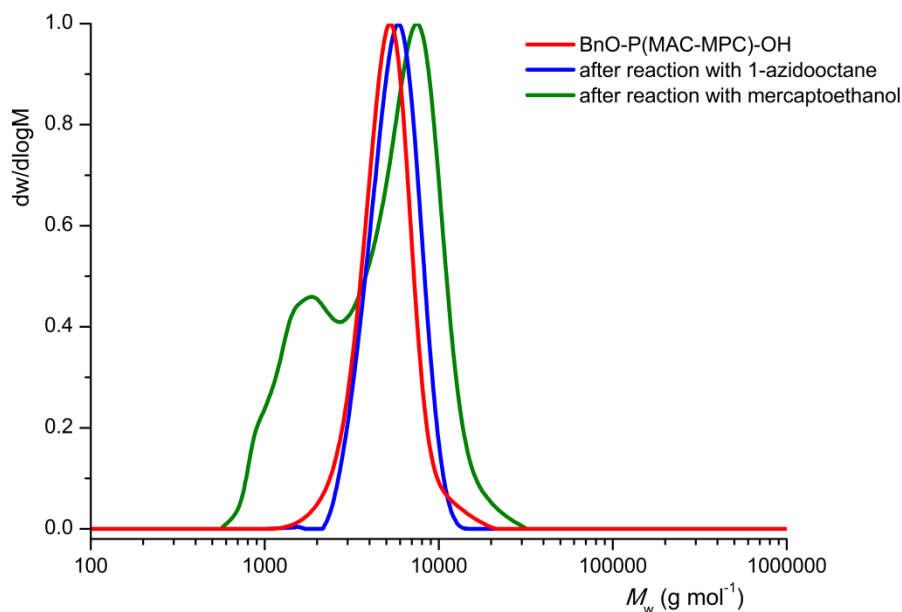


Figure 4.15. GPC traces of BnO-P(MAC-MPC)-OH before functionalisation, after functionalisation of the propargyl groups with 1-azido-octane and after subsequent functionalisation of the allyl groups with mercaptoethanol.

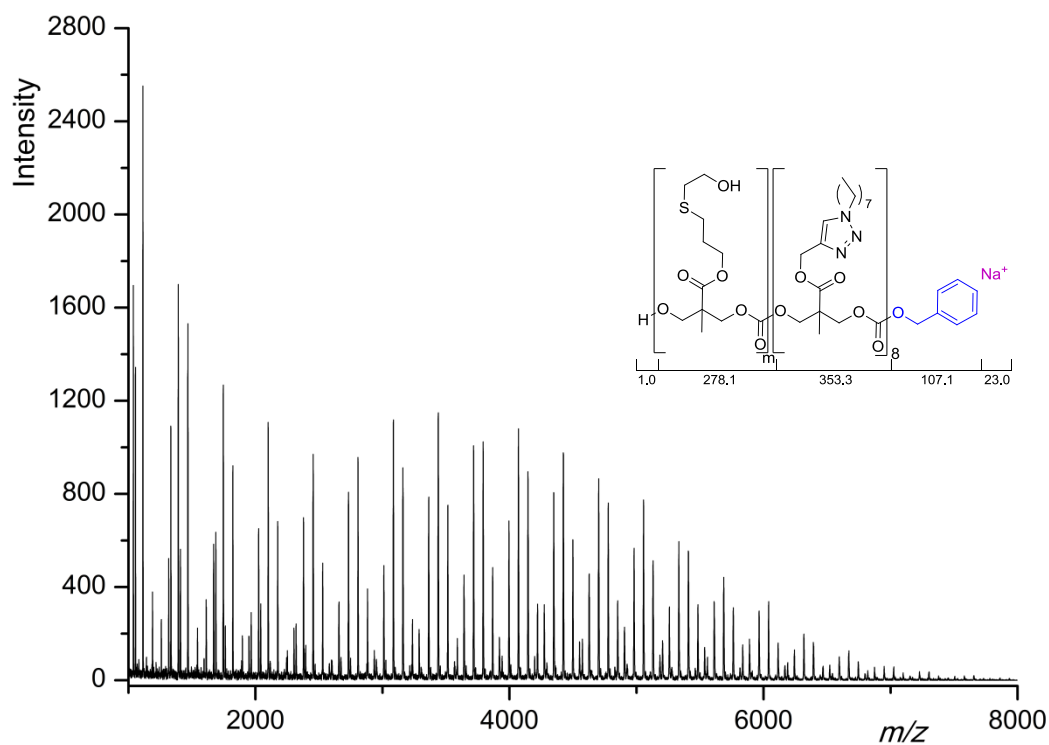


Figure 4.16. The unassigned MALDI-ToF MS spectrum of BnO-P(MAC-*co*-MPC)-OH after orthogonal functionalisation with 1-azido-octane and mercaptoethanol shows a significant low molecular weight shoulder.

Further evidence of polymer degradation was found by analysis of the sample with MALDI-ToF MS, where a complex distribution was found with a high intensity low molecular weight shoulder to the main distributions. This lower molecular weight shoulder partially consists of fully functionalised, sodium charged oligomers with 2-4 repeat units and a benzyl alcohol end group (Figure 4.16). Other unidentified peaks were also found at lower molecular weights. Nonetheless, the rest of the distribution could be fully assigned in a manner similar to that previously for the 1-azidooctane functionalised P(MAC-*co*-MPC). A distribution from the copolymer spectrum consisting of polymer chains with n functionalised MAC repeat units with $m/z = 278$, $8 \times$ 1-azidooctane functionalised MPC repeat units (8×353 m/z), with end groups corresponding to initiation from benzyl alcohol and sodium ionisation was extrapolated (Figure 4.17; Table 4.5). This extrapolated spectrum has a repeat unit of 278 m/z corresponding to the MAC repeating unit with the addition of mercaptoethanol (f MAC) and a main peak at $m/z = 4070$ corresponding to a sodium charged, benzyl alcohol initiated, fully functionalised copolymer chain with a degree of polymerisation of 12 and with a chemical composition of 4 mercaptoethanol functionalised MAC repeat units and $8 \times$ 1-azidooctane functionalised MPC (f MPC) repeat units.

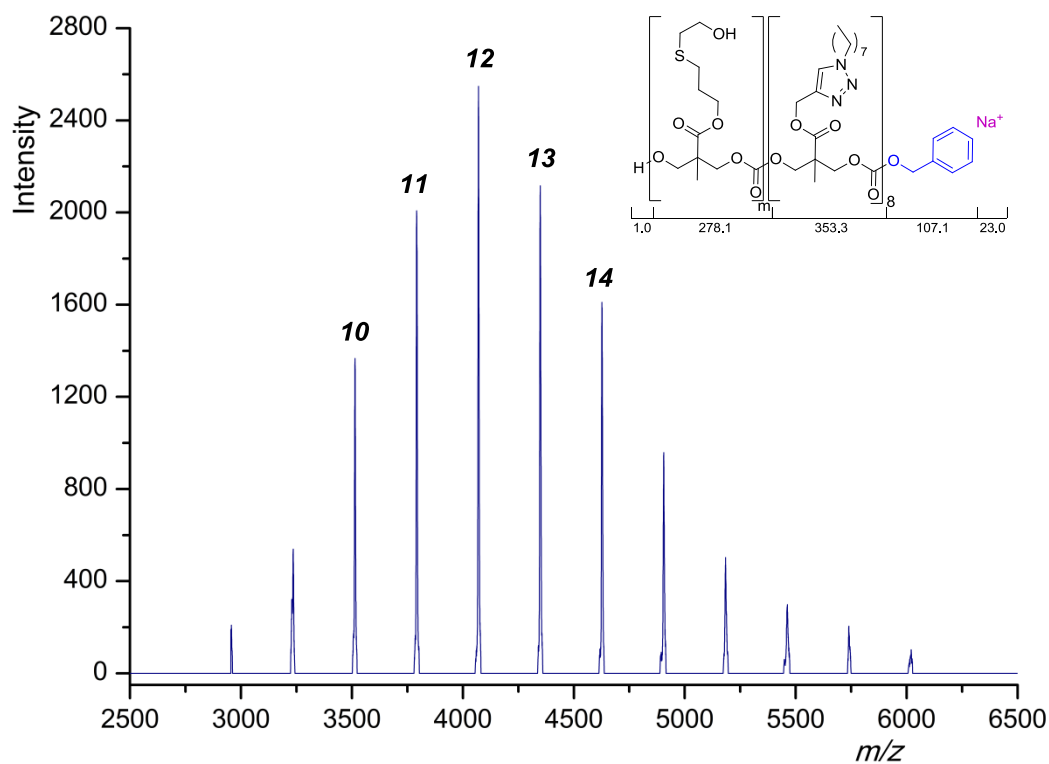


Figure 4.17. Distribution in the MALDI-ToF MS spectrum of BnO-P(MAC-co-MPC)-OH consisting of polymer chains with 8 1-azido-octane functionalised propargyl repeat units and 0-11 functionalised MAC units.

Table 4.5. Theoretical and observed m/z values of the distribution with 8 f MPC repeat units within P(MAC₁₁-co-MPC₁₃) after functionalisation with 1-azido-octane and mercaptoethanol displayed in Figure 4.17.

DP	Experimental m/z	Calculated m/z^a
10	3514.0	3514.8
11	3792.1	3792.9
12	4070.3	4070.9
13	4349.0	4349.0
14	4646.9	4628.1

In a similar manner, distributions within the spectrum could be schematically represented by taking the peak maxima of each peak and then assigning the peak to a distribution corresponding to the amount of functionalised MPC units in its chain. All distributions in this schematic representation correspond to sodium charged, fully functionalised polymer chains with n_1 MAC and n_2 functionalised MPC repeat units and an end group corresponding to initiation from benzyl alcohol (Figure 4.18). No distributions with unfunctionalised MAC or MPC repeating units were found. The copolymer chemical composition was represented in a contour plot (Figure 4.19), which shows the high intensity of lower molecular weight species. The highest intensities in the higher molecular weight area are obtained for copolymer chains with 3 MAC units and 6-7 functionalised propargyl units. These values correspond to a degree of polymerisation of 9-10, which was a little lower than expected but could be explained by the observation of the higher intensity of lower molecular weight species and the low molecular weight shoulder. In addition, the apparent shift in copolymer composition compared to that observed for the copolymer after addition of octyl azide, was ascribed to a discrimination for polymer chains high in Δ MPC repeating unit during the analysis of the copolymer.

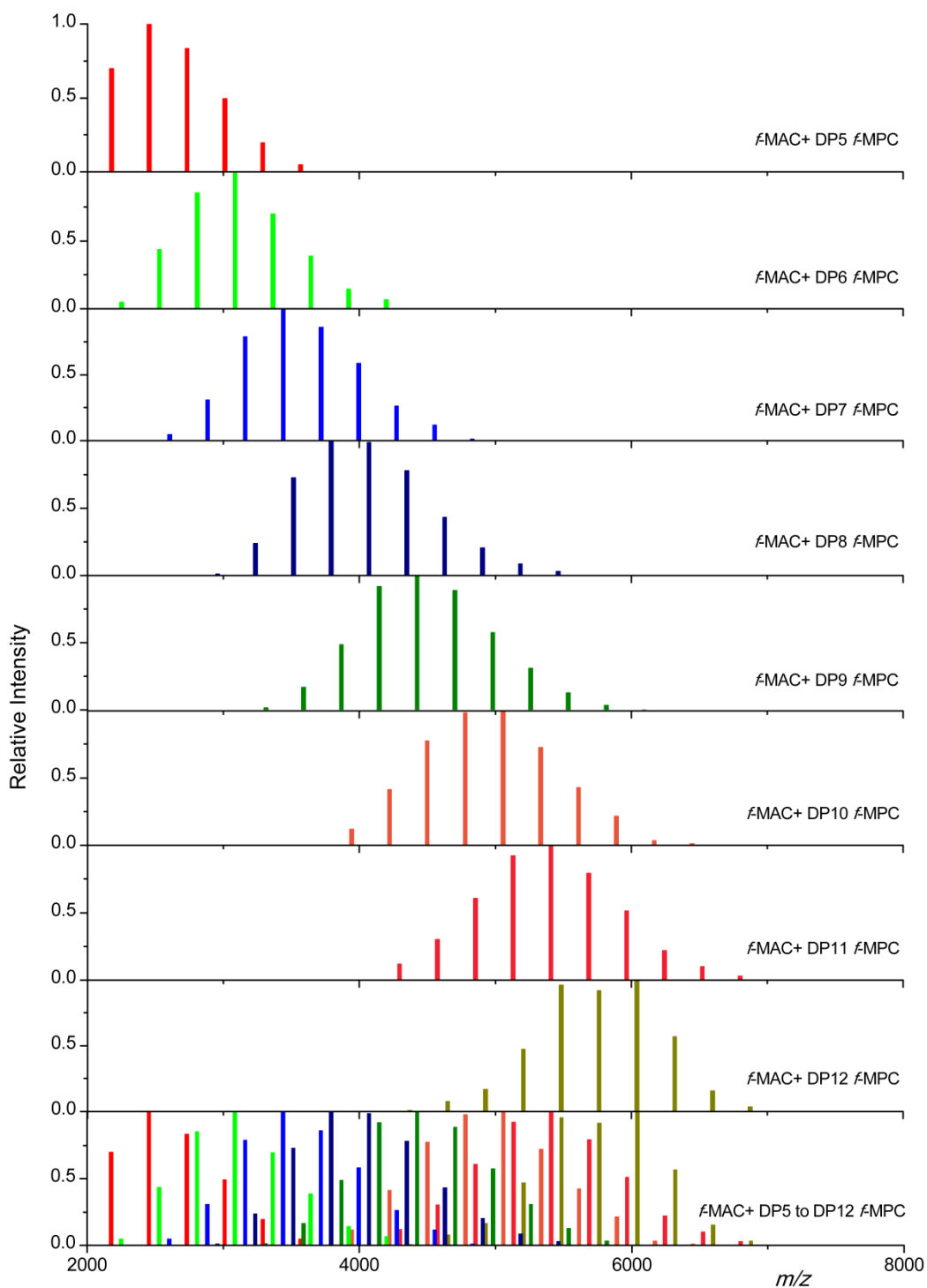


Figure 4.18. Schematic representation of the MALDI ToF MS spectrum of BnO-P(MAC-co-MPC)-OH after functionalisation of the pendant allyl- and propargyl- groups with mercaptoethanol and 1-azido-octane respectively.

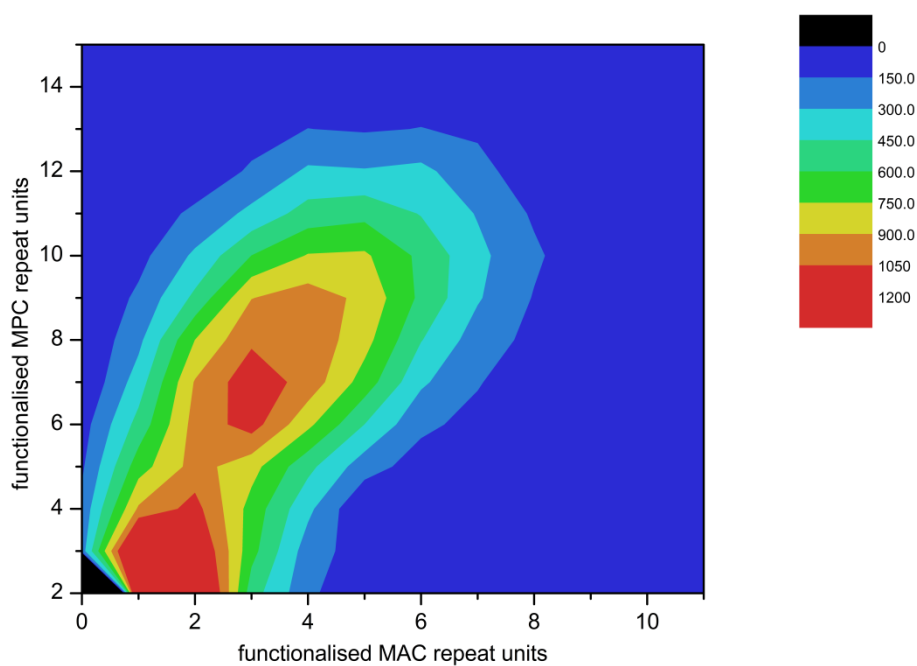


Figure 4.19. Contour plot of P(MAC-*co*-MPC) after functionalisation of the propargyl groups with 1-azidooctane displaying the chemical composition and intensity of the polymer chains as observed by MALDI-ToF MS analysis.

4.3. Conclusions

In conclusion, the controlled ring-opening polymerisation of 5-methyl-5-allyloxycarbonyl-1,3-dioxan-2-one and 5-methyl-5-propargyloxycarbonyl-1,3-dioxan-2-one was achieved successfully using two dual organic catalysts systems under mild conditions. Investigation of the reactivity ratios revealed a higher reactivity for the allyl functional carbonate with values for r_{MAC} and r_{MPC} of 3.73 and 0.92, respectively. The random nature of the copolymer was further confirmed by investigation of the carbonyl region in the ^{13}C NMR spectra and MALDI-ToF MS analysis of the copolymers.

Orthogonal postpolymerisation functionalisation of the pendant propargyl groups and allyl groups in the polymer backbone was realised *via* Huisgen 1,3-dipolar cycloaddition and facile free radical “thiol-ene” addition, leading to the isolation of an amphiphilic aliphatic poly(carbonate). Successful functionalisation was confirmed by extensive MALDI-ToF analysis of the polymer. The orthogonally functionalised polymer however appeared to be unstable and showed signs of degradation by the observation of a low molecular weight shoulder in its GPC trace and its MALDI-ToF MS spectra.

4.4. References

1. Hansell, C. F.; Espeel, P.; Stamenovi, M. M.; Barker, I. A.; Dove, A. P.; Du Prez, F. E.; O'Reilly, R. K. *J. Am. Chem. Soc.* **2011**, *133*, 13828–13831.
2. Barker, I. A.; Hall, D. J.; Hansell, C. F.; Du Prez, F. E.; O'Reilly, R. K.; Dove, A. P. *Macromol. Rapid Commun.* **2011**, *32*, 1362–1366.
3. Stanford M. J.; Dove, A. P. *Macromolecules* **2009**, *42*, 141-147.
4. Malkoch, M.; Thibault, R. J.; Drockenmuller, E.; Messerschmidt, M.; Voit, B.; Russell, T. P.; Hawker, C. J. *J. Am. Chem. Soc.* **2005**, *127*, 14942-14949.
5. Iha, R. K.; Wooley, K. L.; Nyström, A. M.; Burke, D. J.; Kade, M. J.; Hawker, C. J.; *Chem. Rev.* **2009**, *109*, 5620–5686.
6. Pollino, J. M.; Stubbs, L. P.; Weck, M. *J. Am. Chem. Soc.* **2004**, *126*, 563-567.
7. Nurmi, L.; Lindqvist, J.; Randev, R.; Syrett J.; Haddleton, D. M. *Chem. Commun.*, **2009**, 2727–2729.
8. Such, G. K.; Johnston, A. P. R.; Liang, K.; Caruso, F.
doi:10.1016/j.progpolymsci.2011.12.002.
9. Wolf, F. F.; Friedemann, N.; Frey, H. *Macromolecules* **2009**, *42*, 5622–5628.
10. Kose, M. M.; Onbulak, S.; Yilmaz, I. I.; Sanyal, A. *Macromolecules* **2011**, *44*, 2707–2714.

11. Tang H.; Zhang, D. *Polym. Chem.*, **2011**, *2*, 1542-1551.
12. Iha, R. K.; van Horn, B. A.; Wooley, K. L. *J. Polym. Sci. Part A: Polym. Chem.* **2010**, *48*, 3553-3563.
13. van Horn, B. A.; Iha, R. K.; Wooley, K. L. *Macromolecules* **2008**, *41*, 1618-1626.
14. van Herk, A. M. *J. Chem. Educ.* **1995**, *72*, 138..
15. van Herk, A. M.; Manders, B. G.; Smulders, W.; Aerdts, A. *Macromolecules* **1997**, *30*, 322-323.
16. Tidwell, P. W.; Mortimer, G. A. *J. Polym. Sci. Part A: Polym. Chem.* **1965**, *3*, 369-387.

Chapter 5

Synthesis, Stereocomplexation and post-Polymerisation Functionalisation of Functional Poly(Ester-Carbonate)s

Well-defined, crystalline poly(ester-carbonate)s with pendant allyl- or propargyl groups were synthesised *via* the organocatalytic ROP of lactide and cyclic carbonates. The resulting copolymers successfully formed stereocomplexes when blended with (co-)polymers of the opposite chirality *via* solution casting or in the melt. Post-polymerisation modification of the pendant functionality in the individual poly(ester-carbonate)s did not disrupt stereocomplexation and led to the observation of stereocomplexes with more than one functional group.

5.1. Introduction

Biodegradable polymers such as poly(ester)s and poly(carbonate)s are important materials that can be utilised for biomedical and pharmaceutical applications as a consequence of their biodegradability, biocompatibility and low toxicity.¹⁻⁴ In the case of poly(lactic acid) (PLA), materials with higher mechanical performance and higher resistance to hydrolysis are obtained when two isotactic poly(lactic acid)s with opposite configurations co-crystallise to form a so called stereocomplex.^{5,6} Stereocomplexation between poly(*L*-lactic acid) (PLLA) and poly(*D*-lactic acid) (PDLA) was first investigated by Ikada *et al.* in 1987, who reported stereocomplex formation after observing a positive shift in the melting temperature (T_m) for an equimolar blend of PLLA and PDLA by differential scanning calorimetry (DSC) analysis.⁷ Depending on the molecular weight of the polymer, DSC analysis of stereocomplexed PLA can deliver melting points of up to 230-240 °C,^{5,6} which is an increase of *ca.* 50-60 °C compared to that the melting points observed for PLLA and PDLA homocrystallites. The stereocomplex structure can be described as PDLA and PLLA chains packed side by side in a parallel fashion.

Stereocomplexation of poly(lactide) is, however, not restricted to the complexation observed between pure PDLA and PLLA. So-called hetero-stereocomplexation in which *L*- or *D*- poly(lactic acid) forms a stereocomplex with the opposite configuration of another optically active polymer has been

reported as well.⁸ Through hetero-stereocomplexation, the properties of poly(lactide) can be combined with desirable functionalities or properties from other polymers. Examples are stereocomplexation of PDLA with peptides reported by Slager and Domb and stereocomplexation of PDLA and PLLA with poly(*S*-2-hydroxybutyrate) and poly(*R*-2-hydroxybutyrate) reported by Tsuji and co-workers.⁸⁻¹¹ Other efforts to combine the qualities of PLA stereocomplex formation with the qualities of other polymers, have been in the form of block or graft copolymers in which the lactide blocks with opposite configuration form a stereocomplex.¹²⁻¹⁵ Hedrick and co-workers have reported some interesting examples of stereocomplexation between PLA blocks in block-, mikto arm- and graft- copolymers: Stereocomplexation of poly(*N*-isopropylacrylamide)-*b*-poly(*L*-lactide) and poly(ethylene oxide)-*b*-poly(*D*-lactide) block copolymers to form micelles with stabilisation due to the stereocomplex formation in the core was reported as well as the synthesis of mikto arm polymers with an PEO-block, a PLLA and a PDLA block to form stereocomplexes.¹⁶⁻¹⁸ Introducing functionality in the PLA structure can also be achieved by copolymerisation of lactic acid or lactide with other functional monomers. However, copolymerisation might disrupt the ability to form stereocomplexes when too many errors are introduced, as stereocomplexation is preferred when both polymers have an enantiomeric excess of 90% or higher.¹⁹ Nevertheless, crystallinity has been observed in copolymers of *L*- or *D*- lactide with cyclic carbonates and other monomers.²⁰⁻²²

Random copolymerisations that were reported to form stereocomplexes were reported by Yasuda *et al.*²³ They reported the copolymerisation of LLA and DLA with ϵ -caprolactone and DMO (*L*-3-*D,L*-dimethyl-2,5-morpholinedione) and stereocomplexation between the resulting copolymers, with stereocomplexation occurring for lactide/ ϵ -caprolactone copolymers with ϵ -caprolactone incorporations up to 20%.

Herein, the preparation of poly(lactide)s and poly(ester-carbonate)s is reported *via* the organocatalytic ring-opening polymerisation of *L*- or *D*-lactide and their copolymerisation with the functional cyclic carbonate monomers reported in the previous three chapters (Chapters 2, 3 and 4), 5-methyl-5-allyloxycarbonyl-1,3-dioxan-2-one, MAC, and 5-methyl-5-propargyloxycarbonyl-1,3-dioxan-2-one, MPC (Figure 5.1). Furthermore, the crystallinity and stereocomplexation of the resulting poly(ester)s and poly(ester-carbonate)s was investigated by differential scanning calorimetry (DSC) analysis.

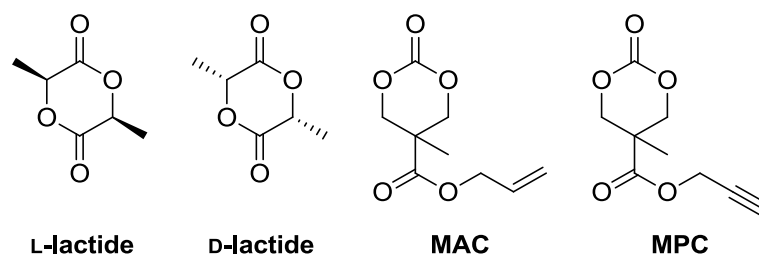
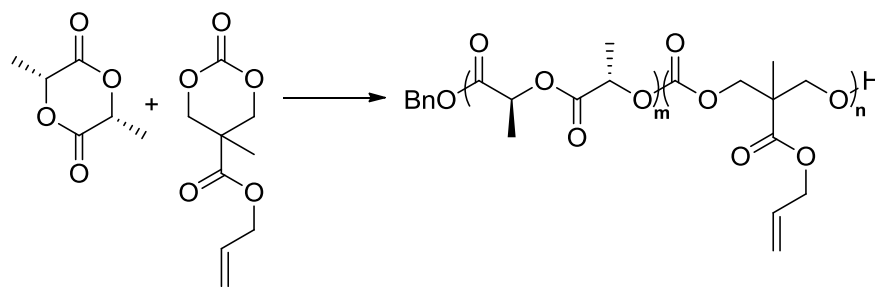


Figure 5.1. Monomers used in the preparation of poly(ester)s and functional poly(ester-carbonate)s.

5.2. Results and Discussion

5.2.1. Copolymerisations of *L*- and *D*-lactide with 5-methyl-5-allyloxycarbonyl-1,3-dioxan-2-one, MAC, and 5-methyl-5-propargyloxycarbonyl-1,3-dioxan-2-one, MPC.

The synthesis of poly(lactide) homopolymers and allyl- or propargyl-functional poly(ester-carbonate) copolymers was realised *via* the organocatalytic ring opening polymerisation of *L*- or *D*- lactide (LLA or DLA) with 5-methyl-5-allyloxycarbonyl-1,3-dioxan-2-one (MAC) or 5-methyl-5-propargyloxycarbonyl-1,3-dioxan-2-one (MPC). Initial studies into the copolymerisation were conducted using a molar fraction of *L*-lactide in the feed (f_{LLA}) of 0.75 and a molar fraction of MAC in the feed (f_{MAC}) of 0.25. Reactions were performed in $CDCl_3$ ($[M] = 0.7$ M) at 25 °C, using benzyl alcohol as initiator with $[M]/[I] = 100$ (Scheme 5.1) and polymerisations were catalysed by the dual catalyst system of 1-(3,5-bis(trifluoromethyl)phenyl)-3-cyclohexylthiourea, **3**, in combination with (-)-sparteine (**2**) or using the dual



Scheme 5.1. Ring-opening polymerisation of 5-methyl-5-allyloxycarbonyl-1,3-dioxan-2-one (MAC) and *L*-lactide (LLA). Conditions: ROH, catalyst system **2/3** or **1/3**, $CDCl_3$, RT.

catalyst system of 5 mol % **3** with 1 mol % 1,8-diazabicyclo[5.4.0]undec-7-ene (**1**, DBU; Figure 5.2). These catalysts have been reported to give excellent results in the ROP of lactide^{24,25} and both catalyst systems were successfully applied in the ROP of functional carbonates.²⁶⁻²⁸ Upon completion of the polymerisation, mixtures were quenched by the addition of Amberlyst™ (acidic) ion exchange resin followed by precipitation in cold methanol.

¹H NMR spectroscopy provided a convenient method to monitor the progress of the copolymerisations. *L*-Lactide consumption was monitored by the reduction of the methine resonance at $\delta = 5.04$ ppm and the appearance of the corresponding multiplet at $\delta = 5.19$ – 5.13 ppm in the polymer backbone, whilst the consumption of MAC could be monitored by the reduction of the methylene resonances in the carbonate ring at $\delta = 4.22$ and 4.72 ppm and the appearance of a broad multiplet at $\delta = 4.45$ – 4.20 ppm for the methylene resonances of the polycarbonate repeat units. MAC and *L*-lactide conversions were monitored until ~90% *L*-lactide conversions for copolymerisations catalysed by **2/3** (10 mol% **3**, 5 mol% **2**) with molar fractions of MAC in the

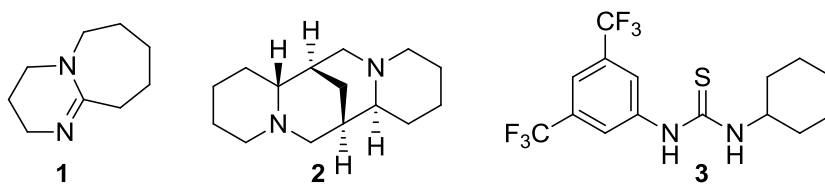


Figure 5.2. Organic catalysts used in the ring-opening polymerisation of MPC.

feed of 0.25 and 0.40 and for a copolymerisation catalysed by **1/3** (5 mol% **3**, 1 mol% DBU) with $f_{\text{MAC}} = 0.25$ (Figure 5.3). Analysis of the resulting polymers by gel permeation chromatography (GPC) analysis revealed narrow molecular weight distributions (PDI = 1.06-1.15) with number average molecular weights of 14 800-23 20 g mol⁻¹. Copolymerisations with 5 mol% **3** and 1 mol% DBU showed *L*-lactide conversions of >95% within 10 minutes, making monitoring the consumption of the monomers challenging. This rapid conversion of *L*-lactide also makes quenching the polymerisation mixture before the formation of a poly(carbonate) block more challenging. To that

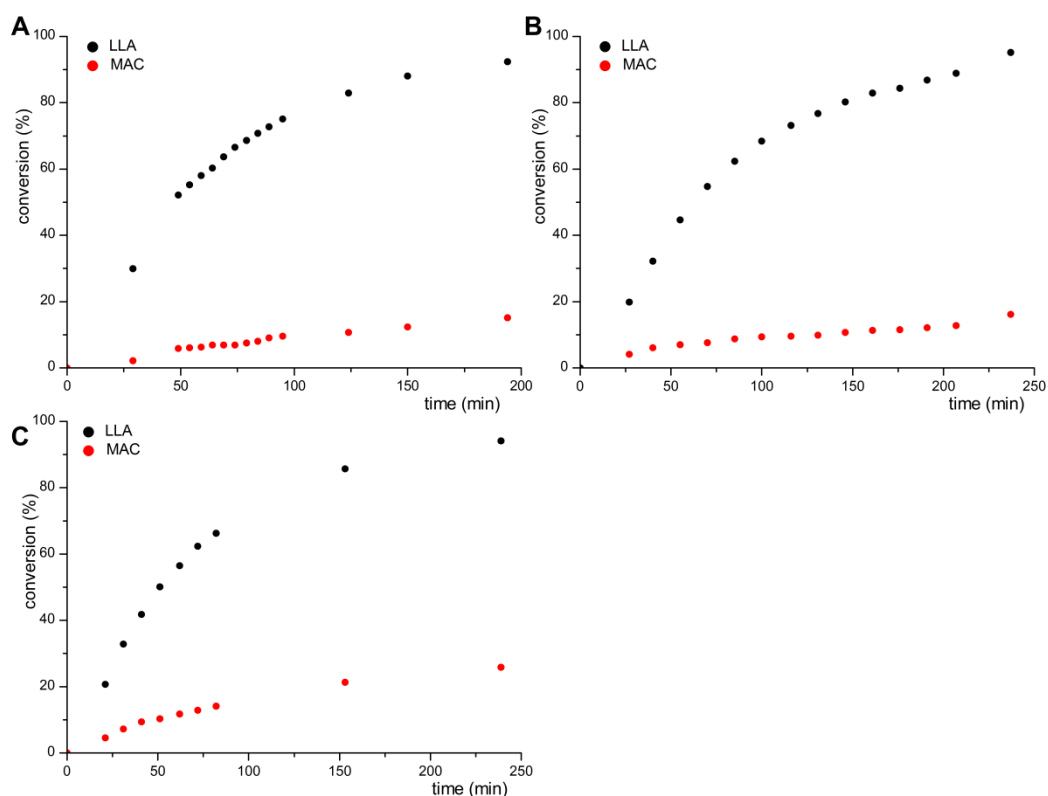


Figure 5.3. Graph showing LLA (●) and MAC (●) conversion against time. The organocatalytic ring-opening polymerisation of *L*-lactide with MAC in CDCl₃ at RT was monitored for copolymerisations catalysed by **1+3** with $f_{\text{MAC}} = 0.25$ (A) and for copolymerisations catalysed by **2+3** with $f_{\text{MAC}} = 0.25$ (B) and 0.4 (C).

end, catalyst loadings were decreased to 1 mol% **3** and 0.2 mol% DBU, showing >95% LLA conversion after 4.3 hours and yielding copolymer with a M_n of 14 840 g mol⁻¹ and PDI = 1.06 (Figure 5.3). In case of polymerisations in which $f_{MAC} = 0.25$ with both the **2/3** and the **1/3** catalyst system, MAC reaches *ca.* 15% conversion at 95% *L*-lactide conversion corresponding with an incorporation of MAC of *ca.* 7% in the final copolymer. As the **1/3** catalyst resulted in similar MAC incorporations compared to the **2/3** catalyst system and because DBU is available commercially, this system was chosen for further use in MAC and LA copolymerisations. A range of copolymerisations of LLA with MAC were performed with MAC molar fractions in the feed (f_{MAC}) of 0.1, 0.25, 0.4 and 0.5 (Table 5.1). Monomer-to-initiator ratios were adjusted so that $[M]/[I] = 75$ for *L*-lactide and polymerisations were precipitated at ~90% *L*-lactide conversion. Compositions of the resulting copolymers were determined by integration of the methine resonance of the PLA repeat units at $\delta = 5.19$ –5.13 ppm those of the methylene resonances originating from the MAC repeat units in the backbone at $\delta = 4.45$ –4.20 ppm, revealing BnO-P(LLA-*co*-MAC)-OH copolymers with MAC incorporations ranging from 1.4% to 15.3%. In addition, a copolymerisation of MAC ($f_{MAC} = 0.5$) with *D*-lactide was performed, yielding a copolymer with a MAC incorporation of 15.6% (Figure 5.4) - comparable to the *L*-lactide result for $f_{MAC} = 0.5$.

Table 5.1. Results from lactide polymerisations and copolymerisation of lactide with MAC.^a

f_{LA}^b	f_{MAC}^c	[M]/[I]	$F_{MAC}^{d,e}$	DP ^f	M_n (NMR) ^e (g mol ⁻¹)	M_n (GPC) ^g (g mol ⁻¹)	PDI ^g
1.0 ^h	0	100	0	96	13 900	27 300	1.05
1.0 ⁱ	0	100	0	114	16 500	25 700	1.10
0.75 ^{h,j}	0.25	145	7.0 ^l	103	15 700	18 400	1.13
0.75 ^h	0.25	100	14.5	77	11 800	14 800	1.06
0.75 ^h	0.25	100	5.4	74	11 000	14 900	1.05
0.90 ^h	0.10	83	1.4	72	10 500	22 900	1.06
0.60 ^h	0.40	125	8.2	98	14 700	22 100	1.07
0.50 ^h	0.50	150	15.3	72	11 100	16 800	1.14
0.50 ⁱ	0.50	150	15.6	45	6990	6910	1.13
0.75 ^h	0.25 ^k	100	10.4 ^k	96	14 500	18 300	1.05

^a Targeted degree of polymerisation (DP) of lactide = 100 (homopolymerisations) or 75 (copolymerisations). Reactions were performed in CDCl₃ at 25 °C, [LA] = 0.7 M (homopolymerisations) or [LA] = 0.53 M (copolymerisations), using 1 mol% **3** and 0.2 mol% **1**. ^b Molar fraction of *L*- or *D*-lactide in the feed. ^c Molar fraction of MAC in the feed. ^d Molar fraction of MAC in the final polymer. ^e Determined by ¹H NMR spectroscopy. ^f Experimental degree of polymerisation measured by ¹H NMR spectroscopy. ^g Determined by GPC analysis in THF. ^h Polymerisation using *L*-lactide. ⁱ Polymerisation using *D*-lactide. ^j Using 10 mol% **3** and 5 mol% **2** as catalysts. ^k Polymerisation using MPC instead of MAC. ^l Conversion at 95% LLA conversion.

Additional analysis could be conducted by integration of the multiplet found at $\delta = 5.05$ ppm corresponding to methine protons found next to a carbonate bond, which revealed an average *L*-lactyl sequence length in the copolymers ranging from 63 for P(LLA-*co*-PMAC_{1.4%}) to 21 for P(DLA-*co*-MAC_{15.6%}). ¹³C analysis of the copolymers also revealed resonances expected for a copolymer with LLA and MAC repeat units.

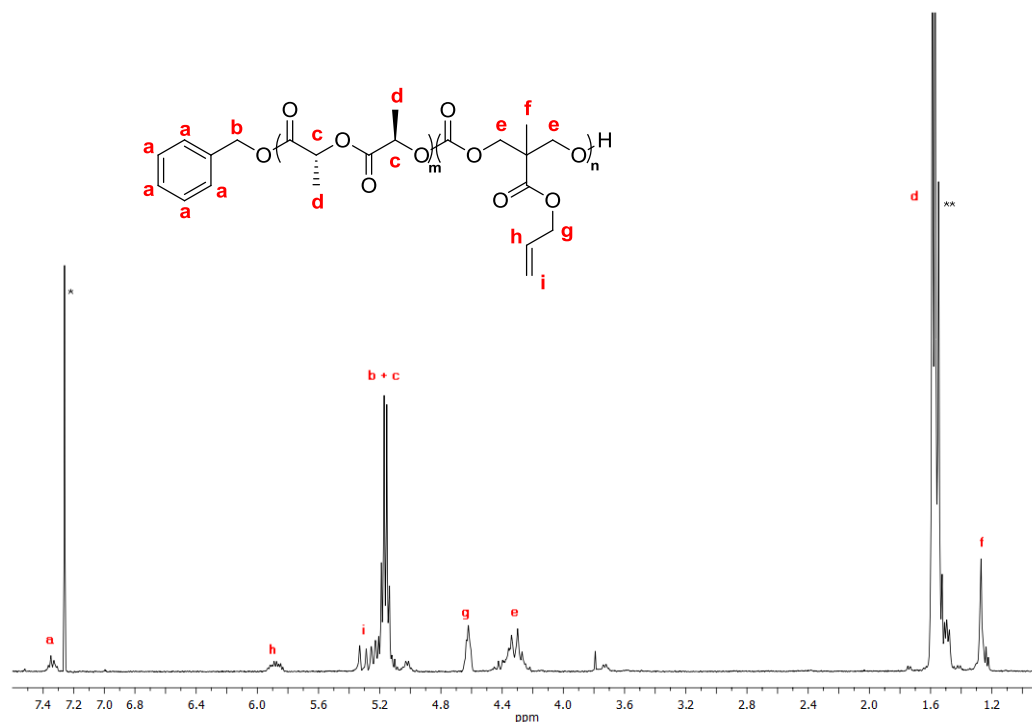


Figure 5.4. ^1H NMR in CDCl_3 of P(DLA-*co*-MAC) initiated from benzyl alcohol using 1 mol% **3** and 0.2 mol% **1** (400 MHz, 298 K; * = residual CDCl_3 , ** = H_2O).

In the carbonyl region, two peaks at $\delta = 154.2$ ppm and at $\delta = 154.5$ ppm were found corresponding to the carbonate carbons. The resonance at $\delta = 154.5$ ppm was assigned to a carbonate group between two MAC repeat units (MAC-MAC dyad) as the same resonance could be found in the ^{13}C NMR spectra of the PMAC homopolymers. It was previously reported for poly(ester-carbonate)s that the carbonyl carbons in the polymer backbone are sensitive to the repeat unit sequence, with a reported shift for the MAC-MAC dyad at $\delta = 154.4$ ppm and at $\delta = 154.1$ ppm for a LA-MAC dyad,^{20,29-31} the higher intensity resonance found at $\delta = 154.2$ ppm in the P(LLA-MAC) copolymers was assigned to the LA-MAC dyad. The carbonyl resonances

corresponding to the carbonyl resonances of the ester groups of the lactyl units were found at $\delta = 167$ -170 ppm. Analysis of the PLA homopolymers and PLA-MAC copolymers by gel permeation chromatography (GPC) revealed narrow polydispersities (PDI = 1.05-1.14) in all cases (Table 5.1; Figure 5.5).

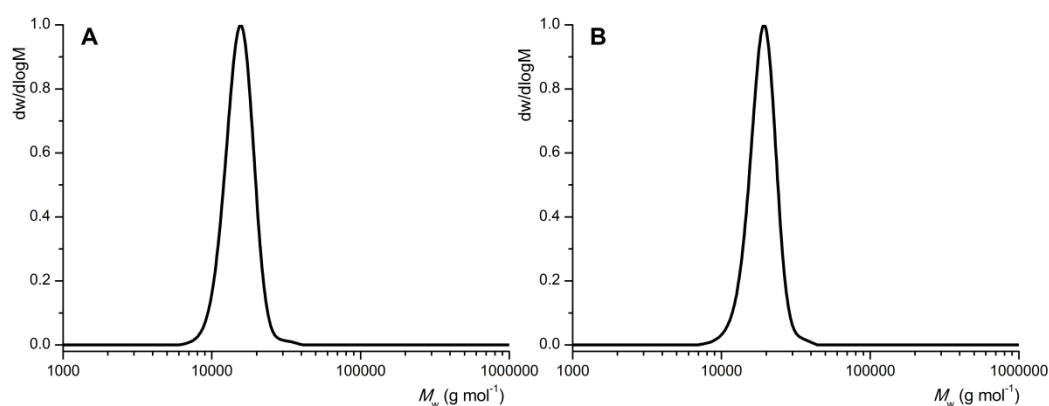


Figure 5.5. GPC traces of (A) P(LLA-*co*-MAC) and (B) P(LLA-*co*-MPC) initiated from benzyl alcohol using 1 mol% **3** and 0.2 mol% **1**.

In a similar manner, the synthesis of a P(MPC-*co*-LLA) copolymer with $f_{\text{MPC}} = 0.25$ was achieved by ROP of *L*-lactide and MPC, catalysed by 1 mol% **3** and 0.2 mol% **1**, using benzyl alcohol as initiator. This copolymerisation afforded a polymer with an MPC incorporation of 10.4% (Figure 5.6), almost twice as much as the incorporation of MAC in a copolymerisation $f_{\text{MAC}} = 0.25$. GPC analysis of the resulting LLA-MPC copolymer showed a narrow, monomodal distribution with a number average molecular weight (M_n) of 14 490 g mol⁻¹ and a PDI of 1.05 (Figure 5.5).

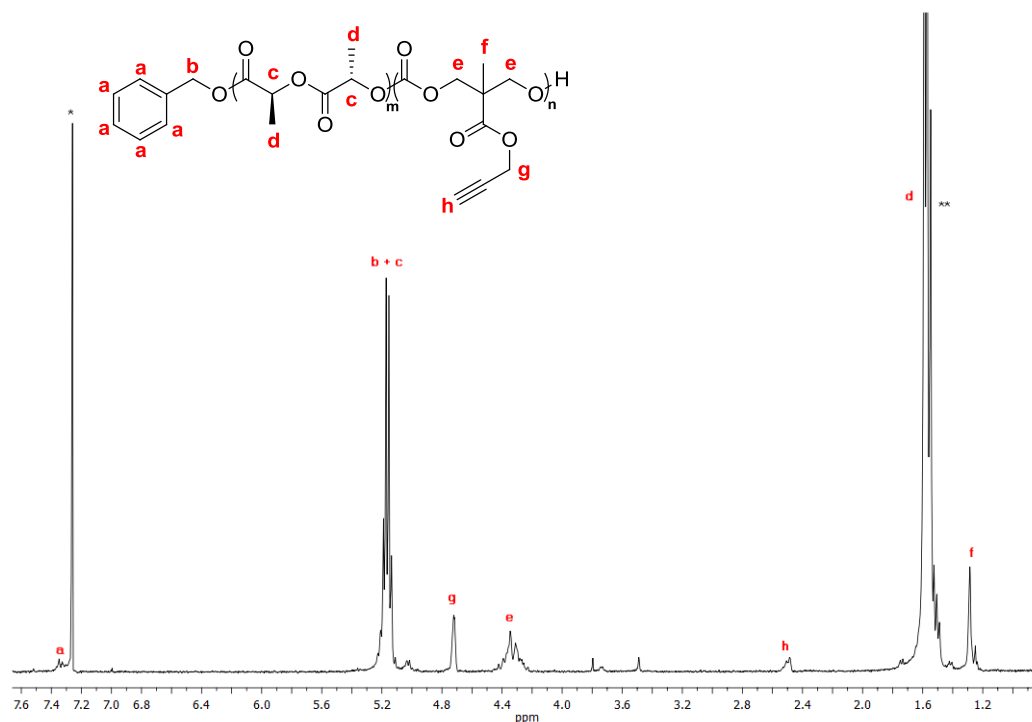
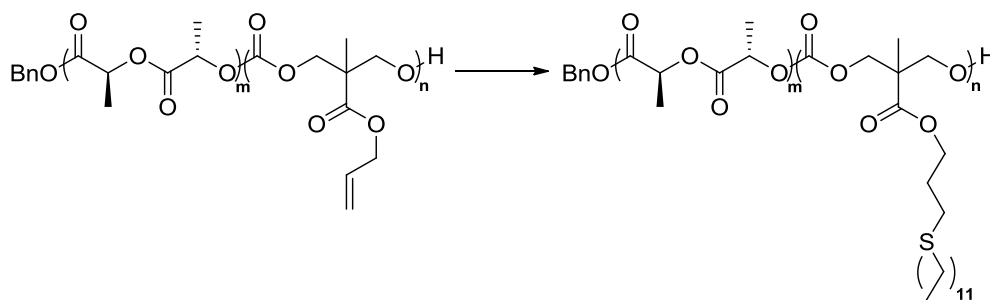


Figure 5.6. ^1H NMR in CDCl_3 of P(LLA-*co*-MPC) initiated from benzyl alcohol using 1 mol% **3** and 0.2 mol% **1** (400 MHz, 298 K; * = residual CDCl_3 , ** = H_2O).

5.2.2. Post-polymerisation functionalisations of allyl- and propargyl functional poly(ester-carbonate)s.

The possibility to further functionalise poly(ester-carbonate)s post-polymerisation, without any degradation occurring, was investigated by radical addition of 1-dodecanethiol to the allyl ester groups of P(LLA-*co*-MAC_{5.4%}) (Scheme 5.2) and by the copper catalysed 1,3-dipolar cycloaddition of 1-azidooctane to the pendant alkyne functional groups in P(LLA-*co*-MPC_{10.4%}). Previous studies on the functionalisation of the pendant allyl ester groups in PMAC homopolymers *via* radical addition (Chapter 2), demonstrated that an excess of thiol was necessary to achieve successful functionalisation of the



Scheme 5.2. Post-polymerisation functionalisation of allyl-functional poly(ester-carbonate)s with 1-dodecanethiol.

allyl groups without cross-linking. Functionalisation of P(LLA-*co*-MAC_{5.4%}) was therefore performed using 20 equivalents of 1-dodecanethiol. After reaction at 90 °C for 16 hours with 20 mol% AIBN under a nitrogen atmosphere, the reaction mixture was precipitated twice in hexanes to afford 1-dodecanethiol functionalised P(LLA-*co*-MAC_{5.4%}). ¹H NMR spectroscopic analysis revealed that >99% conversion of the allyl groups had occurred, evidenced by the disappearance of the vinyl resonances at $\delta = 5.89$ and 5.37-5.21 ppm and by the appearance of new resonances consistent with the 1-dodecanethiol groups (Figure 5.7). Furthermore, GPC analysis revealed a distribution that displayed a small shift to a decreased retention time ($M_n = 16\,300\text{ g mol}^{-1}$) compared to that of the copolymer before post-polymerisation functionalisation ($M_n = 14\,900\text{ g mol}^{-1}$) whilst maintaining a narrow distribution with a polydispersity (PDI = 1.05) similar to that of the unmodified copolymer (Figure 5.8).

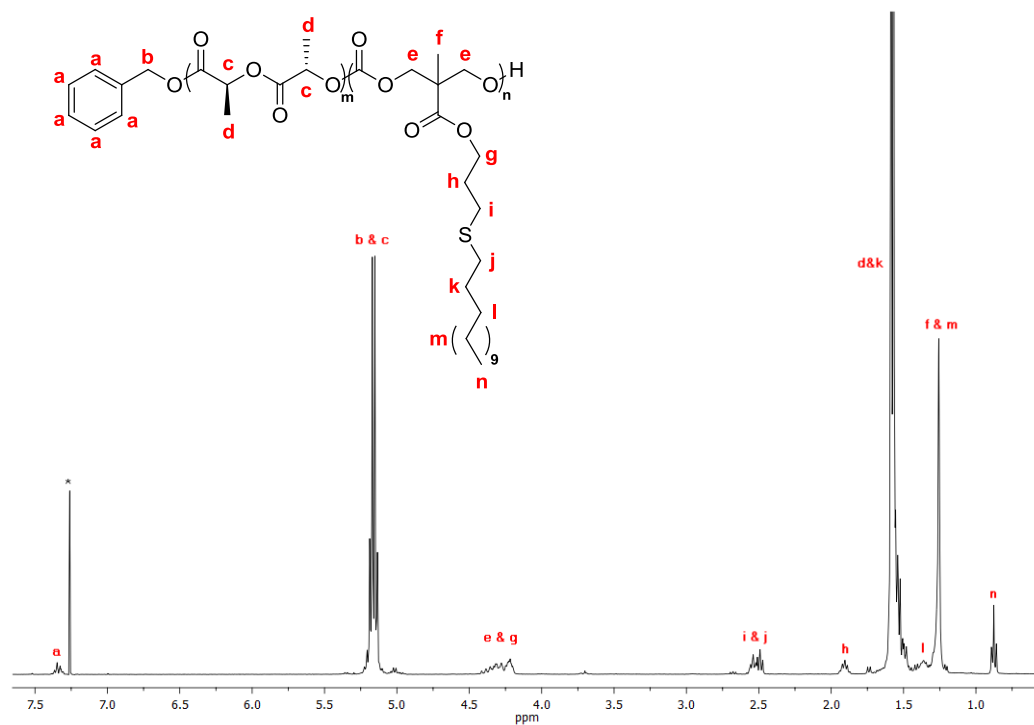


Figure 5.7. ^1H NMR in CDCl_3 of P(LLA-*co*-MAC) after post-polymerisation radical functionalisation with 1-dodecanethiol (400 MHz, 298 K; * = residual CDCl_3).

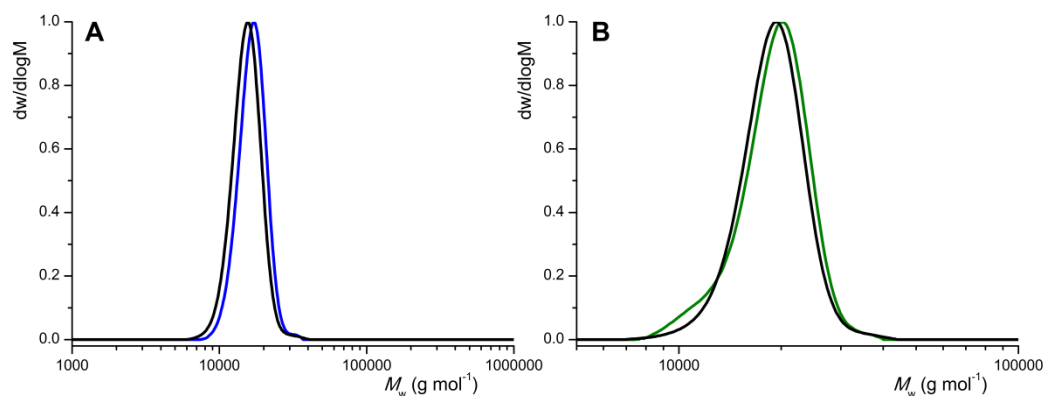
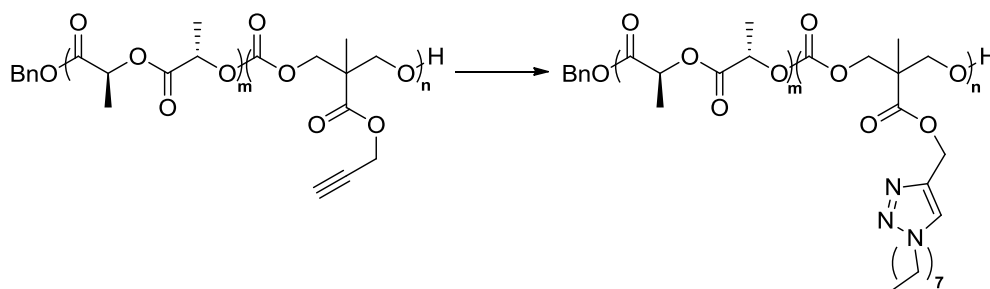


Figure 5.8. GPC traces of (A) P(LLA-*co*-MAC) before (●) and after (●) post-polymerisation functionalisation with 1-dodecanethiol and (B) P(LLA-*co*-MPC) before (●) and after (●) post-polymerisation with 1-azidooctane.

Functionalisation of the pendant alkyne moieties in P(LLA-*co*-MPC_{10.4%}) was carried out in a similar manner to that reported in Chapter 3 for PMPC homopolymers using 1.5 equivalent 1-azidooctane (to alkyne), 0.4 equivalent CuI and 0.8 equivalent of diisopropylethylamine (Scheme 5.3). After reacting in degassed tetrahydrofuran for 24 hours at room temperature, the reaction was quenched with AmberlystTM (acidic) ion exchange resin, followed by the removal of copper and precipitation into hexanes to afford 1-azidooctane functionalised P(LLA-*co*-MPC_{10.4%}). ¹H NMR spectroscopic analysis revealed that >99% conversion of the propargyl groups had occurred, evidenced by the disappearance of the resonance of the propargyl proton at $\delta = 2.49$ ppm, the appearance of for the resonance of the triazole proton at $\delta = 7.62$ ppm as well as those consistent with the 1-octyl groups (Figure 5.9). Furthermore, analysis by GPC revealed a slight shift to a higher molecular weight from $M_n = 18\,290$ g mol⁻¹ (PDI = 1.05) before functionalisation to $M_n = 18\,700$ g mol⁻¹ (PDI = 1.06) after the addition of 1-azidooctane, whilst maintaining a low polydispersity (Figure 5.8).



Scheme 5.3. Post-polymerisation functionalisation of propargyl-functional poly(ester-carbonate)s with 1-azidooctane.

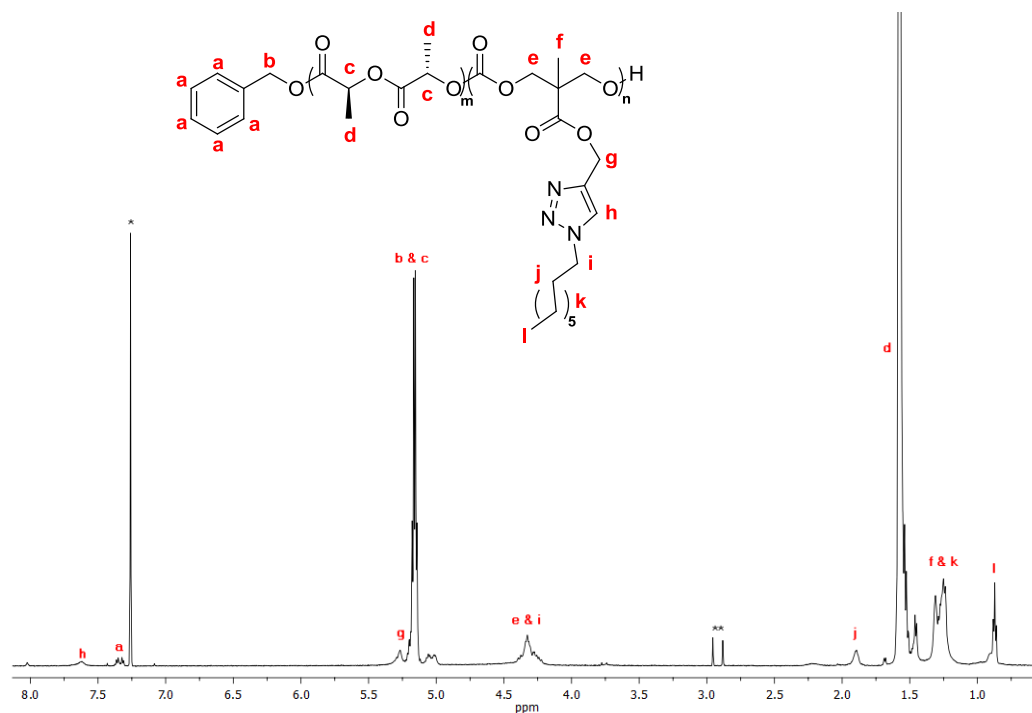


Figure 5.9. ^1H NMR in CDCl_3 of P(LLA-*co*-MPC) after post-polymerisation functionalisation with 1-azidooctane *via* Huisgen 1,3-dipolar cycloaddition (400 MHz, 298 K; * = residual CDCl_3 ; ** = DMF).

5.2.3. Thermal analysis of poly(ester-carbonate)s.

Analysis of allyl- and propargyl- functional poly(ester-carbonate)s by differential scanning calorimetry (DSC) was undertaken to investigate the effect of the MAC and MPC incorporation on the thermal properties of the polymers. All poly(ester-carbonate)s showed a single glass transition temperature (T_g) in their DSC thermograms which is indicative of a random copolymer. Glass transition temperatures obtained for the copolymers ranged from 36.9 °C for P(DLA-*co*-MAC_{15.6%}) (**16**) to 51.3 °C for P(LLA-*co*-MAC_{1.4%}) (**15a**). Copolymers with a low molar fraction of MAC displayed glass transition temperatures that were lower than those with low incorporation of

MAC, revealing a trend for the T_g of P(LLA-*co*-MAC_{1.4%}) (**15a**) > P(LLA-*co*-MAC_{5.4%}) (**15b**) > P(LLA-*co*-MAC_{8.2%}) (**15c**) > P(LLA-*co*-MAC_{15.3%}) (**15d**) > P(DLA-*co*-MAC_{15.6%}) (**16**) (Table 5.2). This observation corresponds to the lower glass transition value observed for PMAC homopolymers ($T_g = -26.4$ °C) compared to that of PLLA (in this work: $T_g = 57.0$ °C, literature: 50-65 °C)^{5,6}.

Table 5.2. Thermal analysis of poly(ester-carbonate)s.

Polymer	Pendant Functionality	T_g^a (°C)	$T_m^{b,c}$ (°C)	H_m^c (J g ⁻¹)	$T_m^{d,e}$ (°C)	H_m^e (J g ⁻¹)	T_c^f (°C)
PDLA	-	56.7 ^h	143.8 ^h	27.6 ^h			-
PLLA	-	57.0 ^h	150.4 ^h	22.4 ^h	150.4 ^h	24.6 ^h	121.9 ^g
P(LLA- <i>co</i> -MAC _{1.4%}) (15a)	allyl	51.3 ^g	139.1 ^h	30.2 ^h	143.2 ^g	34.5 ^g	118.5 ^g
P(LLA- <i>co</i> -MAC _{5.4%}) (15b)	allyl	48.0 ^g	137.3 ^g	29.0 ^g	138.0 ^g	0.3 ^g	
P(LLA- <i>co</i> -MAC _{8.2%}) (15c)	allyl	45.2 ^g	120.7 ^h	15.2 ^h			
P(LLA- <i>co</i> -MAC _{15.3%}) (15d)	allyl	41.0 ^g	111.4 ^h	9.0 ^h			
P(DLA- <i>co</i> -MAC _{15.6%}) (16)	allyl	36.9 ^g					
P(LLA- <i>co</i> -MPC _{10.4%}) (17)	propargyl	45.2 ^g	129.2 ^g	21.9 ^g			
18ⁱ	dodecyl	35.2 ^g	139.7 ^h	15.2 ^h	138.5 ^g	1.1 ^g	
19^j	octyl	35.7 ^g	129.7 ^g	23.8 ^g			

^a Glass transition temperature, measured by DSC analysis at the second scan. ^b Melting point measured by DSC analysis in the first heating run. ^c Samples obtained by solution crystallisation. ^d Melting point measured by DSC analysis in the second heating run. ^e Results obtained from samples in the melt. ^f Crystallisation temperature obtained in the second heating run from samples in the melt. ^g Data was collected using a heating rate of 10 °C/min and a cooling rate of 10 °C/min. ^h Data was collected using a heating rate of 20 °C/min and a cooling rate of 1 °C/min. ⁱ Polymer obtained after functionalisation of **15b** with 1-dodecanethiol. ^j Polymer obtained after functionalisation of **17** with 1-azidooctane.

The expected glass transition temperature of many random copolymers can be calculated if the glass transition temperatures of the respective homopolymers are known following the relation as established by Fox³²:

$$\frac{1}{T_g} = w_B \left(\frac{1}{T_{gB}} - \frac{1}{T_{gA}} \right) + \frac{1}{T_{gA}}$$

Where w_B is the weight fraction of monomer B in the polymer and T_{gA} and T_{gB} represent the glass transition temperatures of the homopolymers of monomer A and B, respectively. The relation of $1/T_g$ (K^{-1}) and weight percentage of monomer is linear for copolymers. Comparison of the experimental values and calculated values for $1/T_g$ and weight percentage of MAC of LLA-MAC copolymers showed that the experimental values were in good agreement with the theoretical values (Figure 5.10). The copolymer of LLA with MPC, P(LLA-MPC_{10.4%}), showed a T_g value of 45.2 °C, which is similar to T_g values copolymers previously reported by Jing and co-workers for P(LA-MAC).³³ Both for P(LLA-*co*-MAC_{5.4%}) and P(LLA-*co*-MPC_{10.4%}) lower values for the glass transition were observed after functionalisation of the allyl- or propargyl-groups with 1-dodecanethiol and 1-azidooctane: T_g = 35.2 °C for **18** and T_g = 35.7 °C for **19** consistent with the introduction of the pendant alkyl chains.

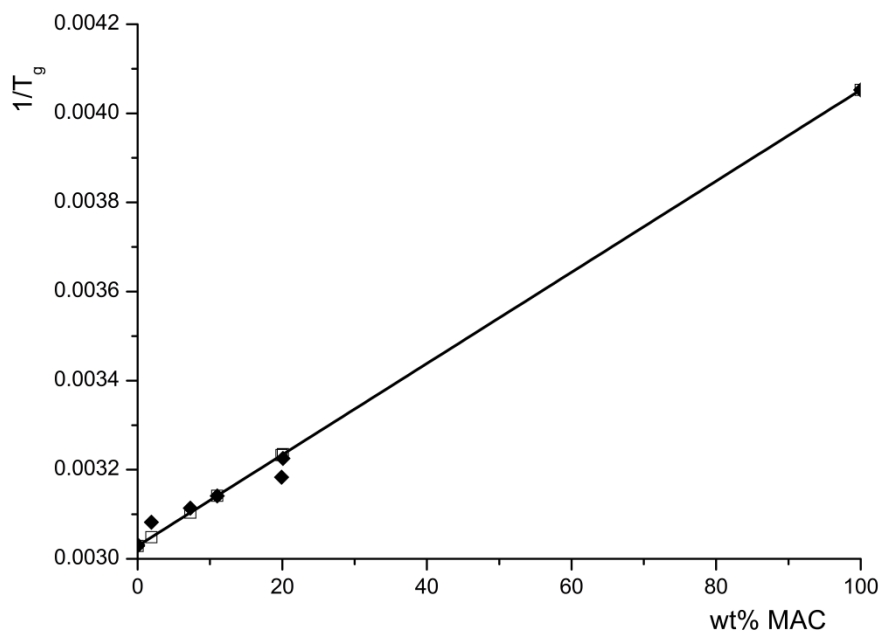


Figure 5.10. Plot of $1/T_g$ (K^{-1}) versus weight percentage of MAC in LA/MAC copolymers. Experimentally obtained values (◆) and calculated values (□) are displayed.

PLLA and PDLA are crystalline materials unlike PDLLA which is amorphous in nature. PLLA and PDLA have a melting point around 180 °C depending on the enantiopurity and its molecular weight. The melting point decreases for higher incorporations of lactyl units with the opposite configuration and crystallinity is lost for incorporations of lactyl units with the opposite configurations over 12%.^{5,6,34-36} DSC analysis of PLLA and PDLA samples prepared *via* organocatalytic ROP of *D*- and *L*-lactide in this work showed melting peaks in solution-crystallised samples at 143.8 °C and 150.4 °C, respectively. Only PLLA showed a crystallisation and melting peak in its DSC thermogram corresponding to crystallisation in the melt ($T_m = 150.5$ °C). The absence of a melting peak in the second analysis of PDLA could be due to a

number of reasons. For example, stereo-errors could have been introduced due to epimerisation during polymerisation or due to transesterification of the polymer samples, but since crystallinity was observed for the sample prepared *via* solution crystallisation it is likely that DSC conditions were not optimal for melt crystallisation of the polymer. DSC thermograms of poly(ester-carbonate)s with incorporations of MAC or MPC of up to 15.6% were also investigated for the presence of a melting peak. Apart from P(DLA-*co*-MAC_{15.6%}) all polymer samples obtained *via* solution crystallisation showed a melting peak at temperatures ranging from 111 to 140 °C. Melting temperature decreases with increasing incorporation of MAC revealing a trend for T_m of P(LLA-*co*-MAC_{1.4%}) (**15a**) > P(LLA-*co*-MAC_{5.4%}) (**15b**) > P(LLA-*co*-MAC_{8.2%}) (**15c**) > P(LLA-*co*-MAC_{15.3%}) (**15d**). A decrease in melting temperature with increasing incorporation of carbonate monomers and a loss of crystallinity in case of incorporations of >20% has previously been reported for poly(ester-carbonate)s.³⁷⁻³⁹ Poly(ester-carbonate)s **15a** and **15b**, which have low incorporations of MAC, also show a melting peak at ~140 °C from crystallisation that had occurred in the melt during heating. The observation of a melting peak in the DSC thermograms of the melt crystallised sample (140 °C) as well as the solution crystallised sample (139 °C) of **18** shows that functionalisation of the allyl groups with a 1-dodecanethiol does not disrupt crystallisation (Figure 5.11). A melting peak is also observed in the DSC thermogram of **19** at 130 °C (solution crystallisation) demonstrating that

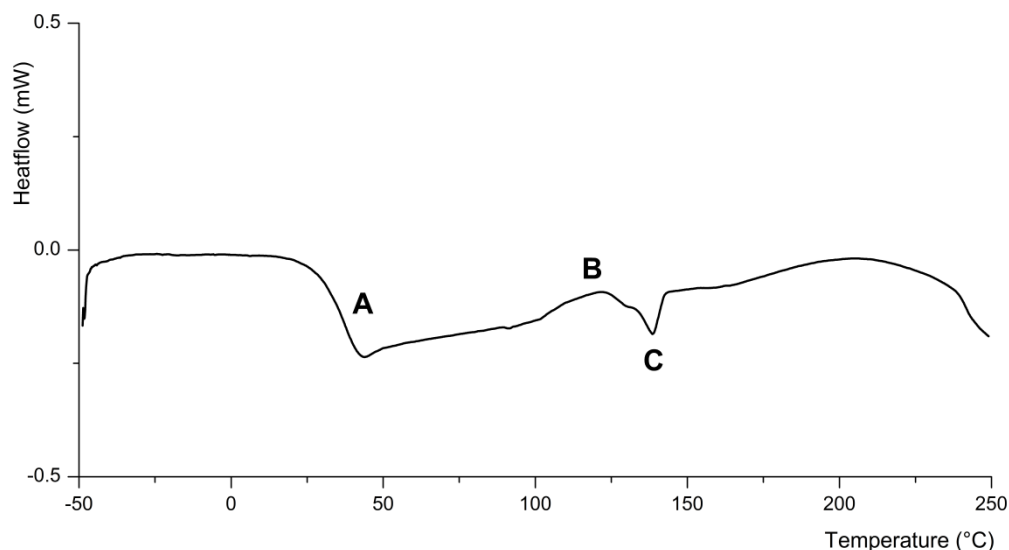


Figure 5.11. DSC thermogram of P(LLA-*co*-MAC_{5.4%}) after functionalisation with 1-dodecanethiol (**18**) obtained by melt crystallisation showing a clear glass transition (A), crystallisation (B) and melting peak (C).

further functionalisation of propargyl functional poly(ester-carbonate)s is also possible. The observation of a small crystallisation peak as well as a small melting peak in the second heating run for some samples indicates that although crystallisation takes place during heating, conditions are not optimal. Slow cooling from 250 °C to -50 °C in 5 hours of the samples was attempted to induce crystallisation followed by a heating at a faster rate than the initial analysis of the samples resulted in DSC thermograms in which no crystallisation or melting peaks were observed at all. Heating for extended periods of time (annealing) or slower heating rates are most likely necessary for full crystallisation to take place. Thermal analysis of P(LA-*co*-MAC) has previously been reported by Storey and co-workers⁴⁰ and Jing and co-workers³¹. However, *rac*-lactide was used in preference to *L*- or *D*-lactide

leading to the formation of amorphous polymers. Crystalline PEO-*b*-P(MPC-*co*-LA) polymers were reported by Jing and co-workers which revealed melting temperatures between 110 and 150 °C.²²

5.2.4. Thermal analysis of poly(ester-carbonate) blends.

Since crystallinity was observed for poly(ester-carbonate)s with low incorporations of MAC or MPC, stereocomplexation of copolymers with opposite chirality might be possible. To that end, equimolar blends were prepared *via* solution casting which was carried out by combining solutions of the polymers in chloroform in equimolar amounts, followed by slow evaporation. This method of stereocomplex formation facilitates reliable results when the solvent is evaporated at a slow rate, as the critical concentration for stereocomplex crystallite formation is lower than that of PLLA and PDLA homocrystallisation. However, formation of homocrystallites is often favoured, when polymers with increasing molecular weights are used.⁴¹ Due to the large radii of the PLLA and PDLA molecules stereocomplex crystallite nucleation is retarded, resulting in the formation of a larger amount of homocrystallites. After analysis of the solution-casted blends by differential scanning calorimetry, the samples were cooled from 250 °C to -50 °C in 30 minutes in an attempt to induce crystallisation upon cooling in the melt.

As control experiment, an equimolar blend of PDLA and PLLA was prepared to form the PDLA/PLLA stereocomplex, SC-[PLLA/PDLA]. DSC analysis of the sample obtained after solution casting revealed melting peaks corresponding PLLA and PDLA homocrystallites between 130 and 150 °C as well as a melting point for SC-[PLLA/PDLA] at 198 °C (Table 5.3). Although some crystallisation was observed during cooling, melt crystallisation of SC-[PLLA/PDLA] was observed mainly in the DSC heating run at 99 °C. The DSC thermogram of the PLLA/PDLA blend (Figure 5.12) from the melt thus shows a large crystallisation peak as well as a melting peak ($T_m = 194.9$ °C) of the

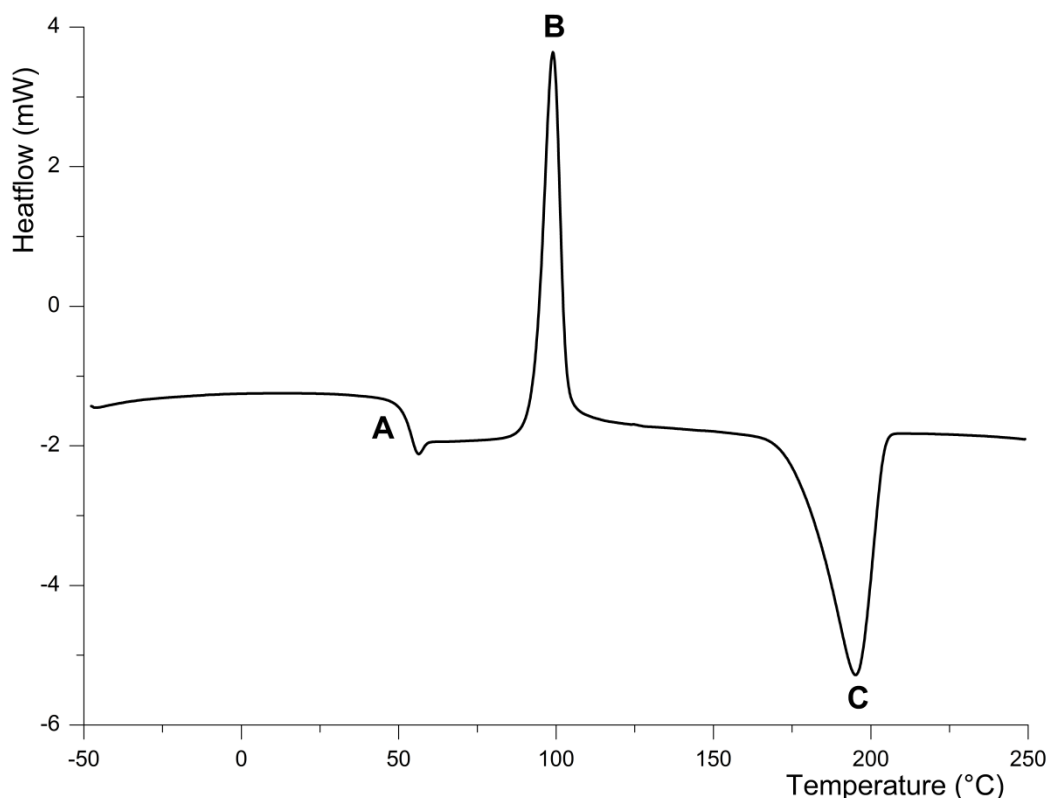


Figure 5.12. DSC thermogram of an equimolar blend of PLLA and PDLA obtained from the melt. The thermogram displays a glass transition (A), crystallisation peak for PDLA and PLLA stereocomplexation (B) and the melting point of the resulting SC-[PLLA/PDLA] (C).

stereocomplex which is an increase of 44.5 °C compared to that of PLLA alone ($T_m = 150.4$ °C). The clear glass transition of the blend was observed at 52.3 °C and no homocrystallisation was observed in the DSC thermogram following crystallisation in the melt.

After stereocomplexation of PLLA and PDLA was confirmed in the melt and in samples prepared *via* solution casting, equimolar blends of poly(ester-carbonate)s P(LLA-*co*-MAC_{1.4%}) (**15a**), P(LLA-*co*-MAC_{5.4%}) (**15b**), P(LLA-*co*-MAC_{8.2%}) (**15c**) P(LLA-*co*-MAC_{15.3%}) (**15d**) and P(LLA-*co*-MPC_{10.4%}) (**17**) with

Table 5.3. Thermal analysis of poly(ester-carbonate)s blends with PDLA.^a

Polymers	T_g^b (°C)	$T_m^{c,d}$ (°C)	H_m^d (J g ⁻¹)	$T_m^{e,f}$ (°C)	H_m^f (J g ⁻¹)	T_g^g (°C)
PLLA ^h	52.3	197.8	23.2	194.9	-38.2	99.1
P(LLA- <i>co</i> -MAC _{1.4%}) (15a) ⁱ	56.3	193.0	22.3	183.6	33.2	118.8 ^j
P(LLA- <i>co</i> -MAC _{5.4%}) (15b) ^h	47.5	191.4	25.7	175.0	20.0	120.7
P(LLA- <i>co</i> -MAC _{8.2%}) (15c) ^h	46.8	183.3	20.4	170.8	2.6	131.0
P(LLA- <i>co</i> -MAC _{15.3%}) (15d) ^h	44.5	177.9	13.2	167.3	0.2	
P(LLA- <i>co</i> -MPC _{10.4%}) (17) ^h	45.9	187.1	21.4	169.3	7.2	123.8
18 ^h	40.3	189.6	29.9	170.8	13.9	115.0
19 ^h	34.2	187.9	23.6	174.0	9.0	

^a Samples were prepared *via* solution casting of the polymers in equimolar amounts. ^b Glass transition temperature of the blend, measured by DSC analysis in the second scan. ^c Melting point measured by DSC analysis in the first heating run. ^d Samples obtained by solution crystallisation. ^e Melting point measured by DSC analysis in the second heating run. ^f Results obtained from samples in the melt. ^g Crystallisation temperature obtained in the second heating run from samples in the melt. ^h Data was collected using a heating rate of 10 °C/min and a cooling rate of 10 °C/min. ⁱ Data was collected using a heating rate of 20 °C/min and a cooling rate of 1 °C/min. ^j Crystallisation occurred in the cooling run.

PDLA were prepared and analysed by DSC. The DSC thermograms of the blends after solution casting show melting points that are at temperatures 35-65 °C higher than observed for their respective homopolymers, indicative of stereocomplex formation (Table 5.3). Most thermograms of solution-casted blends also display melting peaks corresponding to homocrystallites. Crystallisation in the melt was observed for each sample, with melting peaks of SC-[**15a**/PDLA], SC-[**15b**/PDLA], SC-(**15c**/PDLA) and SC-[**15d**/PDLA] obtained by melt crystallisation were found at 184 °C, 175 °C, 171 °C, 167 °C and 169 °C respectively (Figure 5.13).

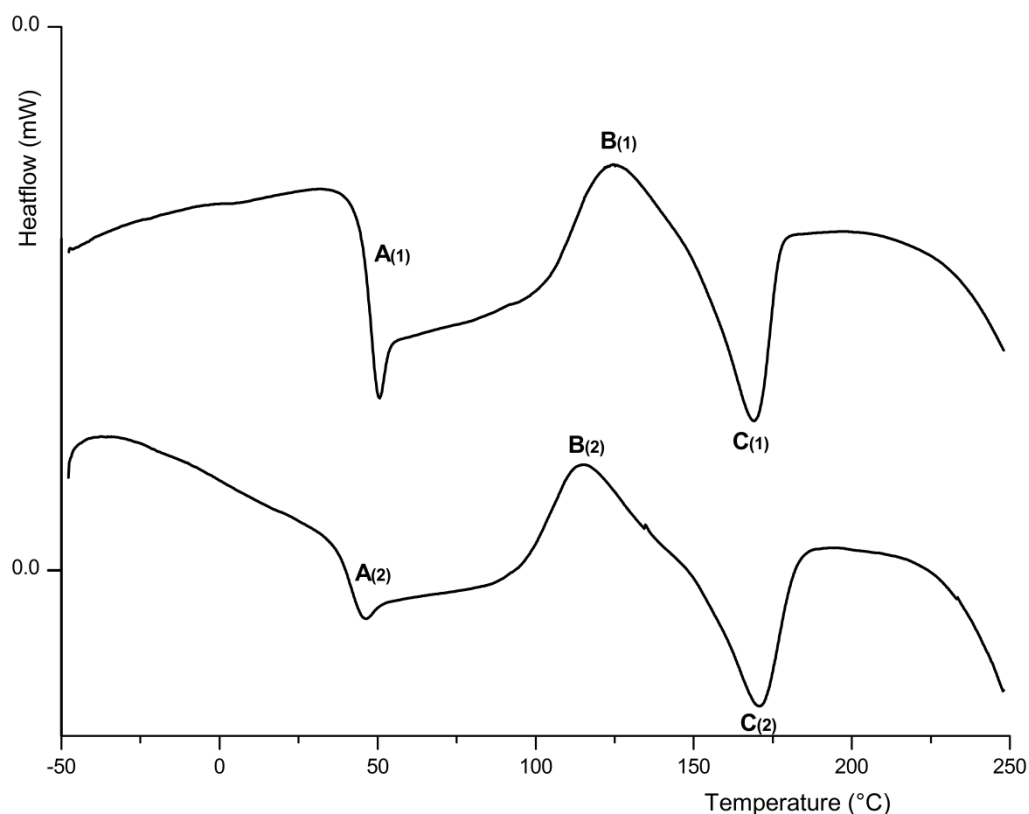


Figure 5.13. DSC thermograms of blends of PDLA with **17** (top; 1) and **18** (bottom, 2) from melt crystallised samples. The DSC thermograms display peaks corresponding to the glass transition of the blend (A(1); A(2)) and crystallisation (B(1); B(2)) and melting peak (C(1); C(2)) of SC-[PDLA/**17**] and SC-[PDLA/**18**].

These values are $\sim 40^\circ\text{C}$ higher than the values found for the respective melting points of the individual polymers.

Stereocomplexation was also observed in blends of PDLA with poly(ester-carbonate)s that had been further functionalised post-polymerisation with dodecanethiol (**18**) or 1-azidooctane (**19**), demonstrating that the incorporation of a new functionality in the poly(ester-carbonate) backbone does not affect stereocomplexation. Peaks corresponding to SC-[**18**/PDLA] crystallisation and melting were found at 115°C and 171°C respectively for melt samples (Figure 5.13), while for samples prepared *via* solution casting the melting peak corresponding to SC-[**18**/PDLA] was observed at 190°C . In addition, blends **18** and PDLA prepared *via* solution casting reveal melting peaks of **18** and PDLA homocrystallites (Figure 5.14). Peaks corresponding to SC-[**19**/PDLA] were observed at 188°C (solution casting) and 174°C (melt).

Although the melting enthalpy is reported to be maximum in the case of stereocomplexation between equimolar mixing PLLA and PDLA homopolymers, stereocomplexation is still observed for blends in which the polymers are present in different ratios.⁴² It was investigated whether this was true for blends of PDLA and the poly(ester-carbonate) P(LLA-*co*-MAC_{5.4%}) (**15b**) with PDLA/**15b** ratios of 95:5, 75:25, 50:50, 25:75 and 5:95. Samples were prepared by solution casting, and from the melt. Analysis of samples prepared by solution casting by DSC thermogravimetric analysis, revealed melting peaks for PDLA homocrystallites at 135°C , **15b** homocrystallites at

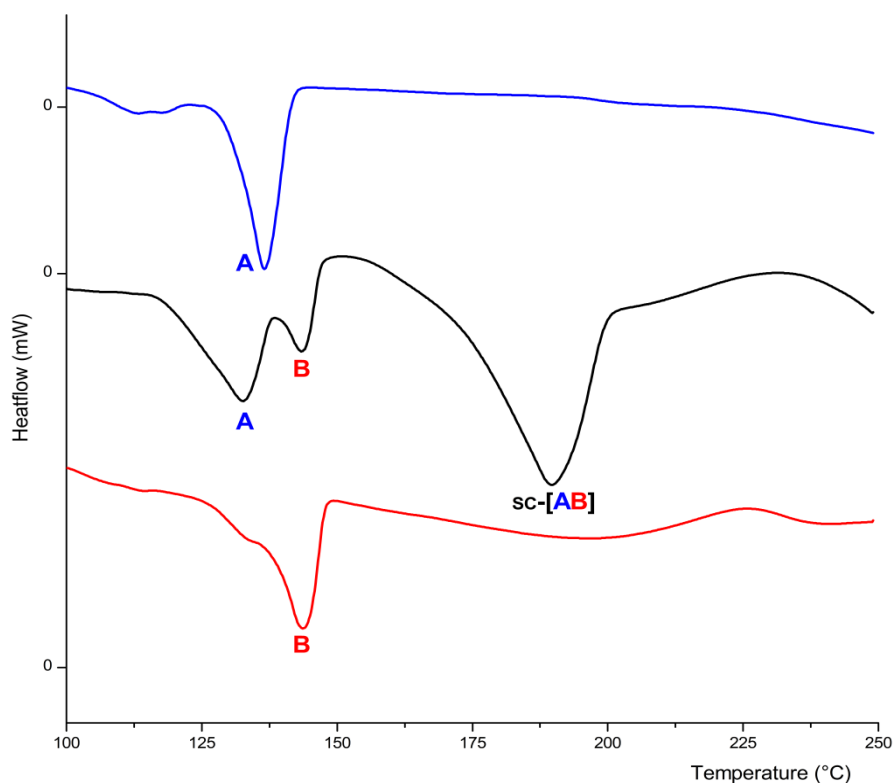


Figure 5.14. DSC thermograms of **18** (blue), PDLA (red) and a blend of PDLA with **18** (black) of samples obtained from solution casting. The thermograms displays peak corresponding to the melting of **18** (A), PDLA (B) and SC-[**18**/PDLA] (SC-[AB]).

145 °C and a melting peak at 190 °C for the stereocomplex, SC-[PDLA/**15b**], in thermograms of the PDLA/**15b** blends (Figure 5.15). As expected, the melting peak corresponding to that of SC-[PDLA/**15b**] was most obvious in that of the 50:50 PDLA/**15b** blend, whereas melting peaks corresponding to the homocrystallites were more dominant in the 95:5 and 5:95 blends. DSC thermograms of the blends prepared by melt crystallisation do not display melting peaks corresponding to PDLA or **15b** homocrystallites.

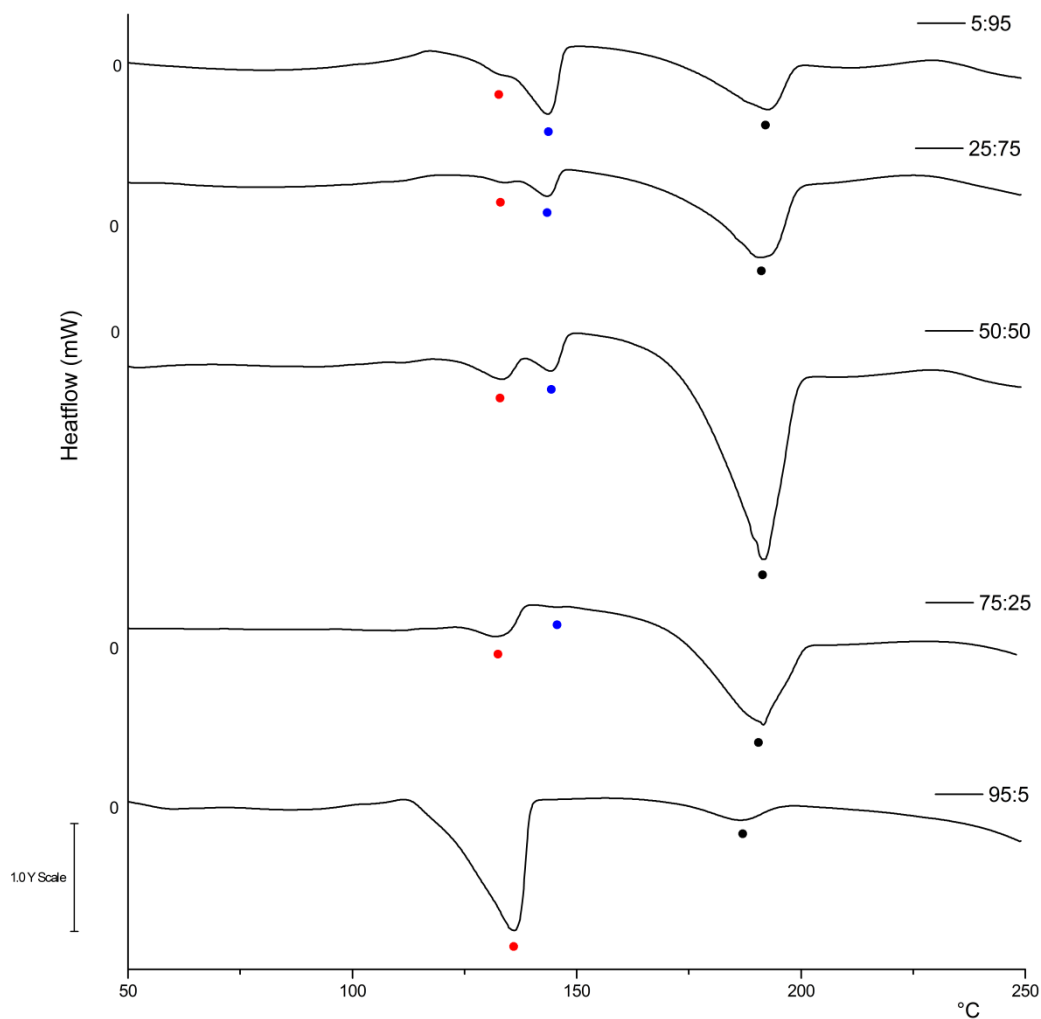


Figure 5.15. DSC thermograms of blends of PDLA with **15b** with ratios of 5:95, 25:75, 50:50, 75:25 and 95:5 (from top to bottom) from samples obtained by solution casting. The DSC thermograms display melting peaks for PDLA (●), **15b** (●) and SC-[PDLA/**15b**] (●).

In all cases a melting peak attributed to SC-[PDLA/**15b**] could be observed, however, intensities were low for the 95:5 and 5:95 blends. Peaks in the 50:50 and 75:25 PDLA/**15b** blends were most prominent and thermograms of these blends also displayed peaks corresponding to the crystallisation of the stereocomplex (Figure 5.16).

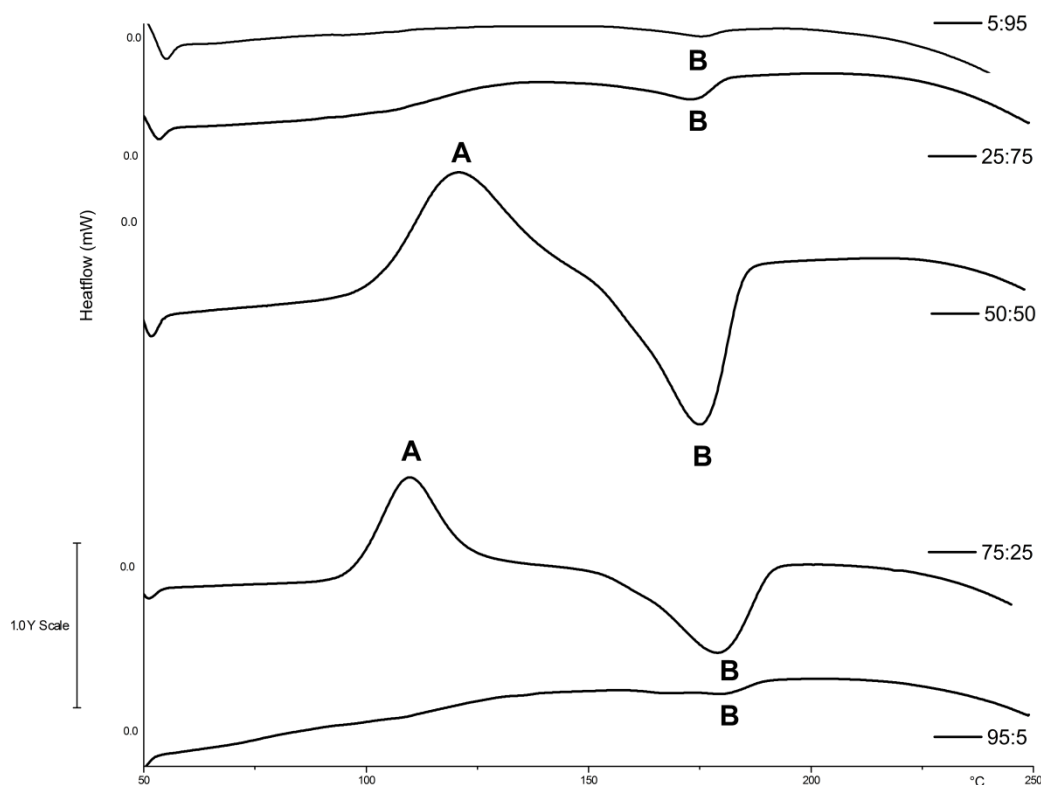


Figure 5.16. DSC thermograms of blends of PDLA with **15b** with ratios of 5:95, 25:75, 50:50, 75:25 and 95:5 (from top to bottom) from melt crystallised samples. The DSC thermograms display peaks corresponding to crystallisation (A) and melting (B) of SC-[PDLA/**15b**].

As stereocomplexation between poly(ester-carbonate)s and PDLA was observed either in samples obtained from solution casting and/or from the melt, stereocomplexation between poly(ester-carbonate)s with opposite chirality was investigated by preparing blends of P(DLA-*co*-MAC_{15.6%}) (**16**) and **15a-15b**, **17**, **18** and **19**. Crystallisation by solution casting revealed stereocomplexation in all cases with an increase in melting temperature $\Delta T_m = 35\text{-}70\text{ }^\circ\text{C}$, whilst only blends of **17** with of **15a-c** and **18** show crystallisation in the melt. Melting peaks for SC-[**15a/16**], SC-[**15b/16**], SC-[**15c/16**] and SC-[**17/16**] were observed at 165, 169, 179 and 166 °C respectively (Figure 5.17).

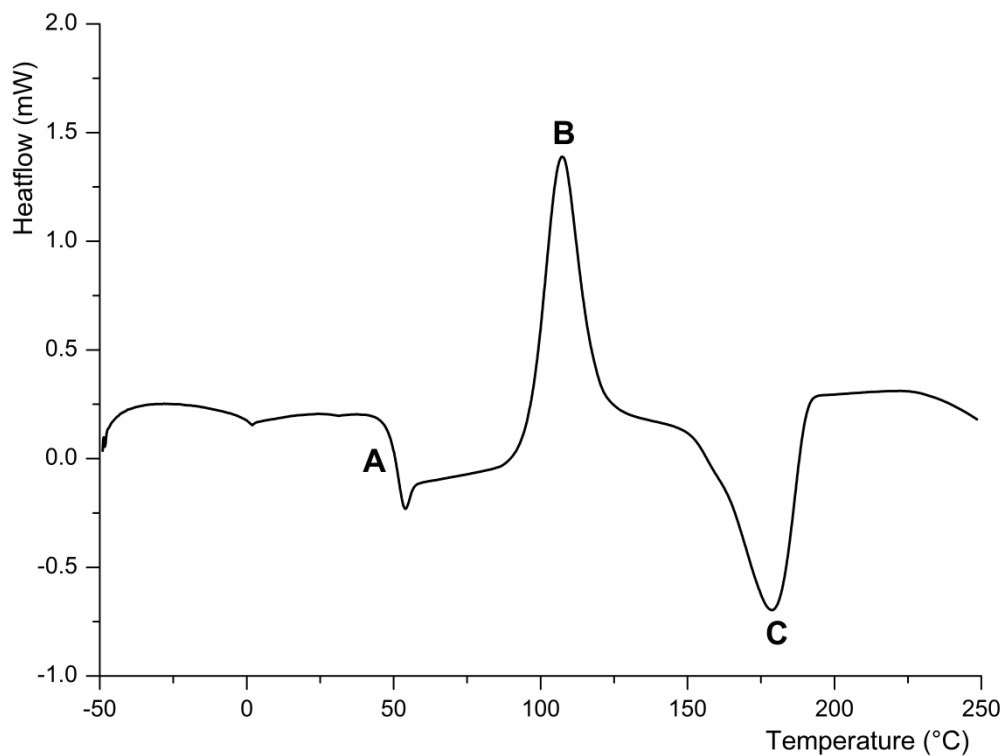


Figure 5.17. DSC thermogram of blends of **16** with **15c** from melt crystallised samples. The DSC thermograms display peaks corresponding to glass transition (A), crystallisation (B) and melting peak (C) of SC-[**16/15c**].

These results show that stereocomplexation is possible between poly(ester-carbonate)s with opposite chirality. In addition, stereocomplexes with two different functionalities have been prepared by simple blending of poly(ester-carbonate)s with different chirality and pendant functionality.

Table 5.4. Thermal analysis of poly(ester-carbonate)s blends with P(DLA-*co*-MAC_{15.6%}) (**7**).^a

Polymer	T_g^b (°C)	$T_m^{c,d}$ (°C)	H_m^d (J g ⁻¹)	$T_m^{e,f}$ (°C)	H_m^f (J g ⁻¹)	T_g^g (°C)
P(LLA- <i>co</i> -MAC _{1.4%}) (15a) ^h	39.0	176.6	26.8	165.0	3.0	126
P(LLA- <i>co</i> -MAC _{5.4%}) (15b) ^h	40.8	175.2	24.5	168.7	6.6	121.0
P(LLA- <i>co</i> -MAC _{8.2%}) (15c) ^h	49.9	192.9	26.3	178.8	26.3	107.4
P(LLA- <i>co</i> -MAC _{15.3%}) (15d) ^h	35.3	164.8	20.2			
P(LLA- <i>co</i> -MPC _{10.4%})(17) ^h	39.1	171.6	23.7			
18 ^h	35.3	172.4	29.1	166.2	7.5	114.9
19 ^h	30.4	173.2	16.9			

^a Samples were prepared *via* solution casting of the polymers in equimolar amounts. ^b Glass transition temperature of the blend, measured by DSC analysis in the second scan. ^c Melting point measured by DSC analysis in the first heating run. ^d Samples obtained by solution crystallisation. ^e Melting point measured by DSC analysis in the second heating run. ^f Results obtained from samples in the melt. ^g Crystallisation temperature obtained in the second heating run from samples in the melt. ^h Data was collected using a heating rate of 10 °C/min and a cooling rate of 10 °C/min. ⁱ Data was collected using a heating rate of 20 °C/min and a cooling rate of 1 °C/min.

5.3. Conclusions

In conclusion, the organocatalytic ring opening polymerisation of *L*- or *D*-lactide with 5-methyl-5-allyloxycarbonyl-1,3-dioxan-2-one (MAC) or 5-methyl-5-propargyloxycarbonyl-1,3-dioxan-2-one (MPC) was achieved successfully, yielding crystalline polymers that displayed narrow molecular weight distributions. Further functionalisation of a copolymer with pendant allyl functional groups *via* facile radical addition of 1-dodecanethiol and a copolymer with propargyl functionalities *via* the copper catalysed 1,3-dipolar cycloaddition of 1-azidooctane resulted in newly functional polymers that showed no sign of degradation with a retention of the molecular weight distribution at a slightly reduced retention time. Thermal analysis of the polymers revealed a melting peak in all cases and successful stereocomplexation was observed in copolymer/PDLA and copolymer/copolymer blends by differential scanning calorimetry of samples prepared by solution casting. In addition, post-polymerisation functionalisation of the polymers did not disrupt the stereocomplex formation.

In short, this work provides a straightforward but versatile method for the introduction of new functionalities in poly(lactide) stereocomplexes, with the possibility of combining two different functionalities *via* the co-crystallisation of two separately functionalised copolymers.

5.4. References

1. Rokicki, G. *Prog. Polym. Sci.* **2000**, *25*, 259–342.
2. Keul, H. *Polycarbonates*; Wiley-VCH Verlag GmbH & Co. KGaA: New York, **2009**; pp 307-327.
3. Dechy-Cabaret, O.; Martin-Vaca, B.; Bourissou, D. *Chem. Rev.* **2004**, *104*, 6147–6176.
4. Uhrich, K. E.; Cannizzaro, S. M.; Langer, R. S.; Shakesheff, K. M. *Chem. Rev.* **1999**, *99*, 3181–3198.
5. Tsuji, H. *Macromol Biosci.* **2005**, *5*, 569–597.
6. Fukushima, K.; Kimura Y. *Polym. Int.* **2006**, *55*, 626–642.
7. Ikada, Y.; Jamshidi, K.; Tsuji, H.; Hyon, S-H. *Macromolecules* **1987**, *20*, 904-906.
8. Slager, J.; Domb, A.J. *Biomacromolecules* **2003**, *4*, 1308-1315.
9. Slager, J. Domb, A.J.; *Biomacromolecules* **2003**, *4*, 1316-1320.
10. Tsuji, H.; Okumura, A. *Macromolecules* **2009**, *42*, 7263-7266.
11. Tsuji, H; Yamamoto, S; Okumura, A; Sugiura, Y. *Biomacromolecules* **2010**, *11*, 252-258.
12. Spasova, M; Mespouille, L.; Coulembier, O.; Paneva, D.; Mandova, N.; Rashkov, I.; Dubois, P. *Biomacromolecules* **2009**, *10*, 1217-1223.
13. Wanamaker, C. L.; Bluemle, M. J.; Pitet, L. M.; O' Leary, L. E.; Tolman, W. B.; Hilmyer, M. A. *Biomacromolecules* **2009**, *10*, 2904-2911.

14. van Nostrum, C. F.; Veldhuis, T. F. J.; Bos, G. W.; Hennink, W.E. *Macromolecules* **2004**, *37*, 2113-2118.
15. Granchara, G.; Coulembier, O.; Surin, M.; Lazzaroni, R.; Dubois, P. *Macromolecules*, **2010**, *43*, 8957-8964.
16. Kim, S. H.; Tan, J. P. K.; Nederberg, F.; Fukushima, K.; Yang, Y. Y.; Waymouth, R. M.; Hedrick, J.L. *Macromolecules* **2009**, *42*, 25-29.
17. Nederberg, F.; Appel, E.; Tan, J. P. K.; Kim, S. H.; Fukushima, K.; Sly, J.; Miller, R. D.; Waymouth, R. M.; Yang, Y. Y.; Hedrick, J. L. *Biomacromolecules* **2009**, *10*, 1460-1468.
18. Fukushima, K.; Pratt, R.C.; Nederberg, F.; Tan, J. P. K.; Yang, Y. Y.; Waymouth, R. M.; Hedrick, J. L. *Biomacromolecules* **2008**, *9*, 3051-3056.
19. Tsuji, H.; Ikada, Y. *Macromolecules* **1992**, *25*, 5719-5723.
20. Chen, X.; McCarthy, S. P.; Gross, R. A. *Macromolecules* **1998**, *31*, 662-668.
21. Slivniak, R.; Domb A. J. *Macromolecules* **2005**, *38*, 5545-5553.
22. Shi, Q.; Huang, Y.; Chen, X.; Wu, M.; Sun, J.; Jing, X. *Biomaterials* **2009**, *30*, 5077-5085.
23. Shirahama, H.; Ichimaru, A.; Tsutsumi, C.; Nakayama, Y.; Yasuda, H. *J. Polym. Sci., Part A: Polym. Chem.* **2005**, *43*, 438-454.
24. Dove, A. P.; Pratt, R. C.; Lohmeijer, B. G. G.; Waymouth, R. M.; Hedrick, J. L. *J. Am. Chem. Soc.* **2005**, *127*, 13798-13799.

25. Pratt, R. C.; Lohmeijer, B. G. G.; Long, D. A.; Lundberg, P. N. P.; Dove, A. P.; Li, H.; Wade, C. G.; Waymouth, R. M.; Hedrick, J. L. *Macromolecules* **2006**, *39*, 7863-7871.
26. Nederberg, F.; Lohmeijer, B. G. G.; Leibfarth, F.; Pratt, R. C.; Choi, J.; Dove, A. P.; Waymouth, R. M.; Hedrick, J. L. *Biomacromolecules* **2007**, *8*, 153-160.
27. Onbulak, S.; Tempelaar, S.; Pounder, R. J.; Gok, O.; Sanyal, R.; Dove, A. P.; Sanyal, A. DOI: 10.1021/ma2019528.
28. Pratt, R. C.; Nederberg, F.; Waymouth, R. M.; Hedrick, J. L. *Chem. Commun.* **2008**, 114–116.
29. Weiser, J. R.; Zawaneh, P. N.; Putnam, D. *Biomacromolecules* **2011**, *12*, 977–986.
30. Hu, X.; Chen, X.; Xie, Z.; Liu, S.; Jing, X. *J. Polym. Sci., Part A: Polym. Chem.* **2007**, *45*, 5518–5528.
31. Hu, X.; Chen, X.; Liu, S.; Shi, Q.; Jing, X. *J. Polym. Sci., Part A: Polym. Chem.* **2008**, *46*, 1852–1861.
32. a. Fox, T. G. *Bull. Am. Phys. Soc.* **1956**, *1*, 123.;b. Fox, T. G.; Flory, P. J. *J. Polym. Sci.* **1954**, *14*, 315–319.
33. Lu, C.; Shi, Q.; Chen, X.; Lu, T.; Xie, Z.; Hu, X.; Ma, J.; Jing, X. *J. Polym. Sci., Part A: Polym. Chem.* **2007**, *45*, 3204-3217.
34. Tsuji, H. Ikada, Y. *Macromol. Chem. Phys.* **1996**, *197*, 3483-3499.

35. Ahmed, J.; Zhang, J.-X.; Song Z.; Varshney, S. K. *J. Therm. Anal. Cal.* **2009**, *95*, 957–964.
36. Sarasua, J. R.; Prud'homme, R. E.; Wisniewski, M.; Le Borgne, A.; Spassky, N. *Macromolecules* **1998**, *31*, 3895-3905.
37. Kumar, R.; Gao, W.; Gross, R. A. *Macromolecules* **2002**, *35*, 6835-6844.
38. Hu, X.; Chen, X.; Xie, Z.; Cheng, H.; Jing, X. *J. Polym. Sci., Part A: Polym. Chem.* **2008**, *46*, 7022–7032.
39. Hu, X.; Chen, X.; Cheng, H.; Jing, X. *J. Polym. Sci., Part A: Polym. Chem.* **2009**, *47*, 161–169.
40. Mullen, B. D.; Tang, C. N.; Storey, R. F. *J. Polym. Sci., Part A: Polym. Chem.* **2003**, *41*, 1978–1991.
41. Tsuji, H.; Hyon, S. H.; Ikada, Y. *Macromolecules* **1991**, *24*, 5651-5656.
42. Tsuji, H.; Hyon, S. H.; Ikada, Y. *Macromolecules* **1991**, *24*, 5657-5662.

Chapter 6

Conclusions

Concluding remarks on the organocatalytic synthesis and post-polymerisation functionalisations of allyl- and propargyl functional poly(carbonate)s and the stereocomplexation of poly(ester-carbonate)s with pendant allyl- and propargyl- groups as discussed in Chapters 2, 3, 4 and 5.

6.1. Conclusions

In conclusion, the synthesis of a range of new, functional aliphatic poly(carbonate)s has been reported through controlled organocatalytic ring opening polymerisations of cyclic carbonates and subsequent post-polymerisation functionalisations of the resulting polymers. The improved ring-opening polymerisation of 5-methyl-5-allyloxycarbonyl-1,3-dioxan-2-one, MAC, was initially studied using a range of organic catalysts. In particular the application of the dual catalyst system of 1-(3,5-bis(trifluoromethyl)phenyl)-3-cyclohexylthiourea (**3**) and (-)-sparteine, led to the controlled synthesis of allyl-functional poly(carbonate) (PMAC). The versatility of the system was demonstrated by the preparation of a range of telechelic- and block copolymers. Successful, facile and quantitative post-polymerisation of PMAC was achieved *via* radical addition of thiol-containing molecules to the pendant allyl ester groups leading to new, functional poly(carbonate)s with a range of different physical properties without notable polymer degradation.

The application of a poly(carbonate) scaffolds as precursors in the preparation of functional aliphatic poly(carbonate)s was extended by the synthesis of propargyl-functional poly(carbonate)s (PMPC) *via* the organocatalytic ring-opening polymerisation of 5-methyl-5-propargyloxycarbonyl-1,3-dioxan-2-one, MPC. Although the system of **3** and (-)-sparteine did not show the same excellent control in the synthesis of PMPC homopolymers as it did for PMAC

homopolymers, the dual organic catalyst system of **1** and 1,8-diazabicyclo[5.4.0]undec-7-ene (DBU) did lead to the observation of a linear evolution of molecular weight with both monomer conversion and monomer-to-initiator ratio and low polydispersities. The versatility of the **3**/DBU system for ROP of MPC was further demonstrated by the synthesis of telechelic polymers and block copolymers of PMPC with poly(ethylene oxide), poly(*L*-lactide) and PMAC. Full functionalisation of the propargyl ester functional poly(carbonate)s could be successfully achieved *via* the copper-catalysed Huisgen 1,3-dipolar cycloaddition and led to the isolation of new aliphatic poly(carbonate)s with a range of pendant functionalities, without notable polymer degradation. This method, however, showed a limitation when homopolymer functionalisation was attempted with an azide with a bulky substituent leading to *ca.* 85% conversion of the propargyl groups. The radical addition of thiols to the pendant propargyl groups in PMPC homopolymers was further investigated as an alternative method to functionalise these polymers post-polymerisation. However, even when using ten equivalent of thiol, cross-linked polymer was obtained. Nonetheless, these methodologies provide attractive routes to the synthesis of biodegradable and biocompatible functional polymers. In addition, the limitations observed due to cross-linking or bulkiness of the azide-containing molecule could possibly be overcome when the functional groups are distributed along the poly(carbonate) *via* copolymerisation with other cyclic monomers.

The random copolymerisation of MAC and MPC was thus investigated in the preparation of poly(carbonate)s with two functionalities. Investigation of the reactivity ratios revealed a higher reactivity for the allyl functional carbonate, however, resulting copolymers were random in nature. These propargyl- and allyl- functional poly(carbonate)s could be orthogonally functionalised *via* Huisgen 1,3-dipolar cycloaddition followed by facile free radical addition of a thiol, leading to the isolation of a new amphiphilic aliphatic poly(carbonate). Successful functionalisation was confirmed by extensive MALDI-ToF analysis of the polymer.

Both MAC and MPC were further applied in the synthesis of novel poly(ester-carbonate) stereocomplexes. This was realised by the preparation of poly(ester-carbonate)s *via* copolymerisation of stereopure lactide with MAC or MPC. Further functionalisation of a copolymer with pendant allyl groups *via* facile radical addition of 1-dodecanethiol and a copolymer with propargyl functionalities *via* the copper catalysed 1,3-dipolar cycloaddition of 1-azidooctane resulted in newly functional poly(ester-carbonate)s that showed no sign of degradation with a retention of the molecular weight distribution at a slightly reduced retention time. Successful stereocomplexation was observed in copolymer/PDLA and copolymer/copolymer blends by differential scanning calorimetry (DSC) of samples prepared by solution casting. In addition, post-polymerisation

functionalisation of the polymers did not disrupt the stereocomplex formation.

In short, the work presented in this thesis provides facile and versatile methodologies for the synthesis of functional aliphatic poly(carbonate)s, a straightforward method for the introduction of functionalities in poly(lactide) stereocomplexes and could be used as a platform in the preparation of functional biodegradable materials for specific applications.

Chapter 7

Experimental

Experimental procedures from Chapter 2 (Organocatalytic Synthesis and post-Polymerisation Functionalisation of Allyl-Functional Poly(carbonate)s), Chapter 3 (Organocatalytic Synthesis and post-Polymerisation Functionalisation of Propargyl-Functional Poly(Carbonate)s), Chapter 4 (Synthesis and Orthogonal post-Polymerisation Functionalisation of Allyl and Propargyl Functional Poly(Carbonate)s) and Chapter 5 (Synthesis, Stereocomplexation and post-Polymerisation Functionalisation of Functional Poly(Ester-Carbonate)s).

7.1. Materials

rac-, *L*- and *D*-Lactide were purified from dry methylene chloride and sublimed twice before use and stored under inert atmosphere. Poly(ethylene oxide) methyl ethers were purchased from Sigma-Aldrich, dried in a desiccator over P₂O₅ and stored under inert atmosphere. CDCl₃, 1,8-diazabicyclo[5.4.0]undec-7-ene (DBU), (-)-sparteine and $\alpha,\alpha,\alpha',\alpha'$ -tetrakis(trifluoromethyl)-1,3-benzenedimethanol were dried over CaH₂, distilled, degassed, and stored under inert atmosphere. Benzyl alcohol and 1,3-propanediol were dried and stored over 4 Å molecular sieves under inert atmosphere. 2-Hydroxyethyl disulfide was purchased from Aldrich and dried and purified by distillation from CaH₂. Methylene chloride was purified over an Innovative Technology SPS alumina solvent column and degassed before use. Silica gel (pore size = 40 Å) was obtained from Fisher Scientific and used as received. Thiourea catalysts **3** and **4** were synthesised as previously reported¹ and then dried over calcium hydride in dry tetrahydrofuran and recrystallised from dry methylene chloride. Alcohols **8** and **9** were received from M. J. Stanford and S. Onbulak, dried over calcium hydride in dry tetrahydrofuran and stored under inert atmosphere. Azides were synthesised (in collaboration with D. J. Hall, V. Truong and C. R. Becer) as previously reported.^{2,3,4} All other solvents and chemicals were obtained from Sigma-Aldrich or Fisher Scientific and used as received.

7.2. General considerations.

Polymerisations were performed under inert atmosphere in a glovebox. Polymer functionalisations were carried out under oxygen-free conditions using standard Schlenk-line techniques. ^1H NMR and ^{13}C NMR spectra were recorded on a Bruker DPX-300, DPX-400, DRX-500, AV II-600 or AV II-700 spectrometer at 293 K unless stated otherwise. Chemical shifts are reported as δ in parts per million (ppm) and referenced to the residual solvent signal (CDCl_3 : ^1H , $\delta = 7.26$ ppm; ^{13}C , $\delta = 77.16$ ppm; $(\text{CD}_3)_2\text{SO}$: ^1H , $\delta = 2.50$; ^{13}C , $\delta = 39.52$). Mass spectra were acquired by MALDI-ToF (matrix-assisted laser desorption ionisation-time of flight) mass spectrometry using a Bruker Daltonics Ultraflex II MALDI-ToF mass spectrometer, equipped with a nitrogen laser delivering 2 ns laser pulses at 337 nm with positive ion ToF detection performed using an accelerating voltage of 25 kV. Solutions of trans-2-[3-(4-tertbutylphenyl)-2-methyl-2-propylidene]malonitrile (DCTB) as a matrix (0.3 μL of a 10 g L^{-1} solution in methylene chloride or tetrahydrofuran), sodium trifluoroacetate as a cationisation agent (0.3 μL of a 10 g L^{-1} solution in methylene chloride or tetrahydrofuran), and analyte (0.3 μL of a 1 g L^{-1} solution in methylene chloride or tetrahydrofuran) were applied sequentially to the target followed by solvent evaporation to prepare a thin matrix/analyte film. The samples were measured in linear and reflectron ion mode and calibrated by comparison to 2×10^3 and 5×10^3 g mol^{-1} poly(ethylene oxide) monomethyl ether standards. Gel-permeation

chromatography (GPC) was used to determine the molecular weights and polydispersities of the synthesized polymers. GPC in THF was conducted on a system composed of a Varian 390-LC-Multi detector suite fitted with differential refractive index (DRI), light scattering (LS), and ultraviolet (UV) detectors equipped with a guard column (Varian Polymer Laboratories PLGel 5 μM , 50 \times 7.5 mm) and two mixed D columns (Varian Polymer Laboratories PLGel 5 μM , 300 \times 7.5 mm). The mobile phase was either tetrahydrofuran eluent or tetrahydrofuran with 5% triethylamine eluent at a flow rate of 1.0 mL min⁻¹, and samples were calibrated against Varian Polymer Laboratories Easi-Vials linear poly(styrene) standards (162-3.7 \times 10⁵ g mol⁻¹) using Cirrus v3.3. GPC in DMF was conducted on a system composed of a Varian 390-LC-Multi detector suite fitted with differential refractive index (DRI) and ultraviolet (UV) detectors equipped with a guard column (Varian Polymer Laboratories PLGel 5 μM , 50 \times 7.5 mm) and two mixed D columns (Varian Polymer Laboratories PLGel 5 μM , 300 \times 7.5 mm). The mobile phase was DMF with 5% LiBr eluent at a flow rate of 1.0 mL min⁻¹, and samples were calibrated against Varian Polymer Laboratories Easi-Vials linear poly(methyl methacrylate) standards (690-1.9 \times 10⁶ g mol⁻¹) using Cirrus v3.3. Differential scanning calorimetry (DSC) analyses for Chapter 2 were performed in a T zero aluminium pan under a flow of nitrogen using a Q2000 DSC from TA Instruments in a custom mode (stabilisation at -90 °C, heating ramp of 10 °C min⁻¹ from -90 to 80 °C, cooling ramp of 10 °C min⁻¹ from 80 C to -90 °C,

stabilisation at -90 °C, second heating ramp of 10 °C min⁻¹ from -90 to 80 °C). Data were reported from the second scan (Chapter 2). DSC analyses for Chapter 5 were performed in a T zero aluminium pan under a flow of nitrogen using a DSC1-STAR from Mettler Toledo in custom mode (as described in Chapter 5). Thermogravimetric analysis (TGA) was performed under a nitrogen flow using a Q5000 TGA from TA Instruments with a conventional ramp of 20 °C/min from ambient to 700 °C.

7.3. Experimental details for Chapter 2.

7.3.1. Synthesis of 5-methyl-5-allyloxycarbonyl-1,3-dioxan-2-one, MAC.

2,2-bis(hydroxymethyl)propionic acid (5.00g, 37.3 mmol) and potassium hydroxide (2.40 g, 42.9 mmol) were dissolved in dimethylformamide (25 mL). The mixture was stirred at 100 °C for 1h. Allyl bromide (3.07 mL, 35.4 mmol) was added at 45 °C and the mixture was stirred at that temperature for 48 h before dimethylformamide was concentrated and the residue was dissolved in methylene chloride (100 mL) and washed with water (2x 25 mL). The organic phase was dried over MgSO₄ and volatiles were removed *in vacuo* yielding a pale yellow oil (1.98 g, 32% yield). Allyl-2,2-bis-(hydroxymethylpropionate (3.40 g, 19.5 mmol), ethyl chloroformate (5.60 mL, 58.8 mmol) were added to ice cold tetrahydrofuran (60 mL) and the mixture was stirred for 30 minutes, before triethylamine (8.20 mL, 58.8 mmol) was added drop-wise over 30 minutes at 0 °C. The mixture was stirred for another 2 hours after addition of triethylamine, after which the NEt₃·HCl salts were filtered off and volatiles were removed giving a yellow oil. The product was recrystallised from methylene chloride and toluene to give fine white crystals (2.74 g, 70% yield). Data was in accordance to that previously reported.⁵ The product was dried over CaH₂ in dry THF at 50-60 °C before further use.

¹H NMR (400 MHz, CDCl₃): δ 6.01-5.75 (m, 1H, CH₂CH=CH₂), 5.44-5.22 (m, 2H, CH₂CH=CH₂), 4.71-4.66 (m, 4H, CH₂CH=CH₂ and OCC₂H₅CH₃), 4.46 (part of dd, 2H, OCC₂H₅CH₃, ²J_{HH} = 200 Hz, ³J_{HH} = 10.8 Hz), 1.35 (s, 3H, CH₃). ¹³C

NMR (101 MHz, CDCl₃): δ 170.2 (C=O), 146.8 (C=O), 130.3 (CH=CH₂), 118.8 (CH=CH₂), 72.3 (OCH₂C(CH₃)), 66.0 (OCH₂CH=CH₂), 39.6 (CCH₃), 16.9 (CH₃).

7.3.2. Organocatalytic ROP of 5-methyl-5-allyloxycarbonyl-1,3-dioxan-2-one (MAC).

In a typical experiment, alcohol initiator, (-)-sparteine (5 mol% to monomer), and 1-(3,5-bis(trifluoromethyl) phenyl)-3-cyclohexylthiourea (10 mol% to monomer) catalyst were weighed and dissolved in dry CDCl₃ or dry methylene chloride. MAC was dissolved separately in the same solvent and added to the initiator/catalyst solution. After the desired time, the polymerisations were precipitated directly into hexanes. 1-(3,5-Bis(trifluoromethyl)phenyl)-3-cyclohexylthiourea and (-)-sparteine impurities were removed by column chromatography on silica gel in hexanes/ethyl acetate (4:1). The polymer-containing fractions were concentrated then dissolved in a minimal amount of methylene chloride and precipitated into hexanes.

¹H NMR (700 MHz, CDCl₃) δ 7.37 (m, OBn-ArH), 5.87 (m, CH_{vinyl}), 5.37-5.20 (m, CH_{2-vinyl}), 5.15 (s, OBn-CH₂), 4.63 (m, OCH₂CHCH₂), 4.45-4.24 (m, OC(O)OCH₂), 3.76-3.69 (m, CH₂OH), 2.46 (t, OH), 1.27 (s, CH₃), 1.22 (s, C(CH₃)CH₂OH). ¹³C NMR (126 MHz, CDCl₃): δ 171.7 (C(O)O), 154.4

(OC(O)O), 135.0 (ArC), 131.6 (CH_{vinyl}), 128.6 (ArC), 118.5 (CH_{2-vinyl}), 68.6 (OC(O)OCH₂), 68.4 (CH₂OH), 65.9 (OCH₂CHCH₂), 46.5 (CCH₃), 17.5 (CH₃).
GPC (THF, RI): M_n (PDI) = 3440 g mol⁻¹ (1.15). GPC (DMF, RI): M_n (PDI) = 3680 g mol⁻¹ (1.10).

7.3.3. Synthesis of PMAC block copolymers.

7.3.3.1. Synthesis of PEO-PMAC block copolymer.

PEO-*b*-PMAC block copolymer was synthesised using the method from 3.2 with commercially available poly(ethylene oxide) monomethyl ether as initiator ($[M]/[I] = 20$).

MeO-PEO₁₁₄-*b*-PMAC₂₀-OH. ¹H NMR (300 MHz, CDCl₃): δ 5.89 (CH_{vinyl}), 5.35-5.19 (CH_{2-vinyl}), 4.63 (OCH₂CHCH₂), 4.45-4.23 (OC(O)OCH₂), 3.64 (OCH₂CH₂), 3.37 (OCH₃), 2.49 (t, OH), 1.27 (s, CH₃), 1.22 (s, C(CH₃)CH₂OH).
GPC (THF, RI): M_n (PDI) = 11 900 g mol⁻¹ (1.06).

7.3.3.2. Synthesis of PLA-PMAC block copolymers.

For the synthesis of PLA-*b*-PMAC block copolymers, benzyl alcohol,(-)-sparteine, and thiourea were weighed and dissolved in dry CDCl₃. *rac*-Lactide (or MAC) was dissolved separately in CDCl₃ and added to the initiator/catalyst solution. After 2 h (>90% conversion), a small aliquot was taken from the mixture and used for GPC analysis, and the reaction mixture

was poured into a vial containing MAC (or *rac*-lactide). The polymerisation was carried out until >90% conversion was reached. The mixture was then precipitated in hexanes, purified by column chromatography on silica gel in hexanes/ ethyl acetate (4:1). The polymer containing fractions were concentrated and then dissolved in a minimal amount of methylene chloride and precipitated into hexanes.

BnO-PMAC₁₆-*b*-PLA₂₃-OH. ¹H NMR (400 MHz, CDCl₃) δ 7.37 (OBn-ArH), 5.89 (CH_{vinyl}), 5.42-5.11 (CH₂-vinyl, PLA-CH and OBn-CH₂), 4.63 (OCH₂CHCH₂), 4.41-4.25 (OC(O)OCH₂ and CHOH), 1.57 (PLA-CH₃), 1.27 (s, PMAC-CH₃). GPC (THF, RI): M_n (PDI) = 6620 g mol⁻¹ (1.28).

BnO-PLA₂₀-*b*-PMAC₂₀-OH. ¹H NMR (400 MHz, CDCl₃) δ 7.31 (OBn-ArH), 5.83 (CH_{vinyl}), 5.35-5.07 (CH₂-vinyl, PLA-CH and OBn-CH₂), 4.59 (OCH₂CHCH₂), 4.41-4.23 (OC(O)OCH₂), 3.68 (CH₂OH), 1.53 (PLA-CH₃), 1.23 (PMAC-CH₃), 1.19 (C(CH₃)CH₂OH). GPC (THF, RI): M_n (PDI) = 7130 g mol⁻¹ (1.17).

7.3.4. Post-polymerisation functionalisation of PMAC.

Stock solutions of polymer and AIBN (20%) in dioxane (50 mg polymer mL⁻¹) and stock solutions of thiol in dioxane were prepared and degassed prior to the reactions. In a typical experiment, an ampoule was charged with 0.78 mL of polymer/AIBN stock solution (*i.e.*, 38.8 mg polymer), after which the

dioxane was removed *in vacuo*. Under a nitrogen atmosphere, 0.15 mL of the degassed benzyl mercaptan stock solution (3.68 M) was added, and the ampoule was placed in an oil bath at 90 °C and stirred for 24 h. The mixture was then concentrated *in vacuo*; the residue was dissolved in a minimal amount of methylene chloride and precipitated into petroleum ether.

11a: ^1H NMR (500 MHz, CDCl_3): δ 7.37 (m, OBn-ArH), 5.15 (s, OBn-CH₂), 4.44-4.25 (m, OC(O)OCH₂), 4.23 (m, OCH₂CH₂CH₂S), 3.70 (m, CH₂OH), 2.55 (m, OCH₂CH₂CH₂S), 2.50 (m, SCH₂(CH₂)₁₀CH₃), 1.91 (m, OCH₂CH₂CH₂S), 1.58 (m, SCH₂CH₂(CH₂)₉CH₃), 1.37 (m, S(CH₂)₂CH₂(CH₂)₈CH₃), 1.26 (m, CCH₃ and (CH₂)₈CH₃), 0.88 (s, (CH₂)₈CH₃). ^{13}C NMR (125 MHz, CDCl_3): δ 171.9 (C(O)O), 154.4 (O(O)O), 68.7 (OC(O)OCH₂), 64.1 (OCH₂CH₂CH₂S), 46.6 (CCH₃), 32.2 (SCH₂(CH₂)₁₀CH₃), 31.9 (CH₂CH₂CH₃), 29.7 (CH₂SCH₂CH₂(CH₂)₉CH₃), 29.3, 29.0, 28.7, 28.5, and 28.3 (CH₂)₇CH₂CH₂CH₃, 22.7 (CH₂CH₂CH₃), 17.4 (CH₃), 14.1 (S(CH₂)₁₁CH₃). GPC (THF, RI): M_n (PDI) = 25 000 g mol⁻¹ (1.22).

11b: ^1H NMR (500 MHz, CDCl_3): δ 7.40-7.22 (m, backbone ArH and OBn-ArH), 5.14 (s, OBn-CH₂), 4.39-4.13 (m, OC(O)OCH₂) and OCH₂CH₂CH₂S), 3.70 (s, CH₂(C₅H₆), 2.44 (m, OCH₂CH₂CH₂S), 1.85 (m, OCH₂CH₂CH₂S), 1.19 (s, CCH₃). ^{13}C NMR (125 MHz, CDCl_3): δ 172.1 (C(O)O), 154.4 (O(O)O), 138.4 (CH₂C_{Ar}), 129.0 (*o*-ArC), 128.6 (*m*-ArC), 127.2 (*p*-ArC), 68.8 (OC(O)OCH₂), 64.2 (OCH₂CH₂CH₂S), 46.7 (CCH₃), 36.7 (SCH₂(C₆H₅), 28.2 (OCH₂CH₂CH₂S),

27.6 (OCH₂CH₂CH₂S), 17.6 (CH₃). GPC (THF, RI): M_n (PDI) = 20 710 g mol⁻¹ (1.19).

11c: ¹H NMR (500 MHz, (CD₃)₂SO) δ 7.38 (m, OBn-ArH), 5.14 (s, OBn-CH₂), 4.72 (m, CH(OH)CH₂OH), 4.53 (m, CH(OH)CH₂OH), 4.34-4.08 (m, OC(O)OCH₂ and OCH₂CH₂CH₂S), 3.57 (m, CH(OH)CH₂OH), 3.34 (m, CH(OH)CH₂OH), 2.63-2.39 (m, OCH₂CH₂CH₂SCH₂), 1.81 (m, OCH₂CH₂CH₂S), 1.18 (m, CCH₃). ¹³C NMR (125 MHz, (CD₃)₂SO): δ 171.7 (C(O)O), 154.0 (C(O)O), 71.5 (CHOH), 68.8 (OC(O)OCH₂), 64.9 (CH₂OH), 64.5 (OCH₂CH₂CH₂S), 46.2 (CCH₃), 35.1 (SCH₂CHOH), 28.2 (OCH₂CH₂CH₂S), 16.8 (CH₃). GPC (DMF, RI): M_n (PDI) = 29 340 g mol⁻¹ (1.34).

11d: ¹H NMR (500 MHz, (CD₃)₂SO): δ 7.38 (m, OBn-ArH), 5.14 (s, OBn-CH₂), 4.73 (m, OH), 4.31-4.17 (m, OC(O)OCH₂), 4.13 (m, OCH₂CH₂CH₂S), 3.52 (m, CH₂OH), 2.54 (m, OCH₂CH₂CH₂SCH₂), 1.81 (m, OCH₂CH₂CH₂S), 1.18 (m, CCH₃). ¹³C NMR (125 MHz, (CD₃)₂SO): δ 171.7 (C(O)O), 153.8 (C(O)O), 68.8 (OC(O)OCH₂), 63.4 (OCH₂CH₂CH₂S), 60.8 (CH₂OH), 46.2 (CCH₃), 33.7 (SCH₂CHOH), 28.2 (OCH₂CH₂CH₂S), 27.6 (OCH₂CH₂CH₂S), 16.8 (CH₃). GPC (DMF, RI): M_n (PDI) = 26 050 g mol⁻¹ (1.27).

11e: ¹H NMR (500 MHz, (CD₃)₂SO): δ 12.62 (br s, COOH), 7.38 (m, OBn-ArH), 5.13 (s, OBn-CH₂), 4.31-4.17 (m, OC(O)OCH₂), 4.13 (m, OCH₂CH₂CH₂S), 3.21 (s, SCH₂CO₂H), 2.61 (m, OCH₂CH₂CH₂S), 1.84 (m, OCH₂CH₂CH₂S), 1.17 (m, CCH₃). ¹³C NMR (125 MHz, (CD₃)₂SO): δ 171.6 (C(O)O), 171.5 (COOH), 153.8 (C(O)O), 68.8 (OC(O)OCH₂), 63.4

(OCH₂CH₂CH₂S), 46.3 (CCH₃), 33.0 (SCH₂COOH), 28.0 (OCH₂CH₂CH₂S), 27.5
(OCH₂CH₂CH₂S), 16.7 (CH₃).

7.4. Experimental details for Chapter 3.

7.4.1. Synthesis of 5-methyl-5-propargyloxycarbonyl-1,3-dioxan-2-one, MPC.

2,2-bis(hydroxymethyl)propionic acid (45.00g, 0.34 mol) and potassium hydroxide (22.5 g, 0.40 mmol) were dissolved in acetone (300 mL). The mixture was refluxed for 1 h. Propargyl bromide solution in toluene (80 wt%, 49.9 mL) was added and the mixture was refluxed for 48 h before solids were filtered off, the mixture was concentrated and the product was distilled under reduced pressure yielding a clear oil (9.40 g, 17.6% yield). Propargyl-2,2-bis(hydroxymethylpropionate (9.40 g, 54.6 mmol), ethyl chloroformate (11.3 mL, 119 mmol) were added to ice cold tetrahydrofuran (150 mL) and the mixture was stirred for 30 minutes, before triethylamine (30 mL, 215 mmol) was added drop-wise over 30 minutes at 0 °C. The mixture was stirred for overnight after addition of triethylamine, after which the NEt_3HCl salts were filtered off and volatiles were removed giving a yellow oil. The product was recrystallised from toluene to give fine white crystals (6.44 g, 59.6% yield).

Data was in accordance to that previously reported.⁶

^1H NMR (400 MHz, CDCl_3): δ 4.79 (d, 2H, $\text{CH}_2\text{C}\equiv\text{CH}$, $^5J_{\text{HH}} = 2.4$ Hz), 4.47 (dd, 4H, $\text{OCCCH}_2\text{CH}_3$, $^2J_{\text{HH}} = 200.4$ Hz, $^3J_{\text{HH}} = 10.8$ Hz), 2.53 (t, 1H, $\text{CH}_2\text{C}\equiv\text{CH}$, $^5J_{\text{HH}} = 2.4$ Hz), 1.37 (s, 3H, CH_3). ^{13}C NMR (101 MHz, CDCl_3): δ 170.5 ($\text{C}=\text{O}$), 147.4 ($\text{C}=\text{O}$), 76.5 ($\text{C}\equiv\text{CH}$), 76.1 ($\text{C}\equiv\text{CH}$), 72.9 ($\text{OCH}_2\text{C}(\text{CH}_3)$), 53.6 ($\text{OCH}_2\text{C}\equiv\text{CH}$), 40.4 (CCH_3), 17.6 (CH_3).

7.4.2. Organocatalytic ROP of 5-methyl-5-propargyloxycarbonyl-1,3-dioxan-2-one (MPC).

In a typical experiment, alcohol initiator, (-)-sparteine (5 mol% to monomer) or DBU (1 mol% to monomer), and 1-(3,5-bis(trifluoromethyl) phenyl)-3-cyclohexylthiourea (10 or 5 mol% to monomer) catalyst were weighed and dissolved in dry CDCl_3 or dry methylene chloride. MPC was dissolved separately in the same solvent and added to the initiator/catalyst solution. After the desired time, the polymerisations were then quenched with Amberlyst® 16 (acidic) ion exchange resin and precipitated into hexanes. Polymers with degrees of polymerisation of 40 or higher were purified by repeated precipitation in hexanes, whereas 1-(3,5-bis(trifluoromethyl)phenyl)-3-cyclohexylthiourea and (-)-sparteine (or DBU) impurities were removed by column chromatography on silica gel in hexanes/ethyl acetate (4:1) when polymers had a DP < 40. The polymer containing fractions were directly precipitated into hexanes.

^1H NMR (600 MHz, CDCl_3 , 298K): δ 7.37 (m, OBn-ArH), 5.15 (s, OBn-CH), 4.73 (m, OCH₂C≡CH) 4.44-4.24 (m, OC(O)OCH₂), 3.73 (m, OC(O)OCH₂), 2.53 (s, CH₂C≡CH), 2.40 (br s, OH), 1.29 (s, CH₃), 1.24 (s, 3H, C(CH₃)CH₂OH). ^{13}C NMR (151 MHz, CDCl_3): δ 171.5 (C(O)O), 154.4 (O(O)O), 135.1, 128.8, 128.6 (ArC), 75.7 (CH₂C≡CH), 70.1 (CH₂C≡CH), 68.6 (OC(O)OCH₂), 64.7 (C(O)OCH₂), 53.0 (CH₂C≡CH), 46.7 (CCH₃), 17.5 (CH₃). GPC (THF, RI): M_n (PDI) = 9 346 g mol⁻¹ (1.11). GPC (DMF, RI): M_n (PDI) = 15 701 g mol⁻¹ (1.13).

7.4.3. Synthesis of PMPC block copolymers.

7.4.3.1. Synthesis of PEO-PMPC block copolymers.

PEO-*b*-PMPC block copolymers were synthesised using the method described in 7.3.2 with commercially available poly(ethylene oxide) monomethyl ethers as initiator ($[M]/[I] = 20$).

MeO-PEO₁₁₄-*b*-PMPC₁₈-OH. ¹H NMR (400 MHz, CDCl₃): δ 4.73 (OCH₂C≡CH), 4.39-4.27 (OC(O)OCH₂), 3.63 (OCH₂CH₂), 3.37 (OCH₃), 2.53 (m, C≡CH), 1.28 (s, CH₃). GPC (THF, RI): M_n (PDI) = 11 020 g mol⁻¹ (1.06).

MeO-PEO₂₁₆-*b*-PMPC₁₂-OH. ¹H NMR (400 MHz, CDCl₃): δ 4.73 (OCH₂C≡CH), 4.40-4.25 (OC(O)OCH₂), 3.63 (OCH₂CH₂), 3.36 (OCH₃), 2.50 (m, C≡CH), 1.28 (s, CH₃). GPC (THF, RI): M_n (PDI) = 17 870 g mol⁻¹ (1.06).

7.4.3.2. Synthesis of PLLA-PMPC block copolymers.

For the synthesis of PLLA-*b*-PMPC block copolymers, benzyl alcohol, (-)-sparteine, and 1-(3,5-bis(trifluoromethyl)phenyl)-3-cyclohexylthiourea were weighed and dissolved in dry CDCl₃. *L*-Lactide (or MPC) was dissolved separately in CDCl₃ and added to the initiator/catalyst solution. After 2 h (>90% conversion), a small aliquot was taken from the mixture and used for GPC analysis, and the reaction mixture was poured in a vial containing MPC (or *L*-lactide). The polymerisation was carried out until >90% conversion was reached. The mixture was then quenched with Amberlyst® 16 (acidic) ion exchange resin and precipitated in hexanes.

BnO-PLLA₁₈-*b*-PMAC₂₀-OH. ¹H NMR (400 MHz, CDCl₃): δ 7.35 (OBn-ArH), 5.21-5.11 (PLLA-CH and OBn-CH₂), 4.72 (OCH₂C≡CH), 4.45-4.24 (OC(O)OCH₂), 3.74 (OC(O)CH₂), 2.54 (C≡CH), 1.57 (PLLA-CH₃), 1.29 (PMPC-CH₃), 1.24 (C(CH₃)CH₂OH). GPC (THF, RI): *M_n* (PDI) = 8740 g mol⁻¹ (1.08).

BnO-PMPC₂₀-*b*-PLLA₂₄-OH. ¹H NMR (400 MHz, CDCl₃): δ 7.37 (OBn-ArH), 5.22-5.11 (PLLA-CH and OBn-CH₂), 4.73 (OCH₂C≡CH), 4.38-4.25 (OC(O)OCH₂ and CHOH), 3.74 (OC(O)CH₂), 2.54 (C≡CH), 1.58 (PLLA-CH₃), 1.29 (PMPC-CH₃). GPC (THF, RI): *M_n* (PDI) = 10350 g mol⁻¹ (1.09).

7.4.3.3. Synthesis of PMPC-PMAC block copolymer.

For the synthesis of PMPC-*b*-PMAC block copolymers, benzyl alcohol, 1,8-diazabicyclo[5.4.0]undec-7-ene, and 1-(3,5-bis(trifluoromethyl)phenyl)-3-cyclohexylthiourea were weighed and dissolved in dry CDCl₃. MPC was dissolved separately in CDCl₃ and added to the initiator/catalyst solution. After 1 h (>90% conversion), a small aliquot was taken from the mixture and used for GPC analysis, and the reaction mixture was poured in a vial containing MAC. The polymerisation was carried out until >90% conversion was reached after 1 h. The mixture was then quenched with Amberlyst® 16 (acidic) ion exchange resin and precipitated in hexanes.

BnO-PMPC₁₇-*b*-PMAC₁₉-OH. ¹H NMR (400 MHz, CDCl₃): δ 7.37 (OBn-ArH), 5.89 (CH_{vinyl}), 5.33-5.23 (CH₂-vinyl), 5.15 (OBn-CH₂), 4.73 (OCH₂C≡CH), 4.63

($\text{OCH}_2\text{CHCH}_2$), 4.45-4.27 (OC(O)OCH_2), 3.72 (OC(O)CH_2), 2.54 ($\text{C}\equiv\text{CH}$), 1.29 (PMPC-CH_3), 1.27 (PMAC-CH_3). GPC (THF, RI): M_n (PDI) = 8110 g mol⁻¹ (1.06).

7.4.4. Post-polymerisation functionalisation of PMPC.

7.4.4.1. Post-polymerisation functionalisation of PMPC *via* Huisgens 1,3-dipolar Cycloaddition.

Stock solutions of polymer in dioxane (50 mg polymer mL⁻¹) and stock solutions of diisopropylamine in THF or DMF were prepared and degassed prior to the reactions. In a typical experiment, an ampoule was charged with 1.00 mL of polymer stock solution (*i.e.*, 50.0 mg polymer, 3.5×10^{-3} mmol), after which the dioxane was removed *in vacuo*. Under a nitrogen atmosphere, CuI (19.1 mg, 0.10 mmol), azide (0.28 mmol) and degassed diisopropylamine stock solution (0.4 M) were added, and the ampoule stirred for 24 h. Amberlyst® 16 (acidic) ion exchange resin and THF or DMF were added and the mixture was stirred vigorously, then passed over a neutral alumina plug. The mixture was then stirred for 16 h with Cuprisorb™ beads to remove residual copper, filtered and concentrated *in vacuo*; the residue was dissolved in a minimal amount of methylene chloride and precipitated into hexanes.

14a: ¹H NMR (600 MHz, CDCl₃): δ 7.71 (br s, N_3CHC), 7.35 (m, OBn-ArH), 5.27 (s, C(O)OCH_2), 5.12 (s, OBn-CH_2), 4.37 (m, NCH_2), 4.30-4.22 (m,

OC(O)OCH₂), 1.91 (m, NCH₂CH₂(CH₂)₅CH₃), 1.36-1.17 (m, N(CH₂)₂(CH₂)₅CH₃ and CCH₃), 0.86 (m, (CH₂)₇CH₃). ¹³C NMR (151 MHz, CDCl₃): δ 172.1 (CC(O)O), 154.4 (OC(O)O), 142.0 (C=CHN₃), 131.7 (CH_{vinyl}), 68.7 (OC(O)OCH₂), 58.7 (OCH₂CCHN₃), 50.7 (N₃CH₂(CH₂)₆CH₃), 46.7 (CCH₃), 31.8, 30.4, 29.2, 29.1 and 26.6 ((CH₂)₅CH₂CH₃), 22.7 ((CH₂)₅CH₂CH₃), 17.5 (m, CH₃), 14.2 ((CH₂)₇CH₃). GPC (THF, RI): *M_n* (PDI) = 12 690 g mol⁻¹ (1.15).

14b: ¹H NMR (400 MHz, CDCl₃): δ 7.59 (s, N₃CHC), 7.39-7.21 (m, OBn-ArH and NCH₂C₆H₅), 5.51 (s, NCH₂C₆H₅), 5.20 (s, C(O)OCH₂), 5.10 (s, OBn-CH₂), 4.27-4.15 (m, OC(O)OCH₂), 1.17 (s, CCH₃). ¹³C NMR (126 MHz, CDCl₃): δ 172.1 (CC(O)O), 154.4 (OC(O)O), 134.7 (N₃CH₂C_{Ar}), 131.7 (CH_{vinyl}), 129.3 (N₃CH₂-*o*-CH_{Ar}), 128.9 (N₃CH₂-*p*-CH_{Ar}), 128.9 (C=CHN₃), 128.8, 128.6 (OCH₂C₆H₆), 128.2 (N₃CH₂-*m*-CH_{Ar}), 70.1 (OCH₂C₆H₆), 68.7 (OC(O)OCH₂), 58.8 (OCH₂CCHN₃), 54.4 (N₃CH₂C_{Ar}), 46.7 (CCH₃), 17.5 (m, CH₃). GPC (THF, RI): *M_n* (PDI) = 9 700 g mol⁻¹ (1.12).

12c: ¹H NMR (400 MHz, CDCl₃): δ 7.88 (br s, N₃CHC), 7.34 (m, OBn-ArH), 5.26 (m, NCH₂CH₂O), 5.11 (s, OBn-CH₂), 4.53 (m, C(O)OCH₂), 4.43-4.13 (m, OC(O)OCH₂), 3.87 (s), 3.79-3.51, 1.21 (s, CCH₃). ¹³C NMR (151 MHz, CDCl₃): δ 172.2 (CC(O)O), 154.4 (OC(O)O), 128.8, 128.6 (C_{Ar}), 73.0, 70.6, 70.4, 69.3, (CH₂-TEG and OCH₂CCHN₃), 68.7 (OC(O)OCH₂), 61.8 (COH-TEG), 46.7 (CCH₃), 17.6 (m, CH₃). GPC (THF, RI): *M_n* (PDI) = 2 480 g mol⁻¹ (1.28).

14d: ¹H NMR (700 MHz, (CD₃)₂SO): δ 8.51 (s, N₃CHC), 8.43 (m, N₃CC₆H₄Ar), 7.57 (m, CH_{Ar}CHCOH), 7.31 (m, OBn-ArH), 6.74 (m, CHCH_{Ar}COH), 6.62 (m,

CHCHC(OH)CH_{Ar}, 5.23 (s, C(O)OCH₂), 5.07 (s, OBn-CH₂), 4.38-3.99 (m, OC(O)OCH₂), 1.12 (s, CCH₃). ¹³C NMR (176 MHz, (CD₃)₂SO): δ 171.5 (C α (O)O), 171.0 (C α (O)O), 166.4 (N₃C α (O)O), 156.4 (COH), 155.3 (O α (O)O), 153.7 (N₃CC(O)OC), 136.6 (N₃CH_{Ar}), 130.7 (CH_{Ar}CHCOH), 129.6, 128.4, 128.2 (ArC-BnO), 125.4 (N₃CH_{triazole}C), 117.0 (N₃C-coumarin), 115.7 (CHCH_{Ar}COH), 108.5 (N₃CCHC), 102.3 (CHCHC(OH)CH_{Ar}), 77.7 (CH₂C \equiv CH), 68.6 (OC(O)OCH₂), 58.1 (C(O)OCH₂), 52.7 (CH₂C \equiv CH), 46.2 (CCH₃), 16.6 (CH₃). GPC (DMF, RI): *M_n* (PDI) = 18 620 g mol⁻¹ (1.23).

14e: ¹H NMR (400 MHz, (CD₃)₂SO): δ 8.26 (s, N₃CHC), 7.37 (m, OBn-ArH), 5.92 (m, N₃CHO), 5.28 (m, OC(N₃)HCH(OH)), 5.21 (m, C(O)OCH₂), 5.12-5.06 (m, OBn-CH₂ and OC(N₃)HCH(OH)CH(OH)), 5.03 (m, OCH(CH₂OH)CH(OH)), 4.61 (m, OCH(CH₂OH)), 4.40 (m, OC(N₃)HCH(OH)), 4.30-4.17 (m, OC(O)OCH₂), 3.84 (m, OC(N₃)HCH(OH)CH(OH)), 3.64-3.52 (m, OCH(CH₂OH)CH(OH)), 3.35 (m, OCH(CH₂OH)CH(OH)), 1.17 (s, CCH₃). ¹³C NMR (176 MHz, CD₃)₂SO): δ 173.0 (C α (O)O), 153.4 (O α (O)O), 142.4 (N₃C_{triazole}CH), 128.5 (ArC), 125.3, 124.5, 124.0 (N₃CH_{triazole}C), 85.7, 80.3, 80.1, 78.4, 74.9, 73.5, 72.3 (OC(O)OCH₂), 71.2, 68.1, 67.6, 66.6, 63.8 (CH₂-mannose), 60.7, 59.6, 58.6, 58.3, 57.7, 57.3, 57.0 (C(O)OCH₂), 48.1 (CCH₃), 16.8 (CH₃). GPC (DMF, RI): *M_n* (PDI) = 13 200 g mol⁻¹ (1.30).

7.4.4.2. Post-polymerisation functionalisation of PMPC *via* radical addition of a thiol.

Stock solutions of polymer and AIBN (20%) in dioxane (50 mg polymer mL⁻¹) and stock solutions of thiol in dioxane were prepared and degassed prior to the reactions. In a typical experiment, an ampoule was charged with 1.00 mL of polymer/AIBN stock solution (*i.e.*, 50.0 mg polymer), after which the dioxane was removed *in vacuo*. Under a nitrogen atmosphere, degassed benzyl mercaptan stock solution was added, and the ampoule was placed in an oil bath at 90 °C and stirred for 24 h. The mixture was then concentrated *in vacuo*; the residue was dissolved in a minimal amount of methylene chloride and precipitated into petroleum ether.

13b: ¹H NMR (600 MHz, CDCl₃): δ 7.36 (m, OBn-ArH), 5.15 (s, OBn-CH₂), 4.46-4.22 (m, OC(O)OCH₂ and OCH₂CH₂CH₂S), 3.70 (m, CH₂OH), 3.00 (m, OCH₂CHCH₂S), 2.76 (m, OCH₂CH₂CH₂S), 2.61-2.50 (m, SCH₂(CH₂)₁₀CH₃), 1.58 (m, SCH₂CH₂(CH₂)₉CH₃), 1.37 (m, S(CH₂)₂CH₂(CH₂)₈CH₃), 1.32-1.19 (m, CCH₃ and (CH₂)₈CH₃), 0.88 (m, (CH₂)₈CH₃). ¹³C NMR (151 MHz, CDCl₃): δ 171.8 (CC(O)O), 154.5 (OC(O)O), 128.7, 128.5 (ArC), 68.9 (OC(O)OCH₂), 65.9 (OCH₂CHCH₂S), 46.8 (CCH₃), 44.6 (OCH₂CHCH₂S), 34.9 (OCH₂CHCH₂S), 33.4 (CHSCH₂(CH₂)₁₀CH₃), 32.1 (CH₂SCH₂(CH₂)₁₀CH₃), 31.7 (CH₂CH₂CH₃), 30.0, 29.9, 29.8, 29.7, 29.5, 29.1, 29.0 (CH₂)₈CH₂CH₂CH₃), 22.8 (CH₂CH₂CH₃), 17.6 (CCH₃), 14.3 (S(CH₂)₁₁CH₃). GPC (THF, RI): *M*_n (PDI) = 18 140 g mol⁻¹ (1.17).

13c: ^1H NMR (600 MHz, CDCl_3): δ 7.41-7.19 (m, backbone ArH and OBn-ArH), 5.14 (s, OBn-CH_2), 4.41-4.18 (m, OC(O)OCH_2) and $\text{OCH}_2\text{CHCH}_2\text{S}$), 3.72 (s, $\text{CH}_2\text{SCH}_2(\text{C}_5\text{H}_6)$), 3.65 ($\text{CHSCH}_2(\text{C}_5\text{H}_6)$), 2.84 (m, $\text{OCH}_2\text{CHCH}_2\text{S}$), 2.64 (m, $\text{OCH}_2\text{CHCH}_2\text{S}$), 1.20 (s, CCH_3). ^{13}C NMR (151 MHz, CDCl_3): δ 171.8 ($\text{C}(\text{O})\text{O}$), 154.5 ($\text{O}(\text{O})\text{O}$), 138.1, 137.9 ($\text{CH}_2\text{C}_{\text{Ar}}$), 129.1, 129.0 ($o\text{-ArC}$), 128.8, 128.7 ($m\text{-ArC}$), 127.4, 127.3 ($p\text{-ArC}$), 68.8 (OC(O)OCH_2), 65.5 ($\text{OCH}_2\text{CHCH}_2\text{S}$), 46.7 (CCH_3), 43.3 ($\text{OCH}_2\text{CHCH}_2\text{S}$), 37.0 ($\text{CH}_2\text{SCH}_2(\text{C}_6\text{H}_5)$), 35.8 ($\text{OCH}_2\text{CHCH}_2\text{S}$), 33.6 ($\text{CHSCH}_2(\text{C}_6\text{H}_5)$), 17.5 (CH_3). GPC (THF, RI): M_n (PDI) = 14 020 g mol^{-1} (1.21).

13d: ^1H NMR (600 MHz, $(\text{CD}_3)_2\text{SO}$) δ 7.38 (m, OBn-ArH), 5.14 (s, OBn-CH_2), 4.80 (m, $\text{CH(OH)CH}_2\text{OH}$), 4.33 (m, $\text{OCH}_2\text{CH}_2\text{CH}_2\text{S}$), 4.29-4.14 (m, OC(O)OCH_2 and $\text{OCH}_2\text{CH}_2\text{CH}_2\text{S}$), 3.53 (m, $\text{CH(OH)CH}_2\text{OH}$), 3.15 (m, $\text{OCH}_2\text{CHCH}_2\text{S}$), 2.85-2.70 (m, $\text{OCH}_2\text{CH}_2\text{CH}_2\text{SCH}_2$), 2.67-2.51 (m, $\text{OCH}_2\text{CH}_2\text{CH}_2\text{SCH}_2$ and $\text{CH(OH)CH}_2\text{OH}$), 1.20 (m, CCH_3). ^{13}C NMR (151 MHz, $(\text{CD}_3)_2\text{SO}$): δ 171.5 ($\text{C}(\text{O})\text{O}$), 153.8 ($\text{O}(\text{O})\text{O}$), 128.5 (ArC), 68.8 (OC(O)OCH_2), 65.4 ($\text{OCH}_2\text{CH}_2\text{CH}_2\text{S}$), 61.2, 60.9, (CH_2OH), 46.3 (CCH_3), 44.0 ($\text{OCH}_2\text{CHCH}_2\text{S}$), 34.8, 34.2 and 33.3 (SCH_2CHOH), 16.8 (CH_3). GPC (DMF, RI): M_n (PDI) = 11 550 g mol^{-1} (1.57).

13e: ^1H NMR (400 MHz, $(\text{CD}_3)_2\text{SO}$): δ 7.38 (m, OBn-ArH), 5.14 (s, OBn-CH_2), 4.38-4.16 (m, OC(O)OCH_2 and $\text{OCH}_2\text{CHCH}_2\text{S}$), 3.53 (m, CH_2OH), 3.15 (m, $\text{OCH}_2\text{CHCH}_2\text{S}$), 2.79 (m, $\text{OCH}_2\text{CHCH}_2\text{S}$), 2.54 (m, $\text{SCH}_2\text{CH}_2\text{OH}$), 1.20 (m, CCH_3). GPC (DMF, RI): M_n (PDI) = 24 830 g mol^{-1} (1.16).

7.5. Experimental details for Chapter 4.

7.5.1. Organocatalytic ROP of 5-methyl-5-allyloxycarbonyl-1,3-dioxan-2-one (MAC) and 5-methyl-5-propargyloxycarbonyl-1,3-dioxan-2-one (MPC).

In a typical experiment, alcohol initiator, (-)-sparteine (5 mol% to monomer) or DBU (1 mol% to monomer), and 1-(3,5-bis(trifluoromethyl) phenyl)-3-cyclohexylthiourea (10 or 5 mol% to monomer) catalyst were weighed and dissolved in dry CDCl_3 or dry methylene chloride. MPC and MAC were dissolved separately in the same solvent and added to the initiator/catalyst solution. After the desired time, the polymerisations were then quenched with Amberlyst® 16 (acidic) ion exchange resin and precipitated into hexanes. Polymers were purified by repeated precipitation in hexanes or by column chromatography on silica gel in hexanes/ethyl acetate (4:1).

^1H NMR (600 MHz, CDCl_3): δ 7.37 (m, OBn-ArH), 5.88 (m, CH_{vinyl}), 5.33-5.23 (m, $\text{CH}_2\text{-vinyl}$), 5.15 (s, OBn-CH), 4.72 (s, $\text{OCH}_2\text{C}\equiv\text{CH}$), 4.63 (m, $\text{OCH}_2\text{CHCH}_2$), 4.34-4.27 (m, OC(O)OCH_2), 3.77-3.69 (m, OC(O)OCH_2), 2.53 (m, $\text{OCH}_2\text{C}\equiv\text{CH}$), 1.28 (s, $\text{CH}_3\text{-MPC}$), 1.27 (s, $\text{CH}_3\text{-MAC}$). ^{13}C NMR (151 MHz, CDCl_3): δ 171.9 (CC(O)O-MAC), 171.5 (CC(O)O-MPC), 154.5 (OC(O)O), 131.7 (CH_{vinyl}), 128.8 (ArC), 118.7 ($\text{CH}_2\text{-vinyl}$), 75.7 ($\text{CH}_2\text{C}\equiv\text{CH}$), 68.8-68.5 (OC(O)OCH_2), 66.0 ($\text{OCH}_2\text{CHCH}_2$), 53.0 ($\text{CH}_2\text{C}\equiv\text{CH}$), 46.7 (CCH_3), 17.7-17.4 (CH_3). GPC (THF, RI): M_n (PDI) = 6170 g mol^{-1} (1.18).

7.5.2. Post-polymerisation functionalisations of P(MAC-*co*-MPC).

7.5.2.1. Functionalisation of the propargyl groups of P(MAC-*co*-MPC).

In a typical experiment, polymer was weighed in a vial, dissolved in methylene chloride and transferred to an ampoule, CuI was added and the methylene chloride was removed *in vacuo*. Under a nitrogen atmosphere, azide and a degassed stock solution of diisopropylamine in THF were added and the mixture was stirred for 24h at RT.

THF and Amberlyst® 16 (acidic) ion exchange resin were added and the mixture was stirred vigorously, then passed over a neutral alumina plug. The mixture was then stirred for 16h with Cuprisorb™ beads to remove residual copper, filtered and concentrated *in vacuo*; the residue was dissolved in a minimal amount of methylene chloride and precipitated into hexanes.

¹H NMR (600 MHz, CDCl₃): δ 7.63 (br s, CCHN₃), 7.36 (m, OBn-ArH), 5.88 (m, CH_{vinyl}), 5.36-5.19 (m, CH_{2-vinyl} and OCH₂CCHN₃), 5.14 (s, OBn-CH₂), 4.63 (m, C(O)OCH₂CHCH₂), 4.45-4.18 (m, OC(O)OCH₂ and N₃-CH₂(CH₂)₆CH₃), 3.79-3.66 (m, OC(O)OCH₂ and CH₂OH), 1.90, (m, N₃-CH₂CH₂(CH₂)₅CH₃), 1.38-1.17 (m, N₃-CH₂CH₂(CH₂)₅CH₃ and CCH₃), 0.86 (m, (CH₂)₇CH₃). ¹³C NMR (151 MHz, CDCl₃): δ 172.1 (CC(O)O-triazole), 171.9 (CC(O)O-allyl), 154.6-154.4 (OC(O)O), 142.2 (C=CHN₃), 131.7 (CH_{vinyl}), 128.8 and 128.5 (ArC, C=CHN₃), 123.8 118.6 (CH_{2-vinyl}), 69.3-68.4 (OC(O)OCH₂), 66.0 (OCH₂CHCH₂), 58.9 (OCH₂CCHN₃), 50.6 (N₃CH₂(CH₂)₆CH₃), 46.7 (CCH₃), 31.8, 30.4, 29.2, 29.1 and 26.6 ((CH₂)₅CH₂CH₃), 22.7 ((CH₂)₅CH₂CH₃), 17.9-

17.2 (m, CH₃), 14.2 ((CH₂)₇CH₃). GPC (THF, RI): M_n (PDI) = 5210 g mol⁻¹ (1.11).

7.5.2.2. Functionalisation of the allyl groups of P(MAC-*co*-MPC).

Stock solutions of polymer and AIBN (20%) in dioxane (50 mg polymer mL⁻¹) and stock solutions of thiol in dioxane were prepared and degassed prior to the reactions. In a typical experiment, an ampoule was charged with 26.0 mg polymer. Under a nitrogen atmosphere, degassed 1-dodecane thiol stock solution was added, and the ampoule was placed in an oil bath at 90 °C and stirred for 24 h. The mixture was then concentrated *in vacuo*; the residue was dissolved in a minimal amount of methylene chloride and precipitated into petroleum ether.

¹H NMR (400 MHz, CDCl₃) δ 7.65 (br s, CCHN₃), 7.37 (m, OBn-ArH), 5.27 (m, OCH₂CCHN₃), 5.15 (s, OBn-CH₂), 4.41-4.20 (m, OC(O)OCH₂, N₃-CH₂(CH₂)₆CH₃ and OCH₂CH₂CH₂S), 3.80-3.66 (m, OC(O)OCH₂ and CH₂CH₂OH), 2.77 (m, OH), 2.71 (OCH₂CH₂CH₂SCH₂), 2.60 (m, OCH₂CH₂CH₂SCH₂), 1.99-1.82 (m, N₃-CH₂CH₂(CH₂)₅CH₃ and OCH₂CH₂CH₂S), 1.36-1.18 (m, N₃-CH₂CH₂(CH₂)₅CH₃ and CCH₃), 0.87 (m, (CH₂)₇CH₃). GPC (THF, RI): M_n (PDI) = 5 210 g mol⁻¹ (1.11). MALDI-ToF: M_n (PDI) = 2 630 g mol⁻¹ (1.10).

7.6. Experimental details for Chapter 5.

7.6.1. Copolymerisations of *L*- and *D*-Lactide with functional cyclic carbonates.

7.6.1.1. Copolymerisations of *L*- or *D*-lactide and MAC.

In a typical experiment, alcohol initiator, (-)-sparteine (5 mol% to monomer) or 1,8-diazabicyclo[5.4.0]undec-7-ene (0.2 mol% to monomer), and 1-(3,5-bis(trifluoromethyl) phenyl)-3-cyclohexylthiourea (10 or 1 mol% to monomer) catalyst were weighed and dissolved in dry CDCl₃ or dry methylene chloride. *L*- or *D*- lactide and MAC were dissolved separately in the same solvent and added to the initiator/catalyst solution. Monomer concentration was kept at 0.7 M for polymerisations with 0% MAC, whilst for other polymerisations the concentration of lactide was kept constant at 0.53 M. At *ca.* 90 % *L*-lactide conversion, the polymerisations were then quenched with Amberlyst® 16 (acidic) ion exchange resin and precipitated into hexanes. Polymers were purified by repeated precipitation in cold methanol.

¹H NMR (500 MHz, CDCl₃, 298K): δ 7.35 (m, OBn-ArH), 5.89 (m, OCH₂CH=CH₂), 5.40-5.07 (m, OCH₂CH=CH₂, CH_{LLA}, OBn-CH₂), 4.64 (m, OCH₂CH=CH₂), 4.43-4.23 (m, OC(O)OCH₂), 1.53 (m, CH_{B-LLA}), 1.27 (m, CH₃).

¹³C NMR (126 MHz, CDCl₃): δ 171.8 (C(O)O), 169.8, 169.6, 169.5 and 169.4 (C(O)O-LLA), 154.3 (O(O)O), 131.7 (CH_{vinyl}), 128.8, 128.7 and 128.4 (ArC), 118.7 (CH_{2-vinyl}), 69.6, 69.4 and 69.2 (CHCH_{3-LLA}), 68.7 (OC(O)OCH₂), 65.8

(OCH₂CHCH₂), 46.6 (CCH₃), 17.6 (CCH₃), 16.8 (CHCH_{3-LLA}). GPC (THF, RI): M_n (PDI) = 14 850 g mol⁻¹ (1.05).

7.6.1.2. Copolymerisations of *L*-lactide and MPC.

1,8-diazabicyclo[5.4.0]undec-7-ene (0.2 mol% to monomer) , and 1-(3,5-bis(trifluoromethyl) phenyl)-3-cyclohexylthiourea (1 mol% to monomer) catalyst were weighed and dissolved in dry CDCl₃. *L*-Lactide (75.0 mg, 0.52 mmol) and MPC (34.4 mg, 0.17 mmol) were dissolved separately in dry CDCl₃ and added to the initiator/catalyst solution. At ca. 90% *L*-lactide conversion, the polymerisation was then quenched with Amberlyst® 16 (acidic) ion exchange resin and precipitated into cold methanol. Polymers were purified by repeated precipitation in cold methanol.

¹H NMR (700 MHz, CDCl₃, 298K): δ 7.35 (m, OBn-ArH), 5.21-5.10 (m, CH_{LLA}, OBn-CH₂), 4.72 (m, CH₂C≡CH), 4.44-4.23 (m, OC(O)OCH₂), 2.49 (s, CH₂C≡CH), 1.57 (s, CH_{3-LLA}), 1.29 (s, CCH₃). ¹³C NMR (176 MHz, CDCl₃): δ 171.5 (CC(O)O), 169.8, 169.6, 169.5 and 169.4 (CC(O)O-LLA), 154.2 (OC(O)O), 128.8, 128.7 and 128.4 (ArC), 75.6 (CH₂C≡CH), 71.8 (OC(O)OCH₂), 69.6, 69.3 and 69.2 (CHCH_{3-LLA}), 53.0 (CH₂C≡CH), 46.7 (CCH₃), 17.5 (CCH₃), 16.8 (CHCH_{3-LLA}). GPC (THF, RI): M_n (PDI) = 16 800 g mol⁻¹ (1.14).

7.6.2. Post-polymerisation functionalisation of poly(ester-carbonate)s.

7.6.2.1. Functionalisation of the allyl groups in P(LLA-*co*-MAC).

Stock solutions of polymer and AIBN (20%) in dioxane (50 mg polymer mL⁻¹) and stock solutions of thiol in dioxane were prepared and degassed prior to the reactions. In a typical experiment, an ampoule was charged with 26.0 mg polymer. Under a nitrogen atmosphere, degassed 1-dodecane thiol stock solution was added, and the ampoule was placed in an oil bath at 90 °C and stirred for 24 h. The mixture was then concentrated *in vacuo*; the residue was dissolved in a minimal amount of methylene chloride and precipitated into petroleum ether.

¹H NMR (400 MHz, CDCl₃): δ 7.35 (m, OBn-ArH), 5.22-5.14 (m, CH_{LLA}, OBn-CH₂), 4.44-4.16 (m, OC(O)OCH₂ and OCH₂CH₂CH₂S), 2.59-2.45 (m, CH₂SCH₂), 1.91 (m, OCH₂CH₂CH₂S), 1.58 (m, CH_{3-LLA} and SCH₂CH₂(CH₂)₉CH₃), 1.36 (m, S(CH₂)₂CH₂(CH₂)₈CH₃), 1.26 (m, CCH₃ and (CH₂)₈CH₃), 0.88 (s, (CH₂)₈CH₃). ¹³C NMR (151 MHz, CDCl₃): δ 172.1 (CC(O)O), 169.7, 169.6, 169.5 and 169.4 (CC(O)O-LLA), 154.2 (OC(O)O), 128.8, 128.7 and 128.4 (ArC), 69.6, 69.4 and 69.1 (CHCH_{3-LLA}), 68.8 (OC(O)OCH₂), 64.3 (OCH₂CH₂CH₂S), 46.6 (CCH₃), 32.2 (SCH₂(CH₂)₁₀CH₃), 32.0 (CH₂CH₂CH₃), 29.8 (CH₂SCH₂CH₂(CH₂)₉CH₃), 29.4, 29.1, 28.6, and 28.5 ((CH₂)₇CH₂CH₂CH₃), 22.8 (CH₂CH₂CH₃), 17.7 (CCH₃), 16.8 (CHCH_{3-LLA}), 14.3 (S(CH₂)₁₁CH₃). *M_n* (PDI) = 16 300 g mol⁻¹ (1.05)

7.6.2.2. Functionalisation of the propargyl groups in P(LLA-*co*-MPC).

Polymer was weighed in a vial, dissolved in methylene chloride and transferred to an ampoule, CuI was added and the methylene chloride was removed *in vacuo*. Under a nitrogen atmosphere, azide and a degassed stock solution of diisopropylamine in THF were added and the mixture was stirred for 24h at RT. THF and Amberlyst® 16 (acidic) ion exchange resin were added and the mixture was stirred vigorously, then passed over a neutral alumina plug. The mixture was then stirred for 16h with Cuprisorb™ beads to remove residual copper, filtered and concentrated *in vacuo*; the residue was dissolved in a minimal amount of methylene chloride and precipitated into hexanes.

¹H NMR (600 MHz, CDCl₃) δ 7.62 (br s, CCHN₃), 7.37-7.30 (m, OBn-ArH), 5.30-5.00 (m, CH_{LLA}, C(O)OCH₂CCH and OBn-CH₂), 4.40-4.22 (m, N₃CH₂(CH₂)₆CH₃ and C(O)OCH₂CHCH₂), 1.90, (m, N₃-CH₂CH₂(CH₂)₅CH₃), 1.58 (m, CH₃-LLA), 1.34-1.21 (m, N₃-CH₂CH₂(CH₂)₅CH₃ and CCH₃), 0.87 (m, (CH₂)₇CH₃). ¹³C NMR (151 MHz, CDCl₃): δ 172.1 (C(O)O), 169.8, 169.6, 169.5 and 169.4 (C(O)O-LLA), 154.1 (O(O)O), 128.8, 128.7 and 128.4 (ArC), 71.7 (OC(O)OCH₂), 69.6, 69.4, 69.3 and 69.2 (CHCH₃-LLA), 58.9 (OCH₂CCHN₃), 50.6 (N₃CH₂(CH₂)₆CH₃), 46.7 (CCH₃), 31.8, 30.4, 29.2, 29.1 and 26.6 ((CH₂)₅CH₂CH₃), 22.7 ((CH₂)₅CH₂CH₃), 17.6 (CCH₃), 16.8 (CHCH₃-LLA), 14.2 ((CH₂)₇CH₃). GPC (THF, RI): M_n (PDI) = 18 700 g mol⁻¹ (1.06).

7.7. References.

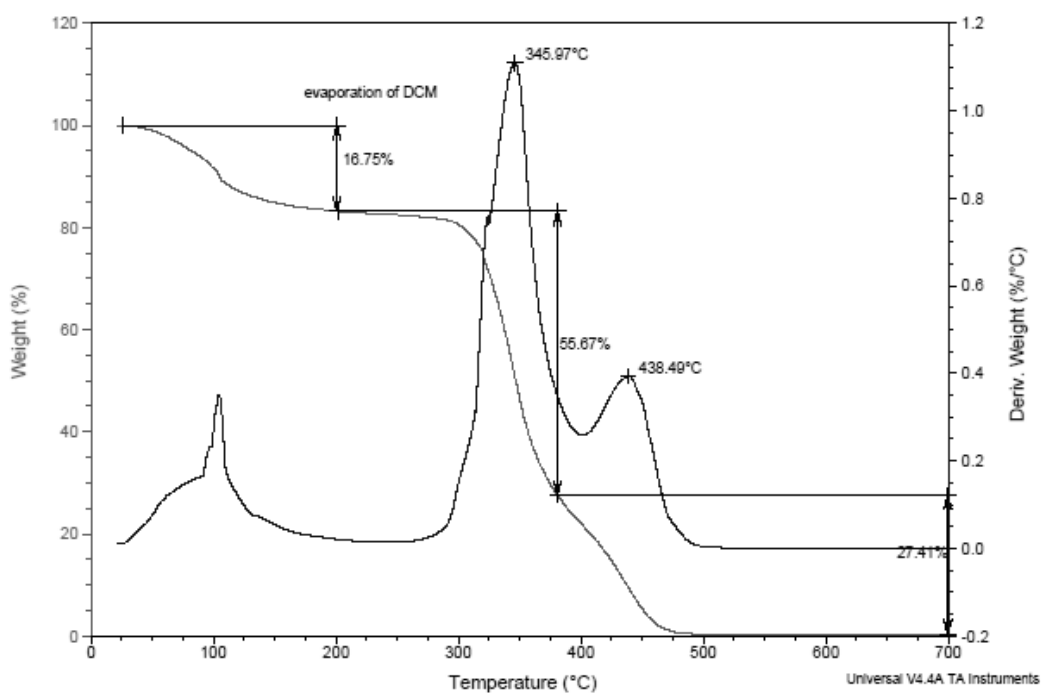
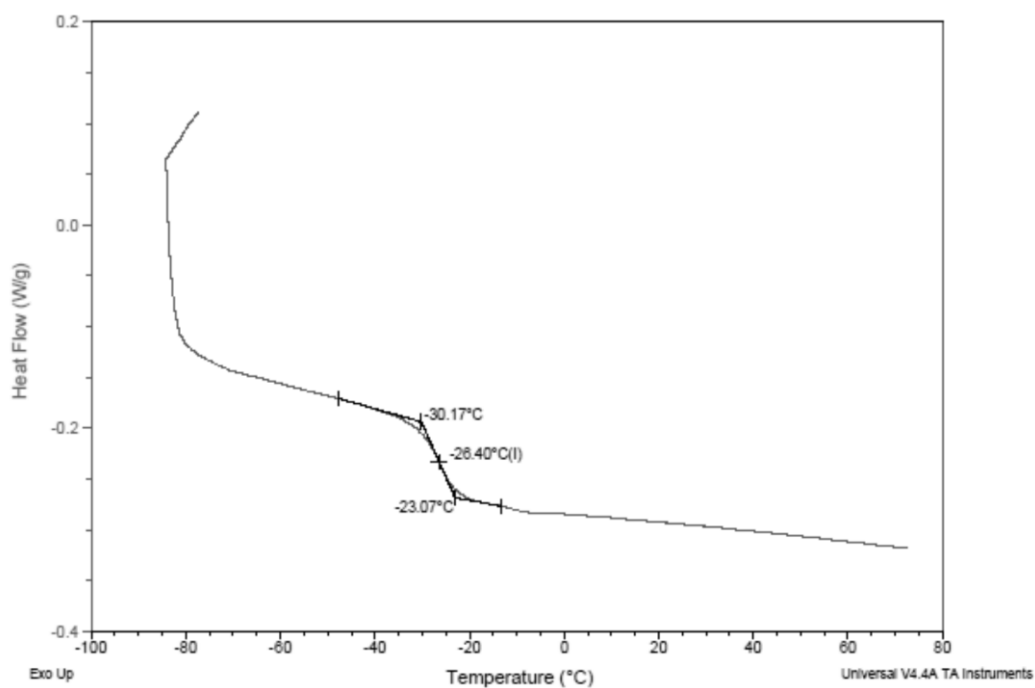
1. Pratt, R. C.; Lohmeijer, B. G. G.; Long, D. A.; Lundberg, P. N. P.; Dove, A. P.; Li, H. B.; Wade, C. G.; Waymouth, R. M.; Hedrick, J. L. *Macromolecules* **2006**, *39*, 7863–7871.
2. Wang, X. L.; Wan, K.; Zhou, C. H. *Eur. J. Med. Chem.* **2010**, *45*, 4631–4639.
3. Sivakumar, K.; Xie, F.; Cash, B. M.; Long, S.; Barnhill, H. N.; Wang, Q. *Org. Lett.* **2004**, *6*, 4603–4606.
4. Vinson, N.; Gou, Y.; Becer, C. R.; Haddleton D. M.; Gibson, M. I. *Polym. Chem.* **2011**, *2*, 107–113.
5. Hu, X.; Chen, X.; Xie, Z.; Liu, S.; Jing, X. *J. Polym. Sci., Part A: Polym. Chem.* **2007**, *45*, 5518–5528.
6. Lu, C.; Shi, Q.; Chen, X.; Lu, T.; Xie, Z.; Hu, X.; Ma, J.; Jing, X. *J. Polym. Sci., Part A: Polym. Chem.* **2007**, *45*, 3204–3217.

UNIVERSITY OF WARWICK

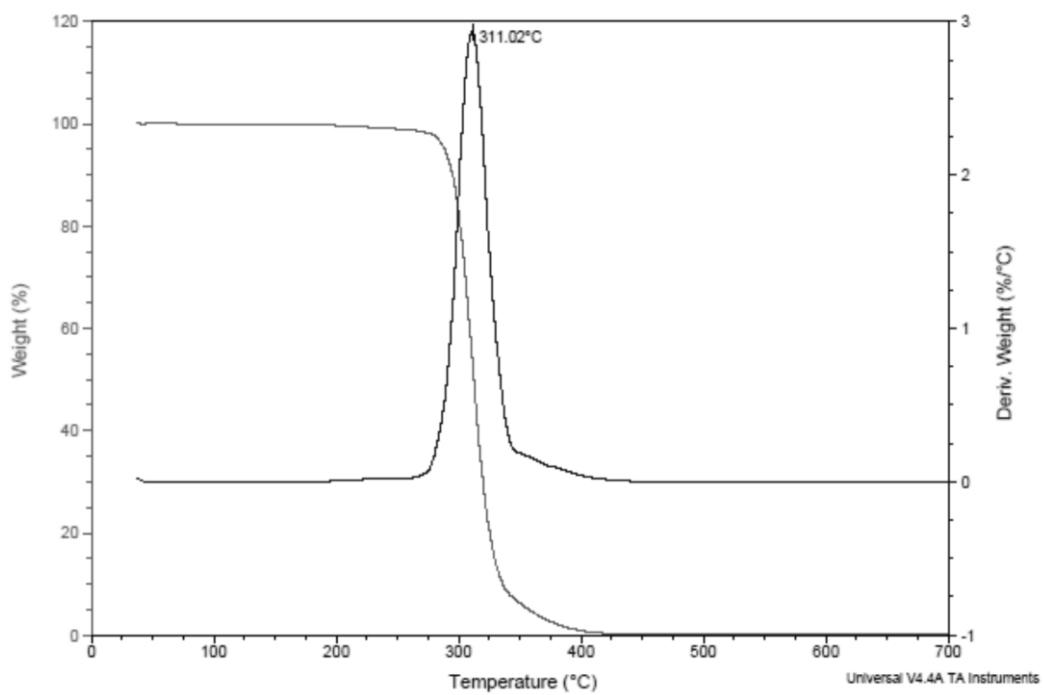
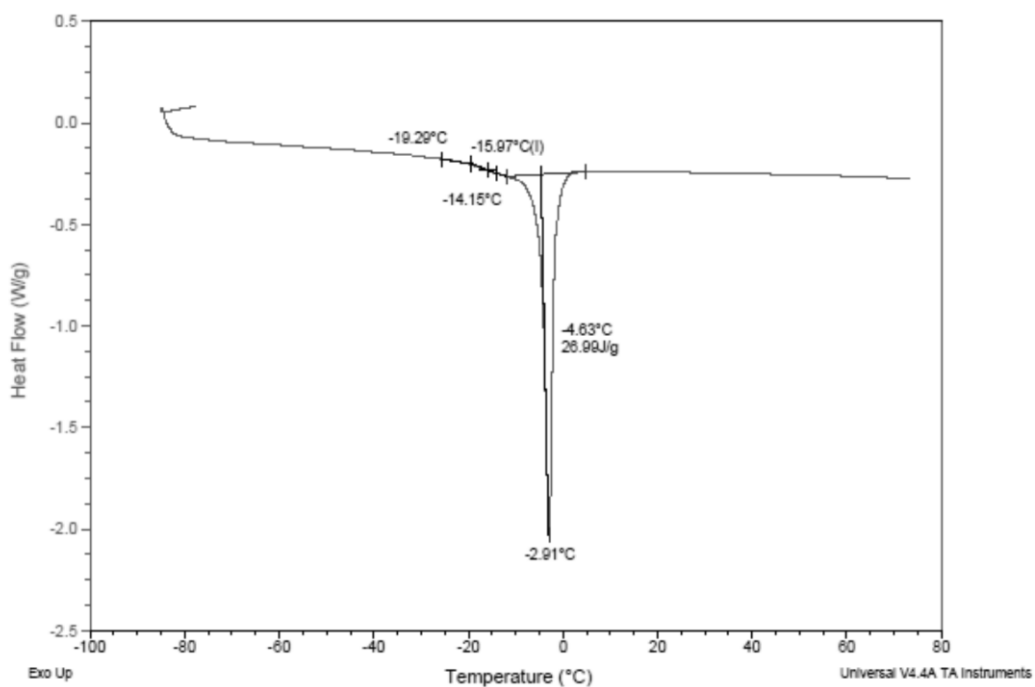
Appendices

Thermal data (DSC and TGA) for Chapter 2

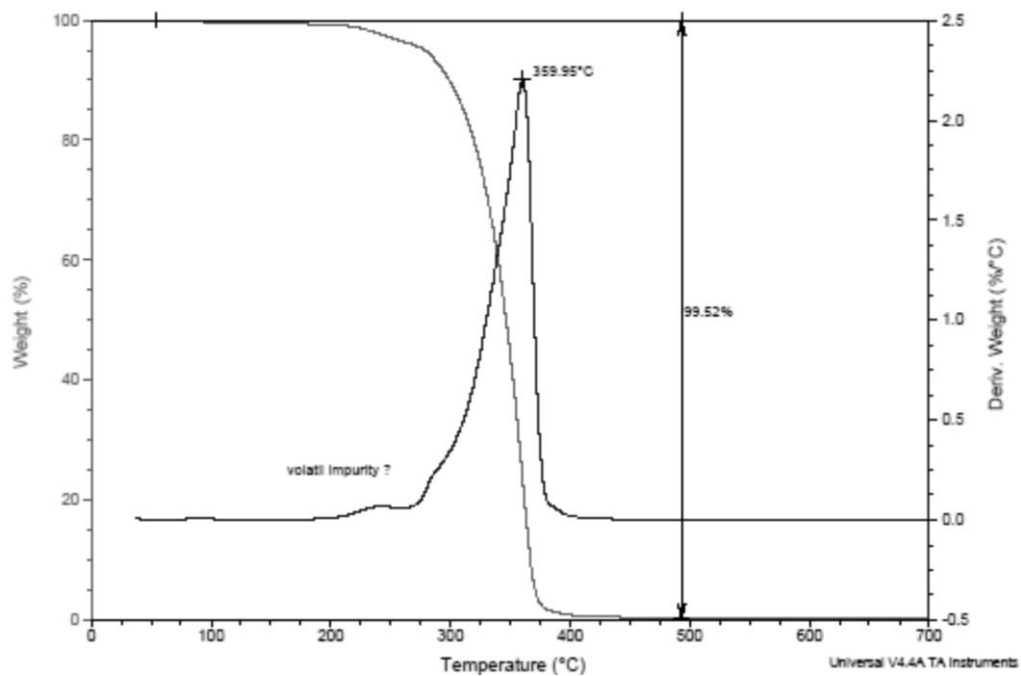
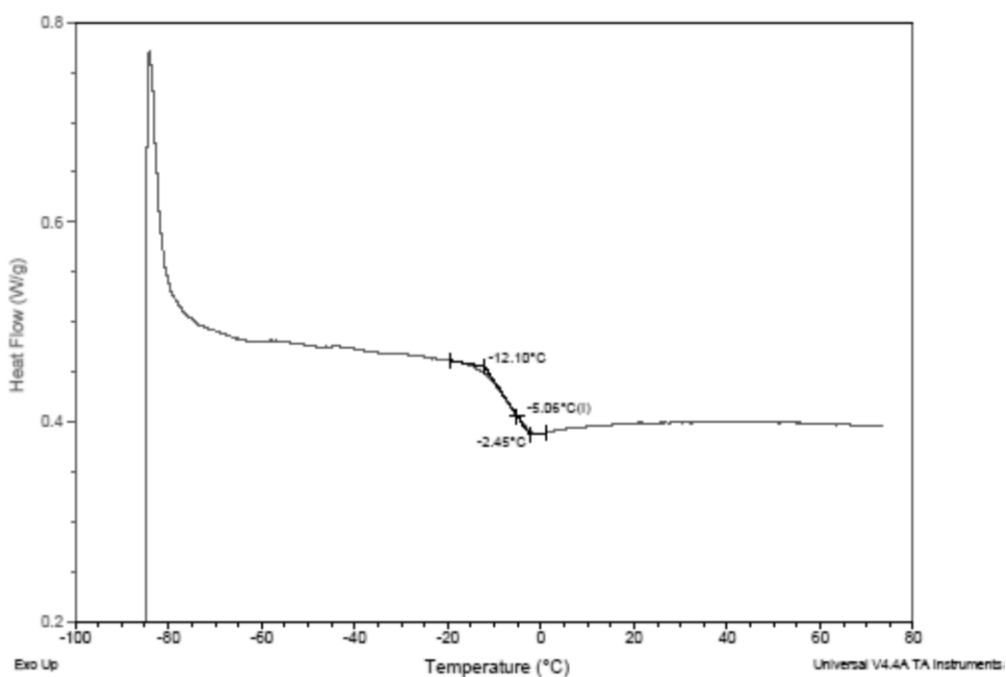
DSC and TGA data BnO-PMAC₁₀₀-OH



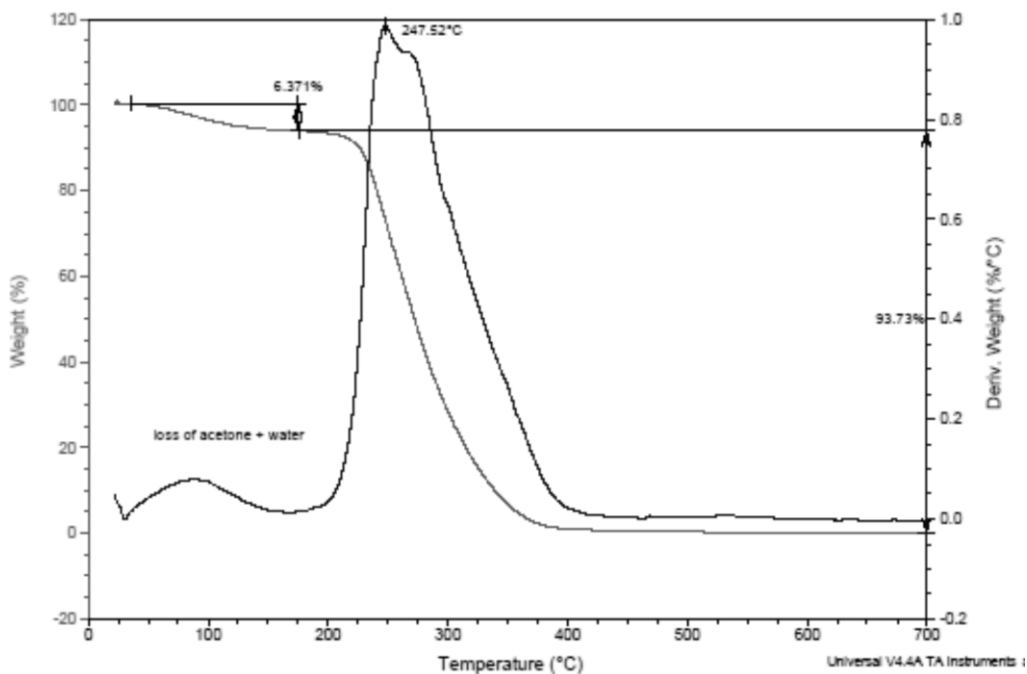
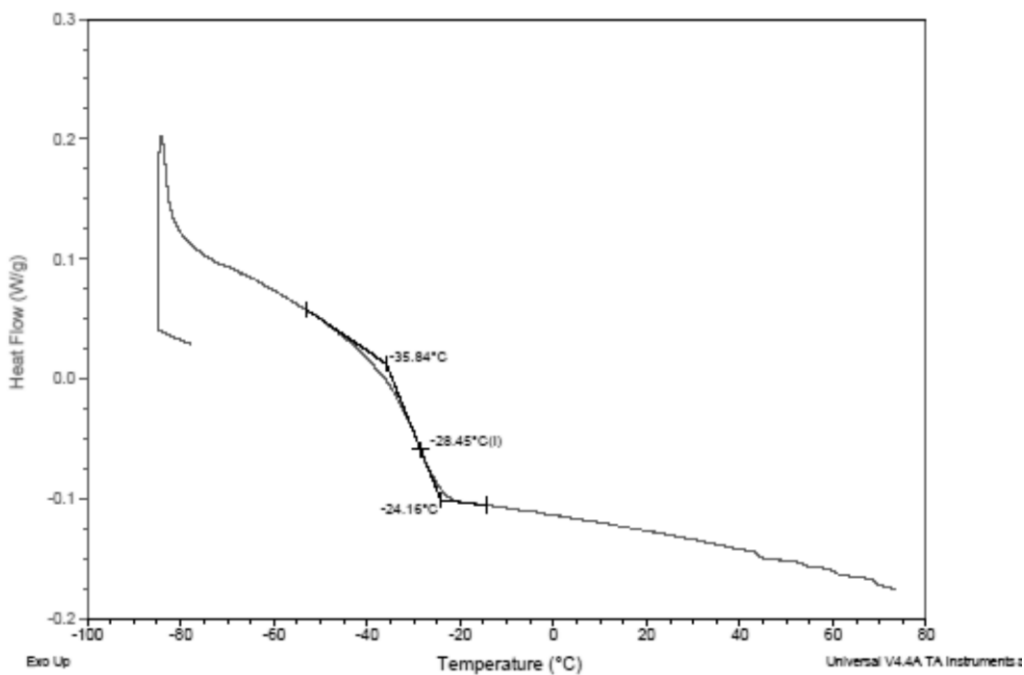
DSC and TGA 11a



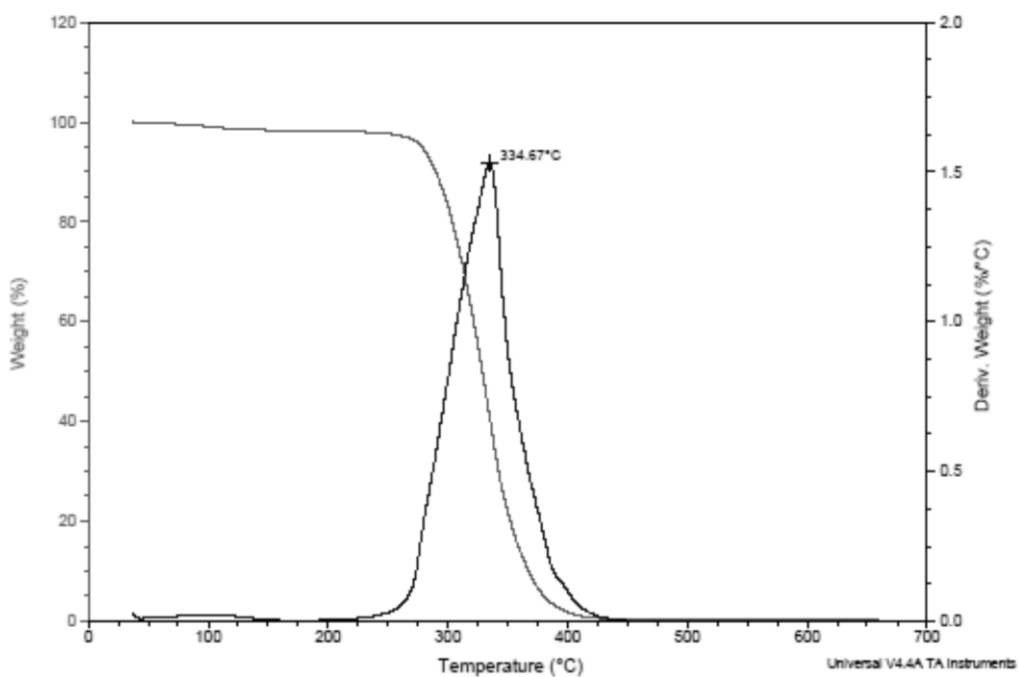
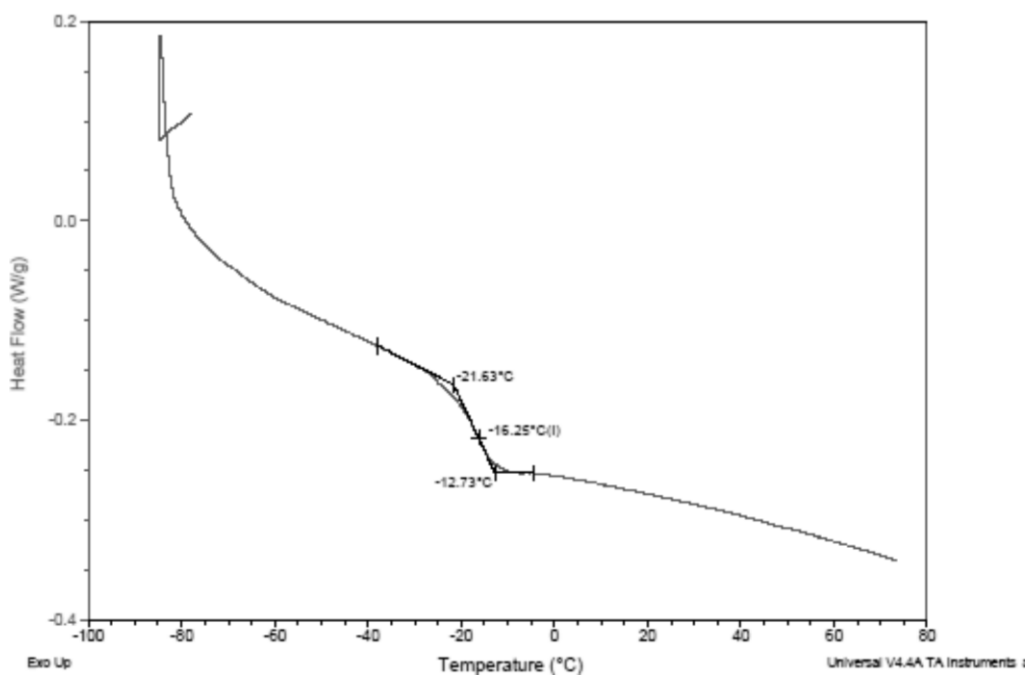
DSC and TGA 11b



DSC and TGA 11c



DSC and TGA 11d



DSC and TGA 11e

